Technical University of Denmark

Full Scale Test of SSP 34m blade, edgewise loading LTT

Data Report 1

Nielsen, Magda; Jensen, Find Mølholt; Nielsen, Per Hørlyk; Berring, Peter; Martyniuk, Karolina; Roczek-Sieradzan, Agnieszka; Sieradzan, Tomasz; Roudnitski, Vatslav; Kucio, Piotr; Bitsche, Robert; Andresen, Peter; Lukassen, Troels Vestergaard; Bialas, Zuzana; Branner, Kim; Bak, Christian; Kallesøe, Bjarne Skovmose; McGugan, Malcolm; Wedel-Heinen, Jakob; Lindby, Torben; Sørensen, Flemming; Jensen, Christian; Knudsen, Henrik Witthøft; Uldahl, Ulla; Rasmussen, Anders Bent; Rasmussen, Jens Jakob Aagaard

Publication date:
2010

Document Version
Publisher's PDF, also known as Version of record

Full Scale Test of SSP 34m blade, edgewise loading LTT. Data Report1

Risø-R-Report

Risø DTU:
Magda Nielsen, Find M. Jensen, Per H. Nielsen, Peter Berring, Karolina Martyniuk, Agnieszka Roczek, Tomasz Sieradzan, Vatslav Roudnitski, Piotr Kucio, Robert Bitsche, Peter Andresen, Troels Lukassen, Zuzana Andrlová, Kim Branner, Christian Bak, Bjarne Kallesøe, Malcolm McGugan, Henrik Knudsen, Ulla Uldahl, Anders B. Rasmussen, Jens Jakob Rasmussen.

Vestas: Jakob Wedel-Heinen
LM-Glasfiber A/S: Torben Lindby
SSP-Technology A/S: Flemming Sørensen
ECC: Christian Jensen

Risø-R-1718(EN)
January 2010
Founded by Energitknologisk Udviklings-og demonstrationsprogram, EUDP-2008

Risø DTU
National Laboratory for Sustainable Energy

Author: Magda Nielsen, Find M. Jensen, Per H. Nielsen, Peter Berring, Karolina Martyniuk, Agnieszka Roczek, Tomasz Sieradzan, Vatslav Roudnitski, Piotr Kucio, Robert Bitsche, Peter Andresen, Troels Lukassen, Zuzana Andrlová, Kim Branner, Christian Bak, Bjarne Kallesøe, Malcolm McGugan, Jakob Wedel-Heinen, Torben Lindby, Flemming Sørensen, Christian Jensen, Henrik Knudsen, Ulla Uldahl, Anders B. Rasmussen, Jens Jakob Rasmussen

Title: Full Scale Test of SSP 34m blade, edgewise loading LTT. Data Report1

Division: Wind Energy Division

Abstract (max. 2000 char.):

This report is a part of the research project "Eksperimentel vingeforskning: Strukturelle mekanismer i nutidens og fremtidens store vinger under kombineret last" where a 34m wind turbine blade from SSP-Technology A/S has been tested in edgewise direction (LTT). The applied load is 60% of an unrealistic extreme event, corresponding to 75% of a certificated extreme load.

This report describes the background, the test set up, the tests and the results.

For this project, a new solution has been used for the load application and the solution for the load application is described in this report as well.

The blade has been submitted to thorough examination. More areas have been examined with DIC, both global and local deflections have been measured, and also 378 strain gauge measurements have been performed.

Furthermore Acoustic Emission has been used in order to detect damage while testing new load areas.

The global deflection is compared with results from a previous test and results from FEM analyses in order to validate the solution as to how the gravity load on the blade was handled. Furthermore, the DIC measurement and the displacement sensors measurements are compared in order to validate the results from the DIC measurements.

The report includes the results from the test and a description of the measurement equipment and the data acquisition.

Risø-R-1718(EN)
January 2010

ISSN 0106-2840
ISBN 978-87-550-3794-6

Contract no.:
J.nr. 63011-0066

Group's own reg. no.:
(psp1120180-01)

Sponsorship: Energitek - nologisk Udviklings - og demonstrationsprogram, EUDP-2008

Cover :

Pages: 158
Tables:
References:

Wind Energy Division
Risø National Laboratory for Sustainable Energy
Technical University of Denmark
P.O.Box 49
DK-4000 Roskilde
Denmark

Contents

Terms and Definitions **1**

1. Introduction **3**

2. Load application **5**

2.1 Equipment for load application 5
2.2 Applying loads 7
2.3 Performing the tests 8
2.4 Comparing deflection 10

3. Measurements **12**

3.1 Planning measurement 12
3.2 Strain gauges measurements 13
3.3 Displacement measurements 13
3.3.1 Global deflection 14
3.3.2 Panels' deformation 14
3.3.3 Deformation and shear distortion of the webs 16
3.4 Optical measurement – Digital Image Correlation 16
3.5 Acoustic Emission 16

4. Data Locking and treatment **17**

4.1 Data acquisition system 18
4.2 Measurement and testing (MGCPlus Assistant) 19
4.3 Measurement and testing (Catman) 19
4.4 Quick View 20
4.5 Data post processing 21

5. Digital Image Correlation (DIC) **23**

5.1 Measuring precision (verification of DIC-system) 23
5.2 DIC-data (measuring results) 25
5.3 Global deformation 26
5.4 Local deformation 27

6. Summary and conclusion **29**

7. References **30**

List of the Appendices **31**

Terms and Definitions

The blade cross section with the main structural features is presented in **Figure 0.1**.

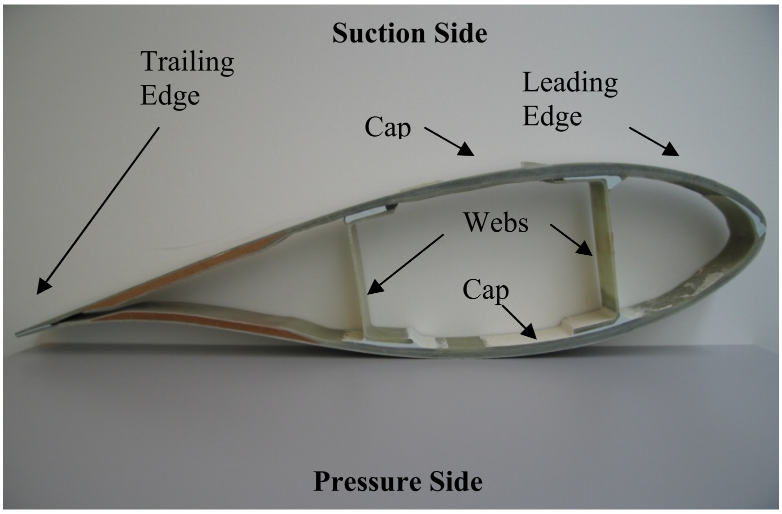

Figure 0.1. Picture of a blade cross-section, indicating construction elements.

Definitions

Blade root:	Part of the wind turbine blade that is closest to the rig
Box girder:	Primary lengthwise structural member of a wind turbine blade
Edgewise:	Direction that is parallel to the local chord of the blade
Flapwise:	Direction that is perpendicular to the surface swept by the non-deformed rotor blade axis
Trailing edge (TE):	Edge of blade pointing opposite travelling direction
Leading edge (LE):	Smooth edge of blade pointing the travelling direction
FEM:	Finite Element Method

Table 0.1. Loading directions, with respect to the blade.

Load case
PTS - pressure side towards suction side
STP - suction side towards pressure side
TTL - trailing edge towards leading edge
LTT - leading edge towards trailing edge

The coordinate system

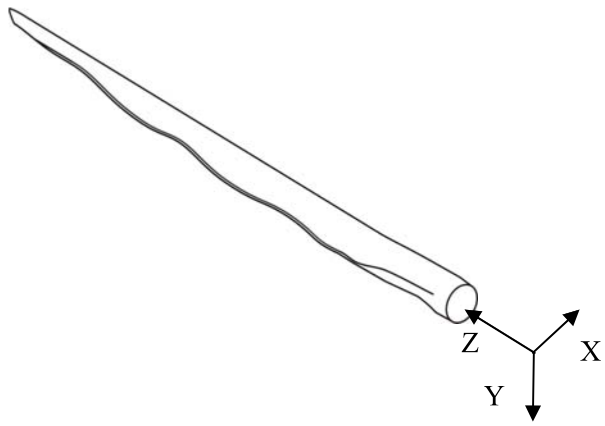

Figure 0.2. Coordinate system.

The x-axis is directed in edgewise (wind) direction, positive towards leading edge. The y-axis is in flapwise direction, positive in direction from pressure to suction side. The z-axis is along the blade, pointed from the root of the blade, as indicated in Figure 0.2.

Measurement equipment

Strain gauges (SG)

UD	Uni Directinal (0° in longitudinal direction)
Bx	Biax (0°/90°)
Tx	Triax-Rosette (0°/45°/90°)
Back to back	One strain gauge on each (inner and outer) side of the blade

Linear transducers (LT)

LT-ASM	Length Transducer from ASM – Cable actuated position sensors
LT-NT	Length Transducer from NovoTechnik

Optical measurement

DIC:	Digital Image Correlation
Aramis:	3D-DIC-system from GOM (www.gom.com)

1. Introduction

This report is part of the EUDP project “Eksperimentel Vingeforskning. Strukturelle mekanismer i nutindes og fremtidens store vinger under kombineret last” The project is sponsored by the Energy Technology Development and Demonstration Program J.No. 63011-0066. Industrial partners in the project are Vestas, LM-Glasfiber A/S, SSP-Technology A/S.

The purpose of this data report is to document the results obtained during full scale testing of a 34m blade in edgewise LTT direction. This is the first data report and it describes the tests and includes results for relatively small loads (approx. 75% of the certification loads). Moreover, in this data report there is a detailed focus on the loading system, the data acquisition and measuring system. The next Risø-R report, Full Scale Test of SSP 34m blade, edgewise loading LTT. Extreme loads + PocInv_E, includes results for extreme LTT load measured with a limited number of measurement equipment located in area where few specific failure modes are to be studied. Furthermore a Risø DTU patent will be implemented and a comparison performed. Later on a data report will be made for combined loading. The coming data reports will focus on the results and if new measuring methods are introduced, they will be described in detail. Evaluation of the results, conclusions, and comparison with FEM will be presented in separate publications (Risø-R- Reports, conference and journal papers). In the present report, one exception is made from the above statement as the global edgewise deflections are compared with an old test carried out in another test facility as well as with FEM. This was done in order to confirm assumptions, calibrations, etc. for the test performed in the new test facility “Experimental Research Facility for Blade Structure” which was opened at Risø in 2008.

The EUDP project aims to further develop the research base needed to understand the structural behaviour of large wind turbine blades which may lead to improved blade designs. This requires research into new methods of measurement and development of test methods for experimental testing. For this purpose, expected in summer 2010, a full-scale test with combined edge- and flapwise loading will be performed. The experimental methods used in all the tests include a large number of strain gauges and displacement sensors. Moreover, advanced digital image correlation (DIC)-system and an acoustic emission measurement system are used.

The main focus of full-scale tests is to understand the structural behaviour and failure mode of the blade. However, areas of the blade which only have interest for dynamic efficiency will also be examined.

Furthermore, these tests enable the researchers to validate the numerical models and allow thorough studies of a wind turbine blade.

The blade tested is from SSP - Technology A/S. It is a 34m blade which has been truncated in 25m, given the part being tested.

For blade data see Table 1.1.

Table 1.1. Blade data.

Type	SSP34
Net weight of the blade	4500 [kg]
Weight of the blade without tip	4200 [kg]
Original blade length	34 [m]
Length of the truncated blade	25 [m]
Diameter at the root	1.8 [m]

2. Load application

The forces applied in the investigated load case are presented in Table 2.1. These values define the so-called Risø load, which is considered the extreme load, and is defined as the design load multiplied by 1.23. The background for this factor is experimental testing of a similar blade, which has carried this amount of load (in flapwise direction) before it failed, see ref. [1], [2].

Table 2.1. The forces applied on the blade in the investigated LTT load case.

Section of application [m from the root]	Applied force [N]
13.21	40013
18.61	31675
24.91	58099

For this test, the blade is mounted on a test rig, see Figure 2.1a and is angled 5 degrees in the vertical direction with respect to horizontal direction, and the tip is tilted 4.4 degree, see Figure 2.1b.

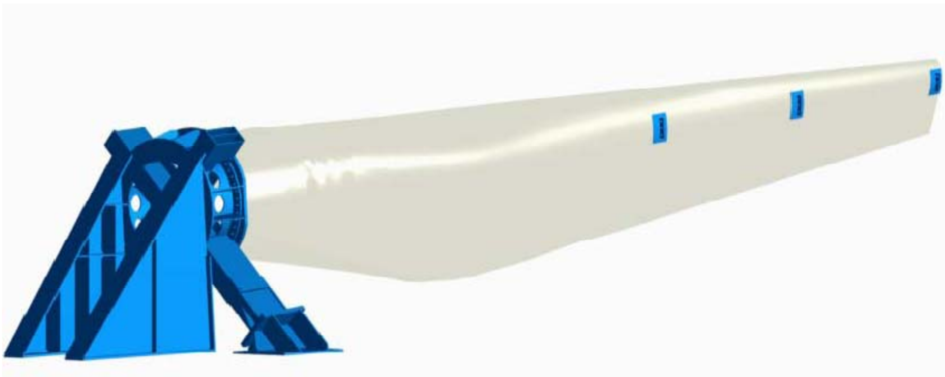

Fig. a

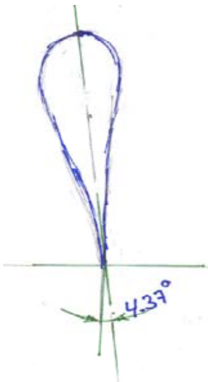

Fig. b

Figure 2.1. Fig. a: Sketch of the blade bolted to the test rig. The tip has been cut off, so only 25m is tested. Fig. b: Cross section of the blade seen from the tip.

2.1 Equipment for load application

The loading system was designed especially for the test facility. The anchor plates transfer the load to the blade thus making the blade free to distort. In particular, transverse shear distortion and out-of-plane deformations are prevented with the traditional loading clamps.

Figure 2.2. The blade with the measurement equipment mounted on the test rig.

The loading system, presented in Figure 2.2, consists of:

- Anchor plates
- Connecting wires
- Winches
- Frequency regulated motors
- Control system

Having being designed and produced, the anchor plates are glued to the surface of the blade at13.2, 18.6 and 24.9 m, see Figure 2.3a and Figure 2.3b.

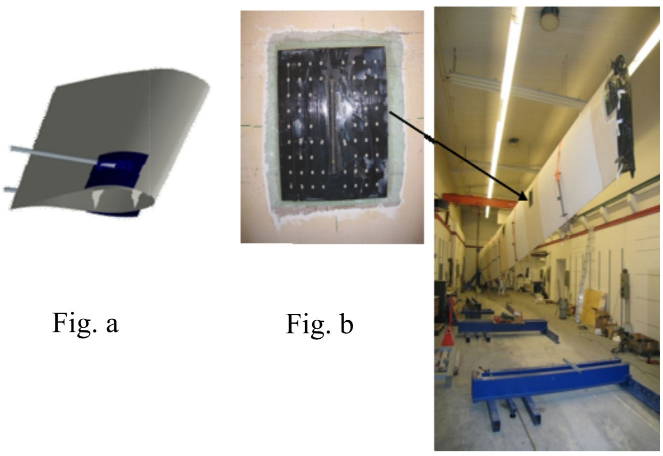

Figure 2.3. Load application at the blade. Fig. a: scheme of anchor plates.   Fig. b: anchor plate glued to the blade at 18.61m.

The wires from the two anchor plates at each side of the blade are assembled in one wire beneath the centreline of the blade. This wire is turned around a block to the winch.

The winch is driven by a frequency regulated motor, and the control system is an on /off system.

The winches can be controlled remotely or from inside the test facility. The steering of the winches from inside the test facility is only used for maintenance or if something needs to be changed inside the facility and the winches are disconnected from the blade.

The remote control system allows the forces to be applied either simultaneously at all loading sections or at each of the three loaded sections separately.

When controlling the winches simultaneously, the frequency regulations of the three motors are set in a predefined ratio to each other. The predefinition is set so that the lengths of the wires connected to the blade are changed according to the expected deflection from the design load on the blade at these loading sections.

The background for the regulation is described shortly in Appendix C.

2.2 Applying loads

The results from the test presented will be compared with a previous test of SSP 34m Blade. When comparing the results obtained in these two tests, there are two main issues that need to be considered:

1) The test is performed on a truncated blade, the tip is cut off at 25 m
2) The blade is placed on the test rig in such a way that the weight of the blade contributes to the actual loading of the blade, i.e. the forces applied on the blade are pulling in the same direction as the weight of the blade itself.

In order to allow comparison between the current test and previous ones, the load caused by the gravity force needed to be considered while establishing the applied load. It was decided to account for the gravity load by reducing the values of the applied load. The gravity load was represented forces loading the blade in the same three sections as the test load is applied. These forces, the gravity related load reduction, are presented in Table 2.2. It was adjusted so that the bending moment distribution was conserved with respect to the previous test of the SSP 34m Blade. The calculation of the moment distribution and the comparison of the moment in the consecutive tests are presented in the Appendix C.

Table 2.2. The force representation of the gravity load, given a load reduction in the three loaded sections.

Blade section	Load reduction
13.21m	10000 N
18.61m	8000 N
24.91m	3500 N

Moreover, the truncated tip needed to be compensated for. Therefore, a preloading was applied at the tip in order to account for the gravity force of the missing part.

In order to prevent the wires at the winches to rewind, all of the sections at which the load was applied needed to be loaded insignificantly. Therefore, after applying the preload, an additional 5% of the load needed to be applied as adjustment forces.

The load acting on the tested blade is thus presented by the following relation (all the forces are given in N). The values are given for 100% of the Risø load and the distribution of the load applied is given below.

Section	Test loads		Weight representation		Preloading		Adjustment forces		Applied loads

$$\begin{bmatrix}13.2\\18.6\\24.9\end{bmatrix} : \begin{bmatrix}40013\\31675\\58099\end{bmatrix} = \underbrace{\begin{bmatrix}10000\\8000\\3500\end{bmatrix} + \begin{bmatrix}0\\0\\11020\end{bmatrix}} + \begin{bmatrix}2001\\1584\\2905\end{bmatrix} + \begin{bmatrix}28012\\22091\\40674\end{bmatrix}$$

$$\begin{bmatrix}13.2\\18.6\\24.9\end{bmatrix} : 100\% = 25\% + 5\% + 70\%$$

Due to the gravity load (including the preloading) and adjustment, the measurements were started at 30% of the Risø load. After applying the preloading and the adjustment forces all the measuring equipment apart from the measurement of the applied forces was set to zero.
To handle the data processing correctly, the data collecting system measured the applied load. The forces representing the gravity load were then added to the measured loads. This sum represented the total load applied to the blade. The total load was used when the data was handled in the data post processing software Graph Tool.

2.3 Performing the tests

During the test there were several crucial safety rules. No one is allowed to be in the test facility while the blade is loaded. However, if the load does not exceed 50% of the loads applied in the previous test, one may enter the test facility.
It was decided that each pull was performed up to 60% of the Risø load for LTT test presented in data report. This decision was made in order not to damage the blade as more tests were planned later on.
During the first test when this load was applied, the blade was monitored with acoustic emission in order to monitor the condition of the blade. The results from the acoustic emission did not indicate any damage at 60% load. In a future data report, results from a coming test performed with extreme loads will be presented.
In this "test" there is a series of tests (called "pulls") since Risø DTU does not have enough channels in the data acquisition system for this amount of data.
The Aramis (DIC) system only measures a limited area at approximately 2m in length and therefore getting measurements at different regions require a pull for each region. More details on this issue are given in Chapters 3 and 4.
The time scale in the Aramis measurement and the time scale for the measurement in the data acquisition system measuring Forces etc. were compared. During load

application, the load at all of three loading sections is kept at approximately the same ratio (%) of the Risø load at these sections.
The result from a pull with the applied forces in % as a function of time can be seen in Figure 2.4. It can be seen that the force at load point 3 FT-3 is corrected during the test.

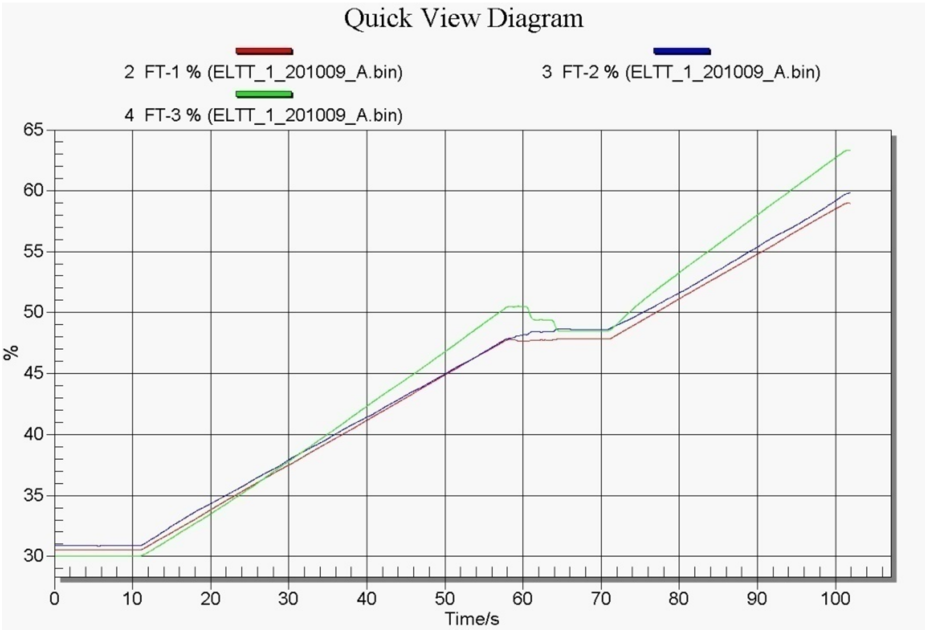

Figure 2.4. The results from a test with the applied forces in % as a function of time.

The small deviation noticeable between the percentages of the applied loads from the three sections has an insignificant influence on the results. The measurements are processed according to local bending moment and thus the results are not very sensitive to this difference. Figure 2.5 presents deflection results from the same pull as in Figure 2.4. The spot at approximately 1020kNm (deflection of 3mm) is where the load is corrected.

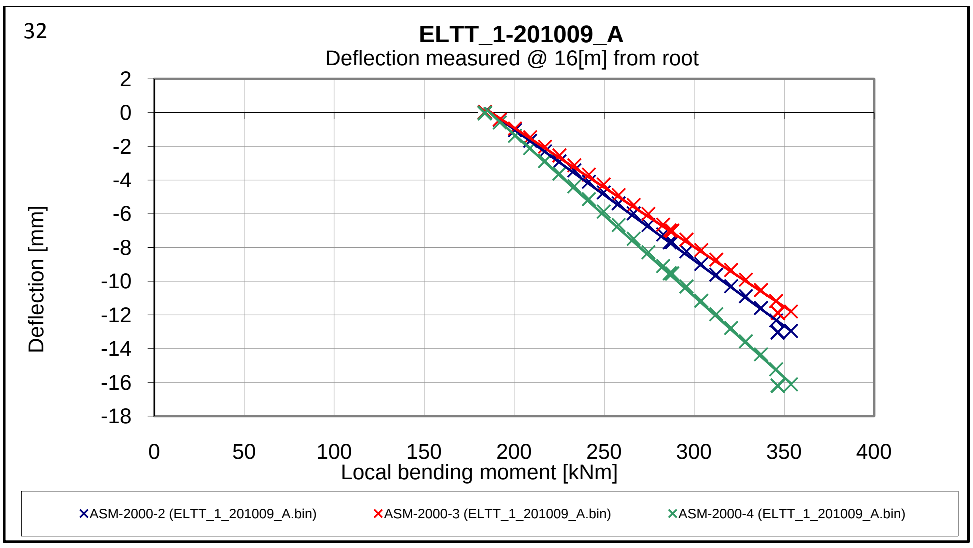

Figure 2.5. Flapwise deflection at 16m, presented by graph tool.

2.4 Comparing deflection

Global edgewise deflections can be compared easily, and therefore these are used for comparison with results from previous tests. This is done in order to make sure that the assumptions, calibration etc. for the new test facility have been performed properly.

The graph in Figure 2.6 shows edgewise deflection of the trailing edge.

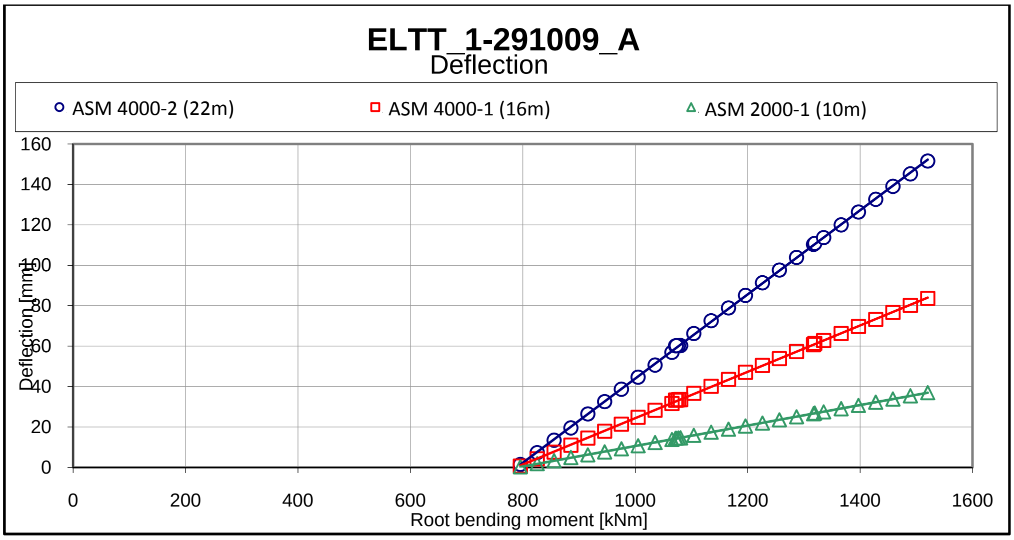

Figure 2.6. The edgewise deflection of the blade trailing edge at 10m, 16m and 22m.

The root bending moment is presented using the total forces (including gravity forces) whereas the deflection is measured from approximately 30% of the Risø load.

As can be seen on the graphs, the global edgewise deflections are linear giving that the total deflection can be determined by extending the lines to intersection with the vertical axes and add the value of the deflection below the horizontal axis to the value above. The readings from the experiment are presented in Table 2.3.

Table 2.3. Comparison of the edgewise displacement of the trailing edge at several cross-sections. The results from the previous blade test are read from plots in ref.[5].

Blade section	Previous measurement Blade test SSP34#2. Nov. 03	Total bending deflection for root bending moment 1500kNm (using the graphs)
10 m	75 mm	75mm
16 m	175 mm	180mm
22 m	325 mm	320mm

In Table 2.3, the results from the experiment are compared with the results from a similar blade, tested at Blaest Test Center (primarily Sparkaer Test Center which has been a part of Risø). This comparison is done in order to check whether all the assumptions, corrections etc. have been done properly. The old test from Blaest Test Center is reported in ref. [5]. The mentioned test was performed with the entire 34m blade rotated by 90°. Thus, the complex issue regarding gravity is not considered in the main (in this case - edgewise) direction studied. The conclusion from this comparison verifies that no wrong assumptions or other errors have been introduced.

While comparing FEM results with the experimental ones, it is important to keep in mind how the test ('SSP-34m-Blade2') was conducted, see Section 2.2. The measurement equipment was set to zero at 30% of the Risø load and the measurements have started.

Thus, while comparing the measurements with FEM results, an easy comparison is to use the following:

RESULT = Result (reached % Risø load) – Result (30% Risø load)

In case of the SSP-34m-Blade2 test, the reached % is 60% and thus we have:

RESULT = Result (60 %) – Result (30%)

The FE-results are also presented in Figure 2.7.

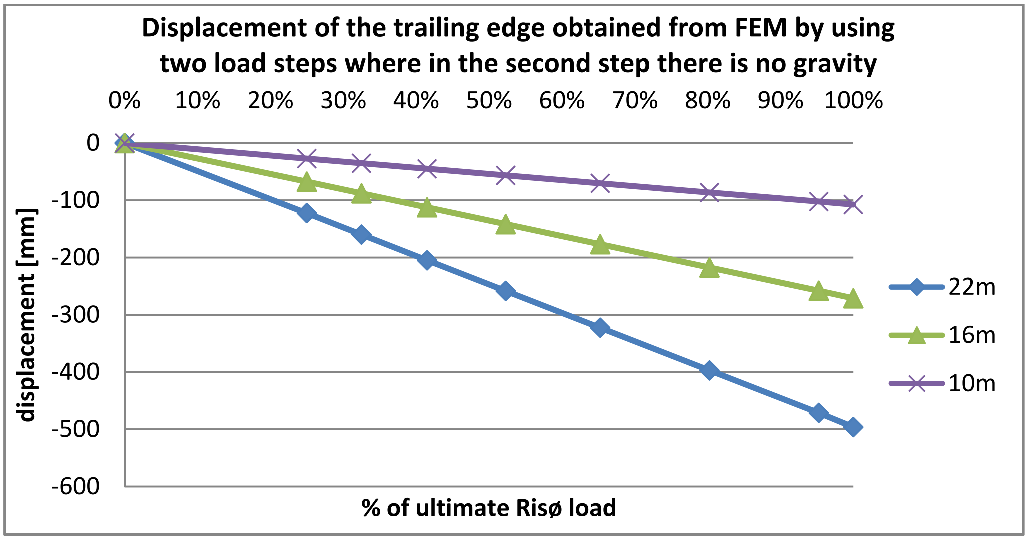

Figure 2.7. Edgewise displacement of the trailing edge at three sections. The results are from a non-linear FE-model performed at Risø DTU.

In Table 2.4, values read from the plots in Figure 2.7 for 60% load are compared to those given in Table 2.3.

Table 2.4. The FE- results for the edgewise displacement of the trailing edge at several cross-sections compared with the experimental readings.

Blade section	FEM results for 60% load	Experimental results (Table 2.3)
10 m	65 mm	75mm
16 m	165 mm	180mm
22 m	297 mm	320mm

The results of FE-analysis deviate by 7-13% from full-scale test results. This difference may be caused by many reasons, e.g. that the material stiffness properties used in the FE-model are too small. This will be evaluated more thoroughly in forthcoming publications, when further experience with the stiffness data is established. Another explanation could be the difference in the actual stiffness of the test rig, which is assumed infinite in the FE-model.

3. Measurements

This chapter describes where and in which way the measurement equipment is placed on the blade and how the measurements are performed.

3.1 Planning measurement

When investigating the blade it is crucial to instrument the blade with measurement equipment in such a way that the structural behaviour can be examined. Therefore, before mounting the measurement equipment, the placement of each single measurement was planned. In this planning, the measurement equipment is placed in positions that allows the addressing of all the relevant deformation behaviour, not only for the edgewise load case.

Four main sections have been chosen, namely 3m, 4m, 7m and 10 m, and they are heavily instrumented in order to get detailed information about the deformations (both local and global) and strains.

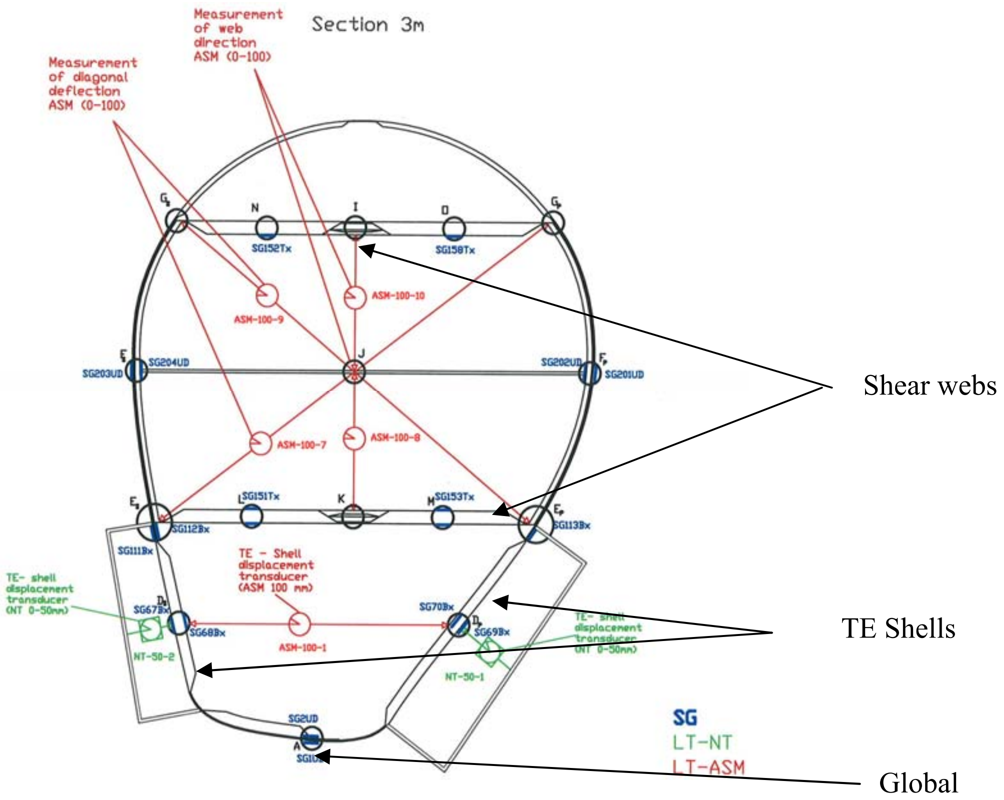

Figure 3.1. Displacement sensors and strain gauges located inside and outside the blade/box

Figure 3.1 presents the drawing with the placement of the measurement equipment at the main section 3m. The letters A, D, E, F, K, L, M, N, I, O, and J are notations for specific placements at each section of the blade. The indices to these letters refer to the side of the blade: S for suction side and P for pressure side.

All over the blade, where it was practically possible, the strain gauges were mounted in the 'back to back' manner. The strain gauges (blue) in the 'back to back' manner can be seen found at several places in Figure 3.1 e.g. at placement with notation L and M.

The LT-NT's measure local panel deformations are mounted with steel frames on the panels on the outside of the blade (marked in green). For further explanations, see ref. [1] and [2].
The shear web deformations are measured with ASM inside the blade (red). A broomstick is placed in the middle of the box girder as a reference frame allowing measuring each web deformation individually. In Figure 3.1 the broomstick is shown as the line between F_s and F_p. Additionally, ASM-sensors are placed in diagonals in order to measure the transverse shear distortion.
Furthermore, at the main sections, the blade was instrumented in several other sections. These remaining sections were not as heavily instrumented as the main sections. Drawings presenting all of the instrumented sections along with the full list of the strain gauges, NT's and ASM's, can be found in Appendix A.

3.2 Strain gauges measurements

Besides the drawings with the strain gauge positions, a list with all the strain gauge positions was made. This list can be found in Appendix A
This list divided the strain gauge positions into:

- Group A Global
- Group B TE- Shell
- Group C Shear Webs
- Group D Caps.

The global was mainly measured with unidirectional UD strain gauges, whereas the main sections were equipped with Tx. At the panels there was primarily used Bx.
The total number of SG used in the tests is 378, and this amount of strain gauges exceeds the amount of channels in the data acquisition system. Consequently, in order to get the results from all of the strain gauges it was necessary to carry out 3pulls at the blade. According to this, the strain gauges were divided into 3 groups, called: Main Section, AED Section + Global and Other Groups.
The lists containing the strain gauges in each group are found in Appendix A2.

3.3 Displacement measurements

For the deformation measurements, two different types of measurement equipment were used, namely NT and ASM. See description of the equipment in Appendix E.
The following were measured:

1. Global deflections
2. Panel deformations
3. Deformation of shear webs and shear distortion of the box girder

3.3.1 Global deflection

The global deflection was measured in the edgewise and flapwise direction, and in order to measure this, position sensors called ASM were mounted outside the blade.
The global edgewise deflection was measured at 10m, 16m, and 22m, and here the position sensors were mounted between the floor and the trailing edge.
To measure flapwise deflection and rotational deformation, ASMs were placed in 4m, 7m, 10m, 16m and 22m. For these measurements the sensors were mounted between the suction sides of the blade and the wall, as shown in Figure 3.2. Two sensors at each section would have been sufficient to find the rotational deformation, but in order to measure bending deformation of the trailing edge, an additional ASM-sensor was placed at the trailing edge. In this data report no evaluation is made. However, in forthcoming publications, it will be considered how dominant the bending deformation is and what influence it has on the structural strength and aerodynamic performance.

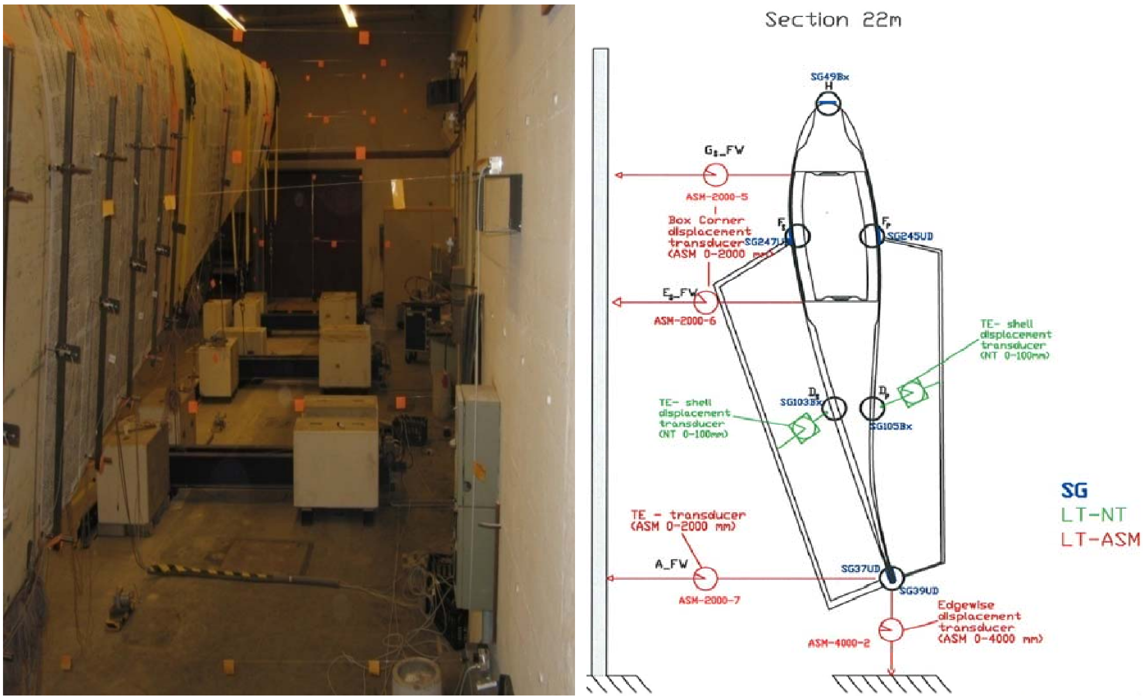

Fig. a. Fig. b

Figure 3.2. Displacement sensors mounted outside the blade shown: a. from the position looking towards the tip, b. from the position looking towards the root.

The complete list of position sensors (LT-ASM) and further information regarding position sensors LT-ASM, can be found in Appendix A3.

3.3.2 Panels' deformation

In order to measure the TE panels' deformation, LT-ASMs were mounted inside the blade, between TE panels in sections: 3m, 4m, 5m, 6m, 7m and 10m (see Appendix A3). In Figure 3.3, the displacement sensors are presented at section 7m from the root. The LT-ASMs are marked with red. Range of the position sensors used inside the blade is 100mm.

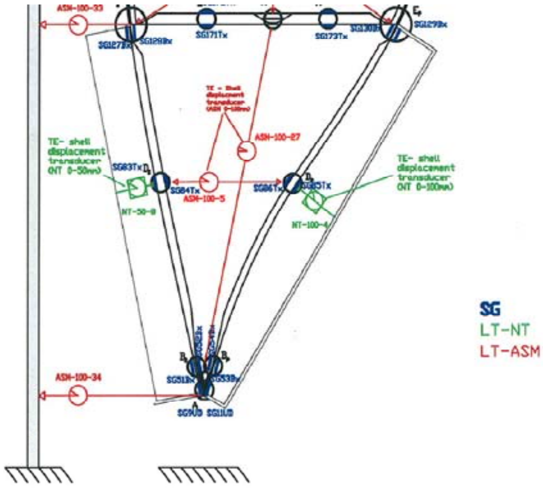

Fig. a. Fig. b

Figure 3.3. Sensors mounted between TE panels at 7m.

The deformations were also measured on the outside of the panels as well. Here the measurements were performed with NT length transducers. The transducers were mounted on frames which were fastened to the blade. The frames were supported at line A and E on the blade, see Figure 3.3b (the NTs are marked in green). Figure 3.4 presents the frames with the NTs mounted on the blade.

Figure 3.4. LT-NT mounted on the frames.

3.3.3 Deformation and shear distortion of the webs

Inside the blade length, transducers were mounted separately between each shear web and the reference frame. This provides information on individual deformation of both webs. The reference frames are shown if Figure 3.5. These measurements were taken at sections: 3m, 4m, 7m and 10m. Additionally, in order to study transverse shear distortion, ASMs were mounted as diagonals in the box girder. The wires for these transducers can be seen in Figure 3.5 as well.

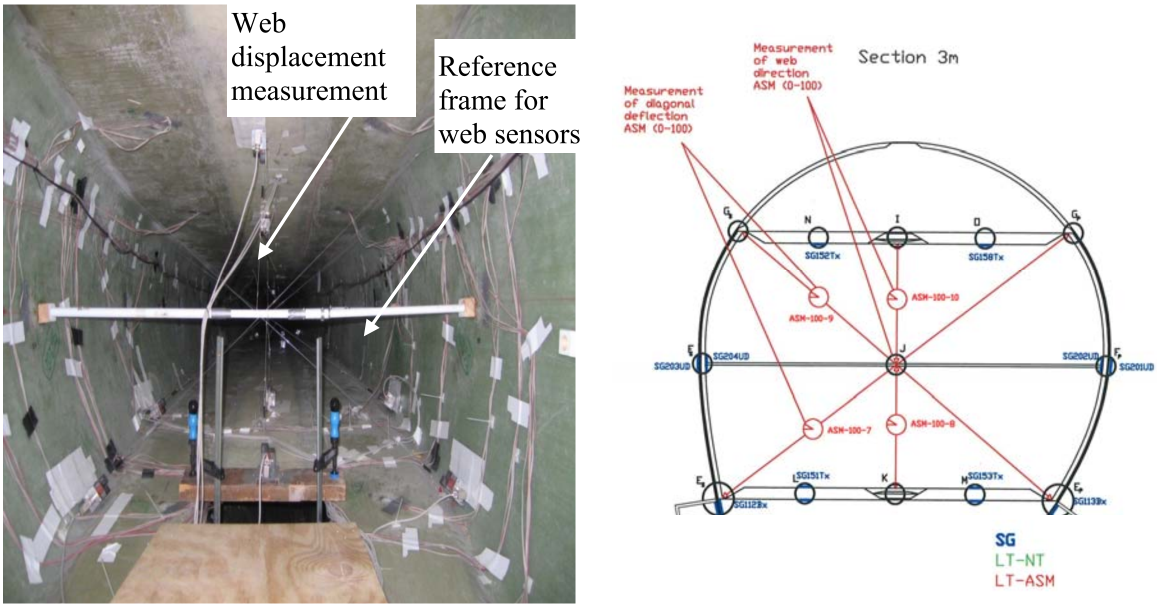

Fig. a　　　　　　　　　　Fig. b

Figure 3.5. The displacement sensors mounted inside the box girder shown. Fig. a: picture – view from the position looking towards the tip, Fig. b: sketch – view from the position looking towards the root.

3.4 Optical measurement – Digital Image Correlation

Digital Image Correlation system, so-called Aramis, performed measurements on the suction and pressure side of the blade at the distance of 4m, 10m and 20m from the root. Aramis is an optical measurement system, able to measure 3D displacement and surface strain of an object by means of image processing. In order to be able to perform Aramis measurements, the blade was covered with a pattern as shown in Figure 3.5a. Further information regarding the Aramis system can be found in Chapter 5.

3.5 Acoustic Emission

During the full-scale tests, a non-destructive testing method was also applied. Acoustic Emission (AE) sensors were mounted on the blade. Moreover, a portable AE system was used to detect cracks or changes in the tested structure. More information regarding the non-destructive test method used can be found in Appendix E. In this data report no results are included since in a coming data report the same blade is tested in the same loading direction, but to extreme load where more acoustic emission measurements is taken.

4. Data Locking and treatment

Before the LTT test series was started, all the pulls carried out on the blade were planed and prepared so that measurements at all positions were performed.
The test series for LTT test included DIC (Aramis) measurement in five different positions namely at 4m and 10m on both pressure and suction side, and at 20 m pressure side.
Strain gauges measurements belonging to different groups, Main, Global and Other groups, together with deflection measurements group were changed according to the plan shown in Table 4.1.
This plan shows that the data collecting system needed 5 templates to cover all the measurements. Each template contains the information about which part of the measurement equipment is connected to the data acquisition system and the calibration of this measurement equipment.
The list with SGs in group Main, Global and Other groups along with the groups for the deflection measurements are in Appendix A4.

Table 4.1. Plan for TTL tests.

Aramis	Group1 Main	Group 2 Global	Group3 Other	Group4 Main B	Group 5 Global B	Test name	Comments
4mP				x		ELTT_4_030909_A	
10mP				x		ELTT_4_131009_A	
16mS	x					ELTT_1_191009_A ELTT_1_201009_A	SG measurement failed
20mS	x					ELTT_1_291009_A	
4mP			x			ELTT_3_041109_A	
4mP		x				ELTT_2_101109_A	
4mS		x				ELTT_2_171109_A	
4mS					x	ELTT_5_181109_A	
4mP					x	ELTT_5_251109_A ELTT_5_251109_B	Aramis was repeated

In Table 4.1, the groups represent different templates. The first column “Aramis” describes the section where the Aramis measurements are performed, e.g. 4mP, means that Aramis is placed in 4m on the Pressure side

All the TTL tests performed are presented in Table 4.1, but only some of them belong to this data report, as some pulls include test of the blade with an additional reinforcement. This reinforcement is part of “Prove of concept for invention E” (Poc_Inv_E, the reinforcement where the trailing edges panels’ are coupled) and will be described in a future report.

The results presented in this report are the results from loading the blade without reinforcing it.
Some of the measurements were repeated but in this data report the results are only presented once. The results from the measurements are presented as plots with

Graph Tool and can be found in Appendix B. The results presented in this data report are as listed below.

Measured strain vs. bending moment - obtained from strain gauges in:

- Main section in test ELTT_1-291009_A
- Global section in test ELTT_2-101109_A
- Other groups section in test ELTT_3-041109_A

The deflection measurements vs. bending moment

- from test ELTT_1-291009_A
- from test ELTT_5-181109_A
  NT-50-17, NT-100-18, NT-50-19, NT-50-20
- ELTT_4-130909_A
  flapwise global deflection measurements in 4 and 7m

4.1 Data acquisition system

The acquisitions system is from HBM and in Figure 4.1, the entire data acquisition system in presented
The measurement equipment from the blade is connected to the Canheads, which again are connected to the data acquisition system MGCPlus through a bus.

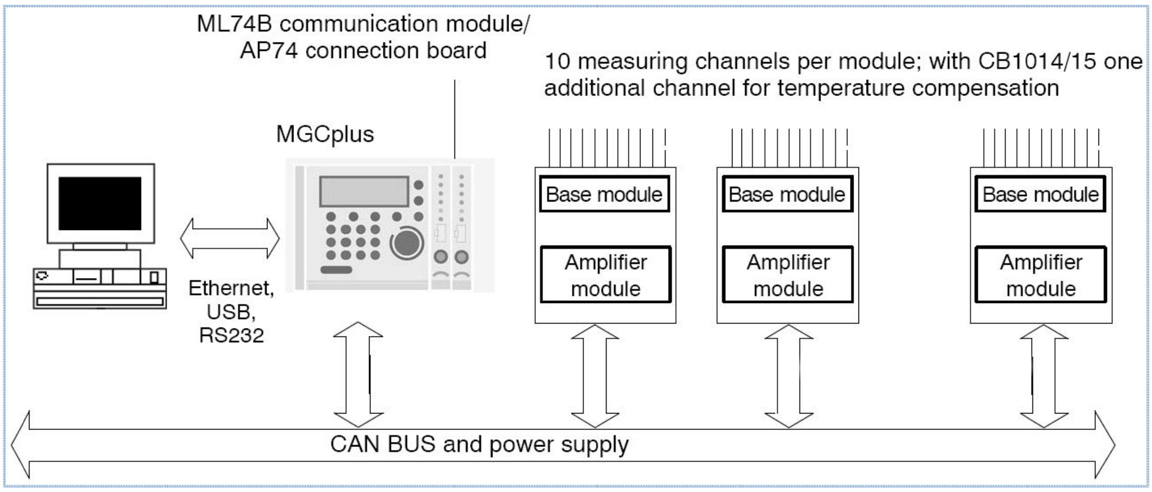

Figure 4.1. The data acquisition system

At the Experimental Research Facility for Blade Structure there are 24 Canheads. 18 out of these are prepared for strain gauge measurements and the remaining 6 are used for Length and Force Transducers.
Each card in the base module card can handle 120 channels, and each card needs its own CAN BUS which gives that at the test facility there are two connecting lines (CAN BUS) connecting the measurement equipment to the data acquisition system. When the measurement equipment is connected to the data acquisition system, the data acquisition system recognizes the Canheads. This is the reason why the order in which the Canheads are connected in the line is free, as long as they are placed in the correct line. However, as the system recognizes the Canheads, the measurement equipment must be connected to the right Canhead in the right order.
For our measurements the data are collected each 0.2 s.

4.2 Measurement and testing (MGCPlus Assistant)

After the Canheads and sensors are connected and before the first measurements, the MGCPlus compatible software "MGCPlus Assistant" is used to calibrate the sensors, setup measurement units, name the channels, etc.

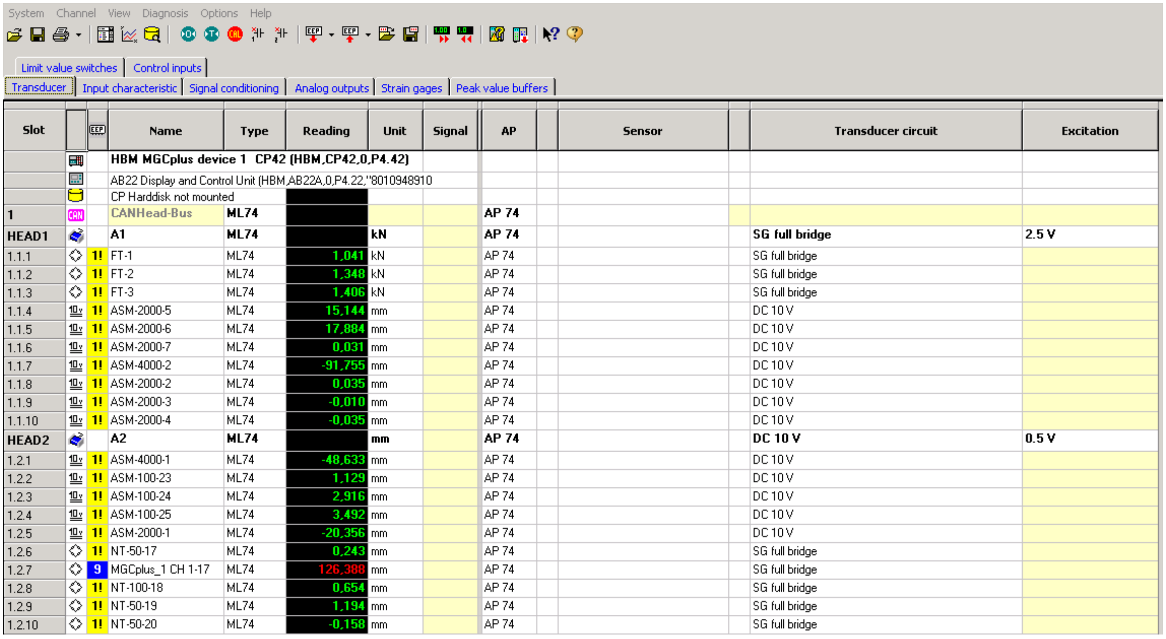

Slot	EEP	Name	Type	Reading	Unit	Signal	AP	Sensor	Transducer circuit	Excitation
		HBM MGCplus device 1 CP42 (HBM,CP42,0,P4.42)								
		AB22 Display and Control Unit (HBM,AB22A,0,P4.22,"8010948910								
		CP Harddisk not mounted								
1		CANHead-Bus	ML74				AP 74			
HEAD1		A1	ML74		kN		AP 74		SG full bridge	2.5 V
1.1.1	1!	FT-1	ML74	1,041	kN		AP 74		SG full bridge	
1.1.2	1!	FT-2	ML74	1,348	kN		AP 74		SG full bridge	
1.1.3	1!	FT-3	ML74	1,406	kN		AP 74		SG full bridge	
1.1.4	1!	ASM-2000-5	ML74	15,144	mm		AP 74		DC 10 V	
1.1.5	1!	ASM-2000-6	ML74	17,884	mm		AP 74		DC 10 V	
1.1.6	1!	ASM-2000-7	ML74	0,031	mm		AP 74		DC 10 V	
1.1.7	1!	ASM-4000-2	ML74	-91,755	mm		AP 74		DC 10 V	
1.1.8	1!	ASM-2000-2	ML74	0,035	mm		AP 74		DC 10 V	
1.1.9	1!	ASM-2000-3	ML74	-0,010	mm		AP 74		DC 10 V	
1.1.10	1!	ASM-2000-4	ML74	-0,035	mm		AP 74		DC 10 V	
HEAD2		A2	ML74		mm		AP 74		DC 10 V	0.5 V
1.2.1	1!	ASM-4000-1	ML74	-48,633	mm		AP 74		DC 10 V	
1.2.2	1!	ASM-100-23	ML74	1,129	mm		AP 74		DC 10 V	
1.2.3	1!	ASM-100-24	ML74	2,916	mm		AP 74		DC 10 V	
1.2.4	1!	ASM-100-25	ML74	3,492	mm		AP 74		DC 10 V	
1.2.5	1!	ASM-2000-1	ML74	-20,356	mm		AP 74		DC 10 V	
1.2.6	1!	NT-50-17	ML74	0,243	mm		AP 74		SG full bridge	
1.2.7	9	MGCplus_1 CH 1-17	ML74	126,388	mm		AP 74		SG full bridge	
1.2.8	1!	NT-100-18	ML74	0,654	mm		AP 74		SG full bridge	
1.2.9	1!	NT-50-19	ML74	1,194	mm		AP 74		SG full bridge	
1.2.10	1!	NT-50-20	ML74	-0,158	mm		AP 74		SG full bridge	

Figure 4.2. Screen-shot from the MGCplus assistant. The calibration is shown.

When all parameters are set, the file is saved as a template so that it can be efficiently loaded to the system again in case the same group of sensors is to perform the measurement again.

4.3 Measurement and testing (Catman)

The Catman software was used for handling the measurement data. It is described in Appendix E. The system gives the opportunity to add additional virtual channels, e.g. to calculate percentages of the load, which is then done automatically. It is here the total load is calculated including the compensation for the gravity load.

During the measurement, visual templates are used in Catman to monitor selected sensors in real-time. A visual template looks as the one used during the tests, presented in Figure 4.3.

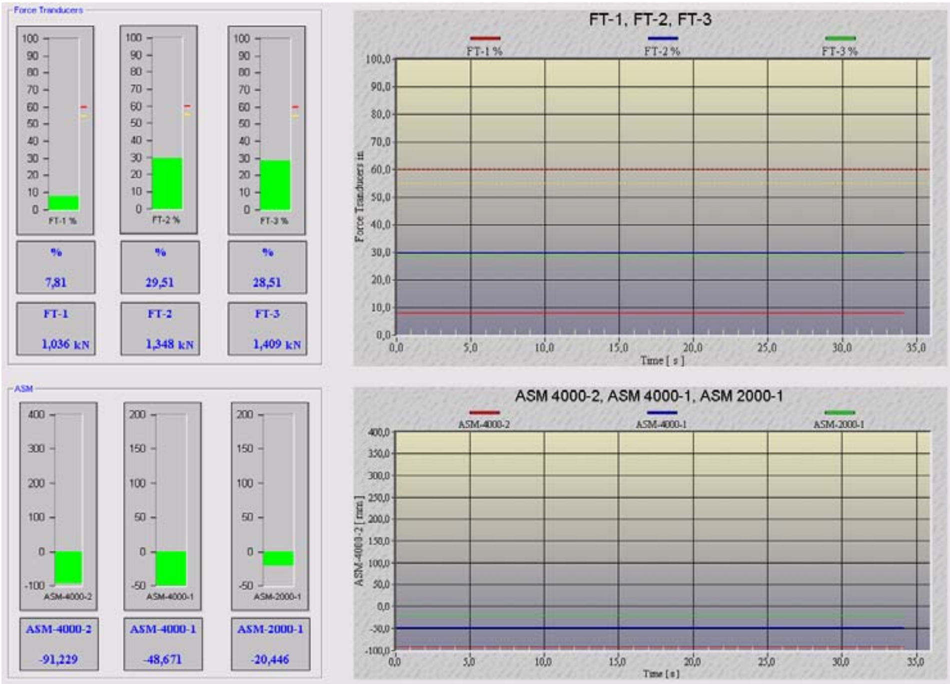

Figure 4.3. Visual template used during test.

The crucial measurement is the forces, and, since the forces with respect to the ultimate loads are to follow each other, this is what is presented during a test at all times. During a pull, the global vertical deflection is shown as well at ASM-4000-2, ASM-4000-1 and ASM-2000-1 (22m, 16m and 10m respectively).

4.4 Quick View

Since we have 240 sensors, it is not possible to monitor all of them at the same time. Consequently, the most important ones are selected and monitored in the real-time.

However, after the measurement is done, it is possible to study any sensor(s) in a 'quick view', where one or several channels can be selected to show the data.
In Figure 4.4, an example of a Quick View Diagram is given. The sensors to be shown are selected in the list to the left. To the right the measurement graphs for the chosen sensors are shown immediately.
The Graph below shows the Forces at load point 2, as a function of Point index (the measurement in the order they are collected).

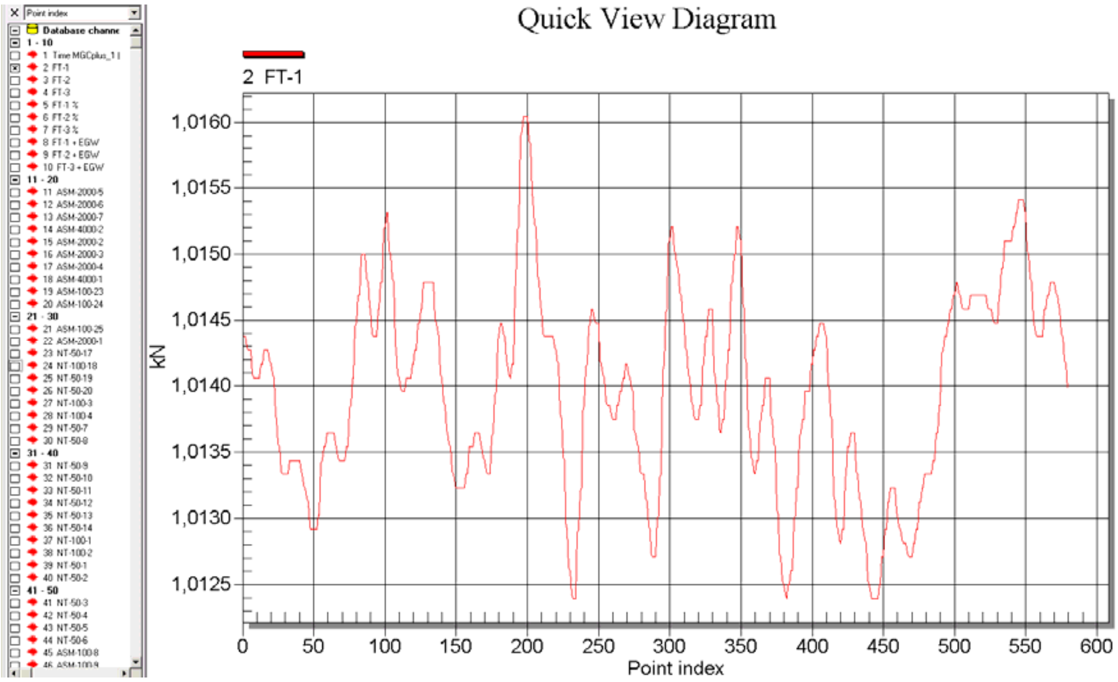

Figure 4.4. Quick view diagram showing the Forces at load point 2, as a function of Point index

4.5 Data post processing

In order to post process the data obtained from full-scale tests, Graph Tool software was used. During the test, all the data was gathered by DAQ system, with the time-delta between each measurement dt=20 ms. However, during the post processing, in order to distribute the results, 30 load increments were used. The blade is preloaded to approximate 30% of the Risø load. Here, the measurement equipment apart from the forces' measurement is set to zero. The graph in Figure 4.5 shows that the deflection measurement is set to zero at the local bending moment of 180kNm (16m section) which is the local bending moment when the measurement start. As visible in Figure 4.5, the deflection is a linear function of the bending moment, so the deflection for the preloading can be found as the value above the horizontal axis where the graph is elongating to zero bending moment.
The total values then become the sum of the values read in the graphs and the values read up to the cross-section.

As an example, the total deflection for ASM 2000-2 at 16m can be found as:
The value deflection above the horizontal axis: a = 14.5mm
below the horizontal axis: b = 12.7mm
gives the total deflection: d = a + b = 14.5 + 12.7 = 27.2mm

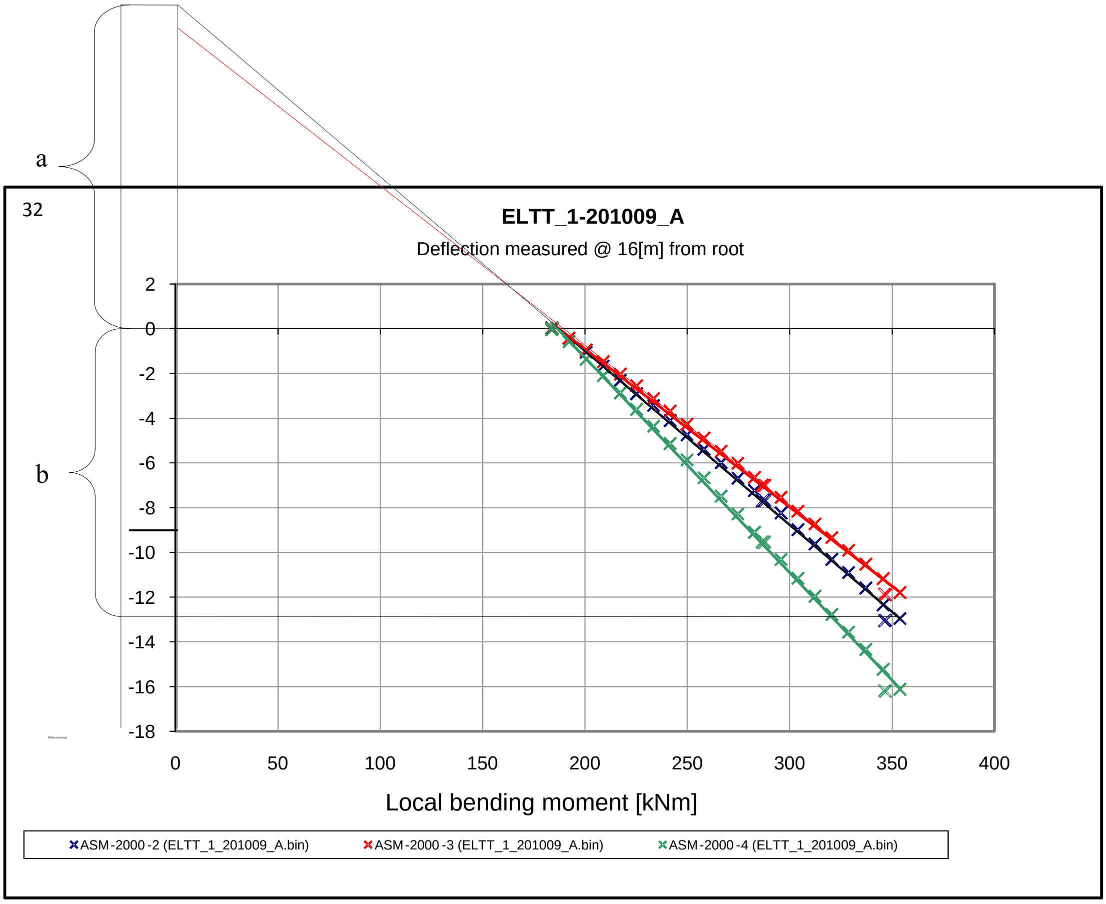

Figure 4.5. Measured deflection as a function of the local bending moment showing how to read the total deflection

5. Digital Image Correlation (DIC)

The following is a short description of how the Digital Image Correlation system was applied in this test and which results were obtained by analyzing the data. All the measuring results can be funded in the Appendix G.

An advanced 3D Digital Image Correlation (DIC), ARAMIS 4M large scale system, was applied in this work. The system records the surface of an object throughout the entire load history using two CCD cameras. The digital images are used to measure the full-field 3D displacements and surface strains of an object by digital image processing. As an aid for the digital image processing, a speckle pattern (typically black spray paint on a white background) has to be applied to the surface of the object. As the system measures a full-field displacements and surface strains, the system is highly suitable for validating FE calculations. Since the surfaces of the blade section are of a considerable size, the random speckle pattern could not be created by simply spraying small dots of black paint on the surface using an aerosol can. A harsher pattern was needed, and the best result was obtained by applying dim black spots of a size around 6 x 6 mm on the surface using a specially designed tool, which can be seen in Figure 5.1.

The system is also well suited for analyzing the global and local response of the wind turbine blade structure. The global response was in this work analyzed by applying a least squares algorithm, which fits a plane through each, deformed cross section, and defines a single set of displacements and rotations (three displacements and rotations) per cross section. This contains valuable information about the beam-like properties (stiffness, location of natural axis and shear centre etc.) of the blade.

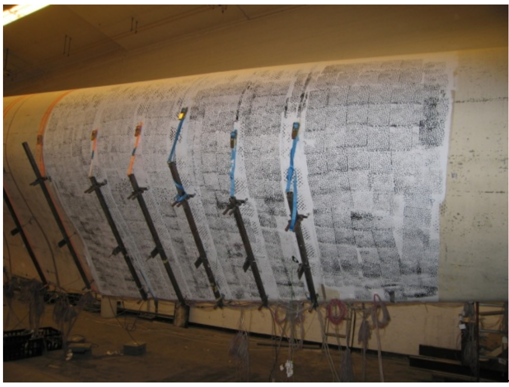

Figure 5.1 Measuring area (speckle pattern)

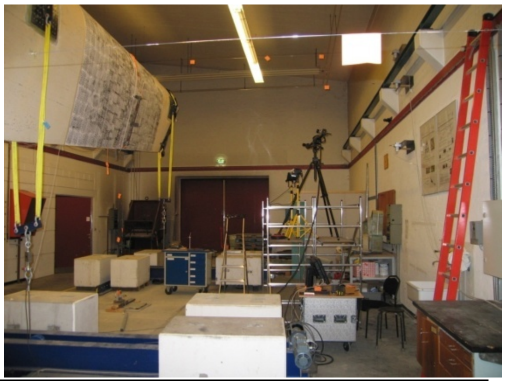

Figure 5.2 Camera setup

5.1 Measuring precision (verification of DIC-system)

The system is then used to measure large scale areas (volumes ~ 3m*3m*3m), and tests have shown an out-of-plane precision within 0.1mm and an in-plane precision which is much better.

To verifier this out-of-plan precision, a comparison was made between the measured local deformations performed with a traditional displacement transducer (called NT), described in Chapter 3.3.2 and the DIC -measurement applying the calculation method illustrated in Figure 5.3. The measurement performed with the displacement transducer is the displacement perpendicular to the panels' surface. To compare the measurements it is necessary to calculate the same distance from the results from DIC system which measure the total displacement of the blade. The method used determines the perpendicular distance from the linear curve, which intercept the two deformed points D* and B* to the location of the deformed point C* (see Figure 5.3b and Eq 1.)

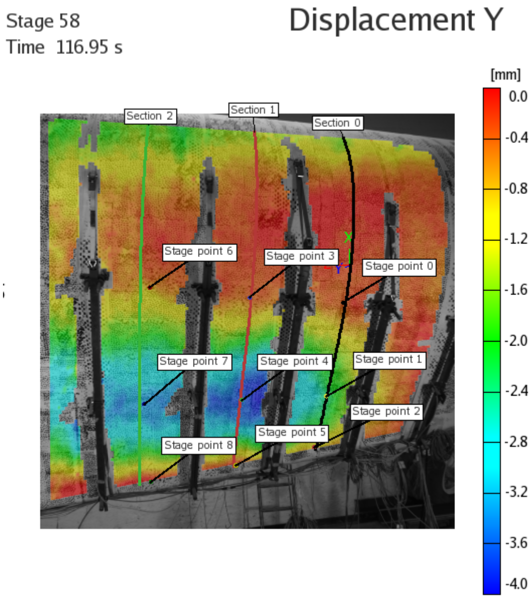

Fig. a

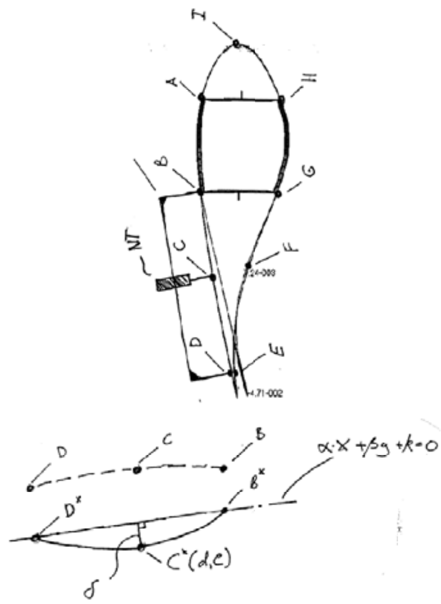

Fig. b

Figure 5.3. DIC-measurement and verification method

If the linear curve is defined based on the two deformed measuring points the perpendicular distance can be determined as:

$$\delta = \frac{\alpha \cdot d + \beta \cdot e + k}{\sqrt{(\alpha^2 + \beta^2)}} \qquad (1)$$

The agreement between the DIC- and NT-measurement during the entire load history is excellent, as shown in Figure 5.4 . It can be concluded that the precision of DIC equipment with the setup used during these tests are usable for analyzing even limited local deformation.

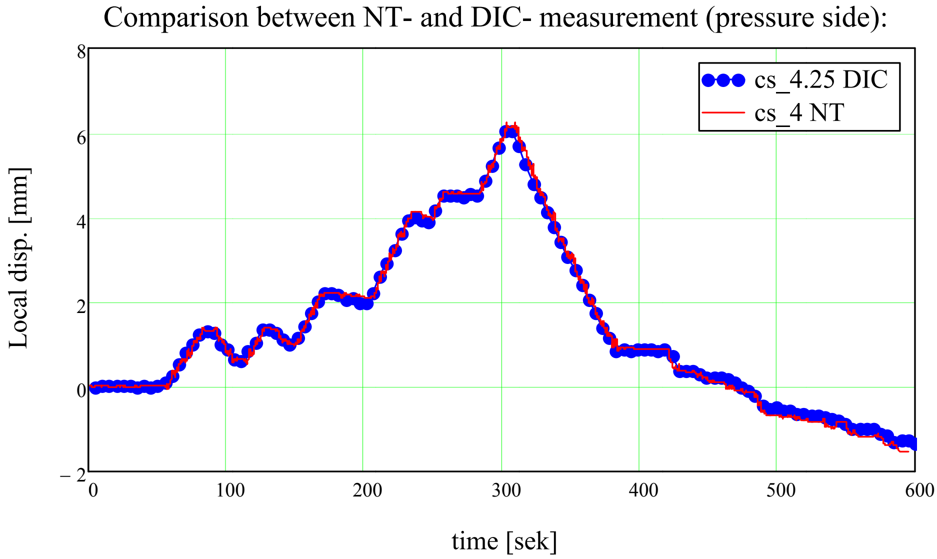

Figure 5.4. Verification of DIC-measurement

5.2 DIC-data (measuring results)

Three measuring areas on the suction and pressure side of the blade were chosen for analyzing. One of these measuring areas is presented in Figure 5.5.

Each measuring area/surface was divided into 3 cross sections, from which the displacements were obtained. Nine stage/measuring points were added per cross section for easy and fast comparison with mechanical measurements (NT measurements).

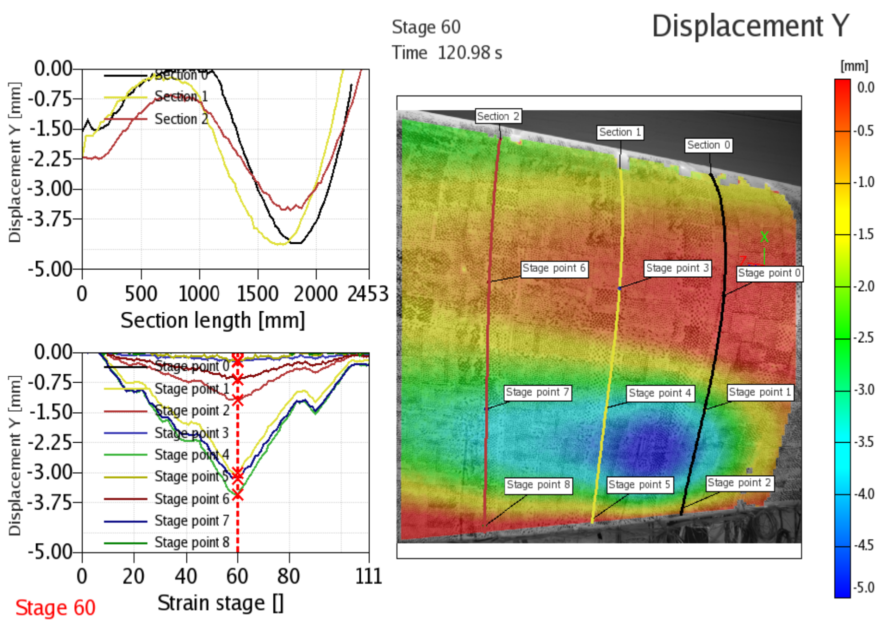

Figure 5.5. Typical measuring area on the blade (showing 3 cross sections and 9 stage points)

5.3 Global deformation

Each of these cross sections consists of a large number of measuring points, and in order to simplify the analysis of the measured data, a least squares algorithm was applied to determine a single set of displacements and rotations (three displacements and rotations) for each cross section. The procedure effectively simplifies the comparison of experimental and numerical results, as only a single set of displacements and rotations per cross section can be compared.
The least squares algorithm consists of the following three steps:

- Computation of displacements (u_x, u_y and u_z)
- Computation of twist angle (r_z)
- Computation of bending slopes (r_x and r_y)

The three displacements were calculated as average values, meaning that all the relative nodal/point displacements are summed up and divided by the number of nodes/points. (Δx, Δy and Δz = relative displacements). This is illustrated in Eq. 2.

$$u_x = \frac{\sum_{i=1}^{n} \Delta x_i}{n}, u_y = \frac{\sum_{i=1}^{n} \Delta y_i}{n}, u_z = \frac{\sum_{i=1}^{n} \Delta z_i}{n} \qquad (2)$$

The cross sectional rotation about the z-axis (twist-angle (r_z)) is determined by fitting a linear least squares regressions curve through the deformed x-coordinates and the relative displacements in the y-direction ($dy = y_{deformed} - y_{undeformed}$). The slope of the curve is then equal to the twist-angle. The curve is given as:

$$y(x) = r_z \cdot x + c \qquad (3)$$

The line is fitted by determining the r_z and c values which minimize the squared residuals (vertical distance between the points and the line).
The theory of linear least squares regression is shown in Eq. 3 (note that dy is equal to the relative displacement in the y-direction):

$$P = \begin{bmatrix} 1 & x_1 \\ 1 & x_2 \\ 1 & .. \\ 1 & x_n \end{bmatrix}, \begin{pmatrix} c \\ r_z \end{pmatrix} = (P^T \cdot P)^{-1} \cdot P^T \cdot \begin{pmatrix} dy_1 \\ dy_2 \\ .. \\ dy_n \end{pmatrix} \qquad (4)$$

The rotations about the x- and y-axis are determined by fitting a linear multiple regression plane through the deformed cross section given as:

$$z(x, y) = b + r_y \cdot x + r_x \cdot y \qquad (5)$$

The two variables x and y describe a plane in the three-dimensional (x,y,z) space. r_y and r_x are the rotations about the y- and x-axis and b is the intersection with the z-axis. In order to make the plane correlate as closely as possible to the measured points in the aggregate, the values of r_y, r_x and b that minimize the sum of the squared residuals are found. The theory of multiple regressions is shown in Eq. 5.

$$F = \begin{bmatrix} 1 & x_1 & y_1 \\ 1 & x_2 & y_2 \\ 1 & .. & .. \\ 1 & x_n & y_n \end{bmatrix}, \begin{pmatrix} b \\ r_y \\ r_x \end{pmatrix} = (F^T \cdot F)^{-1} \cdot F^T \cdot \begin{pmatrix} dz_1 \\ dz_2 \\ .. \\ dz_n \end{pmatrix} \qquad (6)$$

The global response of a measurement conducted at the region 20-23 meter from the root section is illustrated below. The global response is determined based on the least squares algorithm.

Cross section [m]	Disp. Ux [mm]	Disp. Uy [mm]	Disp. Uz [mm]	Rot. Rx [deg]	Rot. Ry [deg]	Rot. Rz [deg]
20.50	-135.9536	-20.4531	7.0808	0.0418	0.6619	0.1693
21.80	-149.2300	-21.6431	7.7095	0.0413	0.6866	0.1658
22.50	-159.9864	-22.4290	8.2046	0.0298	0.7075	0.1604

Figure 5.6. Results of the least squares algorithm (global response)

5.4 Local deformation

Local cross sectional deformations are analyzed by performing a “rigid body movement” transformation of the measured data. This transformation is applied by determining the 3 displacements and 3 rotations of a “stiff” part of the structure and then subtracting these values from the deformed cross sectional data. The displacements and rotations are determined by applying the least squares algorithm, described above. This simplifies the analyses of local deformation of the soft sandwich panels, the trailing edge, the cap etc.

Presented below (see Figure 5.7) is the local deformation of the soft sandwich panels on the pressure side near the adhesive bound in the trailing edge. The “rigid body movement transformation” is in this case applied by determining the displacements and rotations based on measuring points located of the stiff cap (indicated with the two pink circles).

As illustrated in the graph, the unreformed and transformed deformed measuring points located on the cap, is plotted directly on top of each other, which indicate that the transformation works.

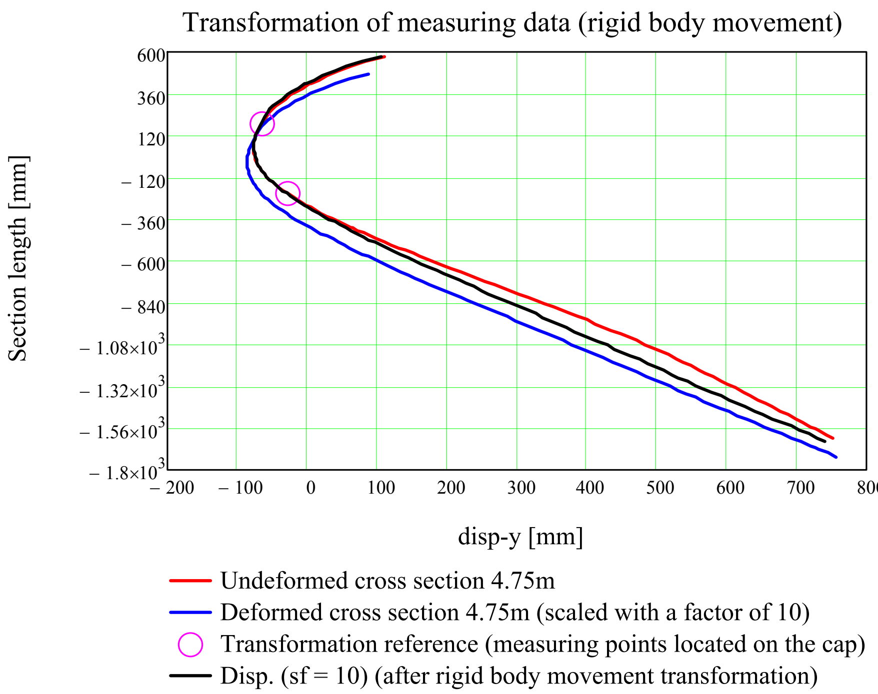

Figure 5.7. Rigid body movement transformation of measuring points

The local deformation of the panels can easily be analyzed after the "rigid body movement transformation" is applied. Depicted in Figure 5.8 is the local deformation of the three cross sections in the region 3-5 meter from the root section. A considerable local out-of-plan response on pressure side of the blade is observed under the edgewise loading. The soft panel near the adhesive bound makes an outwards bulge shape, which is also observed in previous full scale tests and numerical analyzes.

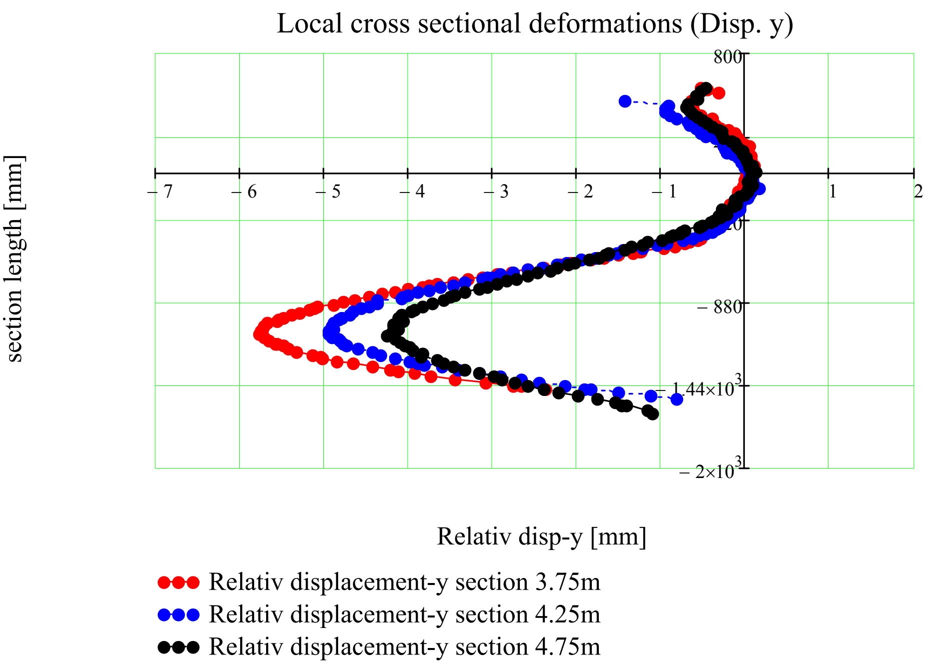

Figure 5.8. Local cross sectional deformation

6. Summary and conclusion

Test has been carried out on a truncated 34m blade from SSP technology A/S, and the LTT tests were carried out up to 60% of extreme load, corresponding to approximately 75% of the certification load. The examination during test and of the results from these tests showed no sign of failure of the blade.
The new invented load application system using anchor plate was used for the tests and this solution was very successful as the blade had a more realistic deformation behavior than when using the traditional loading clamps made by wood.

The global deflection was compared with result from FEM analyses and a previous test to validate the method the gravity load was handled. The agreement was fine especially the comparison between the 2 tests were good.
The test measurement covered all failure mode of the blade and gave a good impression as to where the failure in the blade would occur when the blade was exposed for extreme load.

The comparison between the results obtained with the DIC equipment and the measurements performed with traditional displacement transducers proved that the agreement between the two measuring methods were excellent. The global and local response of the blade measured with the DIC equipment was studied by applying a least squares algorithm. This algorithm determines a beam like response (3 displacements and 3 rotations), which can be used to subtracted the global response from a measuring area making it possible to study the local deformation.

This data report contains the raw data from the measurement. No data treatment of this data has been performed, and more reports will be published explaining the result from this data.

7. References

[1] Jensen, F. M., Branner, K., Nielsen, P. H., Berring, P., Antvorskov, T. S., Nielsen, M., Lund, B., Jensen, C., Reffs, J. H., Nielsen, R. F., Jensen, P. H., McGugan, M., Borum, K., Hansen, R. S., Skamris, C., Sørensen, F., Nielsen, R. S.,Laursen, J. H., Klein, M., Morris, A., Gwayne, A., Stang, H., Wedel-Heinen, J.,Dear, J. P., Puri, A., Fergusson, A. "*Full-scale Test of a SSP34m box girder 1 –Data Report*". Risø-R-RIS88(EN). (March 2008)

[2] Jensen, F.M. , Branner, K., Nielsen., P. H, Berring, P., Antvorskov, T. S., Nielsen, M., Reffs, J.H., Jensen, P.H, McGugan, M., Skamris, C., Sørensen, F.,Nielsen, R.S., Laursen, J.H., Klein, M., Morris, A., Stang, H., Wedel-Heinen, J.,Dear, J.P., Puri, A., Fergusson, A. "*Full-scale Test of a SSP34m box girder 2 –Data Report*". Risø-R-1622(EN) in progress. (April 2008)

[3] Jensen, F. M. *"Ultimate strength of a large wind turbine blade"*, Risø-PhD-34(EN) (May 2008)

[4] Jensen, F. M., Falzon, B.G., Ankersen, J., Stang, H. *"Structural testing and numerical simulation of a 34m composite wind turbine blade",* Composite Structures 76, 2006

[5] Thomsen, C. L., Eisenberg, Y. P. *"Blade Test SSP34#2. Edgewise and Flapwise Final Static test"* Risø National Laboratory, Denmark November 2003

[6] Thomsen C. L., Jørgensen E. R., Borum K. K., McGugan M., Debel C. P., Sørensen B., Jensen F. M. *"V52 Statisk Styrke"*. Risø-I-Report. (April 2003)

List of appendices

A List with measurement equipment and its placement **Page 2**

Strain gauges positions AED sections + global
Strain gauges positions main section
Strain gauge positions other groups
Section on the blade with measurement equipment
Signs for ASM movement
Group with deflection measurements

B Data presented by Graph tool **Page 18**

Measured strain vs. bending moment

B1 Measurements obtained from strain gauges in:
Main section in test ELTT_1-291009_A

B2 Measurements obtained from strain gauges in:
Global section in test ELTT_2-101109_A

B3 Measurements obtained from strain gauges in:
Other groups section in test ELTT_3-041109_A

B4 The deflections measurements vs. local bending moment

Deflections measured in test ELTT_1-291009_A

B5 Deflections measured in test ELTT_5-181109_A
by:
NT-50-17
NT-100-18
NT-50-19
NT-50-20

B6 The flapwise global deflections measurements vs. root bending moment obtained in test ELTT_1-291009_A

C Load comparison **Page 69**

D Test plan **Page 74**

E Measurement equipment **Page 79**

F Calibration of the test equipment **Page 87**

G DIC Result **Page 93**

A List with measurement equipment and its placement

A List with measurement equipment and its placement

Strain gauges positions AED Section + Global

		Group A-Global				Group B-TE-Panels						Group C-Shear Webs				Group D-Caps	
		A	As	Ap	H	Bs	Bp	Ds	Dp	Es	Ep	Ls	Mp	Ns	Op	Fp	Fs
Section					LE	SS_TE	PS_TE	PS_MID	SS_MID			SS_CAP	PS_CAP	SS_CAP	PS_CAP	PS_CAP	SS_CAP
3 m	Outer	SG1UD						SG67Bx	SG69Bx	SG111Bx	SG113Bx					SG201UD	SG203UD
	Inner	SG2UD						SG68Bx	SG70Bx	SG112Bx		SG151Tx	SG153Tx	SG152Tx	SG158Tx	SG202UD	SG204UD
3.5 m	Outer								SG251Bx		SG253Bx						
	Inner								SG250Bx								
3.75 m	Outer								SG303Bx								
	Inner								SG304Bx								
4 m	Outer	SG3Bx			SG41Bx			SG71Tx	SG73Tx	SG115Bx	SG117Bx	SG161Tx	SG163Tx			SG205UD	SG207UD
	Inner	SG4Bx						SG72Tx	SG74Tx	SG116Bx		SG162Tx	SG164Tx	SG166Tx	SG168Tx	SG206UD	SG208UD
4.25 m	Outer								SG307Bx								
	Inner								SG308Bx								
4.5 m	Outer								SG255Bx		SG257Bx						
	Inner								SG254Bx		SG256Bx						
4.75 m	Outer								SG311Bx								
	Inner								SG312Bx								
5 m	Outer	SG5UD						SG75Bx	SG77Bx	SG119Bx	SG121Bx					SG209UD	SG211UD
	Inner	SG6UD						SG76Bx	SG78Bx	SG120Bx	SG122Bx					SG210UD	SG212UD
5.25 m	Outer								SG315Bx								
	Inner								SG316Bx								
6 m	Outer	SG7UD						SG79Bx	SG81Bx	SG123Bx	SG125Bx					SG213UD	SG215UD
	Inner	SG8UD						SG80Bx	SG82Bx	SG124Bx	SG126Bx					SG214UD	SG216UD
7 m	Outer		SG9UD	SG11UD	SG43Bx	SG51Bx	SG53Bx	SG83Tx	SG85Tx	SG127Bx	SG129Bx	SG171Tx	SG173Tx			SG217Bx	SG219Bx
	Inner					SG52Bx	SG54Bx	SG84Tx	SG86Tx	SG128Bx	SG130Bx	SG172Tx	SG174Tx	SG176Tx	SG178Tx	SG218Bx	SG220Bx
7.5 m	Outer		SG297UD	SG299UD													
	Inner																
8 m	Outer		SG13UD	SG15UD		SG55Bx	SG57Bx	SG87Bx	SG89Bx	SG131Bx	SG133Bx					SG221UD	SG223UD
	Inner					SG56Bx	SG58Bx	SG88Bx	SG90Bx	SG132Bx	SG134Bx					SG222UD	SG224UD
8.5 m	Outer		SG261UD	SG263UD													
	Inner																
9 m	Outer		SG17UD	SG19UD		SG59Bx	SG61Bx	SG91Bx	SG93Bx	SG135Bx	SG137Bx					SG225UD	SG227UD
	Inner					SG60Bx	SG62Bx	SG92Bx	SG94Bx	SG136Bx	SG138Bx					SG226UD	SG228UD
9.5 m	Outer		SG265UD	SG267UD													
	Inner																
10 m	Outer		SG21UD	SG23UD	SG45Bx	SG63Bx	SG65Bx	SG95Tx	SG97Tx	SG139Bx	SG141Bx	SG181Tx	SG183Tx			SG229Bx	SG231Bx
	Inner					SG64Bx	SG66Bx	SG96Tx	SG98Tx	SG140Bx	SG142Bx	SG182Tx	SG184Tx	SG186Tx	SG188Tx	SG230Bx	SG232Bx
10.5 m	Outer		SG269UD	SG271UD													
	Inner																
11 m	Outer		SG25UD	SG27UD												SG233UD	SG235UD
	Inner															SG234UD	SG236UD
11.5 m	Outer		SG273UD	SG275UD													
	Inner																
12 m	Outer		SG29UD	SG31UD												SG237UD	SG239UD
	Inner															SG238UD	SG240UD
12.5 m	Outer		SG277UD	SG279UD													
	Inner																
13.5 m	Outer		SG281UD	SG283UD													
	Inner																
14.5 m	Outer		SG285UD	SG287UD													
	Inner																
15.5 m	Outer		SG289UD	SG291UD													
	Inner																
16 m	Outer		SG33UD	SG35UD	SG47Bx			SG99Bx	SG101Bx							SG241UD	SG243UD
	Inner																
22 m	Outer		SG37UD	SG39UD	SG49Bx			SG103Bx	SG105Bx							SG245UD	SG247UD

A List with measurement equipment and its placement

Strain gauges positions Main section

		Group A-Global				Group B-TE-Panels						Group C-Shear Webs				Group D-Caps	
		A	As	Ap	H	Bs	Bp	Ds	Dp	Es	Ep	Ls	Mp	Ns	Op	Fp	Fs
Section					LE	SS_TE	PS_TE	PS_MID	SS_MID			SS_CAP	PS_CAP	SS_CAP	PS_CAP	PS_CAP	SS_CAP
3 m	Outer	SG1UD						SG67Bx	SG69Bx	SG111Bx	SG113Bx					SG201UD	SG203UD
	Inner	SG2UD						SG68Bx	SG70Bx	SG112Bx		SG151Tx	SG153Tx	SG152Tx	SG158Tx	SG202UD	SG204UD
3.5 m	Outer								SG251Bx		SG253Bx						
	Inner								SG250Bx								
3.75 m	Outer								SG303Bx								
	Inner								SG304Bx								
4 m	Outer	SG3Bx			SG41Bx			SG71Tx	SG73Tx	SG115Bx	SG117Bx	SG161Tx	SG163Tx			SG205UD	SG207UD
	Inner	SG4Bx						SG72Tx	SG74Tx	SG116Bx		SG162Tx	SG164Tx	SG166Tx	SG168Tx	SG206UD	SG208UD
4.25 m	Outer								SG307Bx								
	Inner								SG308Bx								
4.5 m	Outer								SG255Bx		SG257Bx						
	Inner								SG254Bx		SG256Bx						
4.75 m	Outer								SG311Bx								
	Inner								SG312Bx								
5 m	Outer	SG5UD						SG75Bx	SG77Bx	SG119Bx	SG121Bx					SG209UD	SG211UD
	Inner	SG6UD						SG76Bx	SG78Bx	SG120Bx	SG122Bx					SG210UD	SG212UD
5.25 m	Outer								SG315Bx								
	Inner								SG316Bx								
6 m	Outer	SG7UD						SG79Bx	SG81Bx	SG123Bx	SG125Bx					SG213UD	SG215UD
	Inner	SG8UD						SG80Bx	SG82Bx	SG124Bx	SG126Bx					SG214UD	SG216UD
7 m	Outer		SG9UD	SG11UD	SG43Bx	SG51Bx	SG53Bx	SG83Tx	SG85Tx	SG127Bx	SG129Bx	SG171Tx	SG173Tx			SG217Bx	SG219Bx
	Inner					SG52Bx	SG54Bx	SG84Tx	SG86Tx	SG128Bx	SG130Bx	SG172Tx	SG174Tx	SG176Tx	SG178Tx	SG218Bx	SG220Bx
7.5 m	Outer		SG297UD	SG299UD													
	Inner																
8 m	Outer		SG13UD	SG15UD		SG55Bx	SG57Bx	SG87Bx	SG89Bx	SG131Bx	SG133Bx					SG221UD	SG223UD
	Inner					SG56Bx	SG58Bx	SG88Bx	SG90Bx	SG132Bx	SG134Bx					SG222UD	SG224UD
8.5 m	Outer		SG261UD	SG263UD													
	Inner																
9 m	Outer		SG17UD	SG19UD		SG59Bx	SG61Bx	SG91Bx	SG93Bx	SG135Bx	SG137Bx					SG225UD	SG227UD
	Inner					SG60Bx	SG62Bx	SG92Bx	SG94Bx	SG136Bx	SG138Bx					SG226UD	SG228UD
9.5 m	Outer		SG265UD	SG267UD													
	Inner																
10 m	Outer		SG21UD	SG23UD	SG45Bx	SG63Bx	SG65Bx	SG95Tx	SG97Tx	SG139Bx	SG141Bx	SG181Tx	SG183Tx			SG229Bx	SG231Bx
	Inner					SG64Bx	SG66Bx	SG96Tx	SG98Tx	SG140Bx	SG142Bx	SG182Tx	SG184Tx	SG186Tx	SG188Tx	SG230Bx	SG232Bx
10.5 m	Outer		SG269UD	SG271UD													
	Inner																
11 m	Outer		SG25UD	SG27UD												SG233UD	SG235UD
	Inner															SG234UD	SG236UD
11.5 m	Outer		SG273UD	SG275UD													
	Inner																
12 m	Outer		SG29UD	SG31UD												SG237UD	SG239UD
	Inner															SG238UD	SG240UD
12.5 m	Outer		SG277UD	SG279UD													
	Inner																
13.5 m	Outer		SG281UD	SG283UD													
	Inner																
14.5 m	Outer		SG285UD	SG287UD													
	Inner																
15.5 m	Outer		SG289UD	SG291UD													
	Inner																
16 m	Outer		SG33UD	SG35UD	SG47Bx			SG99Bx	SG101Bx							SG241UD	SG243UD
	Inner																
22 m	Outer		SG37UD	SG39UD	SG49Bx			SG103Bx	SG105Bx							SG245UD	SG247UD
	Inner																

A List with measurement equipment and its placement

Strain gauges positions other groups

		Group A-Global				Group B-TE-Panels						Group C-Shear Webs				Group D-Caps	
		A	As	Ap	H	Bs	Bp	Ds	Dp	Es	Ep	Ls	Mp	Ns	Op	Fp	Fs
Section					LE	SS_TE	PS_TE	PS_MID	SS_MID			SS_CAP	PS_CAP	SS_CAP	PS_CAP	PS_CAP	SS_CAP
3 m	Outer	SG1UD						SG67Bx	SG69Bx	SG111Bx	SG113Bx					SG201UD	SG203UD
	Inner	SG2UD						SG68Bx	SG70Bx	SG112Bx		SG151Tx	SG153Tx	SG152Tx	SG158Tx	SG202UD	SG204UD
3.5 m	Outer								SG251Bx		SG253Bx						
	Inner								SG250Bx								
3.75 m	Outer								SG303Bx								
	Inner								SG304Bx								
4 m	Outer	SG3Bx			SG41Bx			SG71Tx	SG73Tx	SG115Bx	SG117Bx	SG161Tx	SG163Tx			SG205UD	SG207UD
	Inner	SG4Bx						SG72Tx	SG74Tx	SG116Bx		SG162Tx	SG164Tx	SG166Tx	SG168Tx	SG206UD	SG208UD
4.25 m	Outer								SG307Bx								
	Inner								SG308Bx								
4.5 m	Outer								SG255Bx		SG257Bx						
	Inner								SG254Bx		SG256Bx						
4.75 m	Outer								SG311Bx								
	Inner								SG312Bx								
5 m	Outer	SG5UD						SG75Bx	SG77Bx	SG119Bx	SG121Bx					SG209UD	SG211UD
	Inner	SG6UD						SG76Bx	SG78Bx	SG120Bx	SG122Bx					SG210UD	SG212UD
5.25 m	Outer								SG315Bx								
	Inner								SG316Bx								
6 m	Outer	SG7UD						SG79Bx	SG81Bx	SG123Bx	SG125Bx					SG213UD	SG215UD
	Inner	SG8UD						SG80Bx	SG82Bx	SG124Bx	SG126Bx					SG214UD	SG216UD
7 m	Outer		SG9UD	SG11UD	SG43Bx	SG51Bx	SG53Bx	SG83Tx	SG85Tx	SG127Bx	SG129Bx	SG171Tx	SG173Tx			SG217Bx	SG219Bx
	Inner					SG52Bx	SG54Bx	SG84Tx	SG86Tx	SG128Bx	SG130Bx	SG172Tx	SG174Tx	SG176Tx	SG178Tx	SG218Bx	SG220Bx
7.5 m	Outer		SG297UD	SG299UD													
	Inner																
8 m	Outer		SG13UD	SG15UD		SG55Bx	SG57Bx	SG87Bx	SG89Bx	SG131Bx	SG133Bx					SG221UD	SG223UD
	Inner					SG56Bx	SG58Bx	SG88Bx	SG90Bx	SG132Bx	SG134Bx					SG222UD	SG224UD
8.5 m	Outer		SG261UD	SG263UD													
	Inner																
9 m	Outer		SG17UD	SG19UD		SG59Bx	SG61Bx	SG91Bx	SG93Bx	SG135Bx	SG137Bx					SG225UD	SG227UD
	Inner					SG60Bx	SG62Bx	SG92Bx	SG94Bx	SG136Bx	SG138Bx					SG226UD	SG228UD
9.5 m	Outer		SG265UD	SG267UD													
	Inner																
10 m	Outer		SG21UD	SG23UD	SG45Bx	SG63Bx	SG65Bx	SG95Tx	SG97Tx	SG139Bx	SG141Bx	SG181Tx	SG183Tx			SG229Bx	SG231Bx
	Inner					SG64Bx	SG66Bx	SG96Tx	SG98Tx	SG140Bx	SG142Bx	SG182Tx	SG184Tx	SG186Tx	SG188Tx	SG230Bx	SG232Bx
10.5 m	Outer		SG269UD	SG271UD													
	Inner																
11 m	Outer		SG25UD	SG27UD												SG233UD	SG235UD
	Inner															SG234UD	SG236UD
11.5 m	Outer		SG273UD	SG275UD													
	Inner																
12 m	Outer		SG29UD	SG31UD												SG237UD	SG239UD
	Inner															SG238UD	SG240UD
12.5 m	Outer		SG277UD	SG279UD													
	Inner																
13.5 m	Outer		SG281UD	SG283UD													
	Inner																
14.5 m	Outer		SG285UD	SG287UD													
	Inner																
15.5 m	Outer		SG289UD	SG291UD													
	Inner																
16 m	Outer		SG33UD	SG35UD	SG47Bx			SG99Bx	SG101Bx							SG241UD	SG243UD
	Inner																
22 m	Outer		SG37UD	SG39UD	SG49Bx			SG103Bx	SG105Bx							SG245UD	SG247UD
	Inner																

A List with measurement equipment and its placement

Strain gauges positions

		Group A-Global				Group B-TE-Shells						Group C-Shear Webs				Group D-Caps		No of chanels				
		A	As	Ap	H	Bs	Bp	Ds	Dp	Es	Ep	Ls	Mp	Ns	Op	Fp	Fs	A	B	C	D	SUM
Section					LE	SS_TE	PS_TE	PS_MID	SS_MID			SS_CAP	PS_CAP	SS_CAP	PS_CAP	PS_CAP	SS_CAP					
3 m	Outer	SG1UD						SG67Bx	SG69Bx	SG111Bx	SG113Bx					SG201UD	SG203UD	2	14	12	4	32
	Inner	SG2UD						SG68Bx	SG70Bx	SG112Bx		SG151Tx	SG153Tx	SG152Tx	SG158Tx	SG202UD	SG204UD					
3.5 m	Outer								SG251Bx		SG253Bx							0	6	0	0	6
	Inner								SG250Bx													
3.75 m	Outer								SG303Bx													
	Inner								SG304Bx													
4 m	Outer	SG3Bx			SG41Bx			SG71Tx	SG73Tx	SG115Bx	SG117Bx	SG161Tx	SG163Tx			SG205UD	SG207UD	6	18	18	4	46
	Inner	SG4Bx						SG72Tx	SG74Tx	SG116Bx		SG162Tx	SG164Tx	SG166Tx	SG168Tx	SG206UD	SG208UD					
4.25 m	Outer								SG307Bx													
	Inner								SG308Bx													
4.5 m	Outer								SG255Bx		SG257Bx							0	8	0	0	8
	Inner								SG254Bx		SG256Bx											
4.75 m	Outer								SG311Bx													
	Inner								SG312Bx													
5 m	Outer	SG5UD						SG75Bx	SG77Bx	SG119Bx	SG121Bx					SG209UD	SG211UD	2	16	0	4	22
	Inner	SG6UD						SG76Bx	SG78Bx	SG120Bx	SG122Bx					SG210UD	SG212UD					
5.25 m	Outer								SG315Bx													
	Inner								SG316Bx													
6 m	Outer	SG7UD						SG79Bx	SG81Bx	SG123Bx	SG125Bx					SG213UD	SG215UD	2	16	0	4	22
	Inner	SG8UD						SG80Bx	SG82Bx	SG124Bx	SG126Bx					SG214UD	SG216UD					
7 m	Outer		SG9UD	SG11UD	SG43Bx	SG51Bx	SG53Bx	SG83Tx	SG85Tx	SG127Bx	SG129Bx	SG171Tx	SG173Tx			SG217Bx	SG219Bx	4	28	18	8	58
	Inner					SG52Bx	SG54Bx	SG84Tx	SG86Tx	SG128Bx	SG130Bx	SG172Tx	SG174Tx	SG176Tx	SG178Tx	SG218Bx	SG220Bx					
7.5 m	Outer		SG297UD	SG299UD														2				2
	Inner																					
8 m	Outer		SG13UD	SG15UD		SG55Bx	SG57Bx	SG87Bx	SG89Bx	SG131Bx	SG133Bx					SG221UD	SG223UD	2	24	0	4	30
	Inner					SG56Bx	SG58Bx	SG88Bx	SG90Bx	SG132Bx	SG134Bx					SG222UD	SG224UD					
8.5 m	Outer		SG261UD	SG263UD														2				2
	Inner																					
9 m	Outer		SG17UD	SG19UD		SG59Bx	SG61Bx	SG91Bx	SG93Bx	SG135Bx	SG137Bx					SG225UD	SG227UD	2	24	0	4	30
	Inner					SG60Bx	SG62Bx	SG92Bx	SG94Bx	SG136Bx	SG138Bx					SG226UD	SG228UD					
9.5 m	Outer		SG265UD	SG267UD														2				2
	Inner																					
10 m	Outer		SG21UD	SG23UD	SG45Bx	SG63Bx	SG65Bx	SG95Tx	SG97Tx	SG139Bx	SG141Bx	SG181Tx	SG183Tx			SG229Bx	SG231Bx	4	28	18	8	58
	Inner					SG64Bx	SG66Bx	SG96Tx	SG98Tx	SG140Bx	SG142Bx	SG182Tx	SG184Tx	SG186Tx	SG188Tx	SG230Bx	SG232Bx					
10.5 m	Outer		SG269UD	SG271UD														2				2
	Inner																					
11 m	Outer		SG25UD	SG27UD												SG233UD	SG235UD	2	0	0	4	6
	Inner															SG234UD	SG236UD					
11.5 m	Outer		SG273UD	SG275UD														2				2
	Inner																					
12 m	Outer		SG29UD	SG31UD												SG237UD	SG239UD	2	0	0	4	6
	Inner															SG238UD	SG240UD					
12.5 m	Outer		SG277UD	SG279UD														2				2
	Inner																					
13.5 m	Outer		SG281UD	SG283UD														2				2
	Inner																					
14.5 m	Outer		SG285UD	SG287UD														2				2
	Inner																					
15.5 m	Outer		SG289UD	SG291UD														2				2
	Inner																					
16 m	Outer		SG33UD	SG35UD	SG47Bx			SG99Bx	SG101Bx							SG241UD	SG243UD	4	4	0	2	10
	Inner																					
22 m	Outer		SG37UD	SG39UD	SG49Bx			SG103Bx	SG105Bx							SG245UD	SG247UD	4	4	0	2	10
	Inner																					
																	SUM:	54	190	66	52	362
																	TOTAL:					378

A Sections on blade with measurement equipment

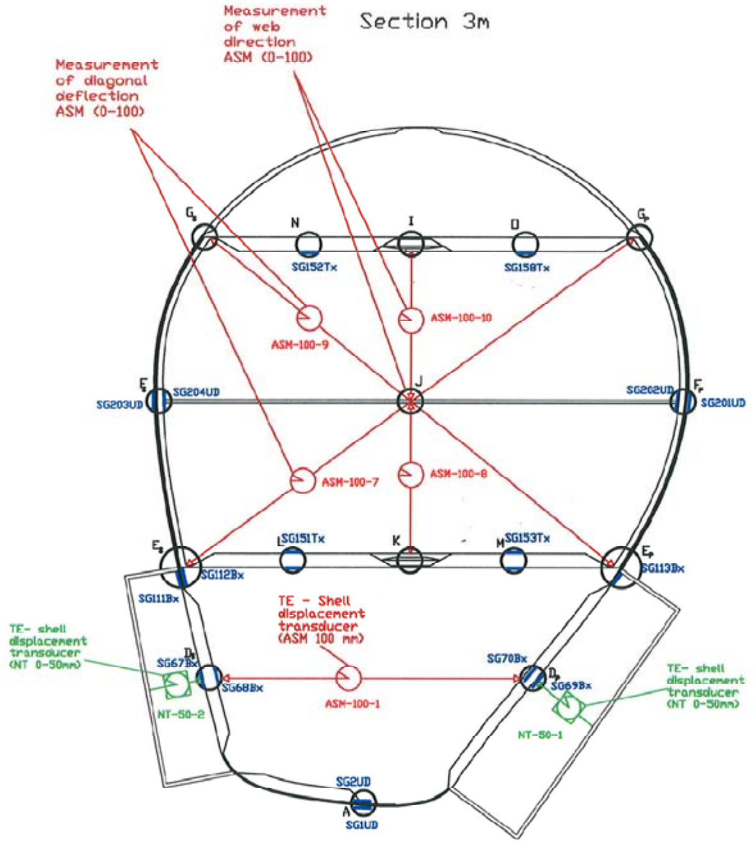

Section 3.5m based on the 3m. section

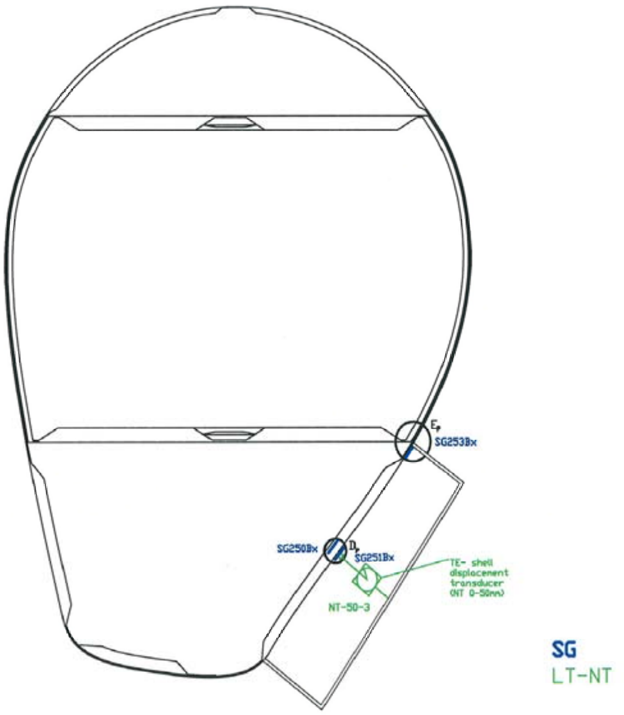

A

Section 4m based on the 3m section

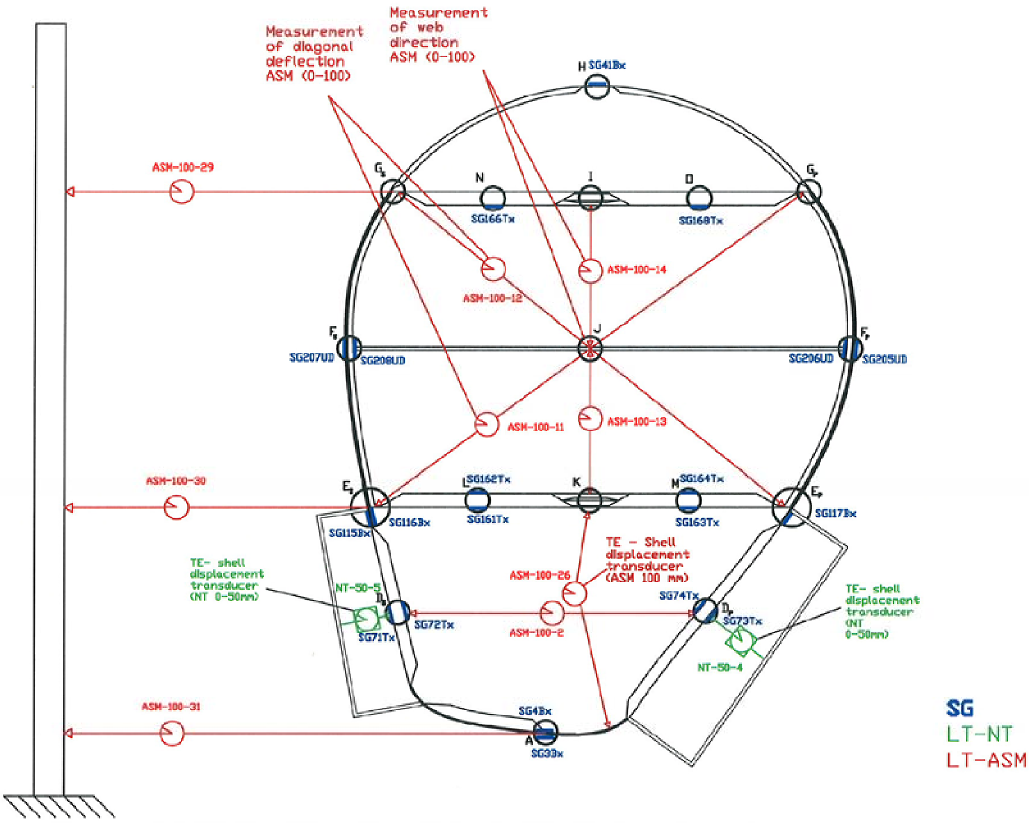

Section 4.5m based on the 3m. section

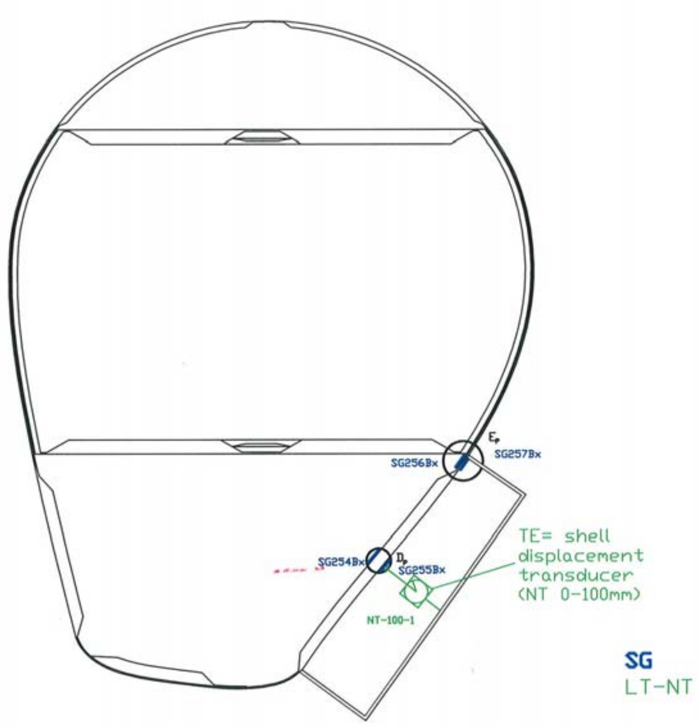

A

Section 5m based on the 3m section

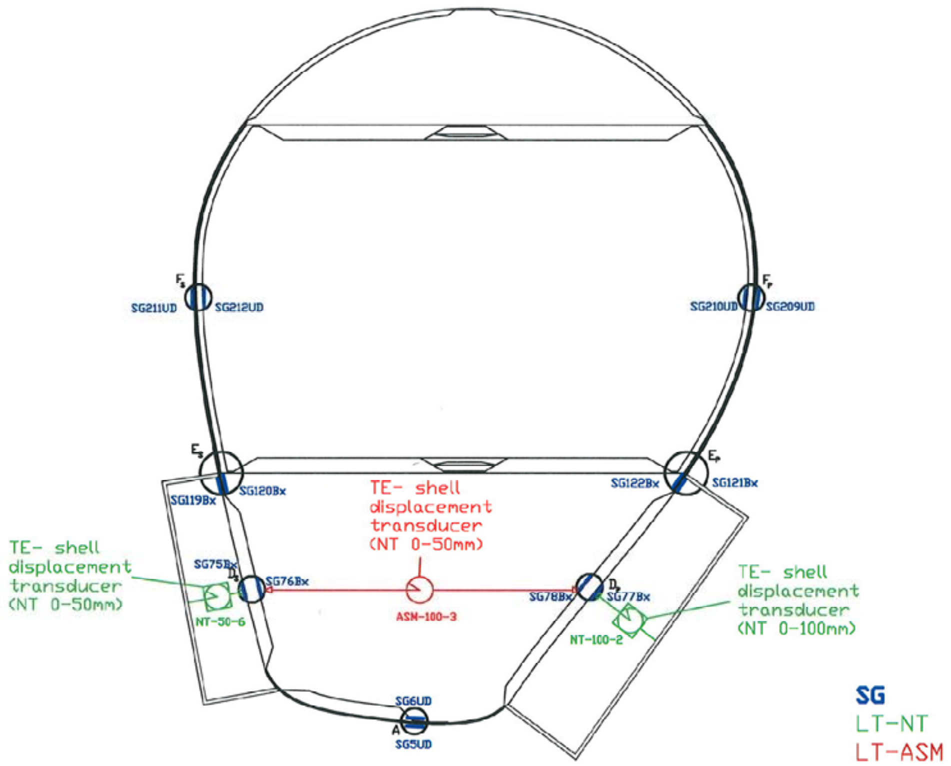

Section 6m based on the 3m section

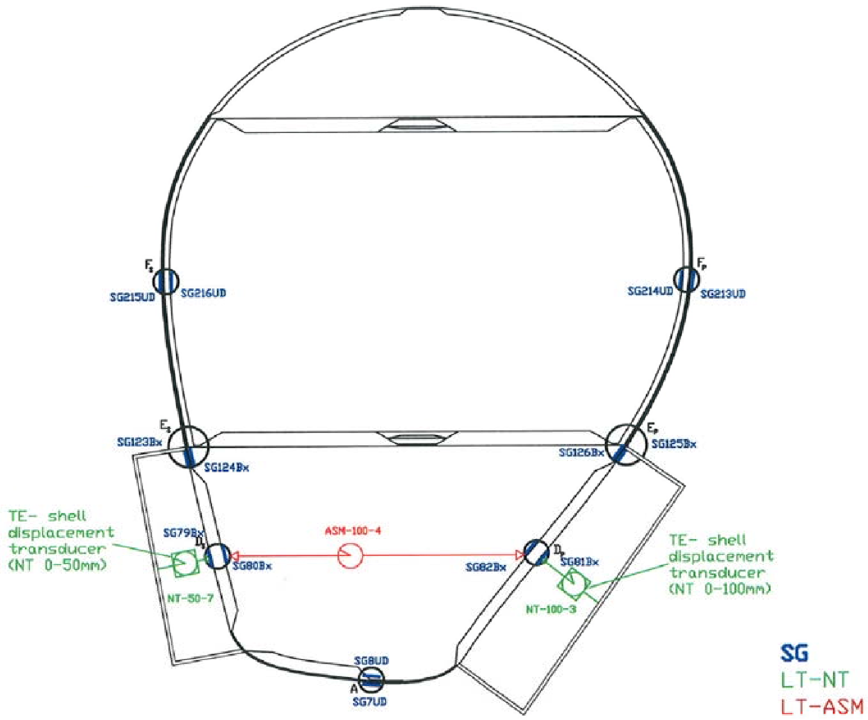

A

Section 7m Main section

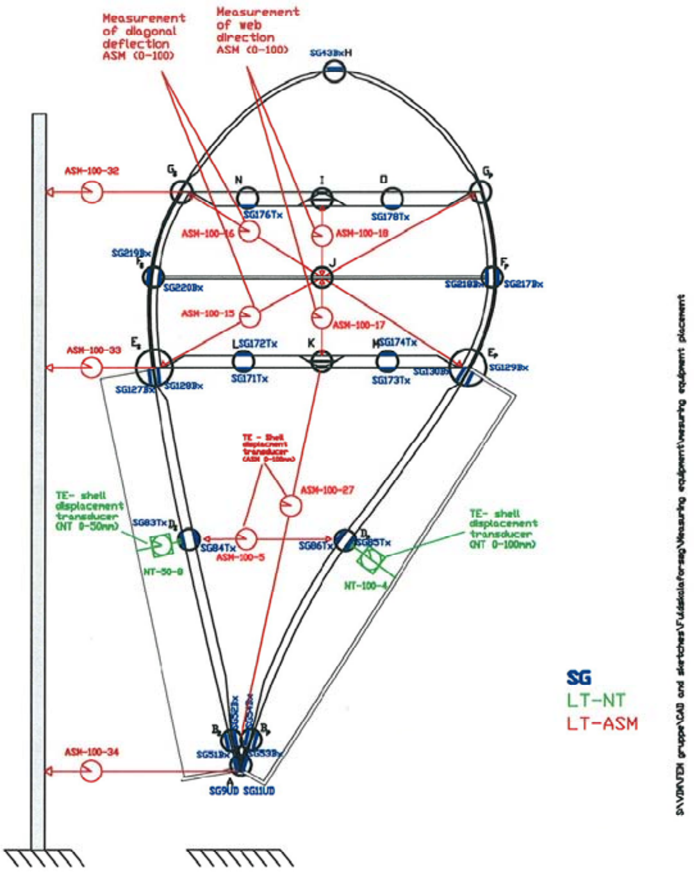

Section 8m based on 9m Section

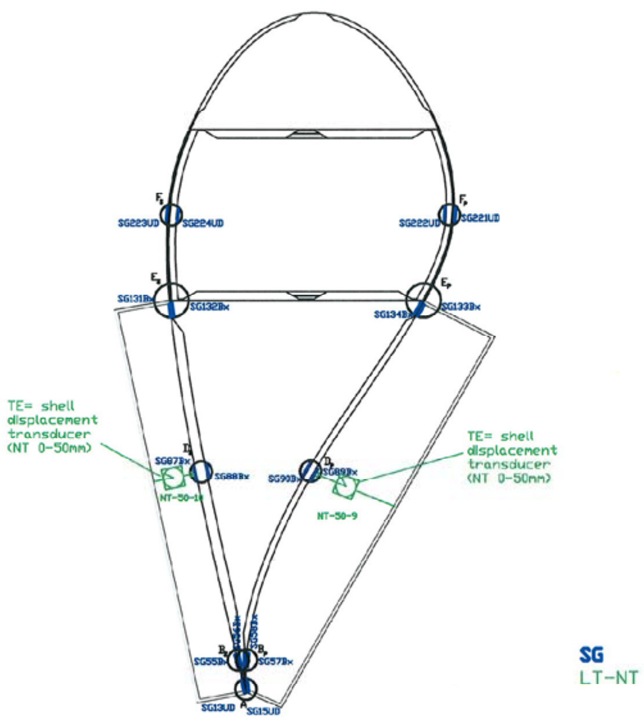

A

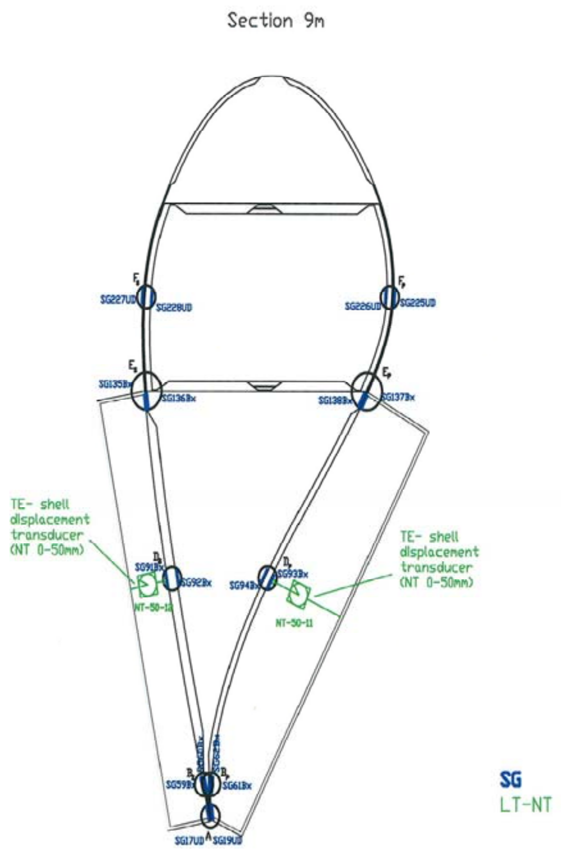
Section 9m
SG227UD
SG228UD
SG226UD
SG225UD
SG135Bx
SG136Bx
SG138Bx
SG137Bx
TE- shell displacement transducer (NT 0-50mm)
SG91Bx
SG92Bx
NT-50-12
SG94Bx
SG93Bx
TE- shell displacement transducer (NT 0-50mm)
NT-50-11
SG59Bx
SG61Bx
SG17UD
SG19UD
SG
LT-NT

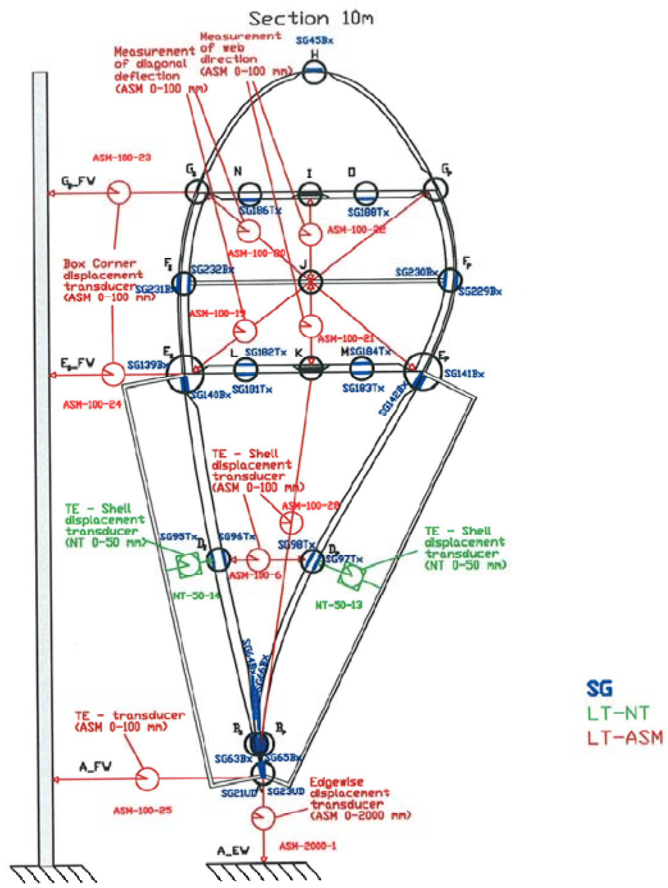
Section 10m
Measurement of diagonal deflection (ASM 0-100 mm)
Measurement of web direction (ASM 0-100 mm)
SG45Bx
H
ASM-100-23
G_FV
N
I
O
SG186Tx
SG188Tx
ASM-100-22
Box Corner displacement transducer (ASM 0-100 mm)
SG232Bx
SG231Bx
J
SG230Bx
SG229Bx
ASM-100-19
ASM-100-21
E_FV
SG139Bx
L
SG182Tx
K
M
SG184Tx
SG141Bx
ASM-100-24
SG140Bx
SG181Tx
SG183Tx
SG142Bx
TE - Shell displacement transducer (ASM 0-100 mm)
ASM-100-20
TE - Shell displacement transducer (NT 0-50 mm)
SG95Tx
SG96Tx
SG98Tx
SG97Tx
TE - Shell displacement transducer (NT 0-50 mm)
ASM-100-6
NT-50-14
NT-50-13
TE - transducer (ASM 0-100 mm)
SG63Bx
SG65Bx
A_FW
SG21UD
SG23UD
Edgewise displacement transducer (ASM 0-2000 mm)
ASM-100-25
ASM-2000-1
A_EW
SG
LT-NT
LT-ASM

A

Section 11m based on 10m section

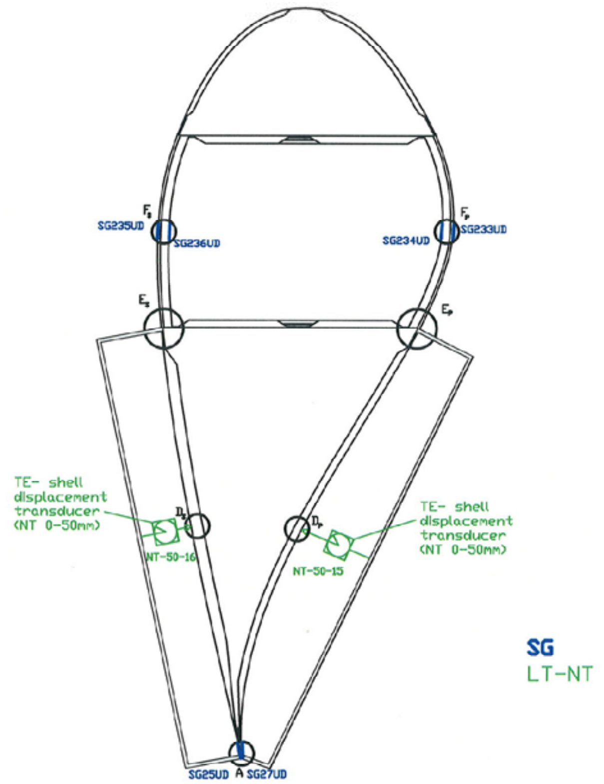

Section 12m based on 10m section

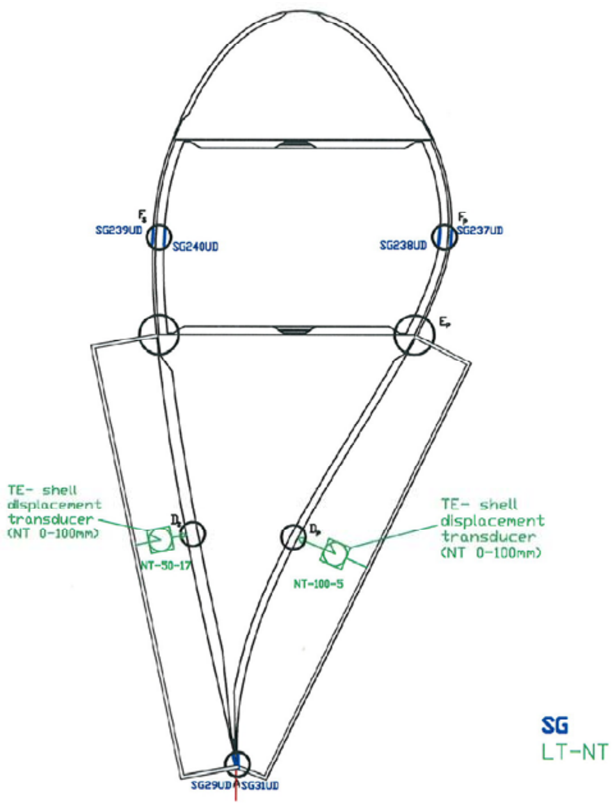

A

Section 16m

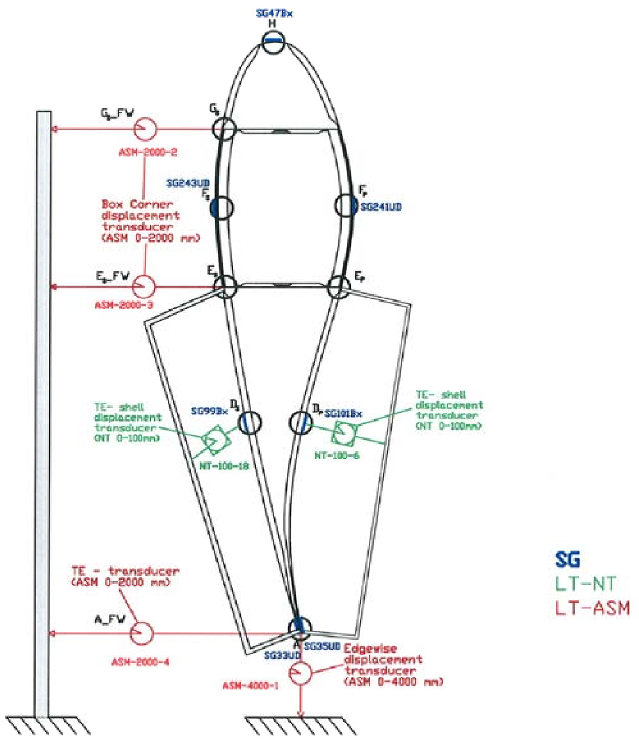

Section 22m

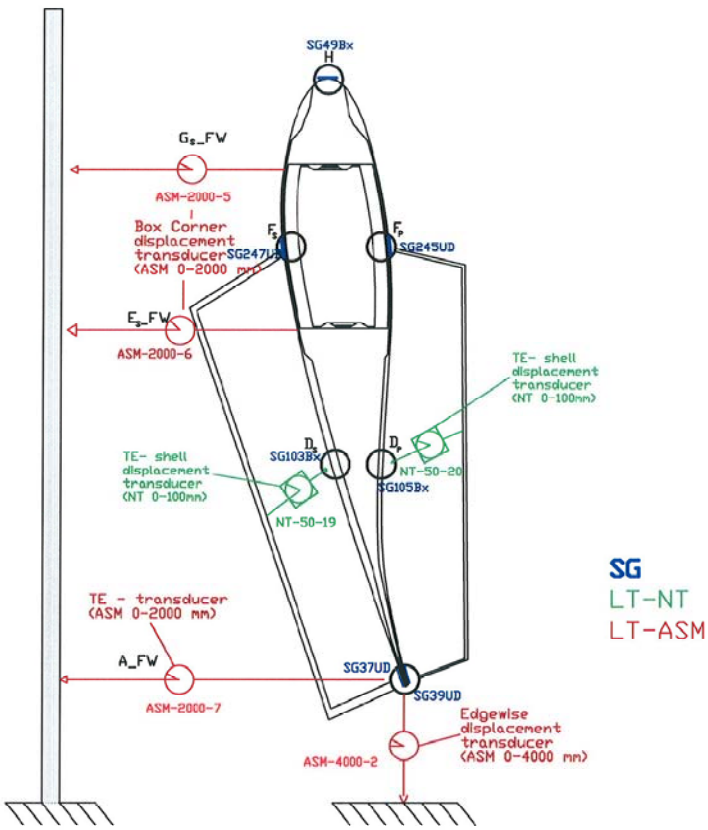

A Sign for ASM-movement

Out is according to the ASM and is when the wire is getting longer.
+ and – refer the sign of the measurement.

ASM no.	out
ASM-100-1	+
ASM-100-2	+
ASM-100-3	+
ASM-100-4	+
ASM-100-5	+
ASM-100-6	+
ASM-100-26	+
ASM-100-27	+
ASM-100-28	+
ASM-100-7	+
ASM-100-8	+
ASM-100-9	+
ASM-100-10	+
ASM-100-11	+
ASM-100-12	+
ASM-100-13	-
ASM-100-14	+
ASM-100-15	+
ASM-100-16	+
ASM-100-17	+
ASM-100-18	+
ASM-100-19	+
ASM-100-20	+
ASM-100-21	+
ASM-100-22	+
ASM-100-23	-
ASM-100-24	-
ASM-100-25	+
ASM-100-29	-
ASM-100-30	-
ASM-100-31	-
ASM-100-32	-
ASM-100-33	-
ASM-100-34	-
ASM-2000-1	-
ASM-2000-2	-
ASM-2000-3	-

ASM-2000-4	-
ASM-4000-1	-
ASM-4000-2	-

Groups with displacement gauges

Displacement transducers Group 1+2+3

	1	2	3	4	5	6	7	8	9	10
A1	FT-1	FT-2	FT-3	ASM-2000-5	ASM-2000-6	ASM-2000-7	ASM-4000-2	ASM-2000-2	ASM-2000-3	ASM-2000-4
A2	ASM-4000-1	ASM-100-23	ASM-100-24	ASM-100-25	ASM-2000-1	NT-100-5	NT-100-6	*empty*	NT-50-15	NT-50-16
A3	NT-100-3	NT-100-4	NT-50-7	NT-50-8	NT-50-9	NT-50-10	NT-50-11	NT-50-12	NT-50-13	NT-50-14
A4	NT-100-1	NT-100-2	NT-50-1	NT-50-2	NT-50-3	NT-50-4	NT-50-5	NT-50-6	ASM-100-8	ASM-100-9
A5	ASM-100-10	ASM-100-11	ASM-100-12	ASM-100-13	ASM-100-14	ASM-100-17	ASM-100-19	ASM-100-20	ASM-100-21	ASM-100-22
A6	ASM-100-1	ASM-100-2	ASM-100-26	ASM-100-3	ASM-100-4	ASM-100-5	ASM-100-27	ASM-100-6	ASM-100-28	ASM-100-7

Displacement transducers Group 4

	1	2	3	4	5	6	7	8	9	10
A1	FT-1	FT-2	FT-3	ASM-2000-5	ASM-2000-6	ASM-2000-7	ASM-4000-2	ASM-100-32	ASM-100-33	ASM-100-34
A2	ASM-4000-1	ASM-100-29	ASM-100-30	ASM-100-31	ASM-2000-1	NT-100-5	NT-100-6	*empty*	NT-50-15	NT-50-16
A3	NT-100-3	NT-100-4	NT-50-7	NT-50-8	NT-50-9	NT-50-10	NT-50-11	NT-50-12	NT-50-13	NT-50-14
A4	NT-100-1	NT-100-2	NT-50-1	NT-50-2	NT-50-3	NT-50-4	NT-50-5	NT-50-6	ASM-100-8	ASM-100-9
A5	ASM-100-10	ASM-100-11	ASM-100-12	ASM-100-13	ASM-100-14	ASM-100-17	ASM-100-19	ASM-100-20	ASM-100-21	ASM-100-22
A6	ASM-100-1	ASM-100-2	ASM-100-26	ASM-100-3	ASM-100-4	ASM-100-5	ASM-100-27	ASM-100-6	ASM-100-28	ASM-100-7

Group 5 (Global B)

	1	2	3	4	5	6	7	8	9	10
A1	FT-1	FT-2	FT-3	ASM-2000-5	NT-50-12	empty	ASM-4000-2	empty	empty	empty
A2	ASM-4000-1	ASM-100-23	ASM-100-24	ASM-100-25	ASM-2000-1	*NT-50-17*	*empty*	*NT-100-18*	*NT-50-19*	*NT-50-20*
A3	NT-100-3	NT-100-4	NT-50-7	NT-50-8	NT-50-9	NT-50-10	NT-50-11	*empty*	NT-50-13	NT-50-14
A4	NT-100-1	NT-100-2	NT-50-1	NT-50-2	NT-50-3	NT-50-4	NT-50-5	NT-50-6	ASM-100-8	ASM-100-9
A5	ASM-100-10	ASM-100-11	ASM-100-12	ASM-100-13	ASM-100-14	ASM-100-17	ASM-100-19	ASM-100-20	ASM-100-21	ASM-100-22
A6	FT-4	FT-5	ASM-100-15	FT-6	ASM-100-4	ASM-100-5	ASM-100-16	ASM-100-6	ASM-100-18	ASM-100-7

B Data presented by Graph tool

B Measured strain vs. bending moment

B1 Measurements obtained from strain gauges in: **Main section in test ELTT_1-291009_A**

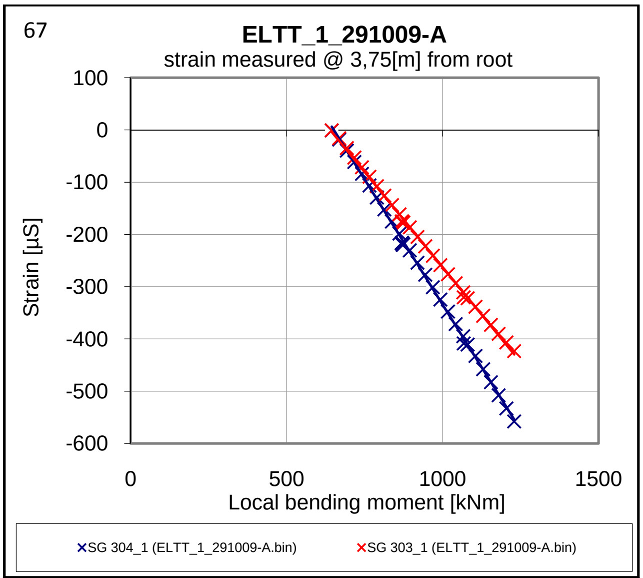

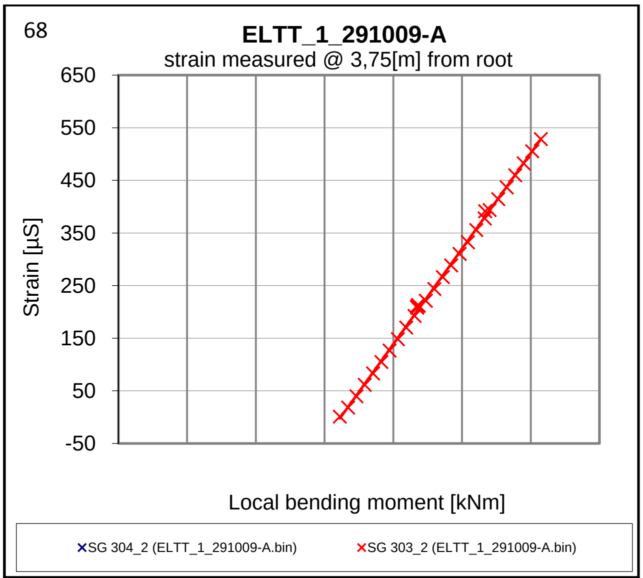

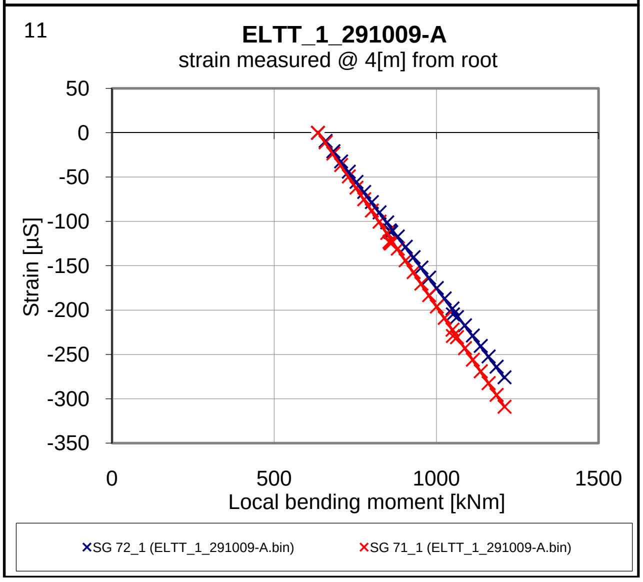

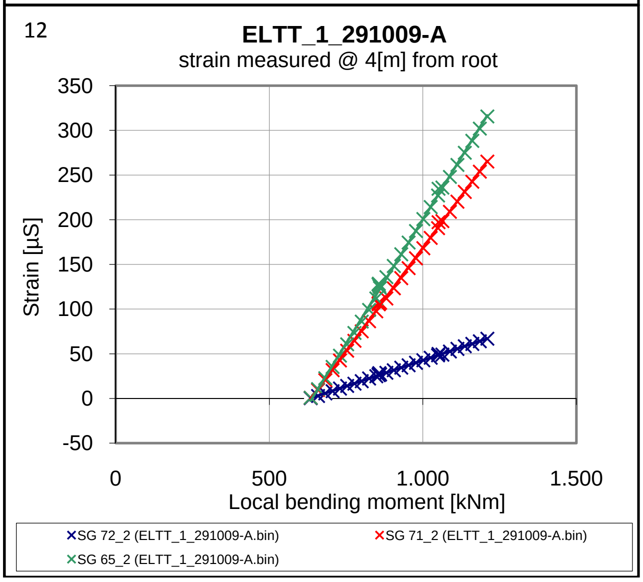

B1

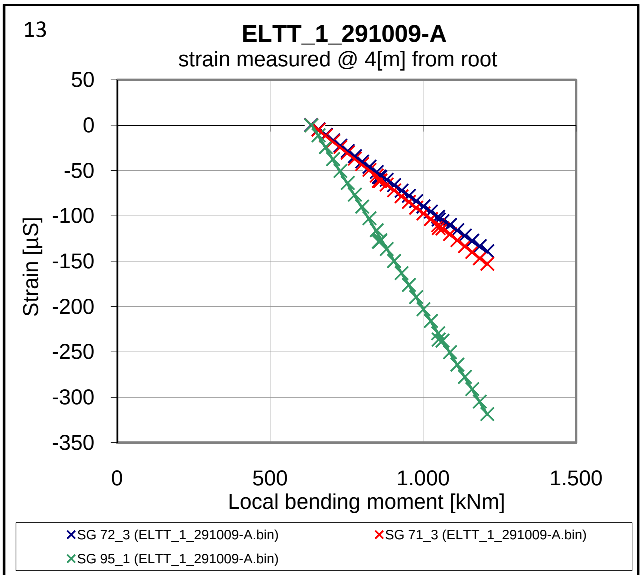
13
ELTT_1_291009-A
strain measured @ 4[m] from root
Strain [µS]
50
0
-50
-100
-150
-200
-250
-300
-350
0
500
1.000
1.500
Local bending moment [kNm]
SG 72_3 (ELTT_1_291009-A.bin)
SG 71_3 (ELTT_1_291009-A.bin)
SG 95_1 (ELTT_1_291009-A.bin)

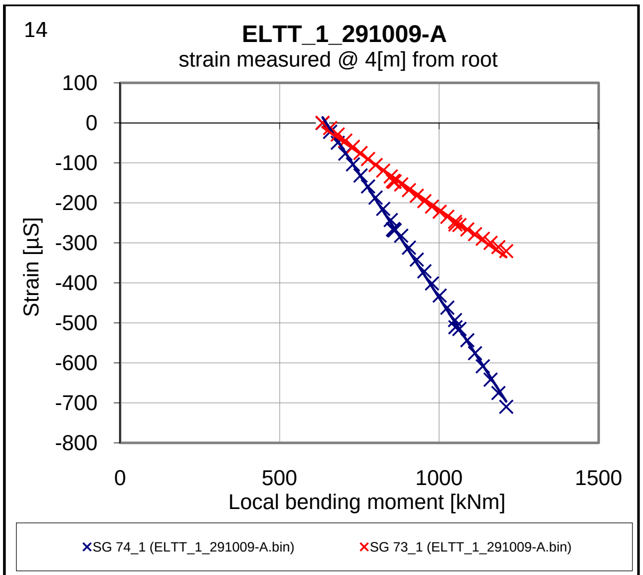
14
ELTT_1_291009-A
strain measured @ 4[m] from root
Strain [µS]
100
0
-100
-200
-300
-400
-500
-600
-700
-800
0
500
1000
1500
Local bending moment [kNm]
SG 74_1 (ELTT_1_291009-A.bin)
SG 73_1 (ELTT_1_291009-A.bin)

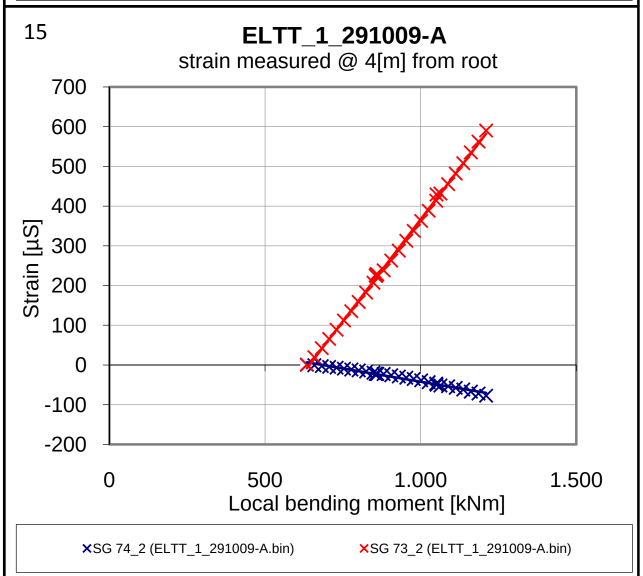
15
ELTT_1_291009-A
strain measured @ 4[m] from root
Strain [µS]
700
600
500
400
300
200
100
0
-100
-200
0
500
1.000
1.500
Local bending moment [kNm]
SG 74_2 (ELTT_1_291009-A.bin)
SG 73_2 (ELTT_1_291009-A.bin)

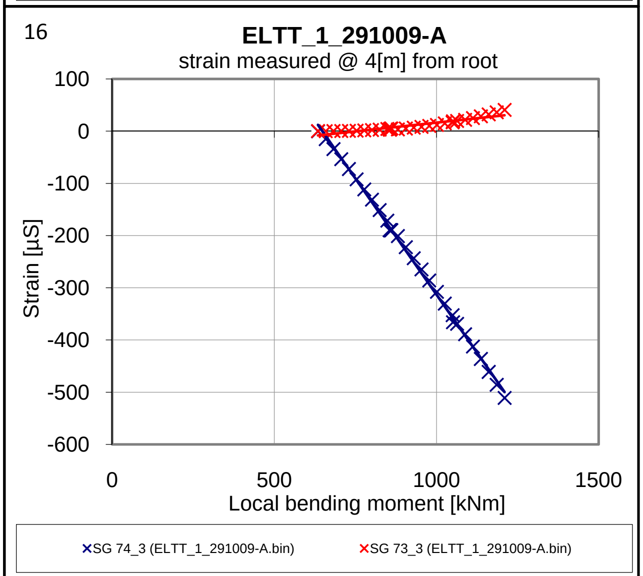
16
ELTT_1_291009-A
strain measured @ 4[m] from root
Strain [µS]
100
0
-100
-200
-300
-400
-500
-600
0
500
1000
1500
Local bending moment [kNm]
SG 74_3 (ELTT_1_291009-A.bin)
SG 73_3 (ELTT_1_291009-A.bin)

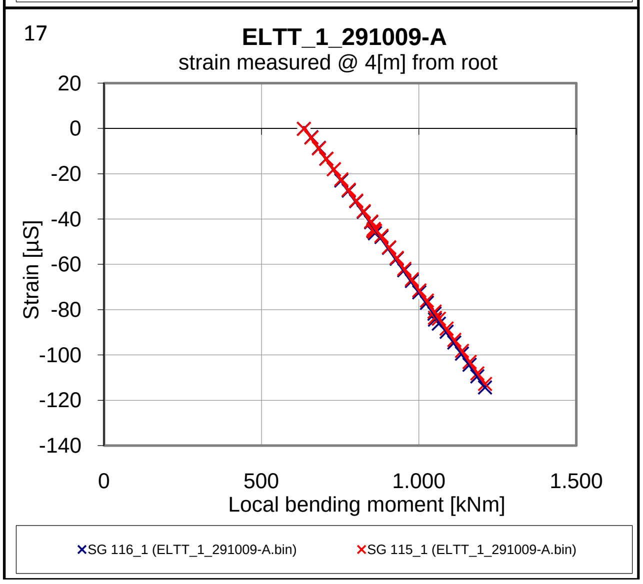
17
ELTT_1_291009-A
strain measured @ 4[m] from root
Strain [µS]
20
0
-20
-40
-60
-80
-100
-120
-140
0
500
1.000
1.500
Local bending moment [kNm]
SG 116_1 (ELTT_1_291009-A.bin)
SG 115_1 (ELTT_1_291009-A.bin)

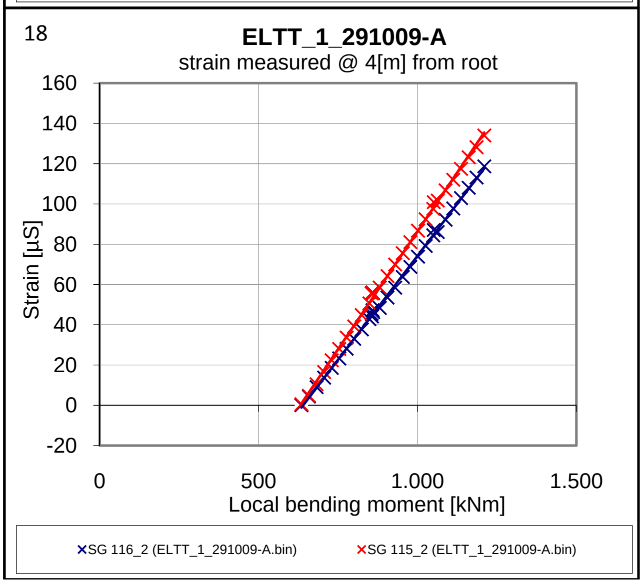
18
ELTT_1_291009-A
strain measured @ 4[m] from root
Strain [µS]
160
140
120
100
80
60
40
20
0
-20
0
500
1.000
1.500
Local bending moment [kNm]
SG 116_2 (ELTT_1_291009-A.bin)
SG 115_2 (ELTT_1_291009-A.bin)

B1

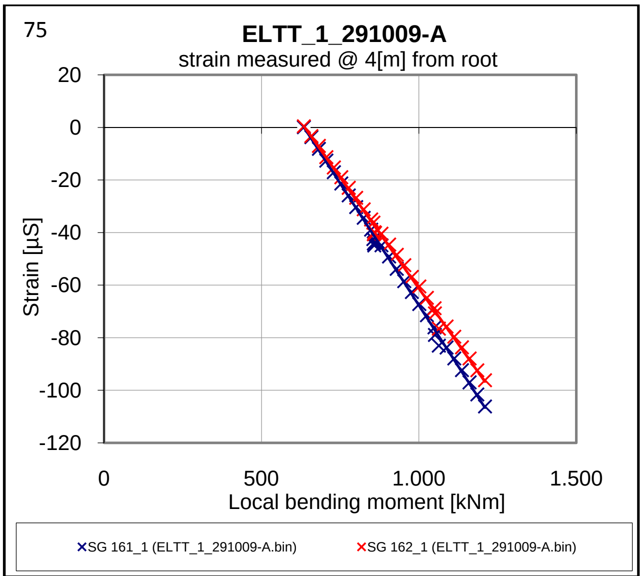

75
ELTT_1_291009-A
strain measured @ 4[m] from root
Strain [µS]
20
0
-20
-40
-60
-80
-100
-120
0
500
1.000
1.500
Local bending moment [kNm]
SG 161_1 (ELTT_1_291009-A.bin)
SG 162_1 (ELTT_1_291009-A.bin)

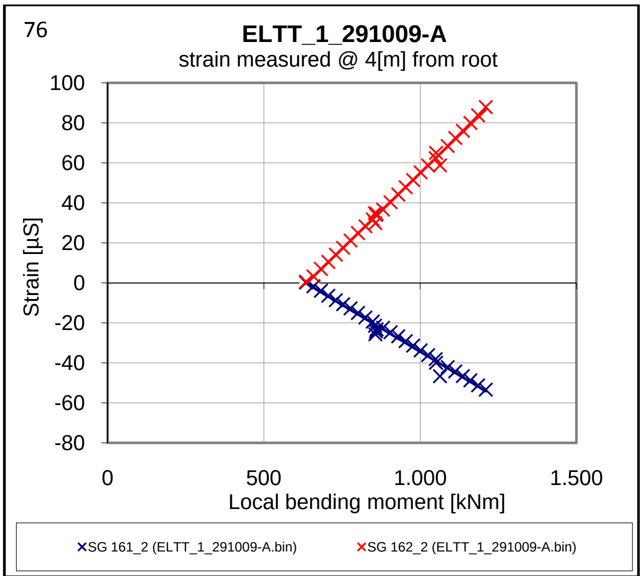

76
ELTT_1_291009-A
strain measured @ 4[m] from root
Strain [µS]
100
80
60
40
20
0
-20
-40
-60
-80
0
500
1.000
1.500
Local bending moment [kNm]
SG 161_2 (ELTT_1_291009-A.bin)
SG 162_2 (ELTT_1_291009-A.bin)

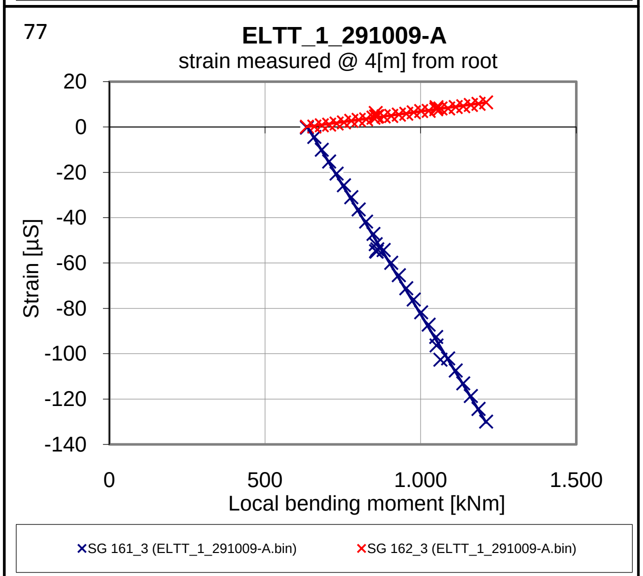

77
ELTT_1_291009-A
strain measured @ 4[m] from root
Strain [µS]
20
0
-20
-40
-60
-80
-100
-120
-140
0
500
1.000
1.500
Local bending moment [kNm]
SG 161_3 (ELTT_1_291009-A.bin)
SG 162_3 (ELTT_1_291009-A.bin)

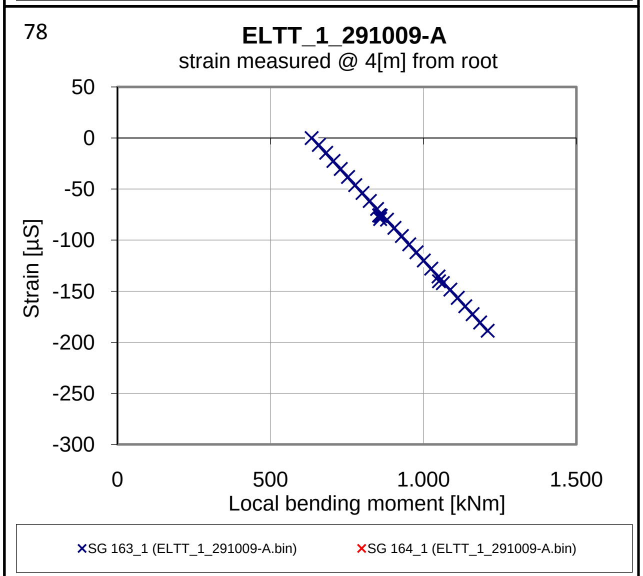

78
ELTT_1_291009-A
strain measured @ 4[m] from root
Strain [µS]
50
0
-50
-100
-150
-200
-250
-300
0
500
1.000
1.500
Local bending moment [kNm]
SG 163_1 (ELTT_1_291009-A.bin)
SG 164_1 (ELTT_1_291009-A.bin)

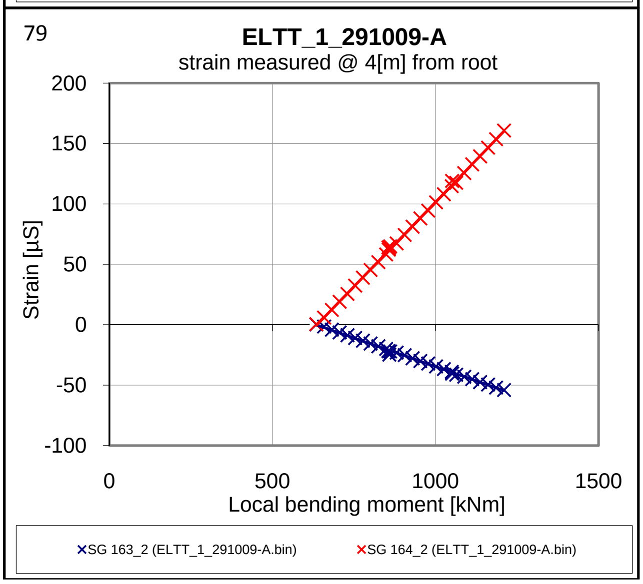

79
ELTT_1_291009-A
strain measured @ 4[m] from root
Strain [µS]
200
150
100
50
0
-50
-100
0
500
1000
1500
Local bending moment [kNm]
SG 163_2 (ELTT_1_291009-A.bin)
SG 164_2 (ELTT_1_291009-A.bin)

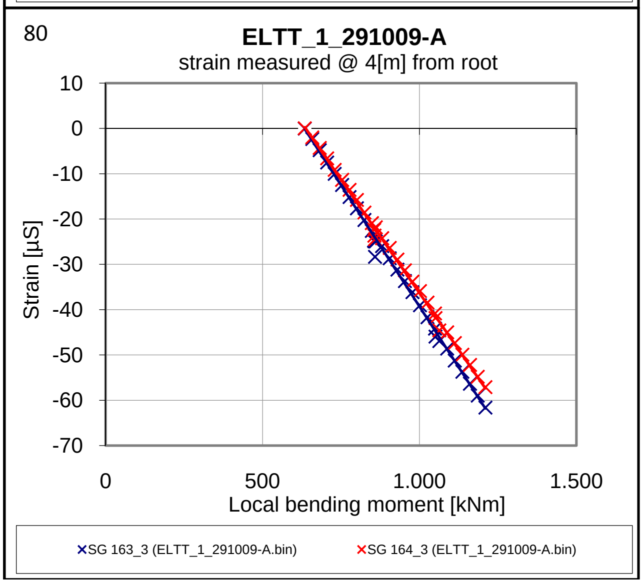

80
ELTT_1_291009-A
strain measured @ 4[m] from root
Strain [µS]
10
0
-10
-20
-30
-40
-50
-60
-70
0
500
1.000
1.500
Local bending moment [kNm]
SG 163_3 (ELTT_1_291009-A.bin)
SG 164_3 (ELTT_1_291009-A.bin)

B1

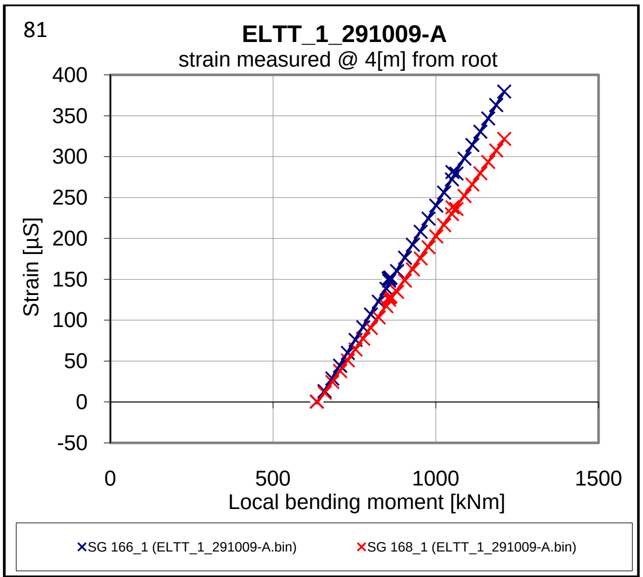
81
ELTT_1_291009-A
strain measured @ 4[m] from root
Strain [µS]
400
350
300
250
200
150
100
50
0
-50
0
500
1000
1500
Local bending moment [kNm]
SG 166_1 (ELTT_1_291009-A.bin)
SG 168_1 (ELTT_1_291009-A.bin)

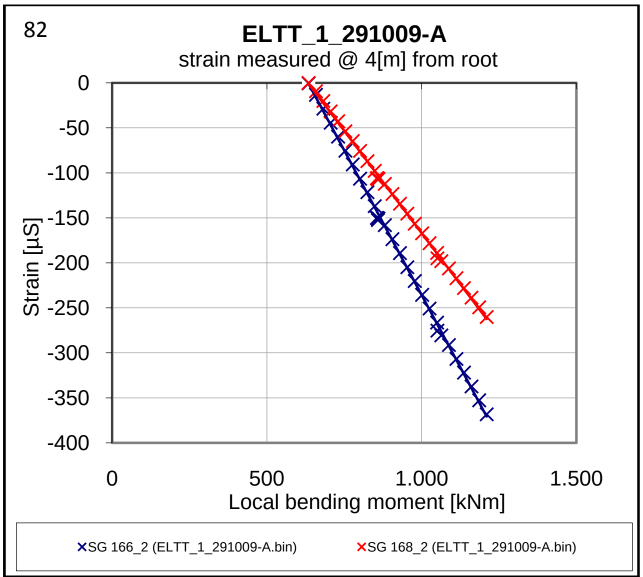
82
ELTT_1_291009-A
strain measured @ 4[m] from root
Strain [µS]
0
-50
-100
-150
-200
-250
-300
-350
-400
0
500
1.000
1.500
Local bending moment [kNm]
SG 166_2 (ELTT_1_291009-A.bin)
SG 168_2 (ELTT_1_291009-A.bin)

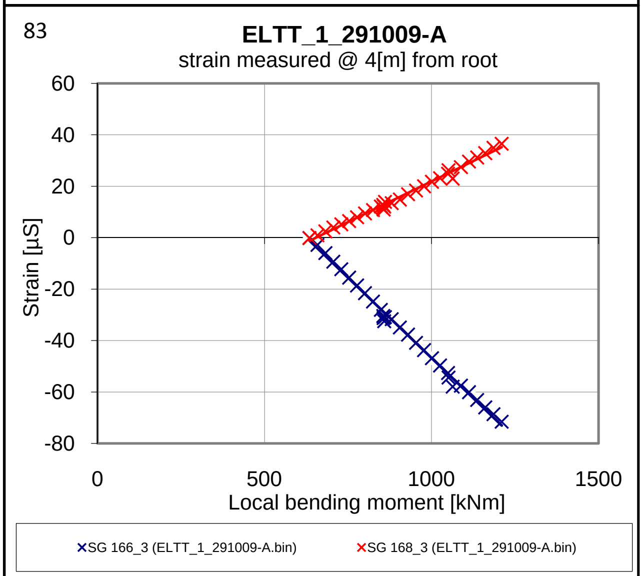
83
ELTT_1_291009-A
strain measured @ 4[m] from root
Strain [µS]
60
40
20
0
-20
-40
-60
-80
0
500
1000
1500
Local bending moment [kNm]
SG 166_3 (ELTT_1_291009-A.bin)
SG 168_3 (ELTT_1_291009-A.bin)

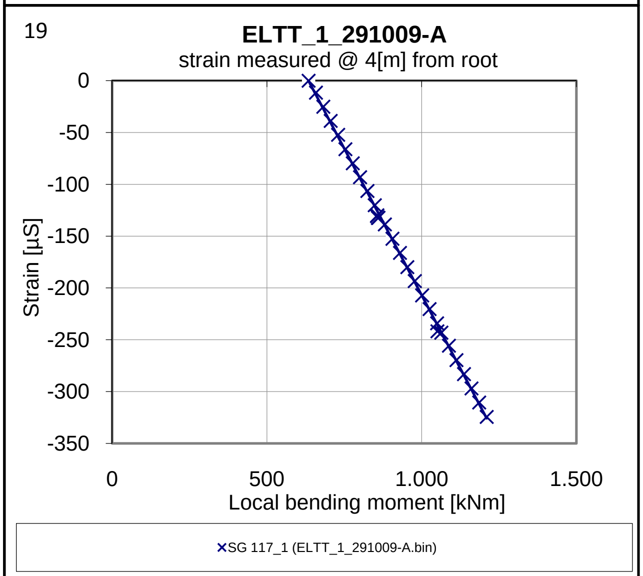
19
ELTT_1_291009-A
strain measured @ 4[m] from root
Strain [µS]
0
-50
-100
-150
-200
-250
-300
-350
0
500
1.000
1.500
Local bending moment [kNm]
SG 117_1 (ELTT_1_291009-A.bin)

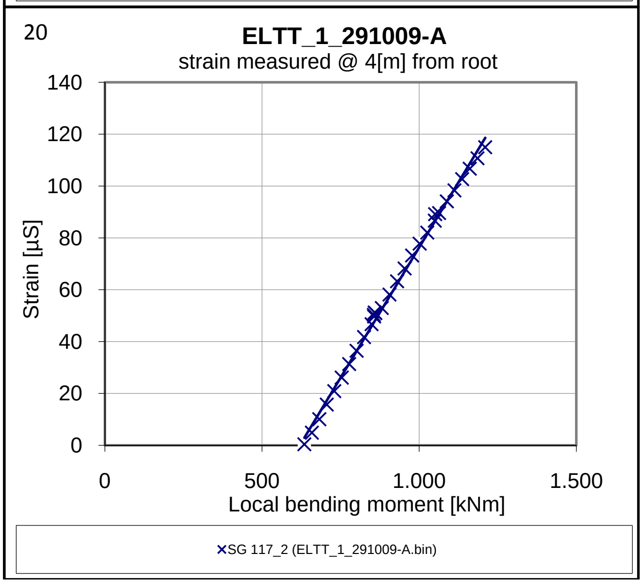
20
ELTT_1_291009-A
strain measured @ 4[m] from root
Strain [µS]
140
120
100
80
60
40
20
0
0
500
1.000
1.500
Local bending moment [kNm]
SG 117_2 (ELTT_1_291009-A.bin)

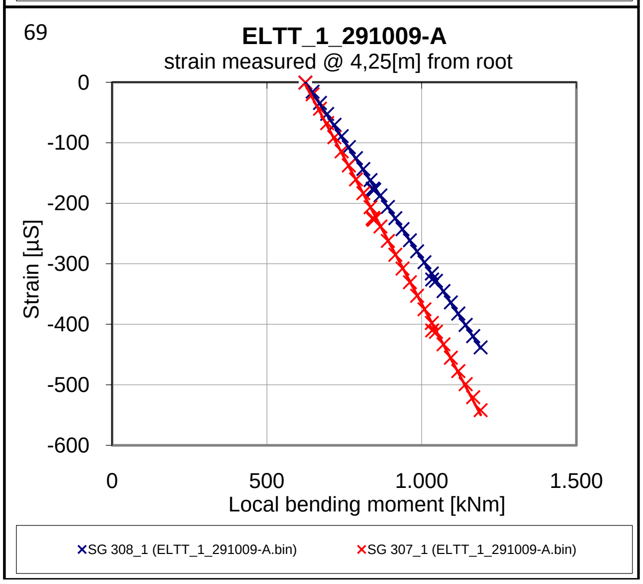
69
ELTT_1_291009-A
strain measured @ 4,25[m] from root
Strain [µS]
0
-100
-200
-300
-400
-500
-600
0
500
1.000
1.500
Local bending moment [kNm]
SG 308_1 (ELTT_1_291009-A.bin)
SG 307_1 (ELTT_1_291009-A.bin)

B1

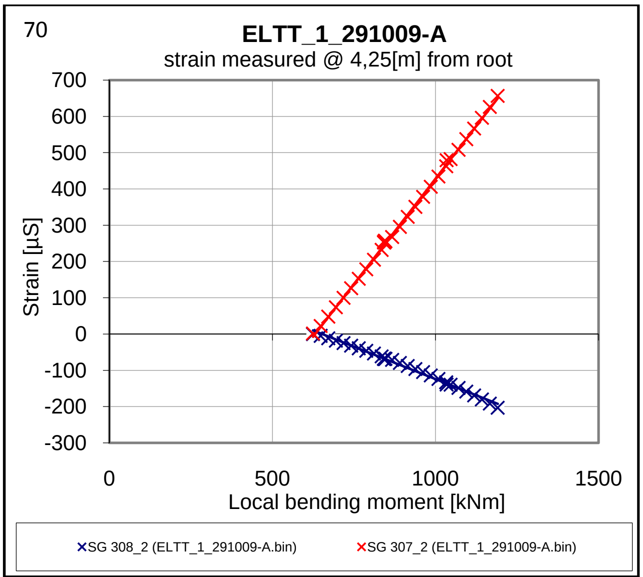
70
ELTT_1_291009-A
strain measured @ 4,25[m] from root
Strain [µS]
700
600
500
400
300
200
100
0
-100
-200
-300
0
500
1000
1500
Local bending moment [kNm]
SG 308_2 (ELTT_1_291009-A.bin)
SG 307_2 (ELTT_1_291009-A.bin)

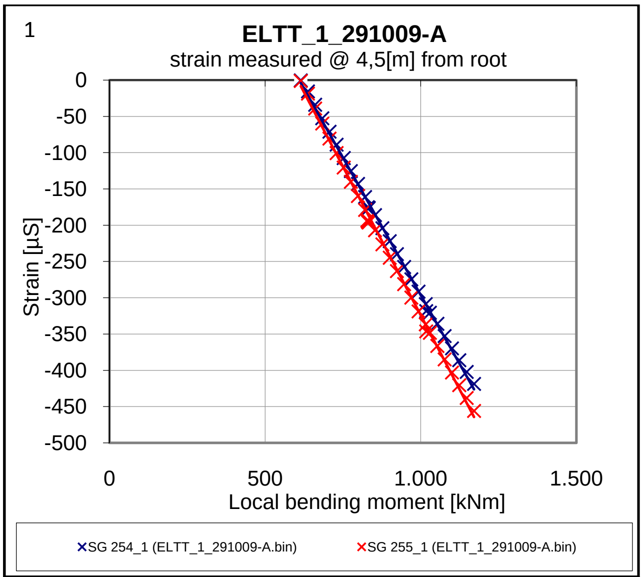
1
ELTT_1_291009-A
strain measured @ 4,5[m] from root
Strain [µS]
0
-50
-100
-150
-200
-250
-300
-350
-400
-450
-500
0
500
1.000
1.500
Local bending moment [kNm]
SG 254_1 (ELTT_1_291009-A.bin)
SG 255_1 (ELTT_1_291009-A.bin)

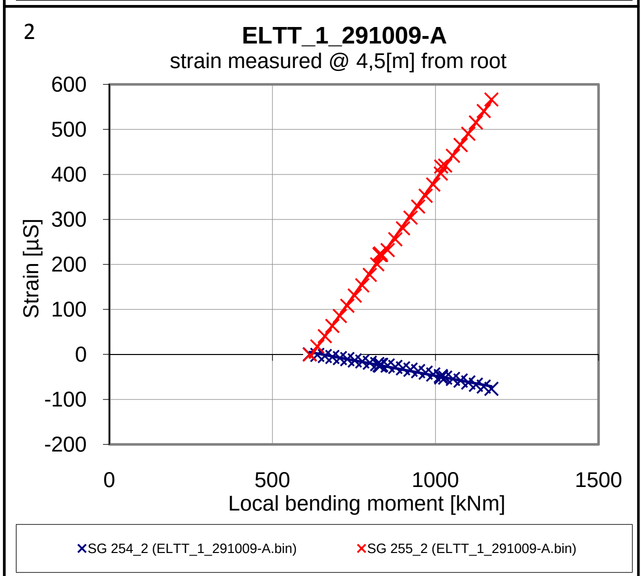
2
ELTT_1_291009-A
strain measured @ 4,5[m] from root
Strain [µS]
600
500
400
300
200
100
0
-100
-200
0
500
1000
1500
Local bending moment [kNm]
SG 254_2 (ELTT_1_291009-A.bin)
SG 255_2 (ELTT_1_291009-A.bin)

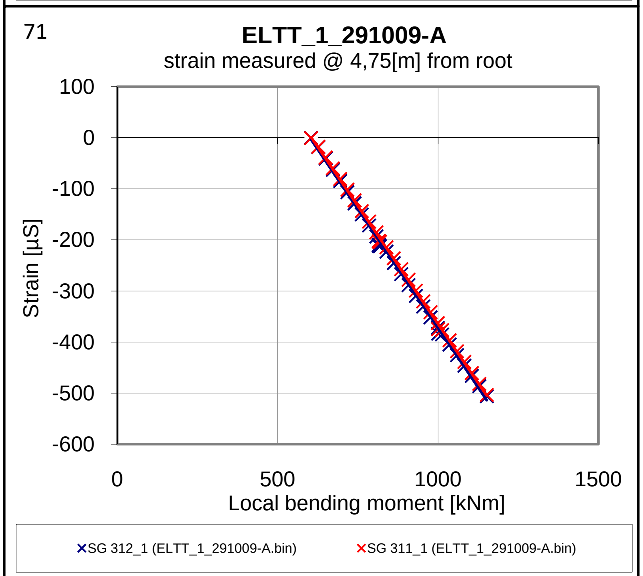
71
ELTT_1_291009-A
strain measured @ 4,75[m] from root
Strain [µS]
100
0
-100
-200
-300
-400
-500
-600
0
500
1000
1500
Local bending moment [kNm]
SG 312_1 (ELTT_1_291009-A.bin)
SG 311_1 (ELTT_1_291009-A.bin)

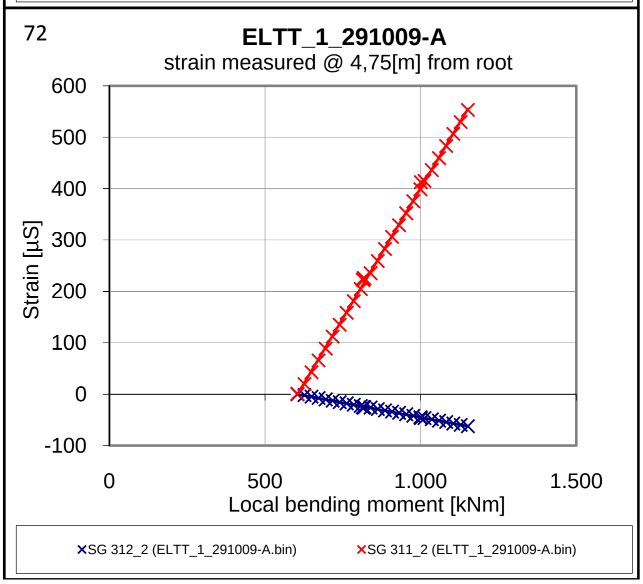
72
ELTT_1_291009-A
strain measured @ 4,75[m] from root
Strain [µS]
600
500
400
300
200
100
0
-100
0
500
1.000
1.500
Local bending moment [kNm]
SG 312_2 (ELTT_1_291009-A.bin)
SG 311_2 (ELTT_1_291009-A.bin)

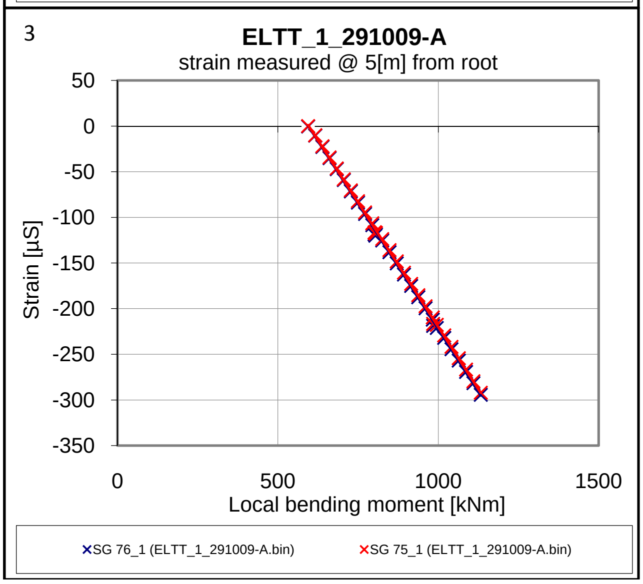
3
ELTT_1_291009-A
strain measured @ 5[m] from root
Strain [µS]
50
0
-50
-100
-150
-200
-250
-300
-350
0
500
1000
1500
Local bending moment [kNm]
SG 76_1 (ELTT_1_291009-A.bin)
SG 75_1 (ELTT_1_291009-A.bin)

B1

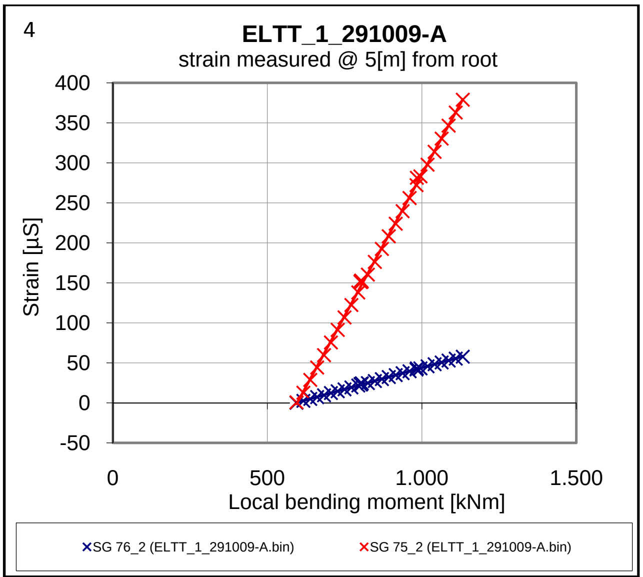
4
ELTT_1_291009-A
strain measured @ 5[m] from root
Strain [µS]
400
350
300
250
200
150
100
50
0
-50
0
500
1.000
1.500
Local bending moment [kNm]
SG 76_2 (ELTT_1_291009-A.bin)
SG 75_2 (ELTT_1_291009-A.bin)

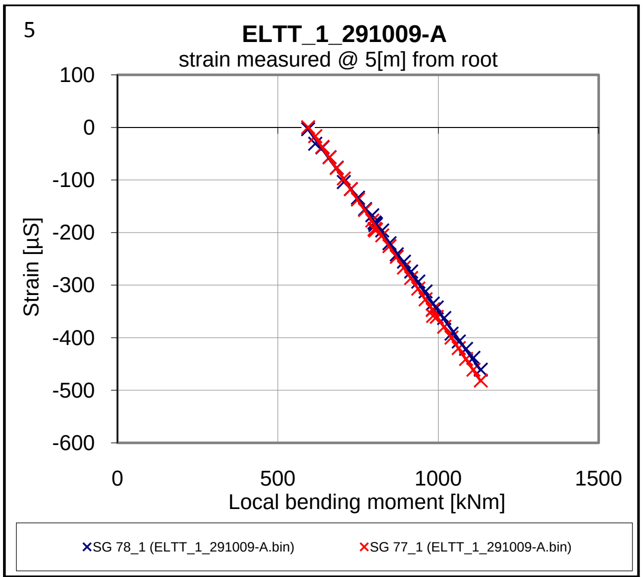
5
ELTT_1_291009-A
strain measured @ 5[m] from root
Strain [µS]
100
0
-100
-200
-300
-400
-500
-600
0
500
1000
1500
Local bending moment [kNm]
SG 78_1 (ELTT_1_291009-A.bin)
SG 77_1 (ELTT_1_291009-A.bin)

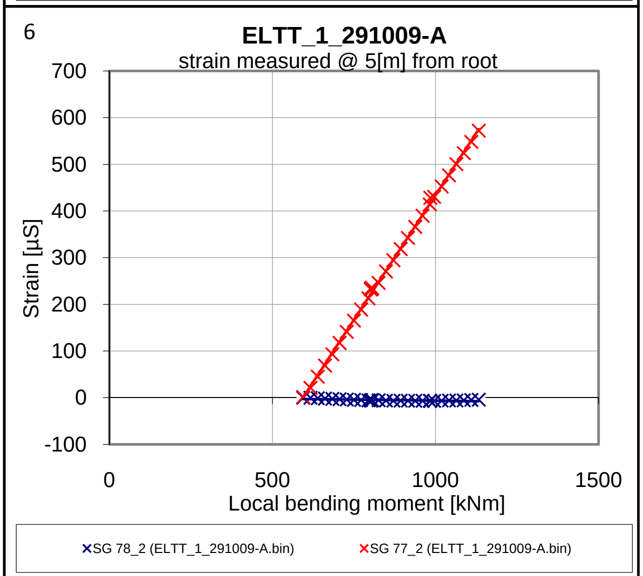
6
ELTT_1_291009-A
strain measured @ 5[m] from root
Strain [µS]
700
600
500
400
300
200
100
0
-100
0
500
1000
1500
Local bending moment [kNm]
SG 78_2 (ELTT_1_291009-A.bin)
SG 77_2 (ELTT_1_291009-A.bin)

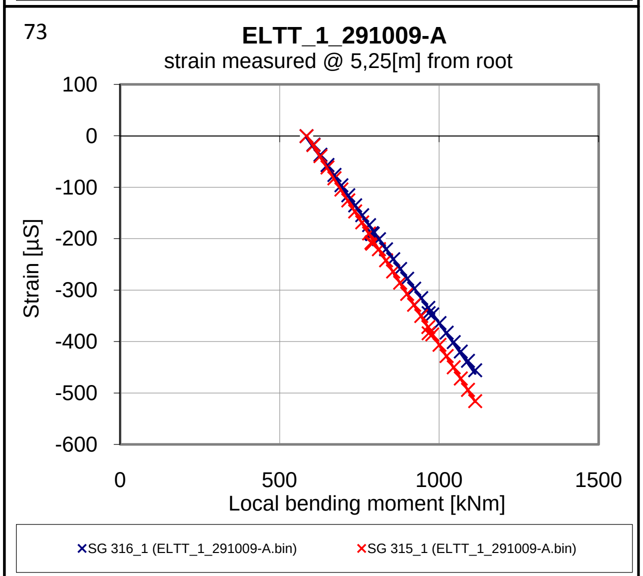
73
ELTT_1_291009-A
strain measured @ 5,25[m] from root
Strain [µS]
100
0
-100
-200
-300
-400
-500
-600
0
500
1000
1500
Local bending moment [kNm]
SG 316_1 (ELTT_1_291009-A.bin)
SG 315_1 (ELTT_1_291009-A.bin)

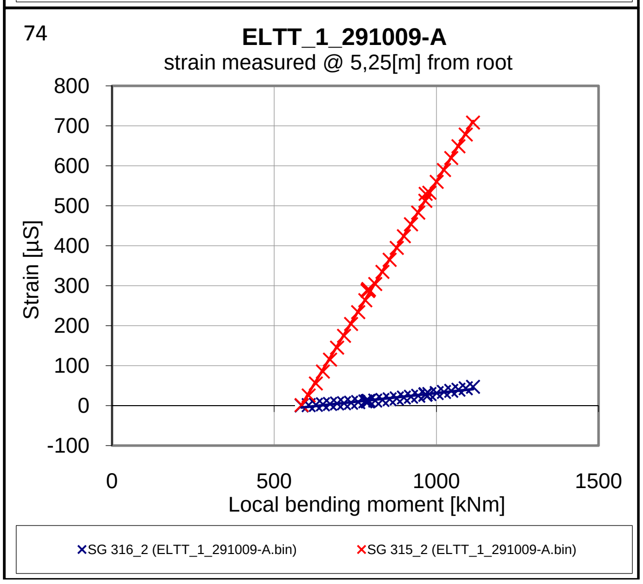
74
ELTT_1_291009-A
strain measured @ 5,25[m] from root
Strain [µS]
800
700
600
500
400
300
200
100
0
-100
0
500
1000
1500
Local bending moment [kNm]
SG 316_2 (ELTT_1_291009-A.bin)
SG 315_2 (ELTT_1_291009-A.bin)

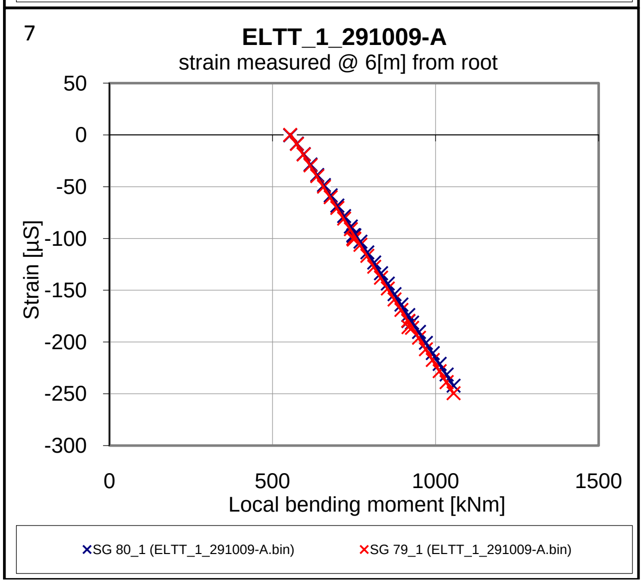
7
ELTT_1_291009-A
strain measured @ 6[m] from root
Strain [µS]
50
0
-50
-100
-150
-200
-250
-300
0
500
1000
1500
Local bending moment [kNm]
SG 80_1 (ELTT_1_291009-A.bin)
SG 79_1 (ELTT_1_291009-A.bin)

B1

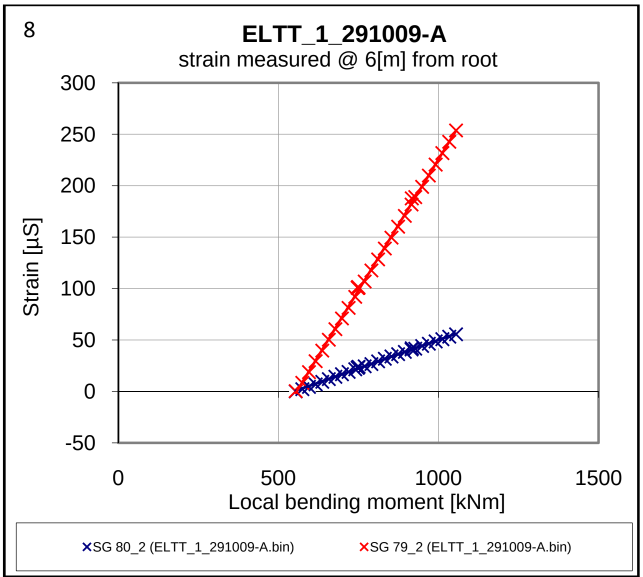
8
ELTT_1_291009-A
strain measured @ 6[m] from root
Strain [µS]
300
250
200
150
100
50
0
-50
0
500
1000
1500
Local bending moment [kNm]
SG 80_2 (ELTT_1_291009-A.bin)
SG 79_2 (ELTT_1_291009-A.bin)

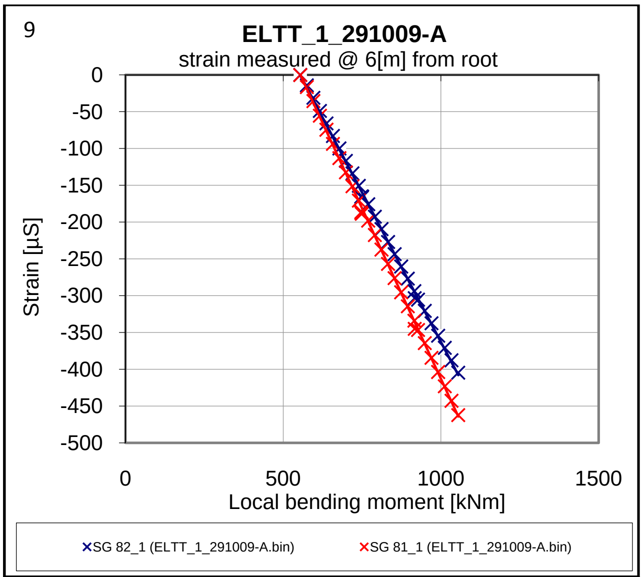
9
ELTT_1_291009-A
strain measured @ 6[m] from root
Strain [µS]
0
-50
-100
-150
-200
-250
-300
-350
-400
-450
-500
0
500
1000
1500
Local bending moment [kNm]
SG 82_1 (ELTT_1_291009-A.bin)
SG 81_1 (ELTT_1_291009-A.bin)

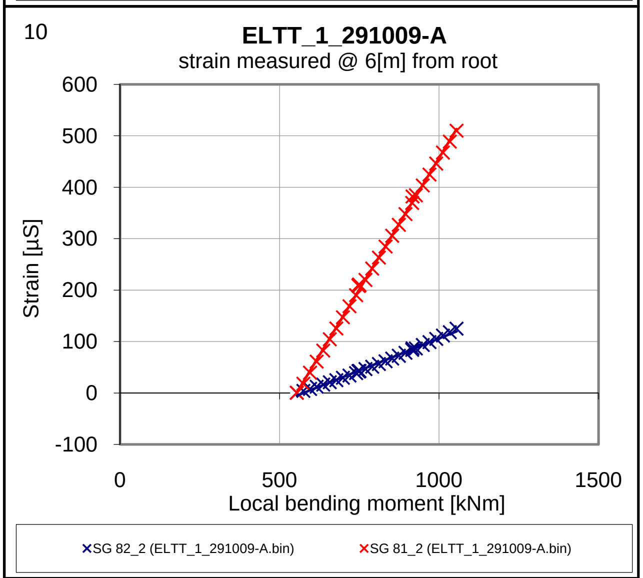
10
ELTT_1_291009-A
strain measured @ 6[m] from root
Strain [µS]
600
500
400
300
200
100
0
-100
0
500
1000
1500
Local bending moment [kNm]
SG 82_2 (ELTT_1_291009-A.bin)
SG 81_2 (ELTT_1_291009-A.bin)

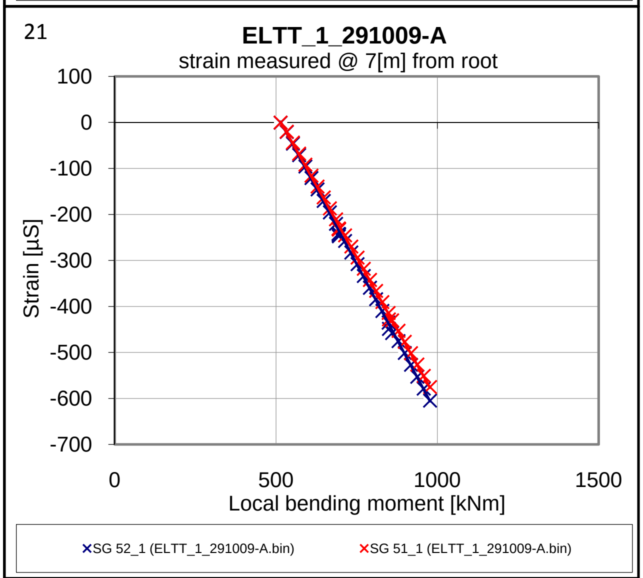
21
ELTT_1_291009-A
strain measured @ 7[m] from root
Strain [µS]
100
0
-100
-200
-300
-400
-500
-600
-700
0
500
1000
1500
Local bending moment [kNm]
SG 52_1 (ELTT_1_291009-A.bin)
SG 51_1 (ELTT_1_291009-A.bin)

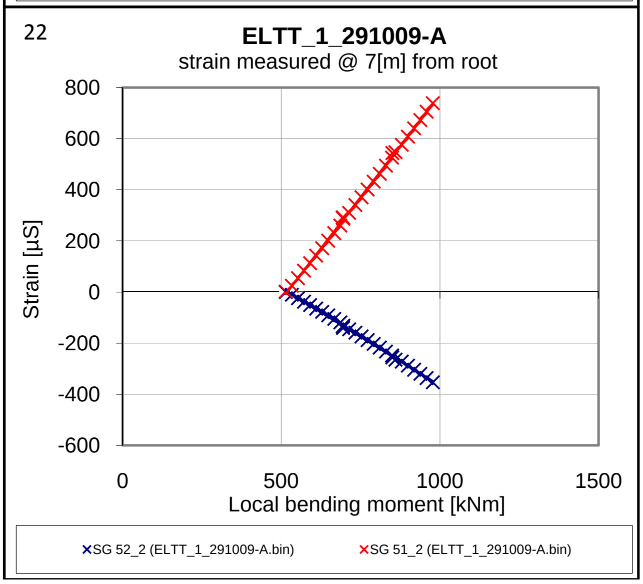
22
ELTT_1_291009-A
strain measured @ 7[m] from root
Strain [µS]
800
600
400
200
0
-200
-400
-600
0
500
1000
1500
Local bending moment [kNm]
SG 52_2 (ELTT_1_291009-A.bin)
SG 51_2 (ELTT_1_291009-A.bin)

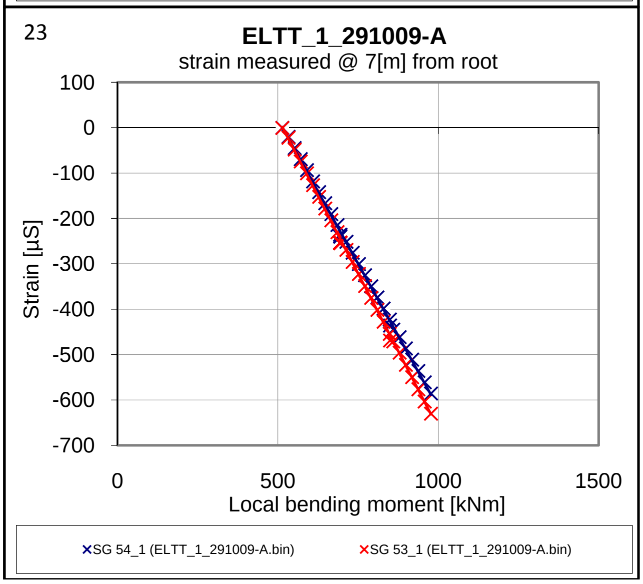
23
ELTT_1_291009-A
strain measured @ 7[m] from root
Strain [µS]
100
0
-100
-200
-300
-400
-500
-600
-700
0
500
1000
1500
Local bending moment [kNm]
SG 54_1 (ELTT_1_291009-A.bin)
SG 53_1 (ELTT_1_291009-A.bin)

B1

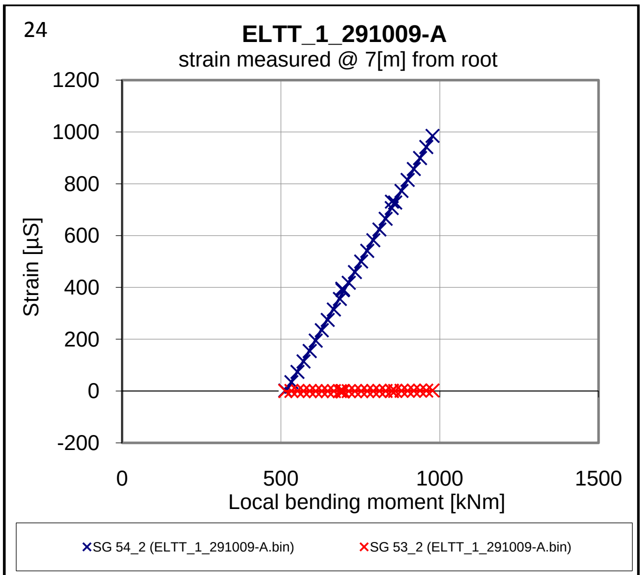
24
ELTT_1_291009-A
strain measured @ 7[m] from root
Strain [µS]
1200
1000
800
600
400
200
0
-200
0
500
1000
1500
Local bending moment [kNm]
SG 54_2 (ELTT_1_291009-A.bin)
SG 53_2 (ELTT_1_291009-A.bin)

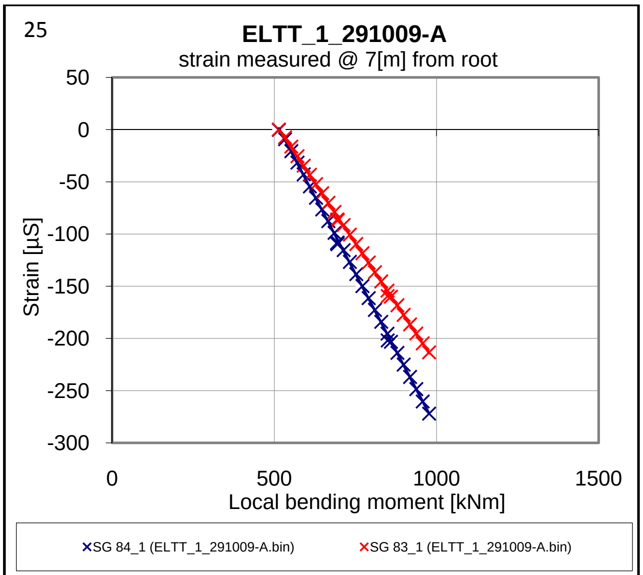
25
ELTT_1_291009-A
strain measured @ 7[m] from root
Strain [µS]
50
0
-50
-100
-150
-200
-250
-300
0
500
1000
1500
Local bending moment [kNm]
SG 84_1 (ELTT_1_291009-A.bin)
SG 83_1 (ELTT_1_291009-A.bin)

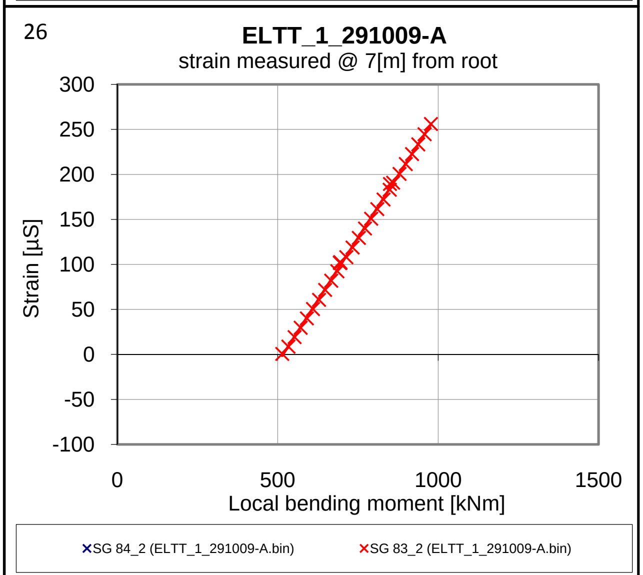
26
ELTT_1_291009-A
strain measured @ 7[m] from root
Strain [µS]
300
250
200
150
100
50
0
-50
-100
0
500
1000
1500
Local bending moment [kNm]
SG 84_2 (ELTT_1_291009-A.bin)
SG 83_2 (ELTT_1_291009-A.bin)

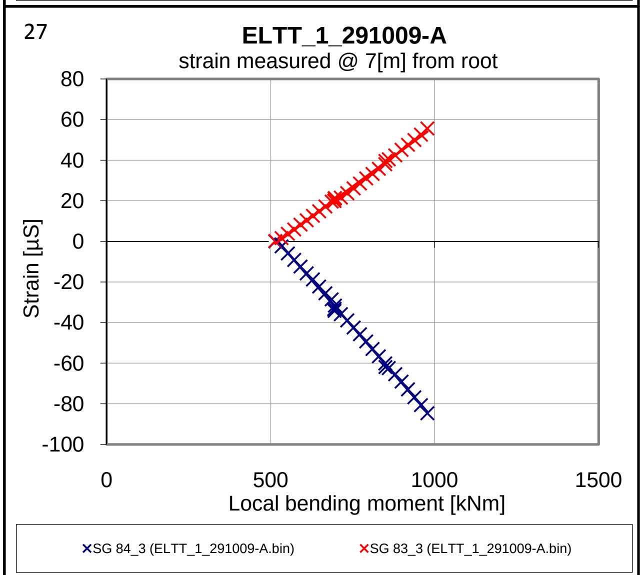
27
ELTT_1_291009-A
strain measured @ 7[m] from root
Strain [µS]
80
60
40
20
0
-20
-40
-60
-80
-100
0
500
1000
1500
Local bending moment [kNm]
SG 84_3 (ELTT_1_291009-A.bin)
SG 83_3 (ELTT_1_291009-A.bin)

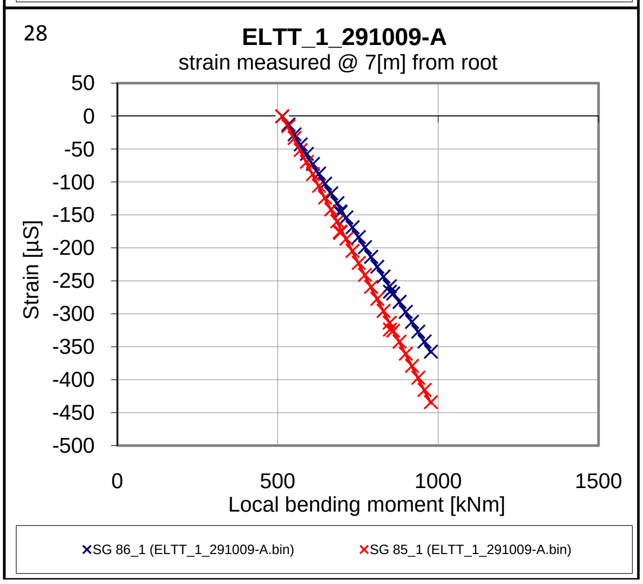
28
ELTT_1_291009-A
strain measured @ 7[m] from root
Strain [µS]
50
0
-50
-100
-150
-200
-250
-300
-350
-400
-450
-500
0
500
1000
1500
Local bending moment [kNm]
SG 86_1 (ELTT_1_291009-A.bin)
SG 85_1 (ELTT_1_291009-A.bin)

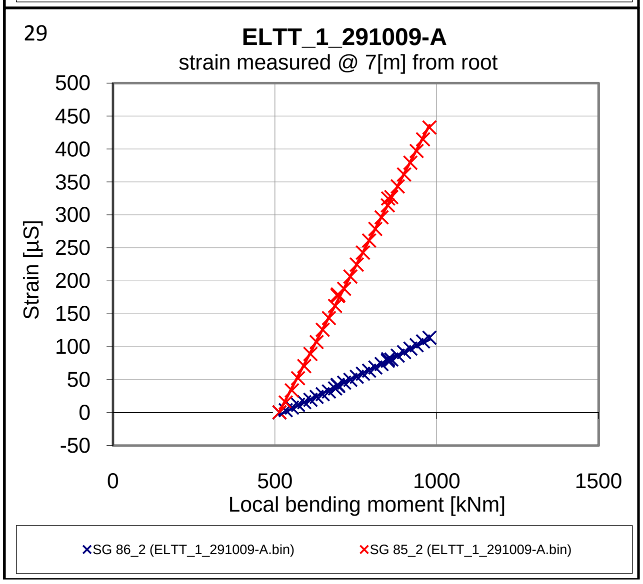
29
ELTT_1_291009-A
strain measured @ 7[m] from root
Strain [µS]
500
450
400
350
300
250
200
150
100
50
0
-50
0
500
1000
1500
Local bending moment [kNm]
SG 86_2 (ELTT_1_291009-A.bin)
SG 85_2 (ELTT_1_291009-A.bin)

B1

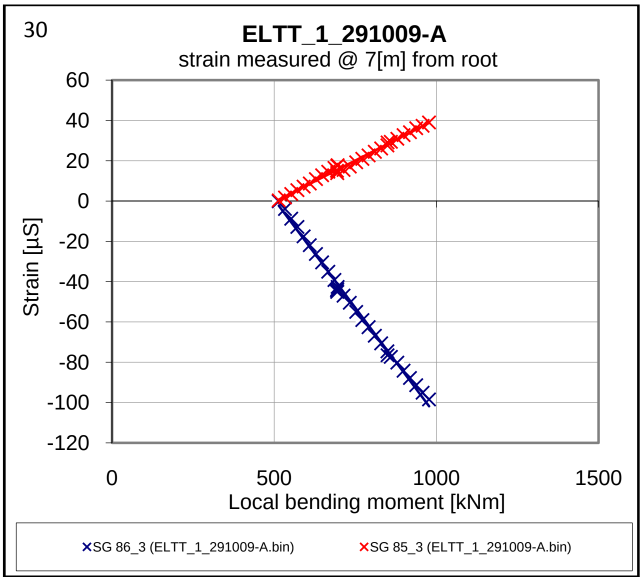
30
ELTT_1_291009-A
strain measured @ 7[m] from root
Strain [µS]
60
40
20
0
-20
-40
-60
-80
-100
-120
0
500
1000
1500
Local bending moment [kNm]
SG 86_3 (ELTT_1_291009-A.bin)
SG 85_3 (ELTT_1_291009-A.bin)

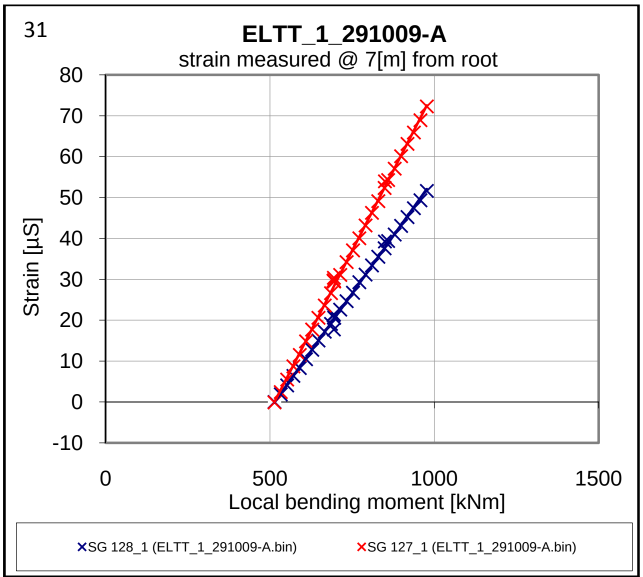
31
ELTT_1_291009-A
strain measured @ 7[m] from root
Strain [µS]
80
70
60
50
40
30
20
10
0
-10
0
500
1000
1500
Local bending moment [kNm]
SG 128_1 (ELTT_1_291009-A.bin)
SG 127_1 (ELTT_1_291009-A.bin)

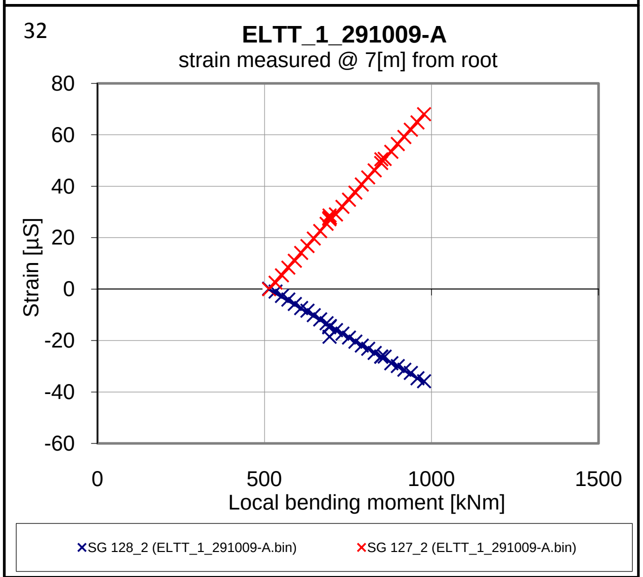
32
ELTT_1_291009-A
strain measured @ 7[m] from root
Strain [µS]
80
60
40
20
0
-20
-40
-60
0
500
1000
1500
Local bending moment [kNm]
SG 128_2 (ELTT_1_291009-A.bin)
SG 127_2 (ELTT_1_291009-A.bin)

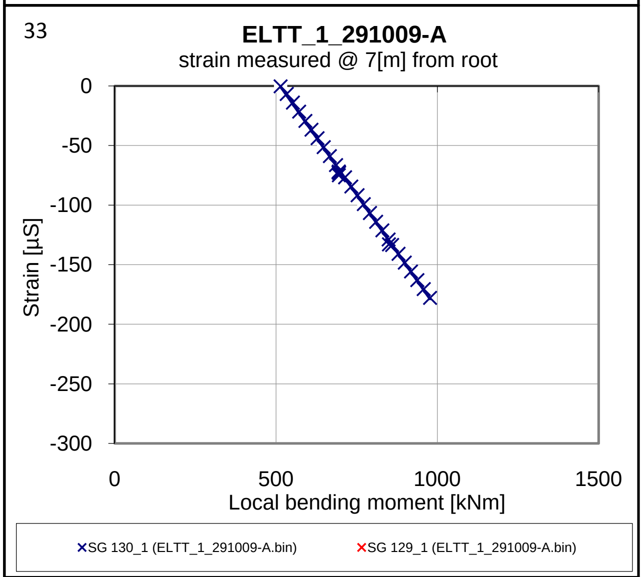
33
ELTT_1_291009-A
strain measured @ 7[m] from root
Strain [µS]
0
-50
-100
-150
-200
-250
-300
0
500
1000
1500
Local bending moment [kNm]
SG 130_1 (ELTT_1_291009-A.bin)
SG 129_1 (ELTT_1_291009-A.bin)

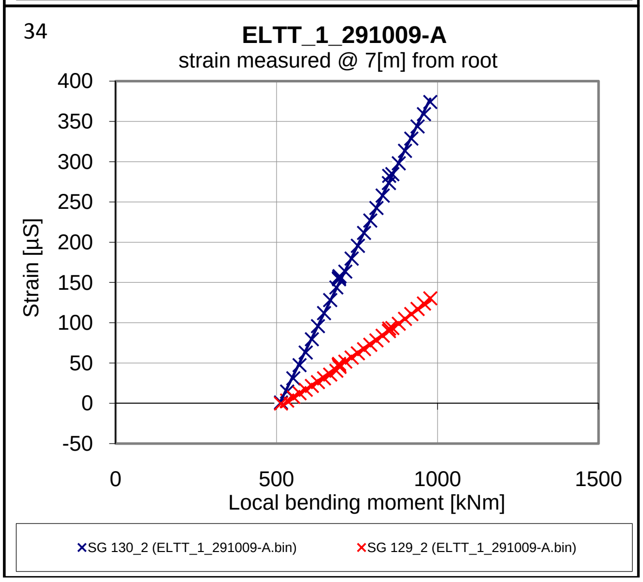
34
ELTT_1_291009-A
strain measured @ 7[m] from root
Strain [µS]
400
350
300
250
200
150
100
50
0
-50
0
500
1000
1500
Local bending moment [kNm]
SG 130_2 (ELTT_1_291009-A.bin)
SG 129_2 (ELTT_1_291009-A.bin)

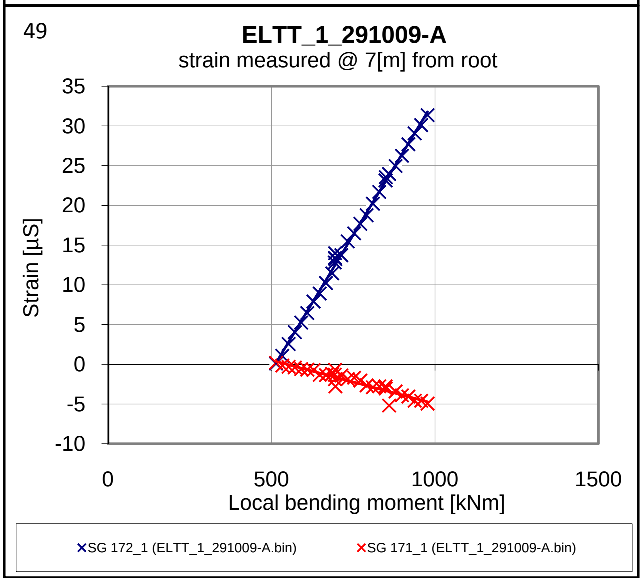
49
ELTT_1_291009-A
strain measured @ 7[m] from root
Strain [µS]
35
30
25
20
15
10
5
0
-5
-10
0
500
1000
1500
Local bending moment [kNm]
SG 172_1 (ELTT_1_291009-A.bin)
SG 171_1 (ELTT_1_291009-A.bin)

B1

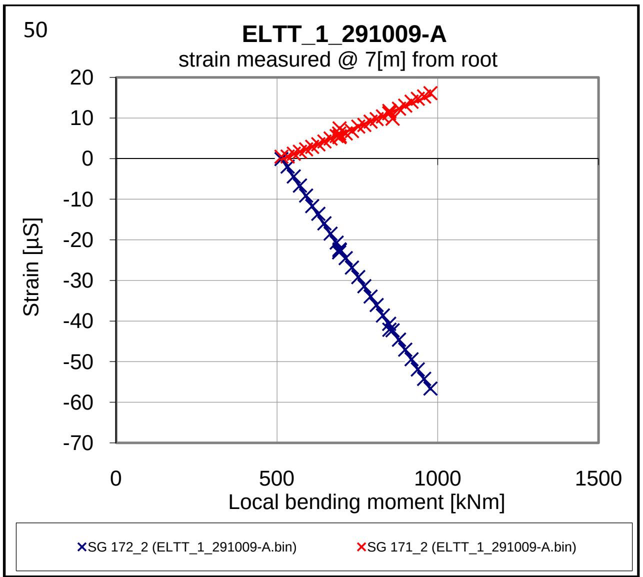
50
ELTT_1_291009-A
strain measured @ 7[m] from root
Strain [µS]
20
10
0
-10
-20
-30
-40
-50
-60
-70
0
500
1000
1500
Local bending moment [kNm]
SG 172_2 (ELTT_1_291009-A.bin)
SG 171_2 (ELTT_1_291009-A.bin)

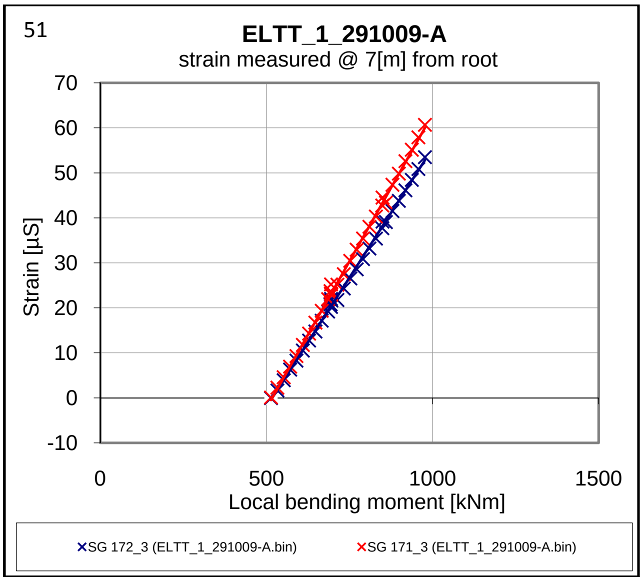
51
ELTT_1_291009-A
strain measured @ 7[m] from root
Strain [µS]
70
60
50
40
30
20
10
0
-10
0
500
1000
1500
Local bending moment [kNm]
SG 172_3 (ELTT_1_291009-A.bin)
SG 171_3 (ELTT_1_291009-A.bin)

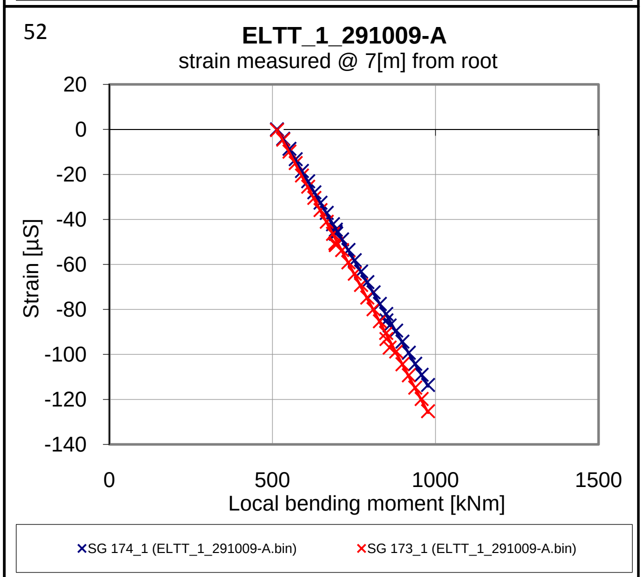
52
ELTT_1_291009-A
strain measured @ 7[m] from root
Strain [µS]
20
0
-20
-40
-60
-80
-100
-120
-140
0
500
1000
1500
Local bending moment [kNm]
SG 174_1 (ELTT_1_291009-A.bin)
SG 173_1 (ELTT_1_291009-A.bin)

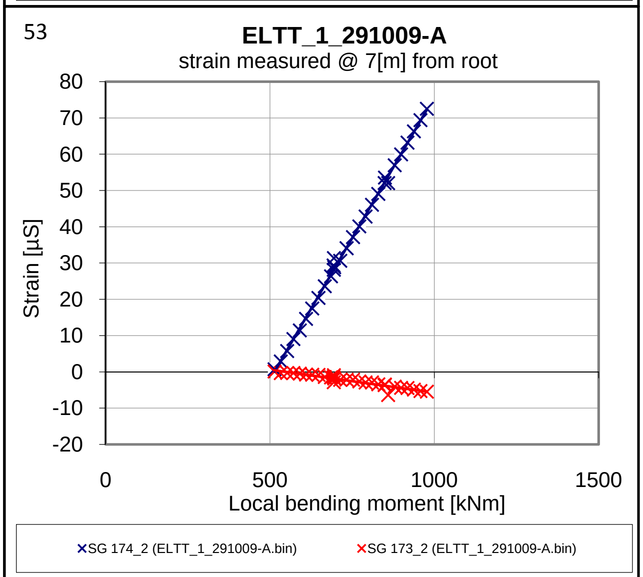
53
ELTT_1_291009-A
strain measured @ 7[m] from root
Strain [µS]
80
70
60
50
40
30
20
10
0
-10
-20
0
500
1000
1500
Local bending moment [kNm]
SG 174_2 (ELTT_1_291009-A.bin)
SG 173_2 (ELTT_1_291009-A.bin)

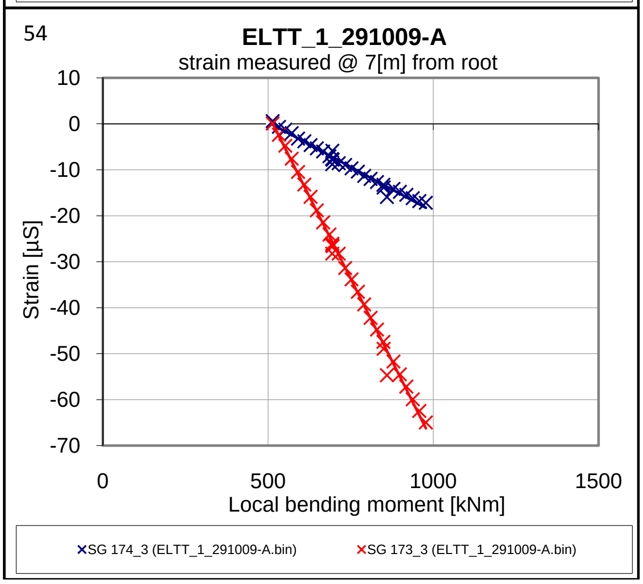
54
ELTT_1_291009-A
strain measured @ 7[m] from root
Strain [µS]
10
0
-10
-20
-30
-40
-50
-60
-70
0
500
1000
1500
Local bending moment [kNm]
SG 174_3 (ELTT_1_291009-A.bin)
SG 173_3 (ELTT_1_291009-A.bin)

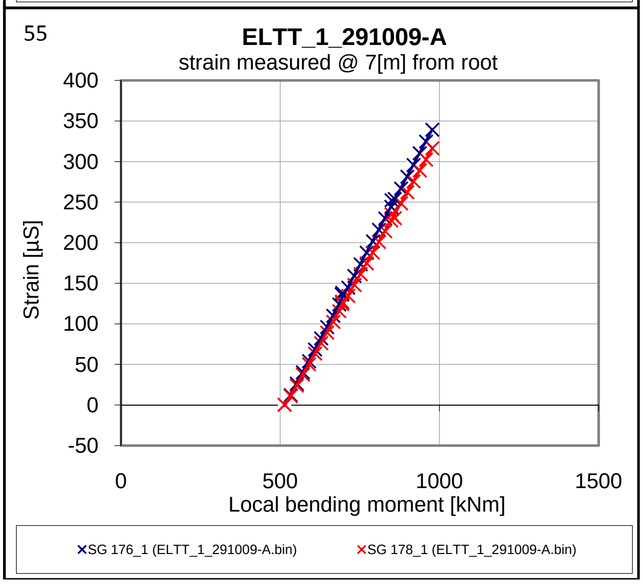
55
ELTT_1_291009-A
strain measured @ 7[m] from root
Strain [µS]
400
350
300
250
200
150
100
50
0
-50
0
500
1000
1500
Local bending moment [kNm]
SG 176_1 (ELTT_1_291009-A.bin)
SG 178_1 (ELTT_1_291009-A.bin)

B1

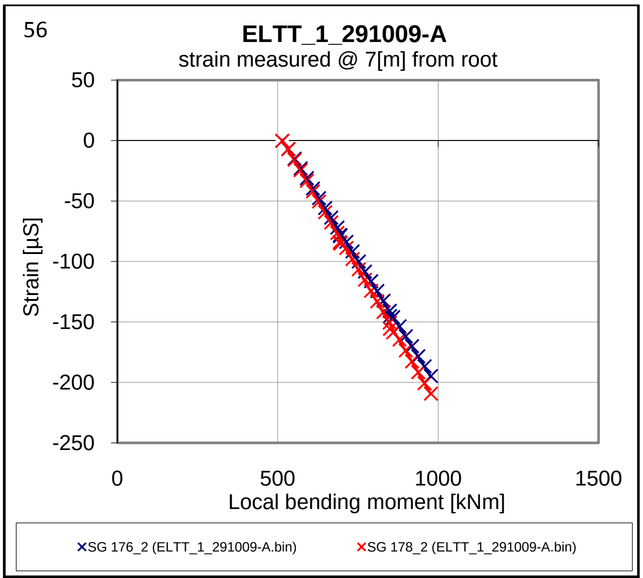
56
ELTT_1_291009-A
strain measured @ 7[m] from root
Strain [µS]
50
0
-50
-100
-150
-200
-250
0
500
1000
1500
Local bending moment [kNm]
SG 176_2 (ELTT_1_291009-A.bin)
SG 178_2 (ELTT_1_291009-A.bin)

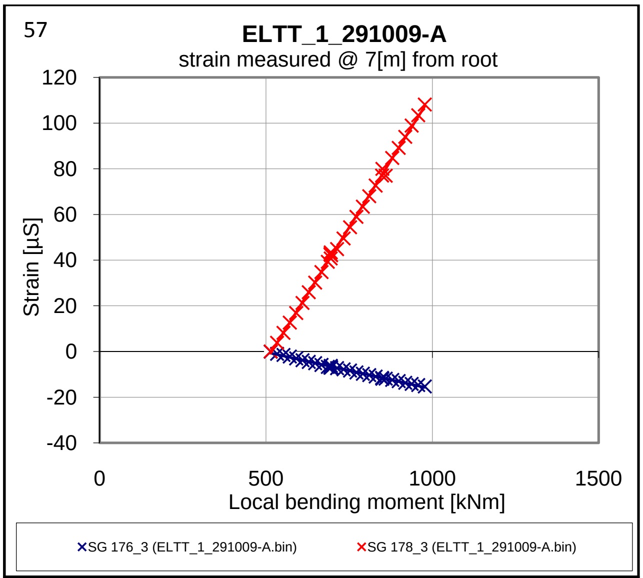
57
ELTT_1_291009-A
strain measured @ 7[m] from root
Strain [µS]
120
100
80
60
40
20
0
-20
-40
0
500
1000
1500
Local bending moment [kNm]
SG 176_3 (ELTT_1_291009-A.bin)
SG 178_3 (ELTT_1_291009-A.bin)

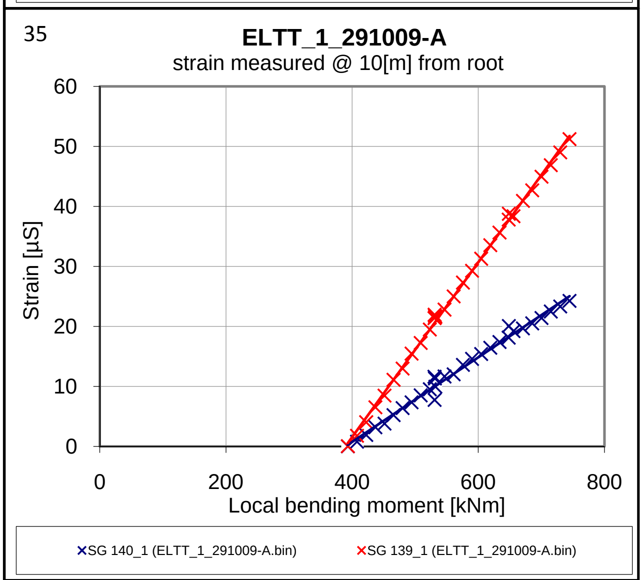
35
ELTT_1_291009-A
strain measured @ 10[m] from root
Strain [µS]
60
50
40
30
20
10
0
0
200
400
600
800
Local bending moment [kNm]
SG 140_1 (ELTT_1_291009-A.bin)
SG 139_1 (ELTT_1_291009-A.bin)

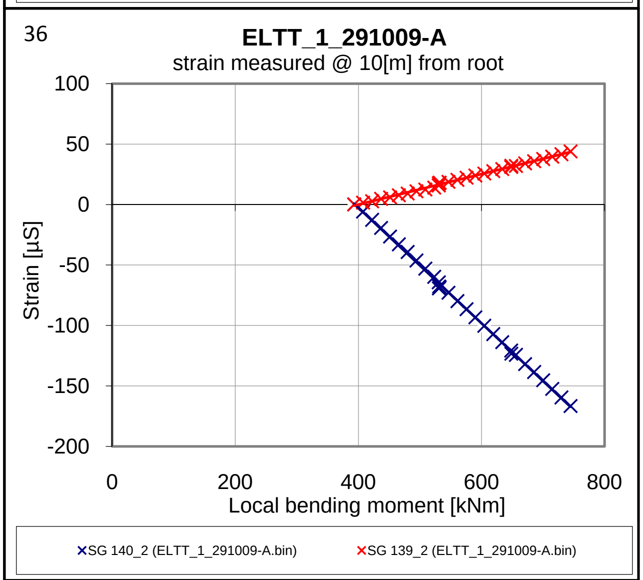
36
ELTT_1_291009-A
strain measured @ 10[m] from root
Strain [µS]
100
50
0
-50
-100
-150
-200
0
200
400
600
800
Local bending moment [kNm]
SG 140_2 (ELTT_1_291009-A.bin)
SG 139_2 (ELTT_1_291009-A.bin)

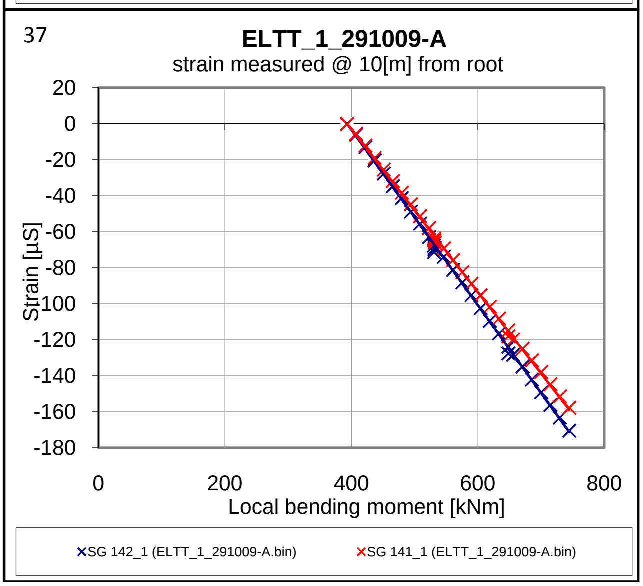
37
ELTT_1_291009-A
strain measured @ 10[m] from root
Strain [µS]
20
0
-20
-40
-60
-80
-100
-120
-140
-160
-180
0
200
400
600
800
Local bending moment [kNm]
SG 142_1 (ELTT_1_291009-A.bin)
SG 141_1 (ELTT_1_291009-A.bin)

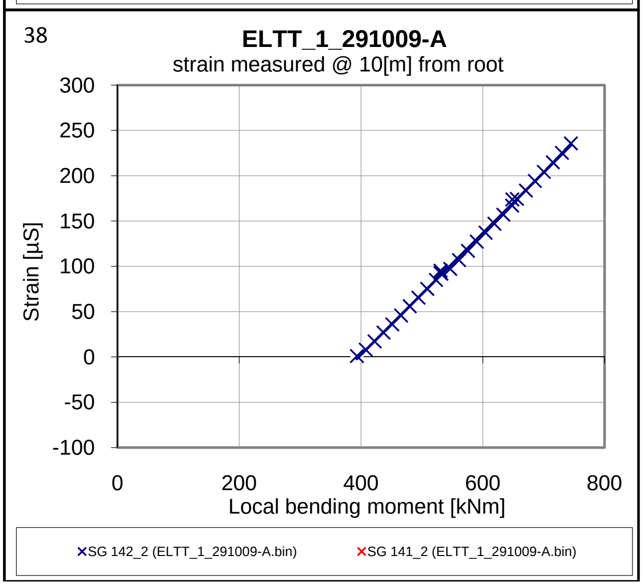
38
ELTT_1_291009-A
strain measured @ 10[m] from root
Strain [µS]
300
250
200
150
100
50
0
-50
-100
0
200
400
600
800
Local bending moment [kNm]
SG 142_2 (ELTT_1_291009-A.bin)
SG 141_2 (ELTT_1_291009-A.bin)

B1

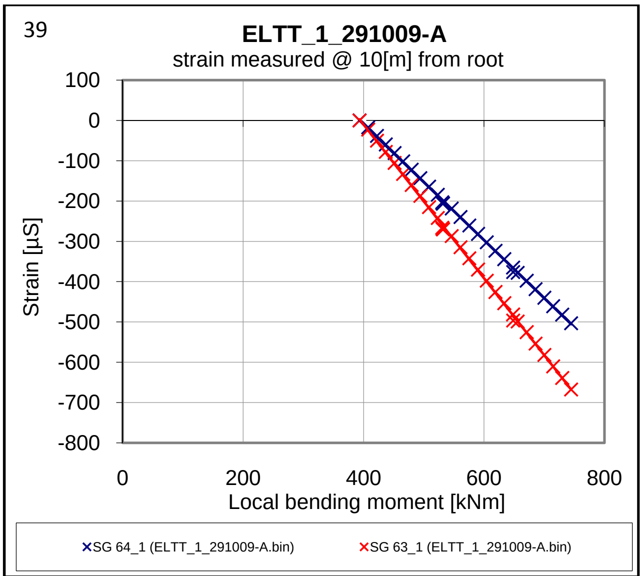
39
ELTT_1_291009-A
strain measured @ 10[m] from root
Strain [µS]
100
0
-100
-200
-300
-400
-500
-600
-700
-800
0
200
400
600
800
Local bending moment [kNm]
SG 64_1 (ELTT_1_291009-A.bin)
SG 63_1 (ELTT_1_291009-A.bin)

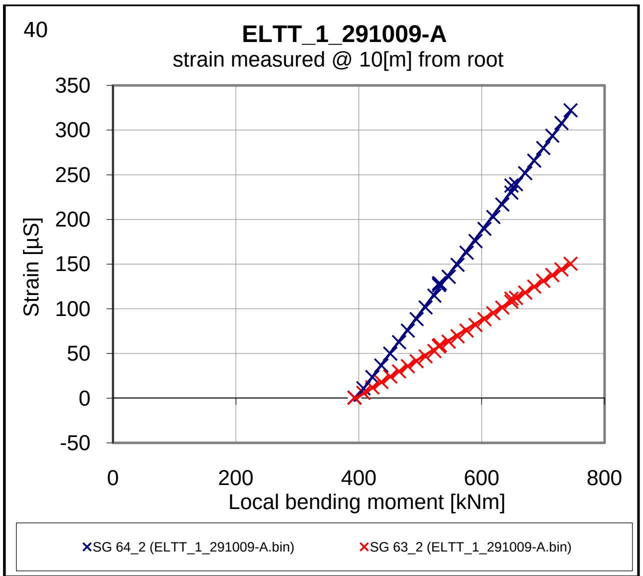
40
ELTT_1_291009-A
strain measured @ 10[m] from root
Strain [µS]
350
300
250
200
150
100
50
0
-50
0
200
400
600
800
Local bending moment [kNm]
SG 64_2 (ELTT_1_291009-A.bin)
SG 63_2 (ELTT_1_291009-A.bin)

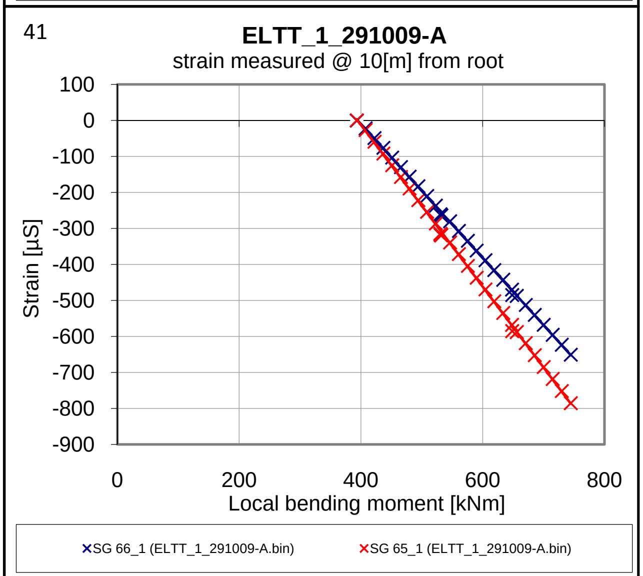
41
ELTT_1_291009-A
strain measured @ 10[m] from root
Strain [µS]
100
0
-100
-200
-300
-400
-500
-600
-700
-800
-900
0
200
400
600
800
Local bending moment [kNm]
SG 66_1 (ELTT_1_291009-A.bin)
SG 65_1 (ELTT_1_291009-A.bin)

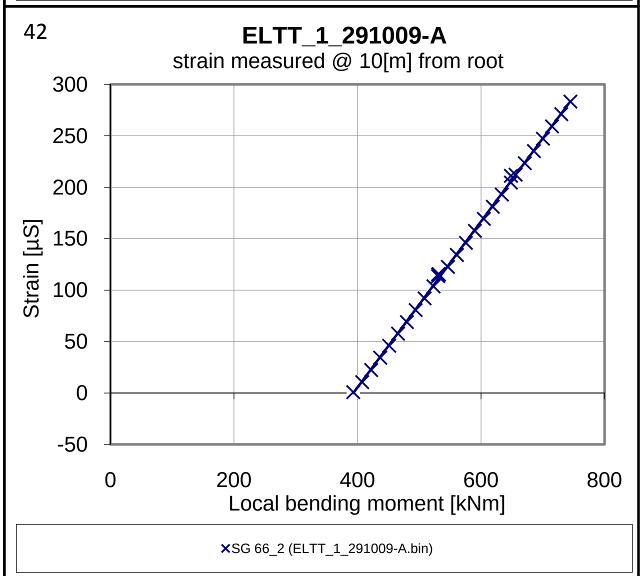
42
ELTT_1_291009-A
strain measured @ 10[m] from root
Strain [µS]
300
250
200
150
100
50
0
-50
0
200
400
600
800
Local bending moment [kNm]
SG 66_2 (ELTT_1_291009-A.bin)

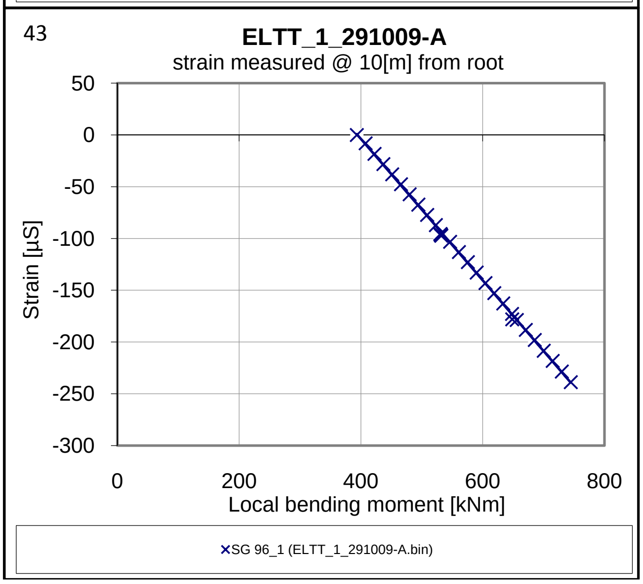
43
ELTT_1_291009-A
strain measured @ 10[m] from root
Strain [µS]
50
0
-50
-100
-150
-200
-250
-300
0
200
400
600
800
Local bending moment [kNm]
SG 96_1 (ELTT_1_291009-A.bin)

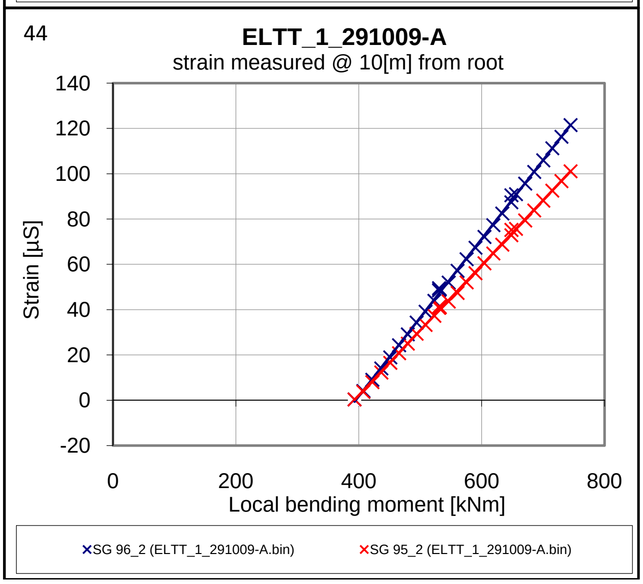
44
ELTT_1_291009-A
strain measured @ 10[m] from root
Strain [µS]
140
120
100
80
60
40
20
0
-20
0
200
400
600
800
Local bending moment [kNm]
SG 96_2 (ELTT_1_291009-A.bin)
SG 95_2 (ELTT_1_291009-A.bin)

B1

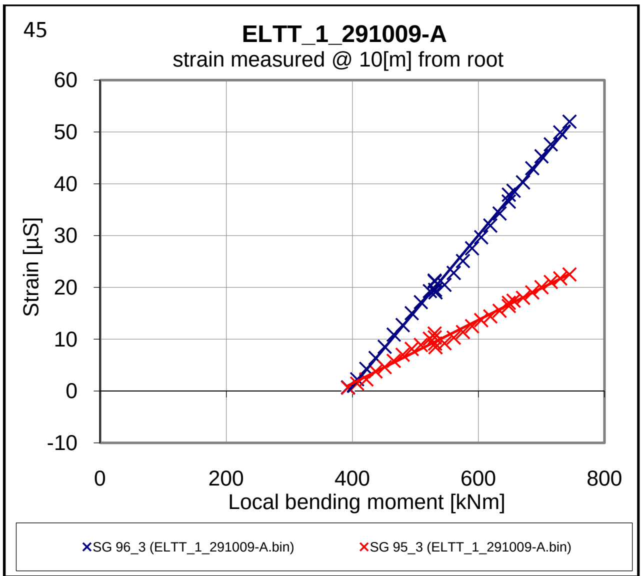
45
ELTT_1_291009-A
strain measured @ 10[m] from root
Strain [µS]
60
50
40
30
20
10
0
-10
0
200
400
600
800
Local bending moment [kNm]
SG 96_3 (ELTT_1_291009-A.bin)
SG 95_3 (ELTT_1_291009-A.bin)

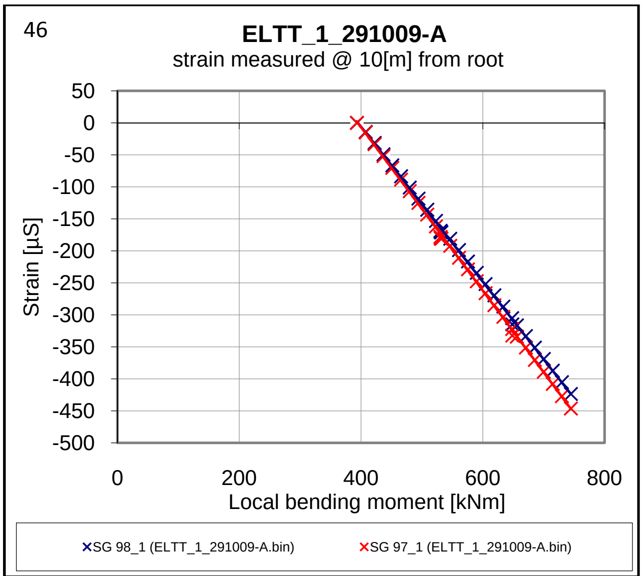
46
ELTT_1_291009-A
strain measured @ 10[m] from root
Strain [µS]
50
0
-50
-100
-150
-200
-250
-300
-350
-400
-450
-500
0
200
400
600
800
Local bending moment [kNm]
SG 98_1 (ELTT_1_291009-A.bin)
SG 97_1 (ELTT_1_291009-A.bin)

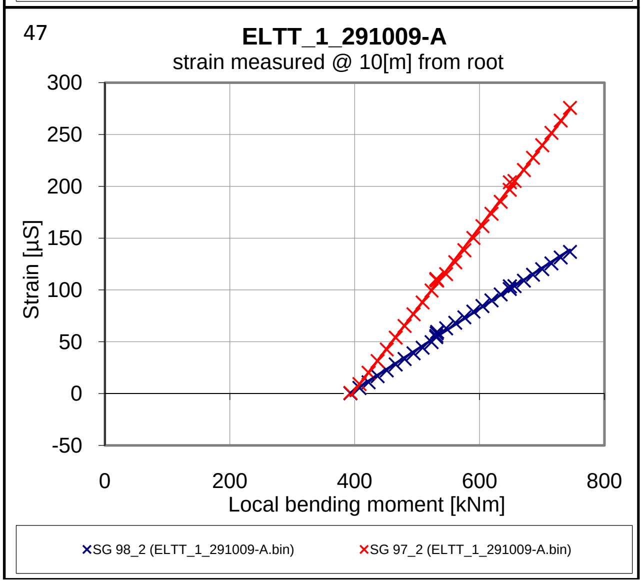
47
ELTT_1_291009-A
strain measured @ 10[m] from root
Strain [µS]
300
250
200
150
100
50
0
-50
0
200
400
600
800
Local bending moment [kNm]
SG 98_2 (ELTT_1_291009-A.bin)
SG 97_2 (ELTT_1_291009-A.bin)

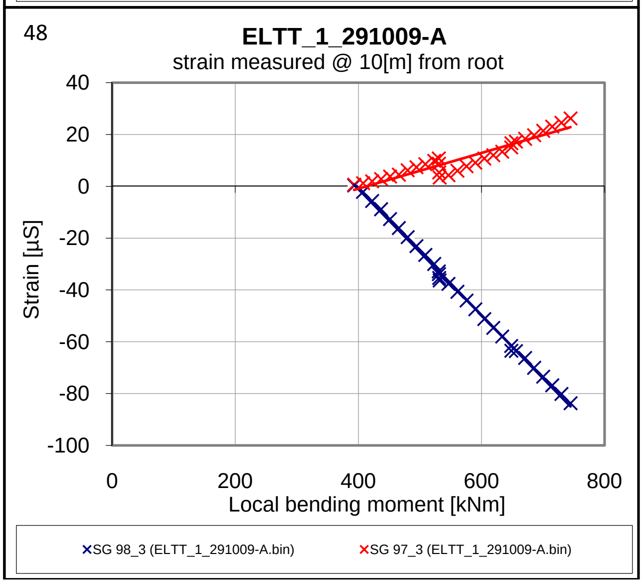
48
ELTT_1_291009-A
strain measured @ 10[m] from root
Strain [µS]
40
20
0
-20
-40
-60
-80
-100
0
200
400
600
800
Local bending moment [kNm]
SG 98_3 (ELTT_1_291009-A.bin)
SG 97_3 (ELTT_1_291009-A.bin)

B1

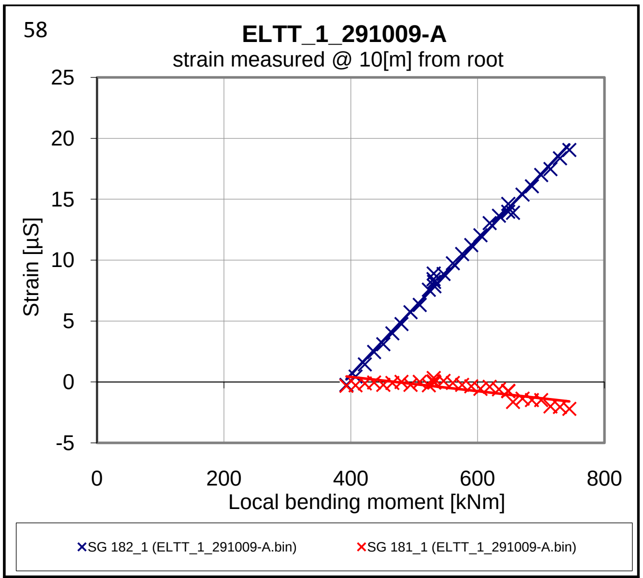
58
ELTT_1_291009-A
strain measured @ 10[m] from root
Strain [µS]
Local bending moment [kNm]
25
20
15
10
5
0
-5
0
200
400
600
800
SG 182_1 (ELTT_1_291009-A.bin)
SG 181_1 (ELTT_1_291009-A.bin)

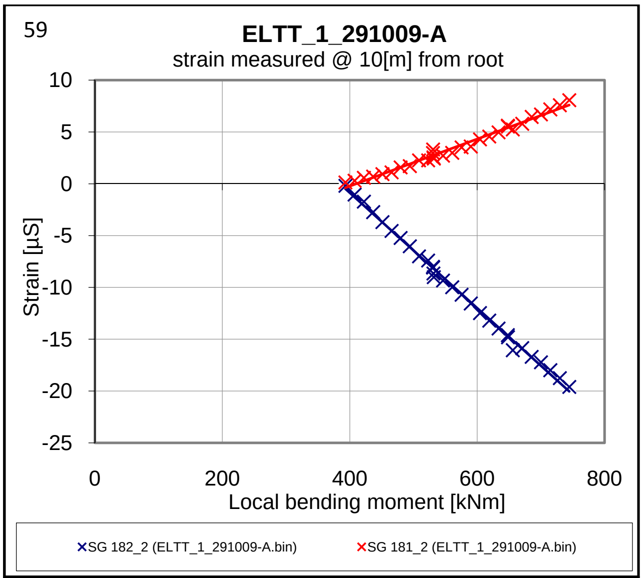
59
ELTT_1_291009-A
strain measured @ 10[m] from root
Strain [µS]
Local bending moment [kNm]
10
5
0
-5
-10
-15
-20
-25
0
200
400
600
800
SG 182_2 (ELTT_1_291009-A.bin)
SG 181_2 (ELTT_1_291009-A.bin)

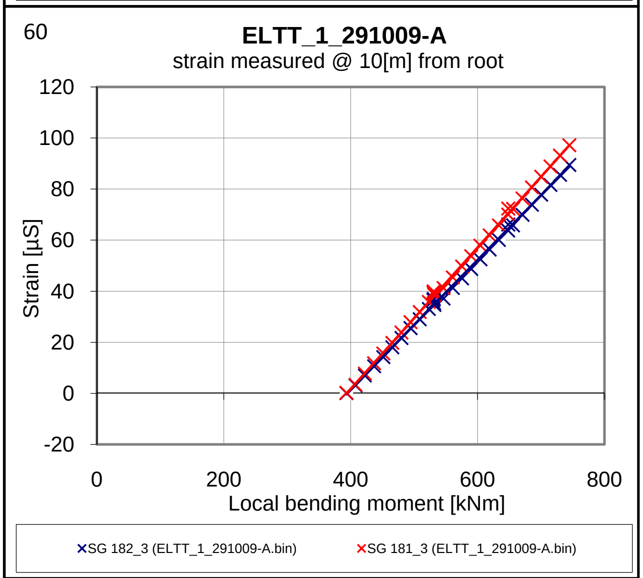
60
ELTT_1_291009-A
strain measured @ 10[m] from root
Strain [µS]
Local bending moment [kNm]
120
100
80
60
40
20
0
-20
0
200
400
600
800
SG 182_3 (ELTT_1_291009-A.bin)
SG 181_3 (ELTT_1_291009-A.bin)

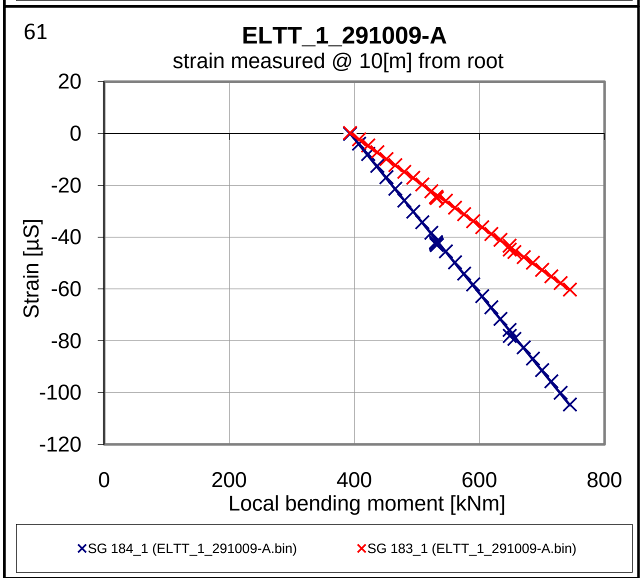
61
ELTT_1_291009-A
strain measured @ 10[m] from root
Strain [µS]
Local bending moment [kNm]
20
0
-20
-40
-60
-80
-100
-120
0
200
400
600
800
SG 184_1 (ELTT_1_291009-A.bin)
SG 183_1 (ELTT_1_291009-A.bin)

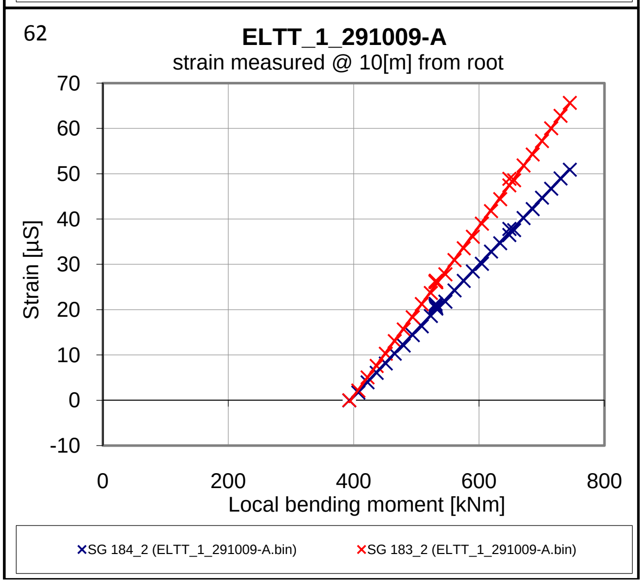
62
ELTT_1_291009-A
strain measured @ 10[m] from root
Strain [µS]
Local bending moment [kNm]
70
60
50
40
30
20
10
0
-10
0
200
400
600
800
SG 184_2 (ELTT_1_291009-A.bin)
SG 183_2 (ELTT_1_291009-A.bin)

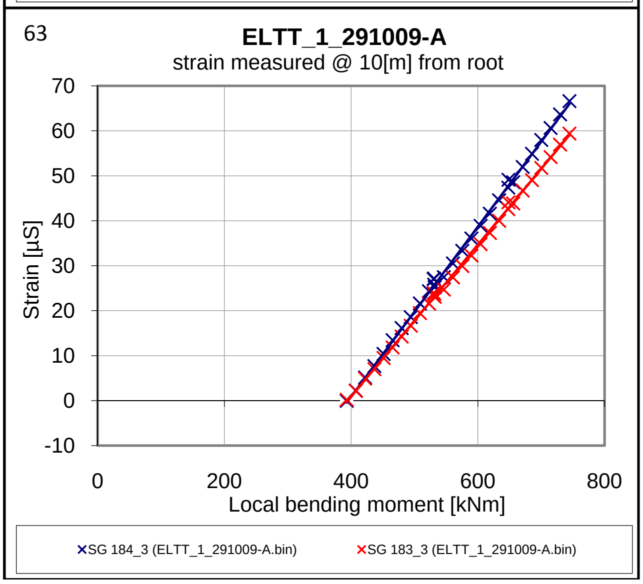
63
ELTT_1_291009-A
strain measured @ 10[m] from root
Strain [µS]
Local bending moment [kNm]
70
60
50
40
30
20
10
0
-10
0
200
400
600
800
SG 184_3 (ELTT_1_291009-A.bin)
SG 183_3 (ELTT_1_291009-A.bin)

B1

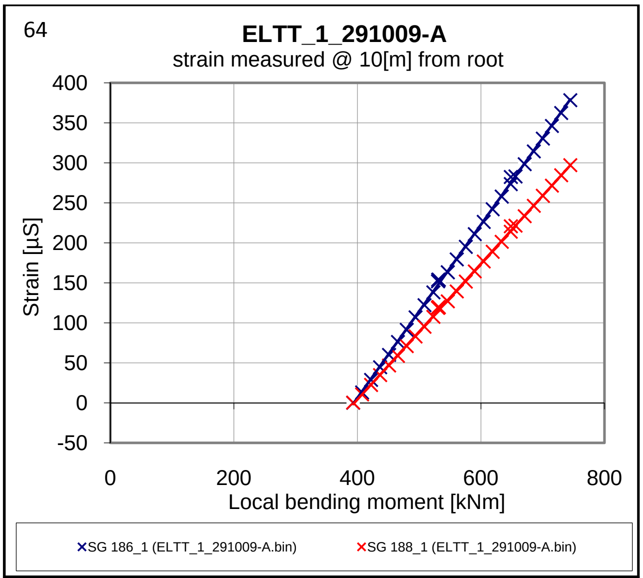
64
ELTT_1_291009-A
strain measured @ 10[m] from root
Strain [µS]
400
350
300
250
200
150
100
50
0
-50
0
200
400
600
800
Local bending moment [kNm]
SG 186_1 (ELTT_1_291009-A.bin)
SG 188_1 (ELTT_1_291009-A.bin)

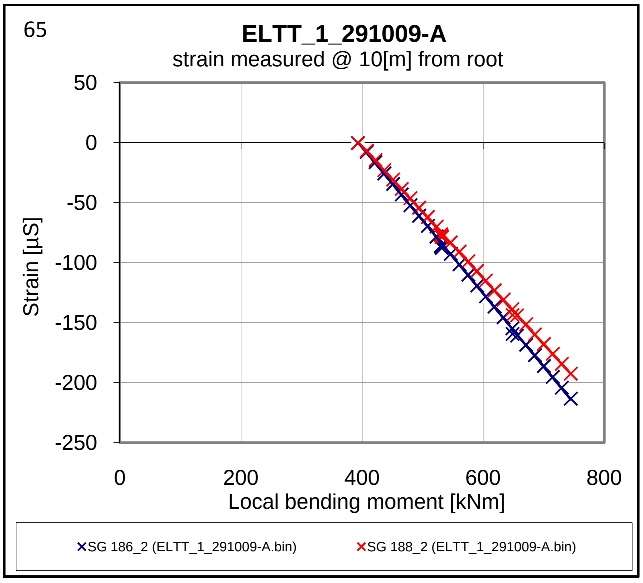
65
ELTT_1_291009-A
strain measured @ 10[m] from root
Strain [µS]
50
0
-50
-100
-150
-200
-250
0
200
400
600
800
Local bending moment [kNm]
SG 186_2 (ELTT_1_291009-A.bin)
SG 188_2 (ELTT_1_291009-A.bin)

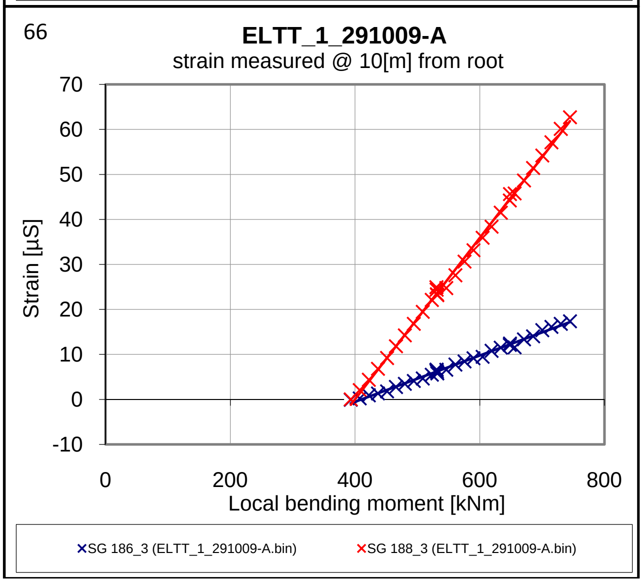
66
ELTT_1_291009-A
strain measured @ 10[m] from root
Strain [µS]
70
60
50
40
30
20
10
0
-10
0
200
400
600
800
Local bending moment [kNm]
SG 186_3 (ELTT_1_291009-A.bin)
SG 188_3 (ELTT_1_291009-A.bin)

B2 Measurements obtained from strain gauges in:
Global section in test ELTT_2-101109_A

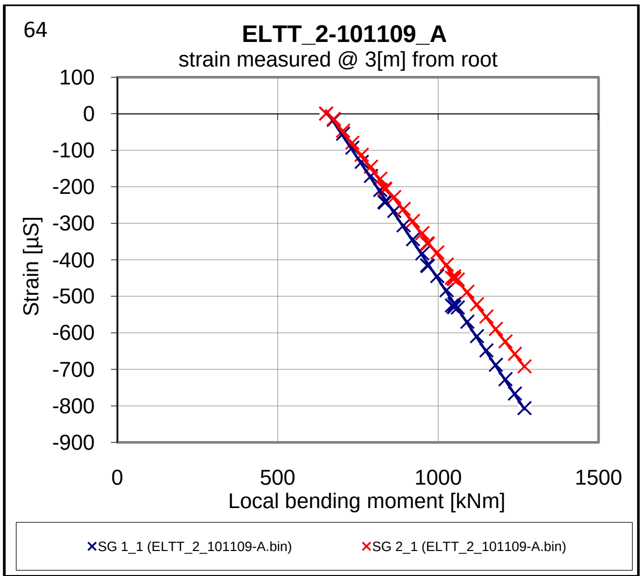

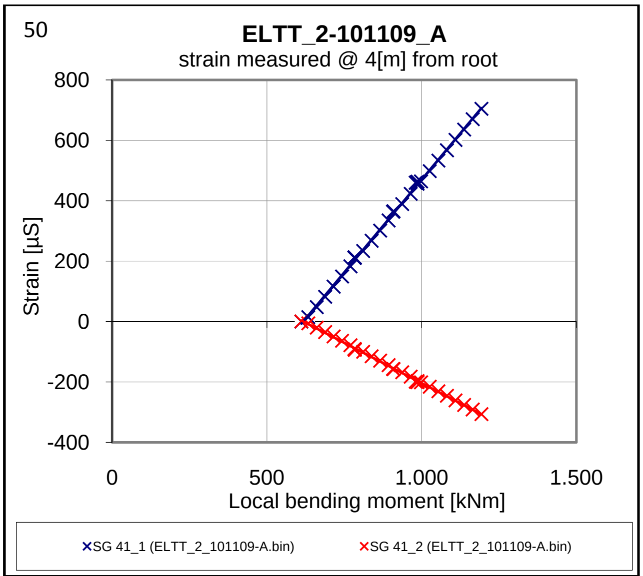

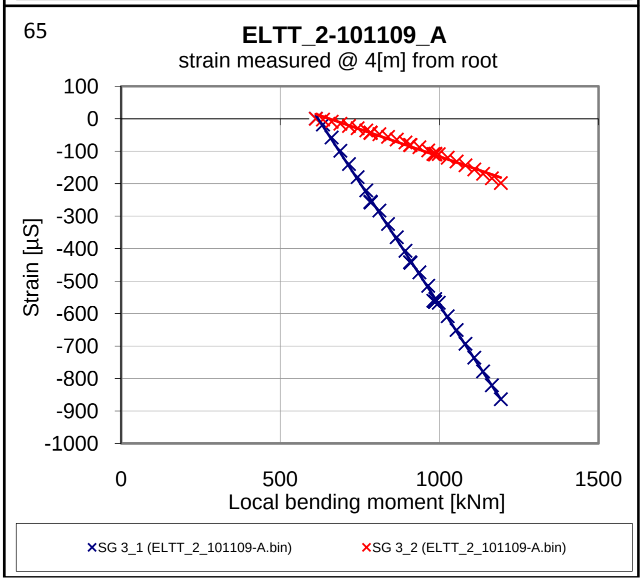

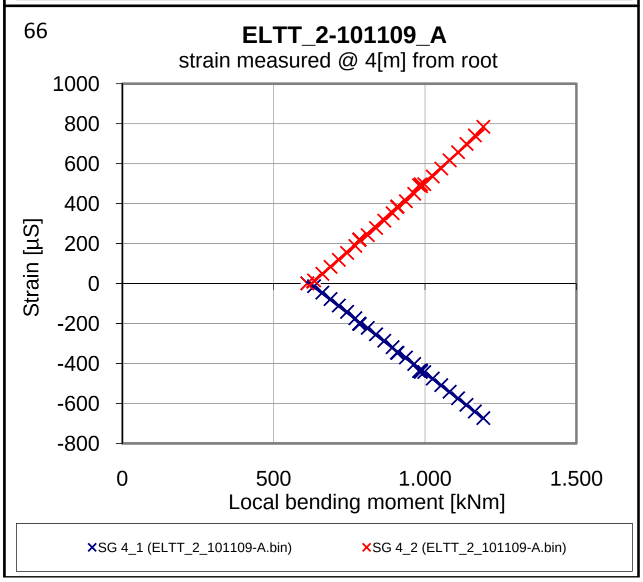

B2

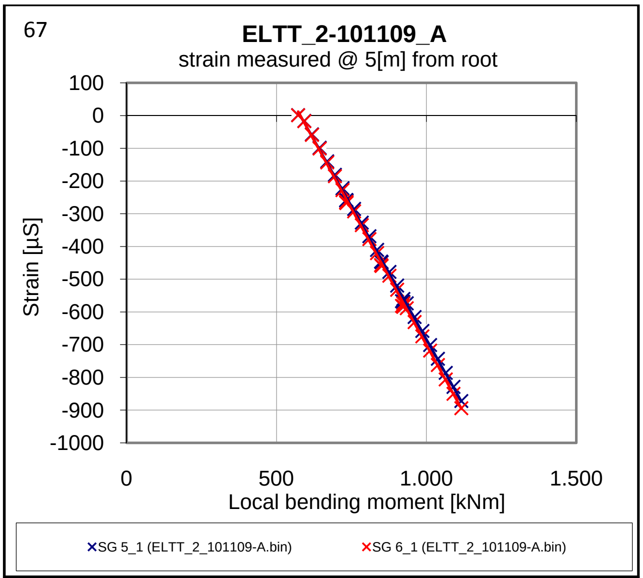
67
ELTT_2-101109_A
strain measured @ 5[m] from root
Strain [µS]
100
0
-100
-200
-300
-400
-500
-600
-700
-800
-900
-1000
0
500
1.000
1.500
Local bending moment [kNm]
SG 5_1 (ELTT_2_101109-A.bin)
SG 6_1 (ELTT_2_101109-A.bin)

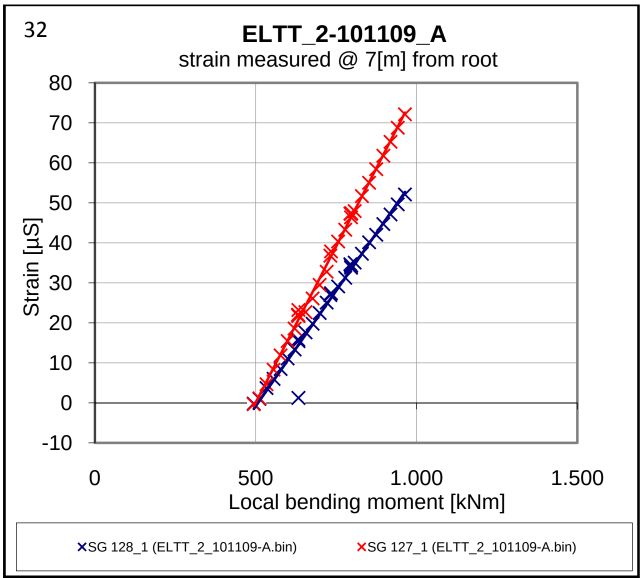
32
ELTT_2-101109_A
strain measured @ 7[m] from root
Strain [µS]
80
70
60
50
40
30
20
10
0
-10
0
500
1.000
1.500
Local bending moment [kNm]
SG 128_1 (ELTT_2_101109-A.bin)
SG 127_1 (ELTT_2_101109-A.bin)

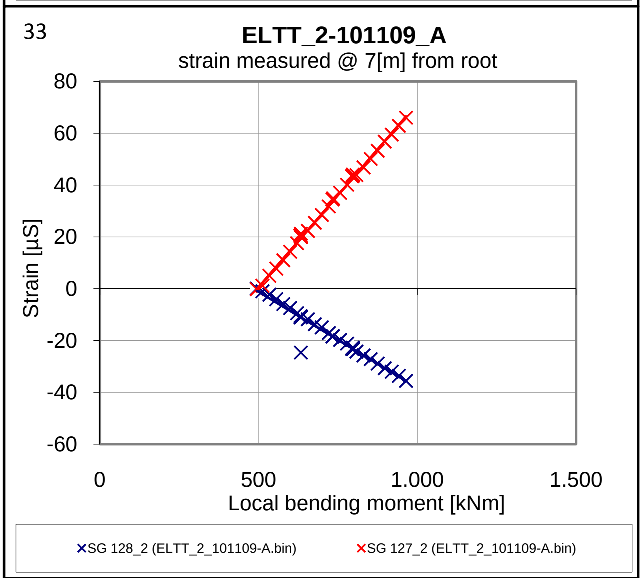
33
ELTT_2-101109_A
strain measured @ 7[m] from root
Strain [µS]
80
60
40
20
0
-20
-40
-60
0
500
1.000
1.500
Local bending moment [kNm]
SG 128_2 (ELTT_2_101109-A.bin)
SG 127_2 (ELTT_2_101109-A.bin)

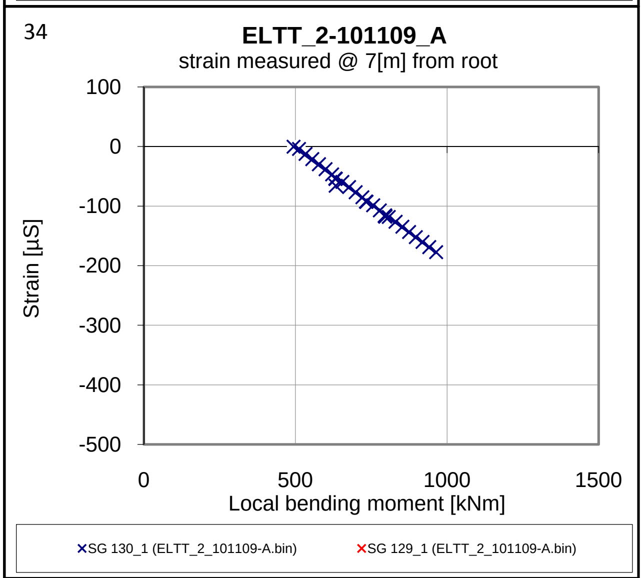
34
ELTT_2-101109_A
strain measured @ 7[m] from root
Strain [µS]
100
0
-100
-200
-300
-400
-500
0
500
1000
1500
Local bending moment [kNm]
SG 130_1 (ELTT_2_101109-A.bin)
SG 129_1 (ELTT_2_101109-A.bin)

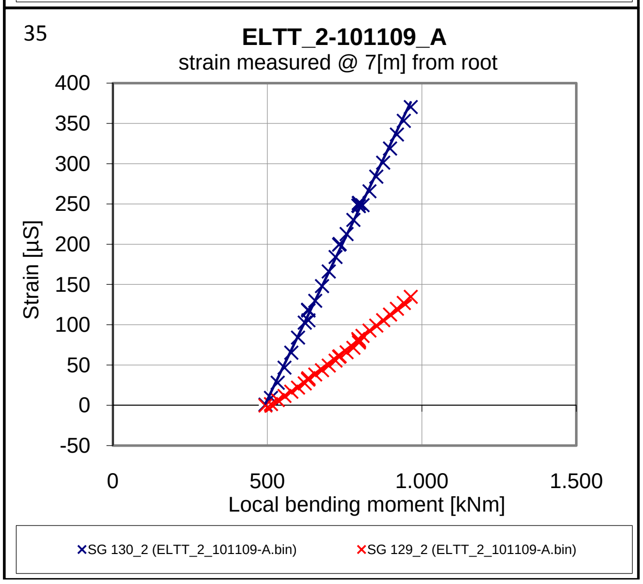
35
ELTT_2-101109_A
strain measured @ 7[m] from root
Strain [µS]
400
350
300
250
200
150
100
50
0
-50
0
500
1.000
1.500
Local bending moment [kNm]
SG 130_2 (ELTT_2_101109-A.bin)
SG 129_2 (ELTT_2_101109-A.bin)

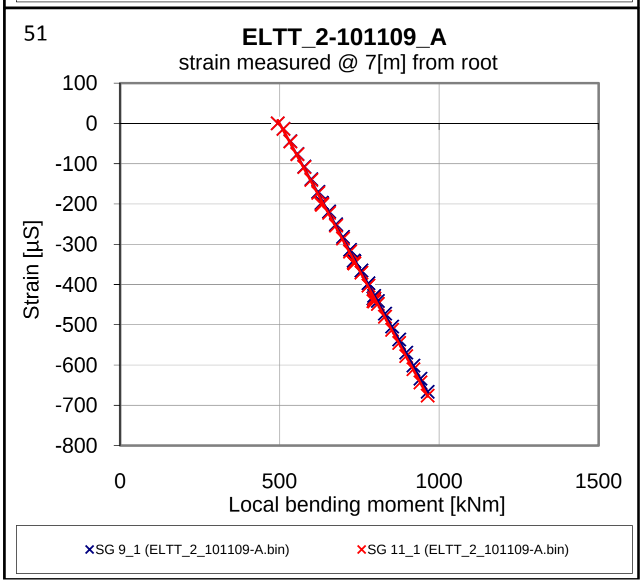
51
ELTT_2-101109_A
strain measured @ 7[m] from root
Strain [µS]
100
0
-100
-200
-300
-400
-500
-600
-700
-800
0
500
1000
1500
Local bending moment [kNm]
SG 9_1 (ELTT_2_101109-A.bin)
SG 11_1 (ELTT_2_101109-A.bin)

B2

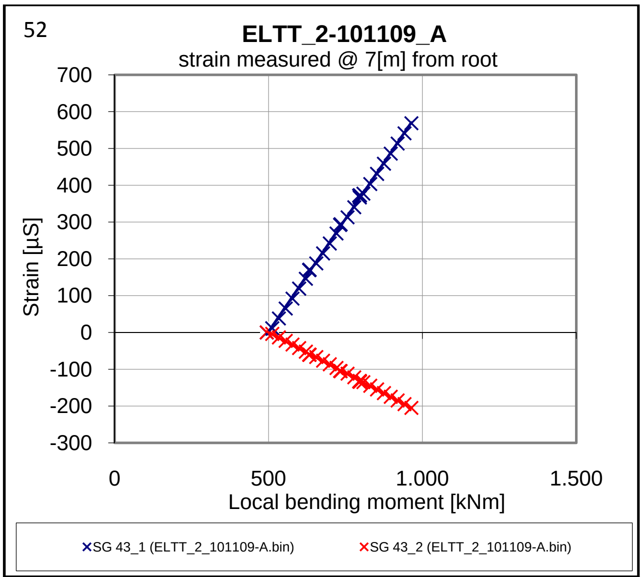
52
ELTT_2-101109_A
strain measured @ 7[m] from root
Strain [µS]
700
600
500
400
300
200
100
0
-100
-200
-300
0
500
1.000
1.500
Local bending moment [kNm]
SG 43_1 (ELTT_2_101109-A.bin)
SG 43_2 (ELTT_2_101109-A.bin)

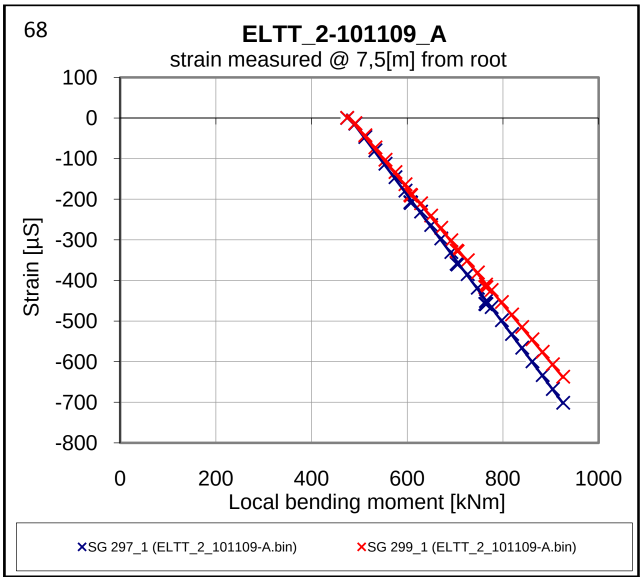
68
ELTT_2-101109_A
strain measured @ 7,5[m] from root
Strain [µS]
100
0
-100
-200
-300
-400
-500
-600
-700
-800
0
200
400
600
800
1000
Local bending moment [kNm]
SG 297_1 (ELTT_2_101109-A.bin)
SG 299_1 (ELTT_2_101109-A.bin)

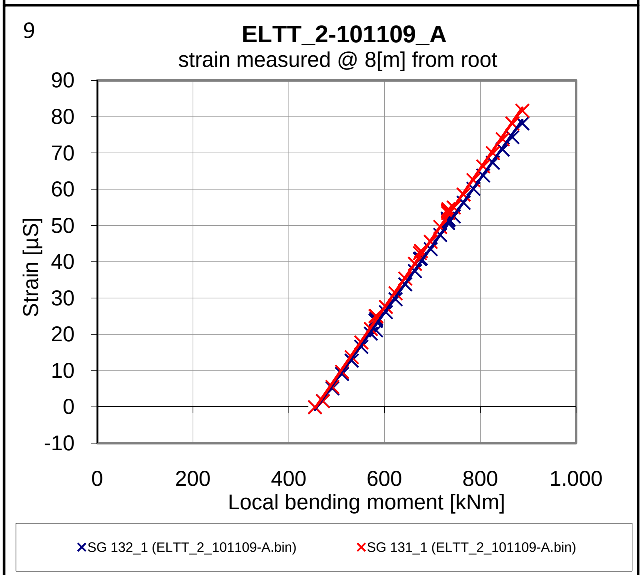
9
ELTT_2-101109_A
strain measured @ 8[m] from root
Strain [µS]
90
80
70
60
50
40
30
20
10
0
-10
0
200
400
600
800
1.000
Local bending moment [kNm]
SG 132_1 (ELTT_2_101109-A.bin)
SG 131_1 (ELTT_2_101109-A.bin)

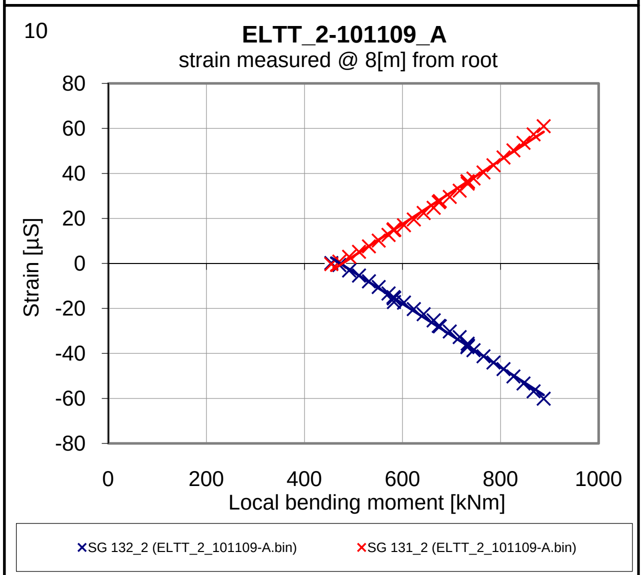
10
ELTT_2-101109_A
strain measured @ 8[m] from root
Strain [µS]
80
60
40
20
0
-20
-40
-60
-80
0
200
400
600
800
1000
Local bending moment [kNm]
SG 132_2 (ELTT_2_101109-A.bin)
SG 131_2 (ELTT_2_101109-A.bin)

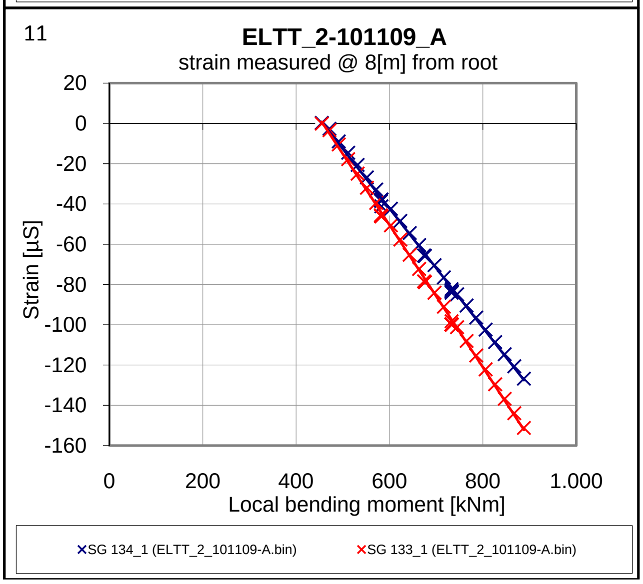
11
ELTT_2-101109_A
strain measured @ 8[m] from root
Strain [µS]
20
0
-20
-40
-60
-80
-100
-120
-140
-160
0
200
400
600
800
1.000
Local bending moment [kNm]
SG 134_1 (ELTT_2_101109-A.bin)
SG 133_1 (ELTT_2_101109-A.bin)

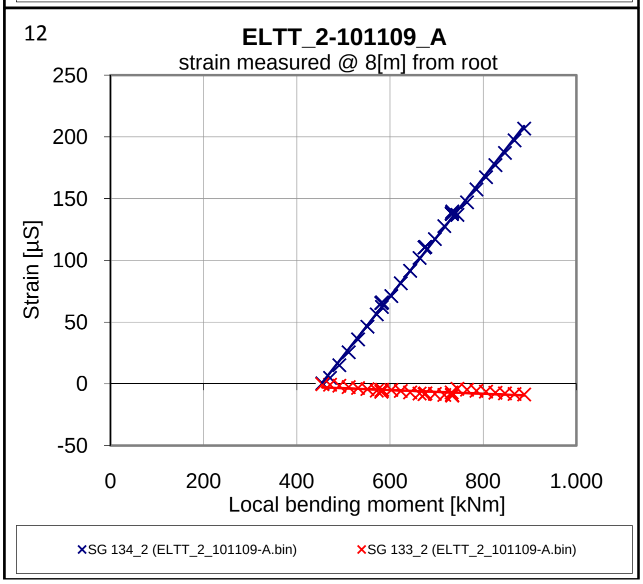
12
ELTT_2-101109_A
strain measured @ 8[m] from root
Strain [µS]
250
200
150
100
50
0
-50
0
200
400
600
800
1.000
Local bending moment [kNm]
SG 134_2 (ELTT_2_101109-A.bin)
SG 133_2 (ELTT_2_101109-A.bin)

B2

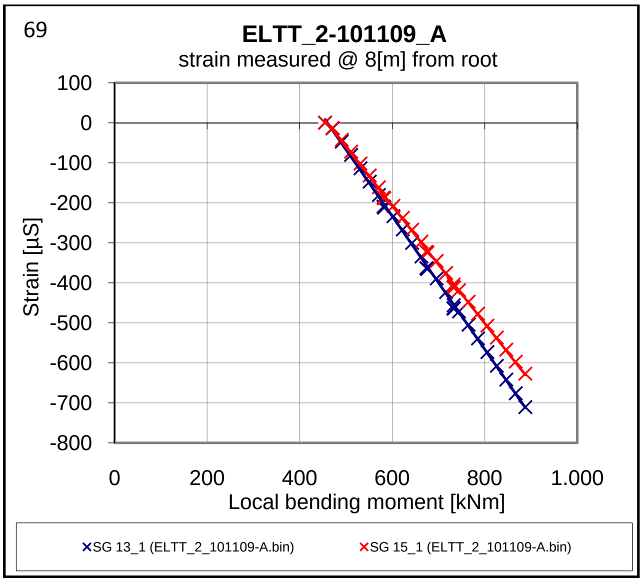
69
ELTT_2-101109_A
strain measured @ 8[m] from root
Strain [µS]
100
0
-100
-200
-300
-400
-500
-600
-700
-800
0
200
400
600
800
1.000
Local bending moment [kNm]
SG 13_1 (ELTT_2_101109-A.bin)
SG 15_1 (ELTT_2_101109-A.bin)

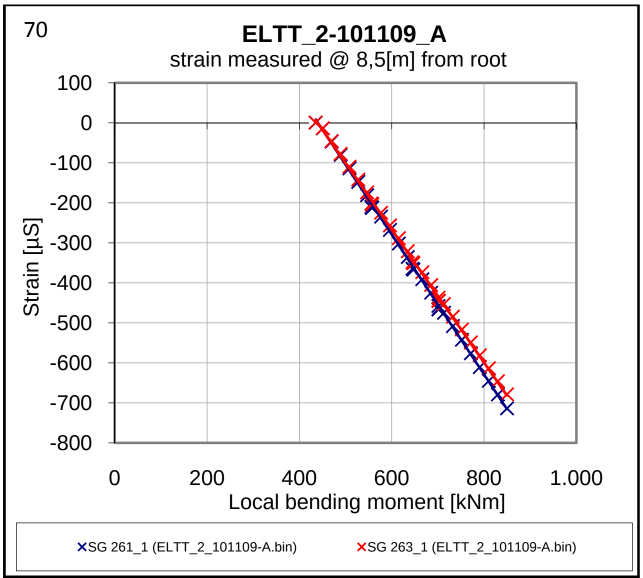
70
ELTT_2-101109_A
strain measured @ 8,5[m] from root
Strain [µS]
100
0
-100
-200
-300
-400
-500
-600
-700
-800
0
200
400
600
800
1.000
Local bending moment [kNm]
SG 261_1 (ELTT_2_101109-A.bin)
SG 263_1 (ELTT_2_101109-A.bin)

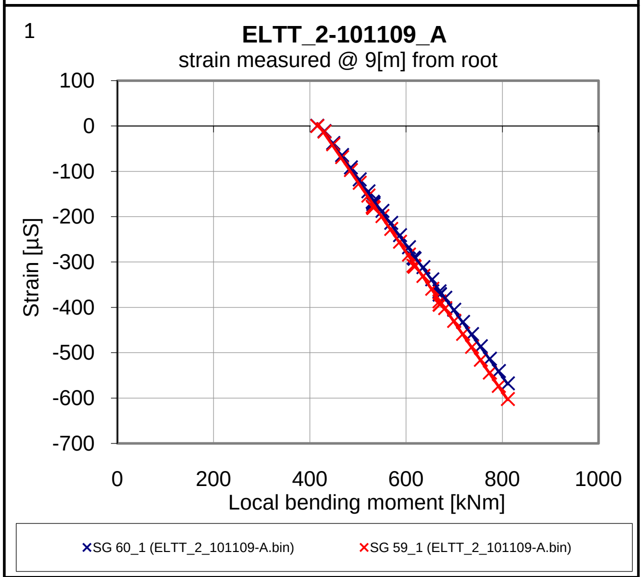
1
ELTT_2-101109_A
strain measured @ 9[m] from root
Strain [µS]
100
0
-100
-200
-300
-400
-500
-600
-700
0
200
400
600
800
1000
Local bending moment [kNm]
SG 60_1 (ELTT_2_101109-A.bin)
SG 59_1 (ELTT_2_101109-A.bin)

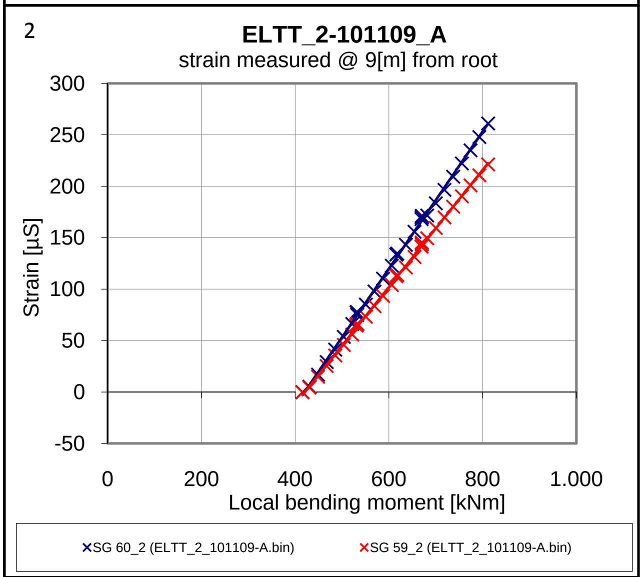
2
ELTT_2-101109_A
strain measured @ 9[m] from root
Strain [µS]
300
250
200
150
100
50
0
-50
0
200
400
600
800
1.000
Local bending moment [kNm]
SG 60_2 (ELTT_2_101109-A.bin)
SG 59_2 (ELTT_2_101109-A.bin)

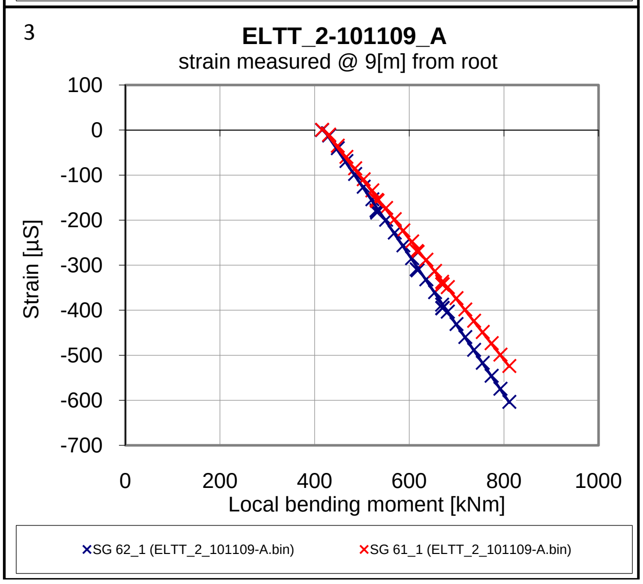
3
ELTT_2-101109_A
strain measured @ 9[m] from root
Strain [µS]
100
0
-100
-200
-300
-400
-500
-600
-700
0
200
400
600
800
1000
Local bending moment [kNm]
SG 62_1 (ELTT_2_101109-A.bin)
SG 61_1 (ELTT_2_101109-A.bin)

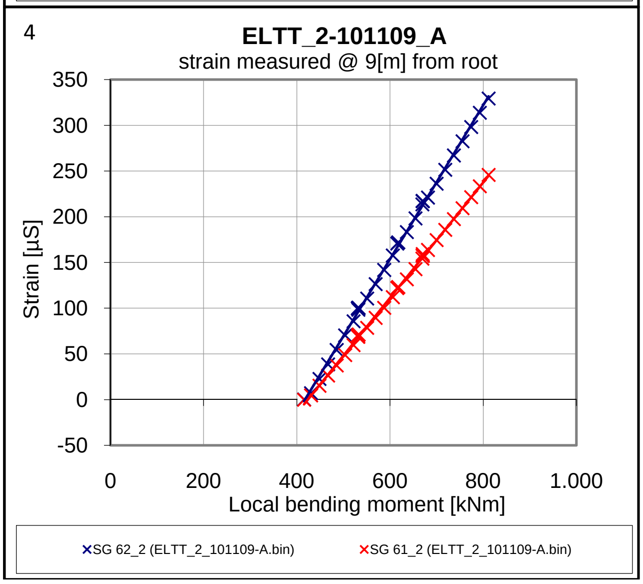
4
ELTT_2-101109_A
strain measured @ 9[m] from root
Strain [µS]
350
300
250
200
150
100
50
0
-50
0
200
400
600
800
1.000
Local bending moment [kNm]
SG 62_2 (ELTT_2_101109-A.bin)
SG 61_2 (ELTT_2_101109-A.bin)

B2

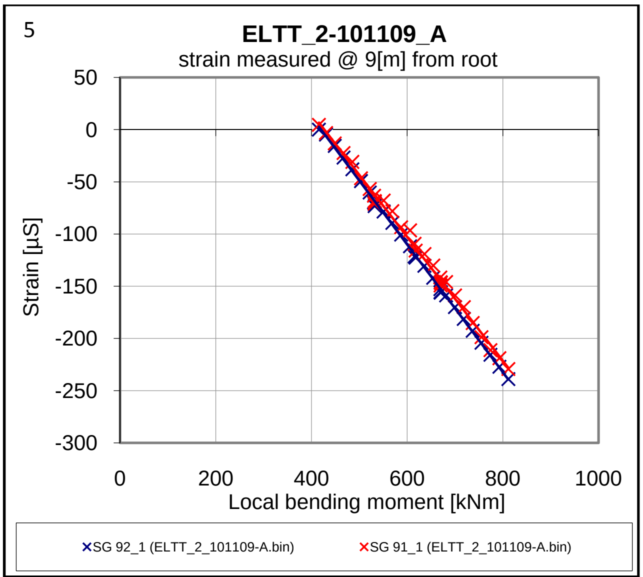
5
ELTT_2-101109_A
strain measured @ 9[m] from root
Strain [µS]
50
0
-50
-100
-150
-200
-250
-300
0
200
400
600
800
1000
Local bending moment [kNm]
SG 92_1 (ELTT_2_101109-A.bin)
SG 91_1 (ELTT_2_101109-A.bin)

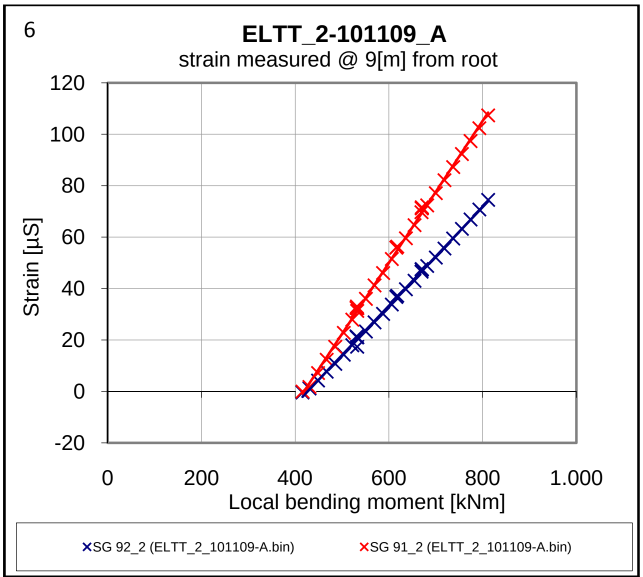
6
ELTT_2-101109_A
strain measured @ 9[m] from root
Strain [µS]
120
100
80
60
40
20
0
-20
0
200
400
600
800
1.000
Local bending moment [kNm]
SG 92_2 (ELTT_2_101109-A.bin)
SG 91_2 (ELTT_2_101109-A.bin)

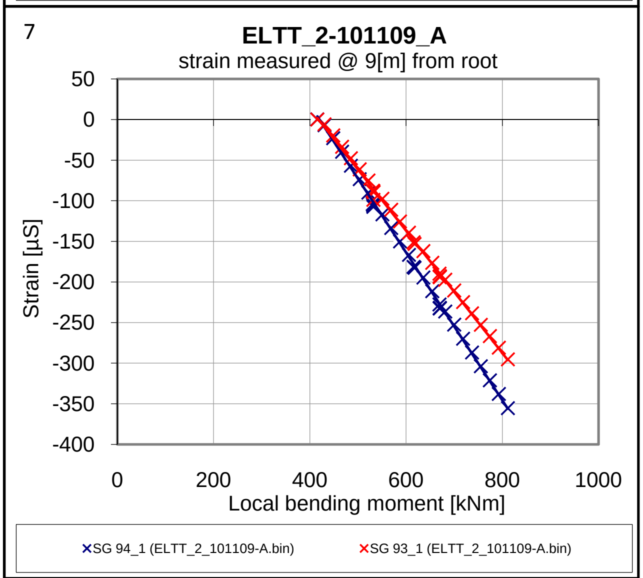
7
ELTT_2-101109_A
strain measured @ 9[m] from root
Strain [µS]
50
0
-50
-100
-150
-200
-250
-300
-350
-400
0
200
400
600
800
1000
Local bending moment [kNm]
SG 94_1 (ELTT_2_101109-A.bin)
SG 93_1 (ELTT_2_101109-A.bin)

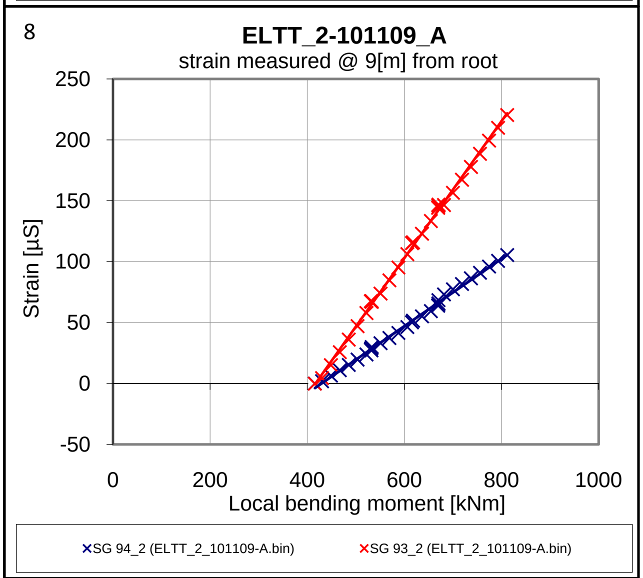
8
ELTT_2-101109_A
strain measured @ 9[m] from root
Strain [µS]
250
200
150
100
50
0
-50
0
200
400
600
800
1000
Local bending moment [kNm]
SG 94_2 (ELTT_2_101109-A.bin)
SG 93_2 (ELTT_2_101109-A.bin)

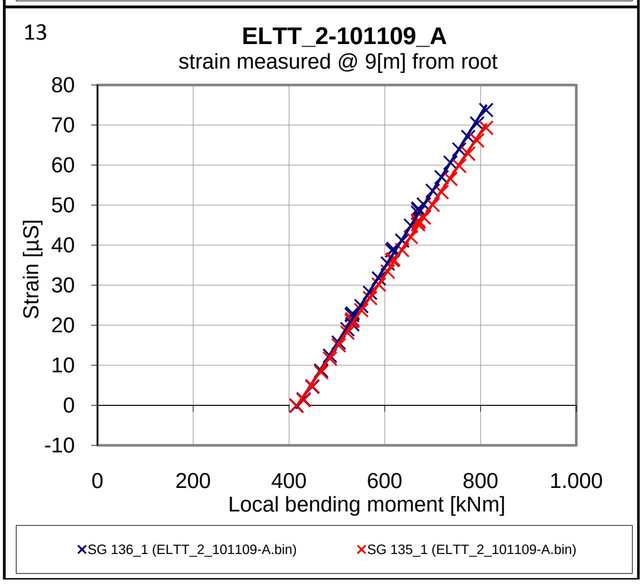
13
ELTT_2-101109_A
strain measured @ 9[m] from root
Strain [µS]
80
70
60
50
40
30
20
10
0
-10
0
200
400
600
800
1.000
Local bending moment [kNm]
SG 136_1 (ELTT_2_101109-A.bin)
SG 135_1 (ELTT_2_101109-A.bin)

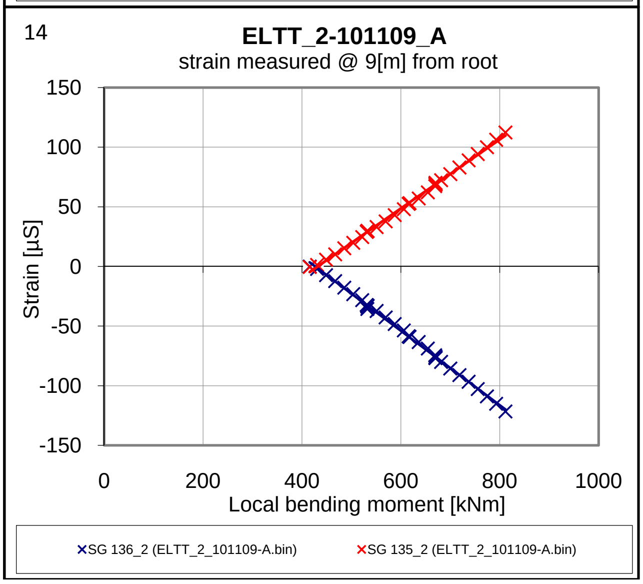
14
ELTT_2-101109_A
strain measured @ 9[m] from root
Strain [µS]
150
100
50
0
-50
-100
-150
0
200
400
600
800
1000
Local bending moment [kNm]
SG 136_2 (ELTT_2_101109-A.bin)
SG 135_2 (ELTT_2_101109-A.bin)

B2

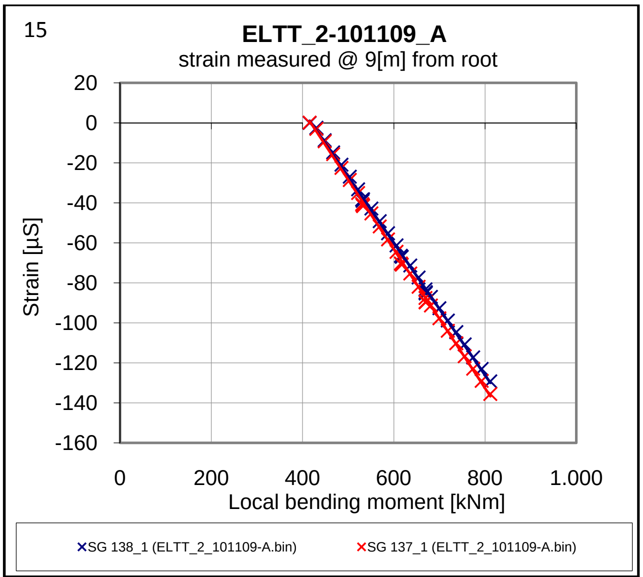
15
ELTT_2-101109_A
strain measured @ 9[m] from root
Strain [µS]
20
0
-20
-40
-60
-80
-100
-120
-140
-160
0
200
400
600
800
1.000
Local bending moment [kNm]
SG 138_1 (ELTT_2_101109-A.bin)
SG 137_1 (ELTT_2_101109-A.bin)

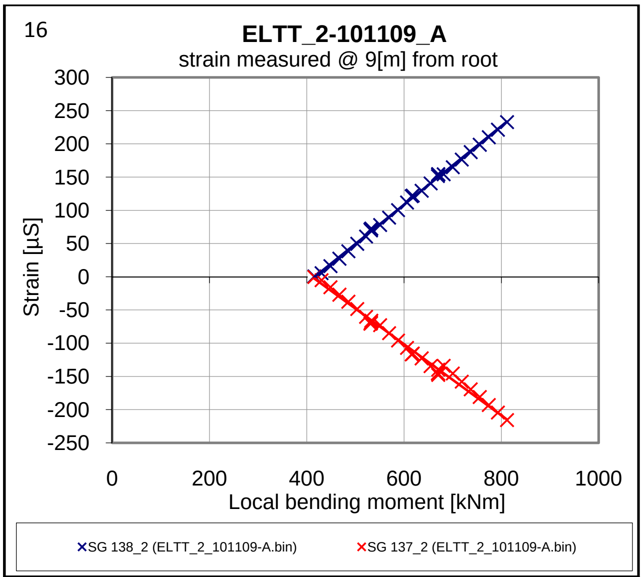
16
ELTT_2-101109_A
strain measured @ 9[m] from root
Strain [µS]
300
250
200
150
100
50
0
-50
-100
-150
-200
-250
0
200
400
600
800
1000
Local bending moment [kNm]
SG 138_2 (ELTT_2_101109-A.bin)
SG 137_2 (ELTT_2_101109-A.bin)

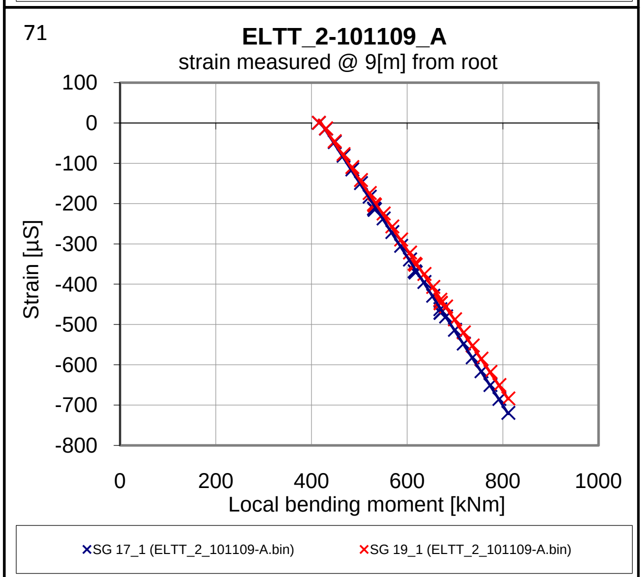
71
ELTT_2-101109_A
strain measured @ 9[m] from root
Strain [µS]
100
0
-100
-200
-300
-400
-500
-600
-700
-800
0
200
400
600
800
1000
Local bending moment [kNm]
SG 17_1 (ELTT_2_101109-A.bin)
SG 19_1 (ELTT_2_101109-A.bin)

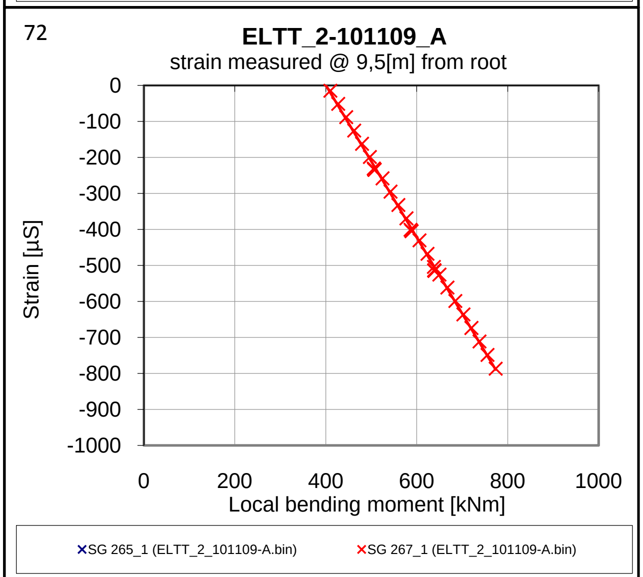
72
ELTT_2-101109_A
strain measured @ 9,5[m] from root
Strain [µS]
0
-100
-200
-300
-400
-500
-600
-700
-800
-900
-1000
0
200
400
600
800
1000
Local bending moment [kNm]
SG 265_1 (ELTT_2_101109-A.bin)
SG 267_1 (ELTT_2_101109-A.bin)

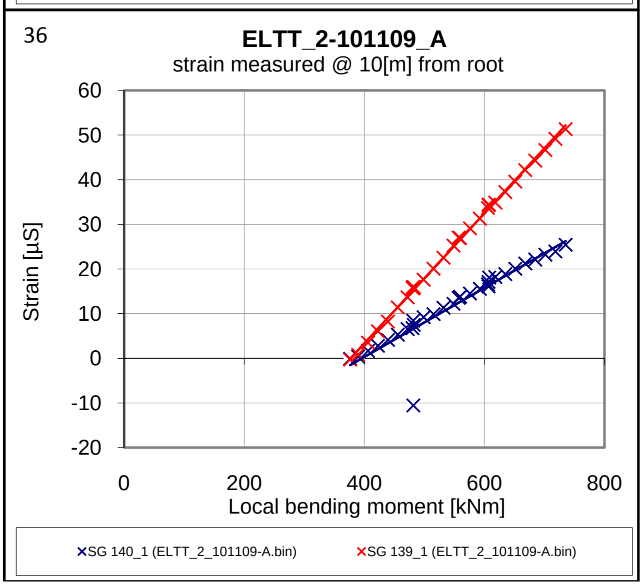
36
ELTT_2-101109_A
strain measured @ 10[m] from root
Strain [µS]
60
50
40
30
20
10
0
-10
-20
0
200
400
600
800
Local bending moment [kNm]
SG 140_1 (ELTT_2_101109-A.bin)
SG 139_1 (ELTT_2_101109-A.bin)

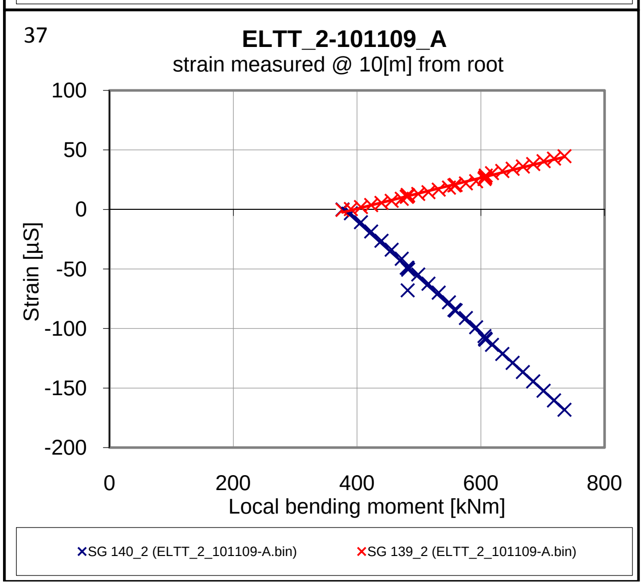
37
ELTT_2-101109_A
strain measured @ 10[m] from root
Strain [µS]
100
50
0
-50
-100
-150
-200
0
200
400
600
800
Local bending moment [kNm]
SG 140_2 (ELTT_2_101109-A.bin)
SG 139_2 (ELTT_2_101109-A.bin)

B2

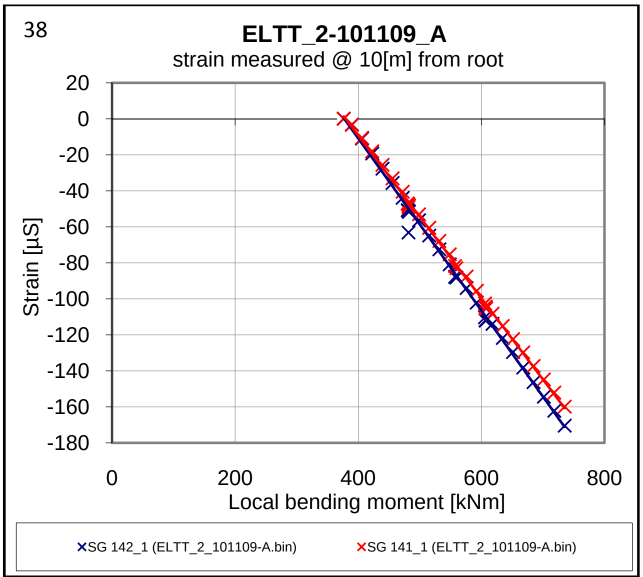
38
ELTT_2-101109_A
strain measured @ 10[m] from root
20
0
-20
-40
-60
-80
-100
-120
-140
-160
-180
Strain [µS]
0
200
400
600
800
Local bending moment [kNm]
SG 142_1 (ELTT_2_101109-A.bin)
SG 141_1 (ELTT_2_101109-A.bin)

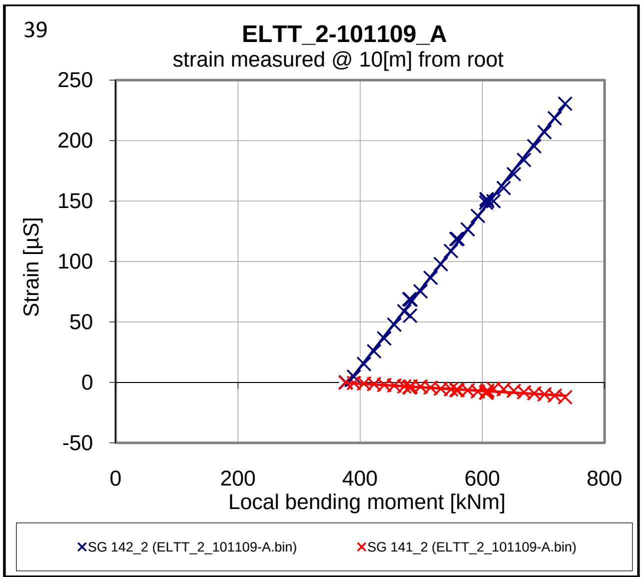
39
ELTT_2-101109_A
strain measured @ 10[m] from root
250
200
150
100
50
0
-50
Strain [µS]
0
200
400
600
800
Local bending moment [kNm]
SG 142_2 (ELTT_2_101109-A.bin)
SG 141_2 (ELTT_2_101109-A.bin)

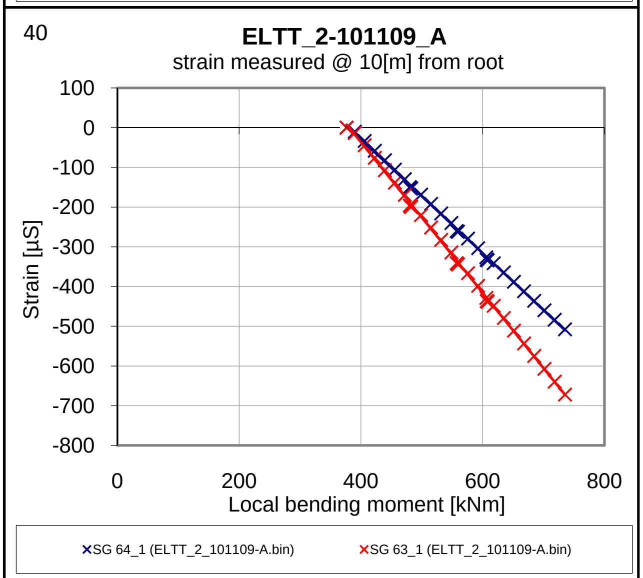
40
ELTT_2-101109_A
strain measured @ 10[m] from root
100
0
-100
-200
-300
-400
-500
-600
-700
-800
Strain [µS]
0
200
400
600
800
Local bending moment [kNm]
SG 64_1 (ELTT_2_101109-A.bin)
SG 63_1 (ELTT_2_101109-A.bin)

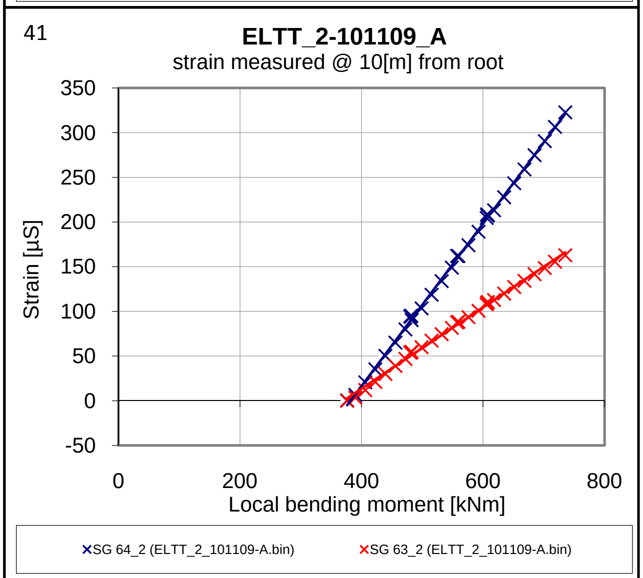
41
ELTT_2-101109_A
strain measured @ 10[m] from root
350
300
250
200
150
100
50
0
-50
Strain [µS]
0
200
400
600
800
Local bending moment [kNm]
SG 64_2 (ELTT_2_101109-A.bin)
SG 63_2 (ELTT_2_101109-A.bin)

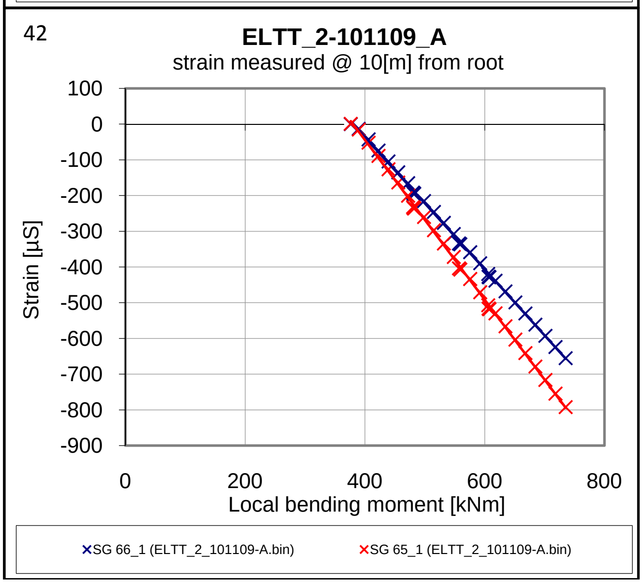
42
ELTT_2-101109_A
strain measured @ 10[m] from root
100
0
-100
-200
-300
-400
-500
-600
-700
-800
-900
Strain [µS]
0
200
400
600
800
Local bending moment [kNm]
SG 66_1 (ELTT_2_101109-A.bin)
SG 65_1 (ELTT_2_101109-A.bin)

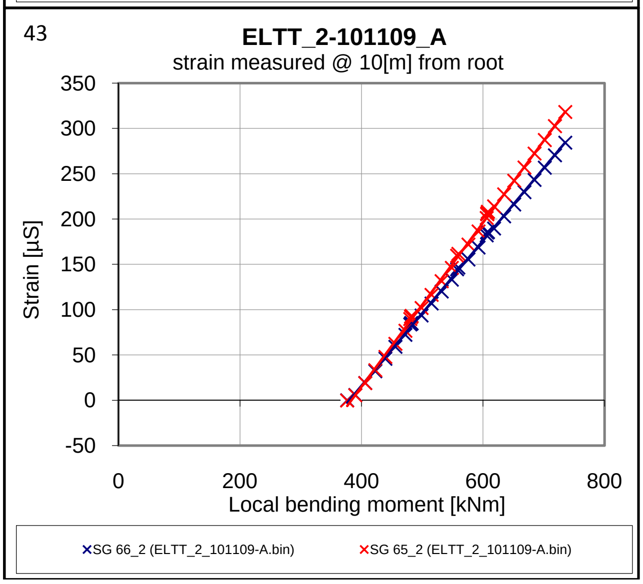
43
ELTT_2-101109_A
strain measured @ 10[m] from root
350
300
250
200
150
100
50
0
-50
Strain [µS]
0
200
400
600
800
Local bending moment [kNm]
SG 66_2 (ELTT_2_101109-A.bin)
SG 65_2 (ELTT_2_101109-A.bin)

B2

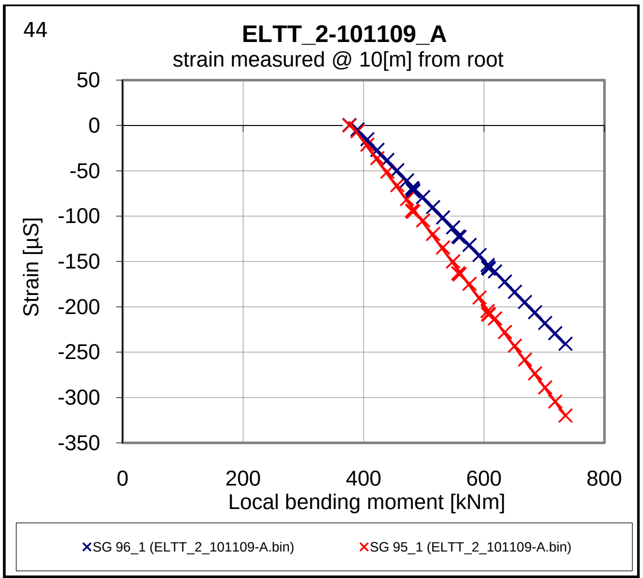
44
ELTT_2-101109_A
strain measured @ 10[m] from root
Strain [µS]
50
0
-50
-100
-150
-200
-250
-300
-350
0
200
400
600
800
Local bending moment [kNm]
SG 96_1 (ELTT_2_101109-A.bin)
SG 95_1 (ELTT_2_101109-A.bin)

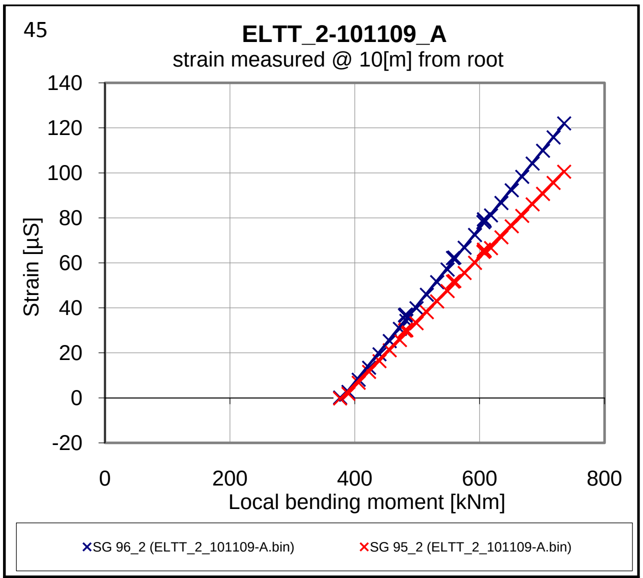
45
ELTT_2-101109_A
strain measured @ 10[m] from root
Strain [µS]
140
120
100
80
60
40
20
0
-20
0
200
400
600
800
Local bending moment [kNm]
SG 96_2 (ELTT_2_101109-A.bin)
SG 95_2 (ELTT_2_101109-A.bin)

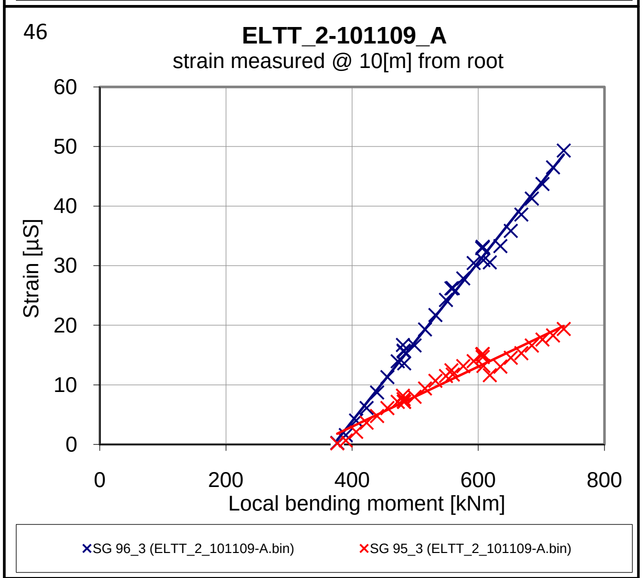
46
ELTT_2-101109_A
strain measured @ 10[m] from root
Strain [µS]
60
50
40
30
20
10
0
0
200
400
600
800
Local bending moment [kNm]
SG 96_3 (ELTT_2_101109-A.bin)
SG 95_3 (ELTT_2_101109-A.bin)

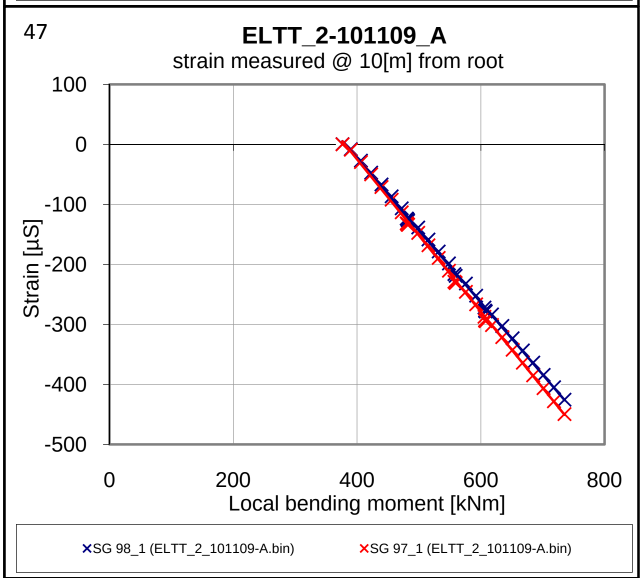
47
ELTT_2-101109_A
strain measured @ 10[m] from root
Strain [µS]
100
0
-100
-200
-300
-400
-500
0
200
400
600
800
Local bending moment [kNm]
SG 98_1 (ELTT_2_101109-A.bin)
SG 97_1 (ELTT_2_101109-A.bin)

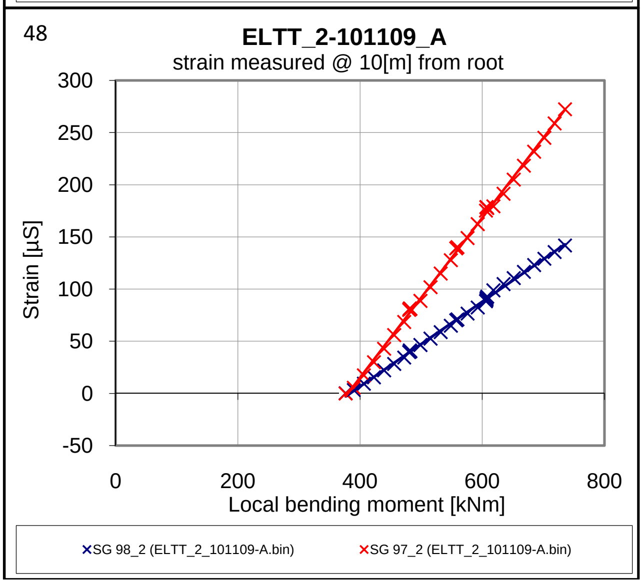
48
ELTT_2-101109_A
strain measured @ 10[m] from root
Strain [µS]
300
250
200
150
100
50
0
-50
0
200
400
600
800
Local bending moment [kNm]
SG 98_2 (ELTT_2_101109-A.bin)
SG 97_2 (ELTT_2_101109-A.bin)

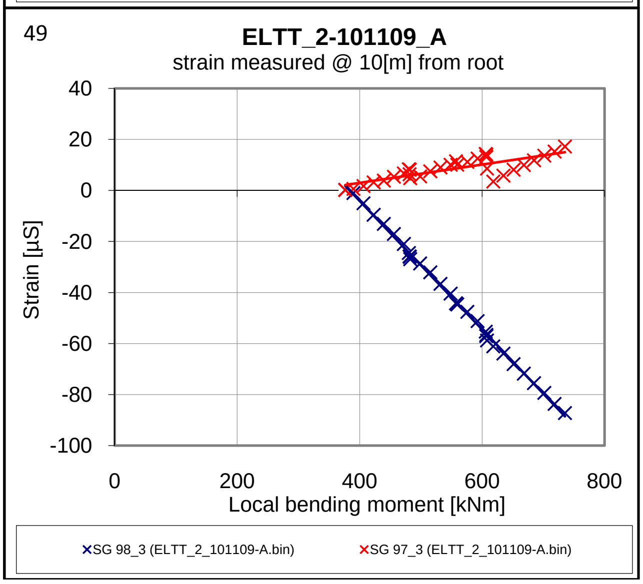
49
ELTT_2-101109_A
strain measured @ 10[m] from root
Strain [µS]
40
20
0
-20
-40
-60
-80
-100
0
200
400
600
800
Local bending moment [kNm]
SG 98_3 (ELTT_2_101109-A.bin)
SG 97_3 (ELTT_2_101109-A.bin)

B2

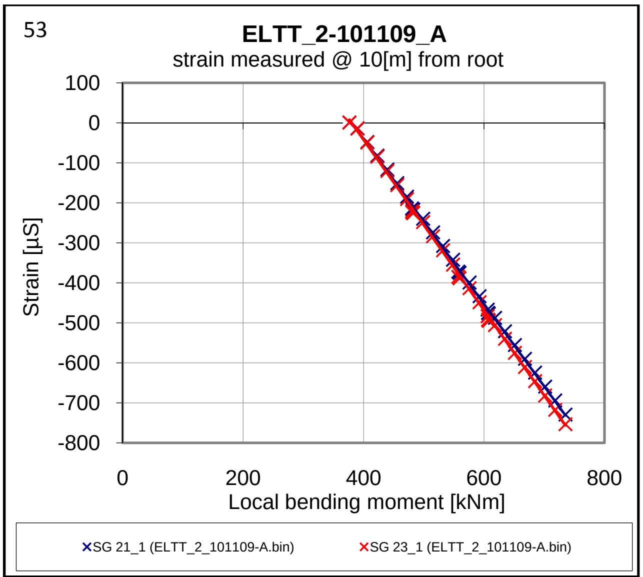
53
ELTT_2-101109_A
strain measured @ 10[m] from root
Strain [µS]
100
0
-100
-200
-300
-400
-500
-600
-700
-800
0
200
400
600
800
Local bending moment [kNm]
SG 21_1 (ELTT_2_101109-A.bin)
SG 23_1 (ELTT_2_101109-A.bin)

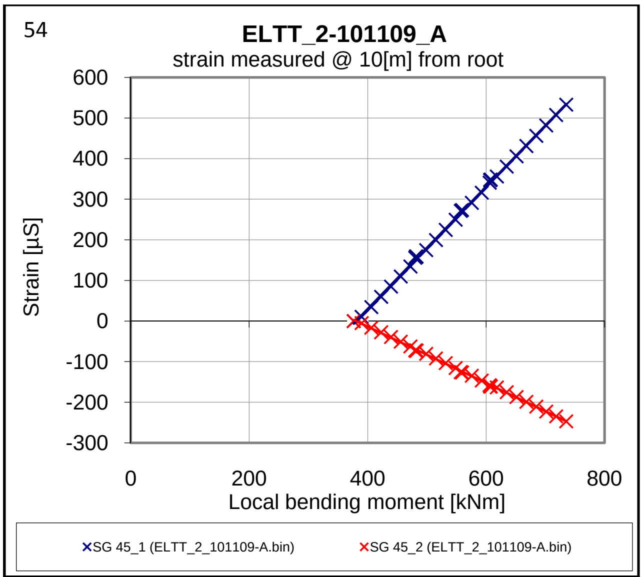
54
ELTT_2-101109_A
strain measured @ 10[m] from root
Strain [µS]
600
500
400
300
200
100
0
-100
-200
-300
0
200
400
600
800
Local bending moment [kNm]
SG 45_1 (ELTT_2_101109-A.bin)
SG 45_2 (ELTT_2_101109-A.bin)

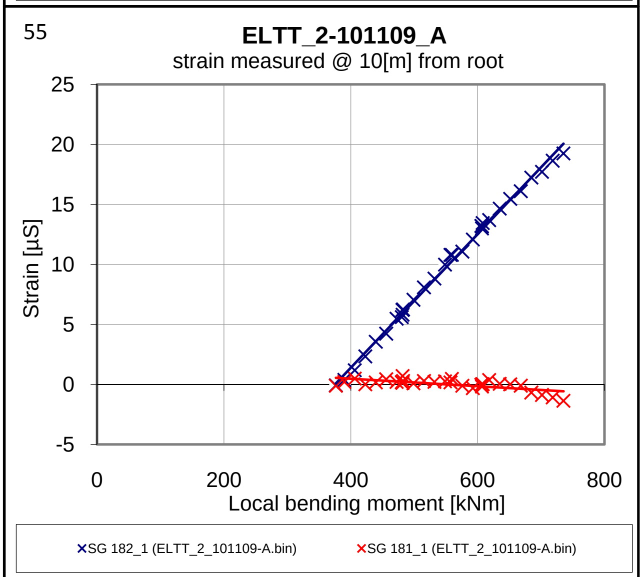
55
ELTT_2-101109_A
strain measured @ 10[m] from root
Strain [µS]
25
20
15
10
5
0
-5
0
200
400
600
800
Local bending moment [kNm]
SG 182_1 (ELTT_2_101109-A.bin)
SG 181_1 (ELTT_2_101109-A.bin)

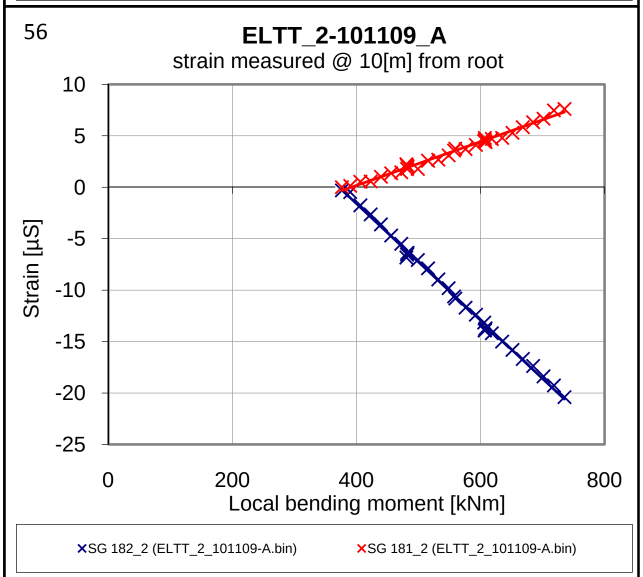
56
ELTT_2-101109_A
strain measured @ 10[m] from root
Strain [µS]
10
5
0
-5
-10
-15
-20
-25
0
200
400
600
800
Local bending moment [kNm]
SG 182_2 (ELTT_2_101109-A.bin)
SG 181_2 (ELTT_2_101109-A.bin)

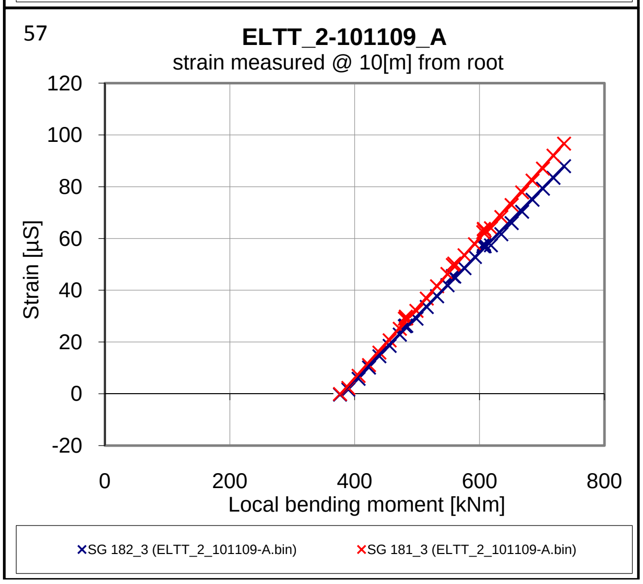
57
ELTT_2-101109_A
strain measured @ 10[m] from root
Strain [µS]
120
100
80
60
40
20
0
-20
0
200
400
600
800
Local bending moment [kNm]
SG 182_3 (ELTT_2_101109-A.bin)
SG 181_3 (ELTT_2_101109-A.bin)

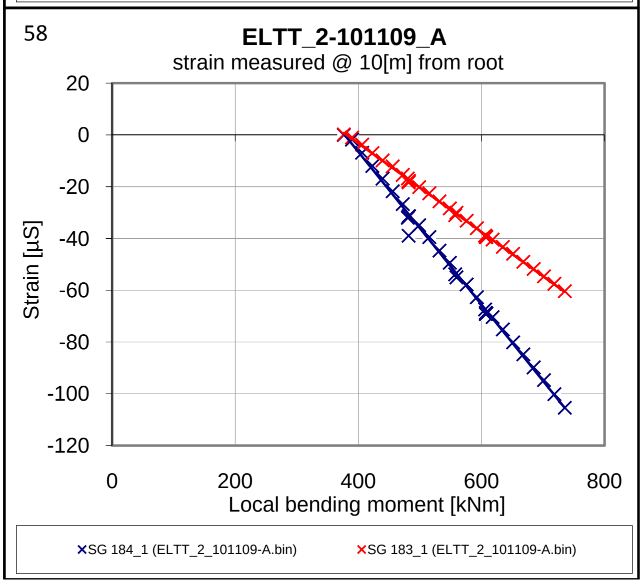
58
ELTT_2-101109_A
strain measured @ 10[m] from root
Strain [µS]
20
0
-20
-40
-60
-80
-100
-120
0
200
400
600
800
Local bending moment [kNm]
SG 184_1 (ELTT_2_101109-A.bin)
SG 183_1 (ELTT_2_101109-A.bin)

B2

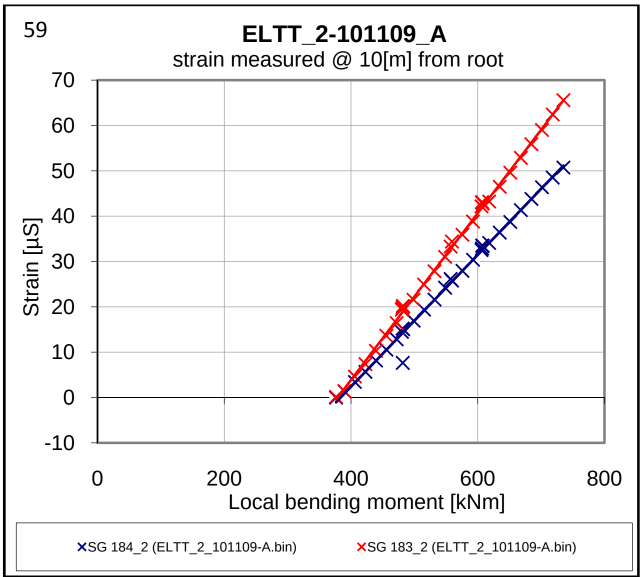
59
ELTT_2-101109_A
strain measured @ 10[m] from root
Strain [µS]
Local bending moment [kNm]
SG 184_2 (ELTT_2_101109-A.bin)
SG 183_2 (ELTT_2_101109-A.bin)

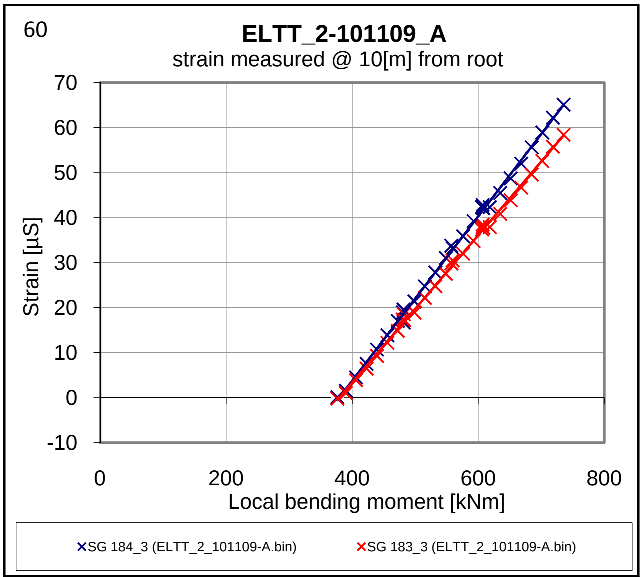
60
ELTT_2-101109_A
strain measured @ 10[m] from root
Strain [µS]
Local bending moment [kNm]
SG 184_3 (ELTT_2_101109-A.bin)
SG 183_3 (ELTT_2_101109-A.bin)

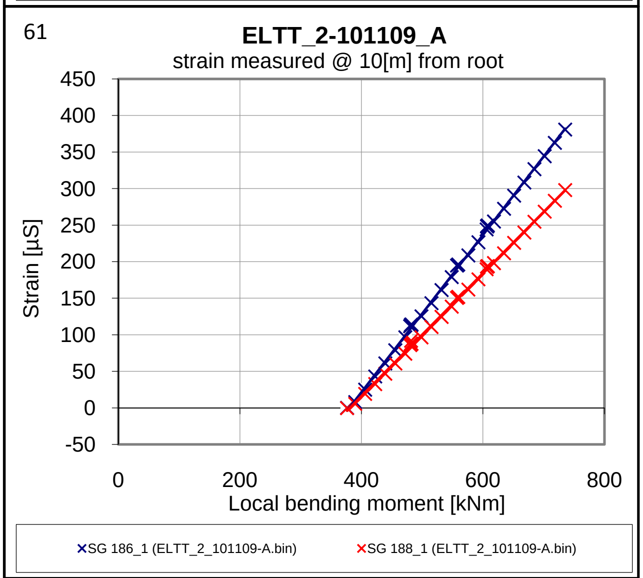
61
ELTT_2-101109_A
strain measured @ 10[m] from root
Strain [µS]
Local bending moment [kNm]
SG 186_1 (ELTT_2_101109-A.bin)
SG 188_1 (ELTT_2_101109-A.bin)

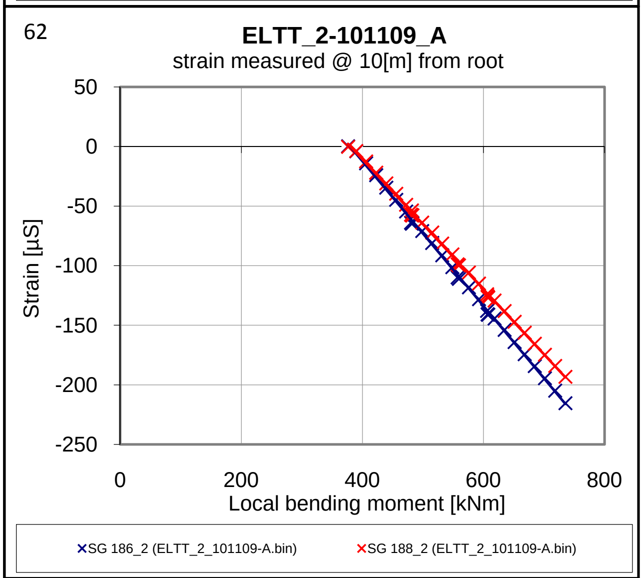
62
ELTT_2-101109_A
strain measured @ 10[m] from root
Strain [µS]
Local bending moment [kNm]
SG 186_2 (ELTT_2_101109-A.bin)
SG 188_2 (ELTT_2_101109-A.bin)

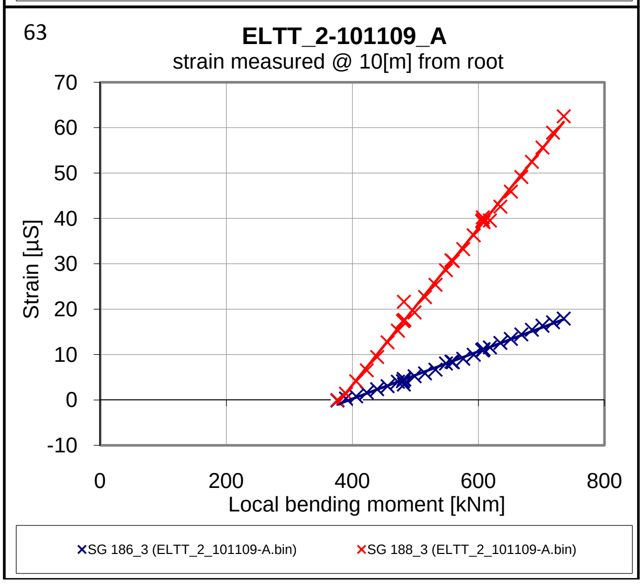
63
ELTT_2-101109_A
strain measured @ 10[m] from root
Strain [µS]
Local bending moment [kNm]
SG 186_3 (ELTT_2_101109-A.bin)
SG 188_3 (ELTT_2_101109-A.bin)

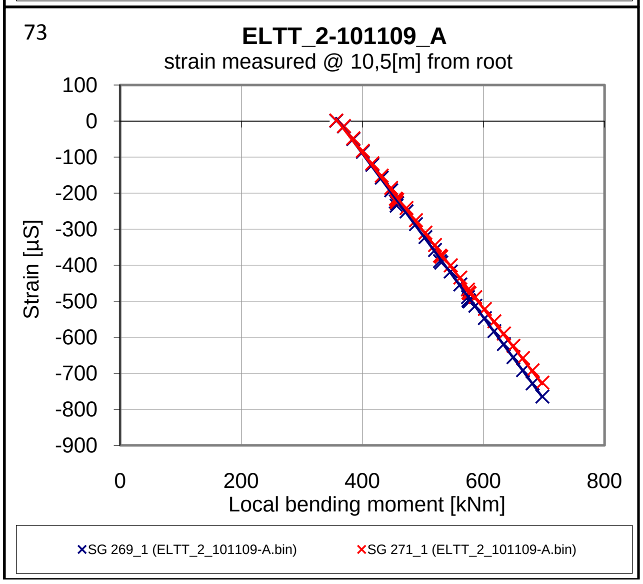
73
ELTT_2-101109_A
strain measured @ 10,5[m] from root
Strain [µS]
Local bending moment [kNm]
SG 269_1 (ELTT_2_101109-A.bin)
SG 271_1 (ELTT_2_101109-A.bin)

B2

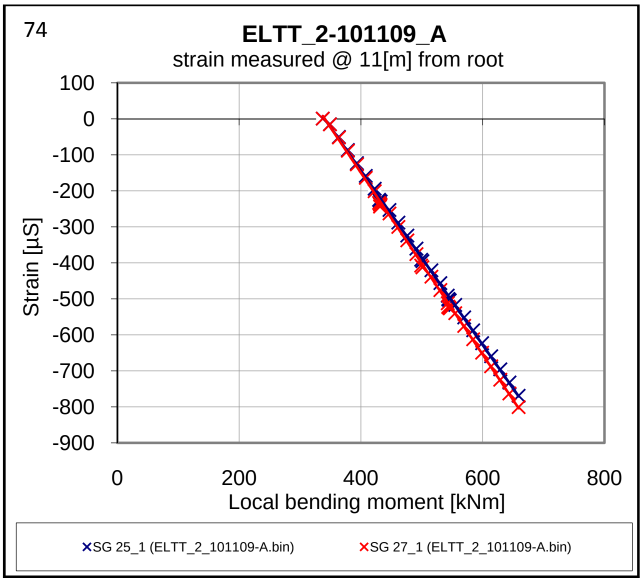
74
ELTT_2-101109_A
strain measured @ 11[m] from root
Strain [µS]
Local bending moment [kNm]
SG 25_1 (ELTT_2_101109-A.bin)
SG 27_1 (ELTT_2_101109-A.bin)

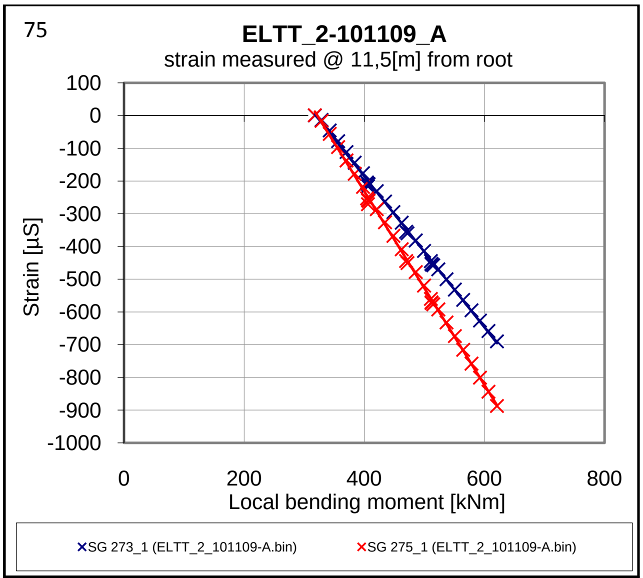
75
ELTT_2-101109_A
strain measured @ 11,5[m] from root
Strain [µS]
Local bending moment [kNm]
SG 273_1 (ELTT_2_101109-A.bin)
SG 275_1 (ELTT_2_101109-A.bin)

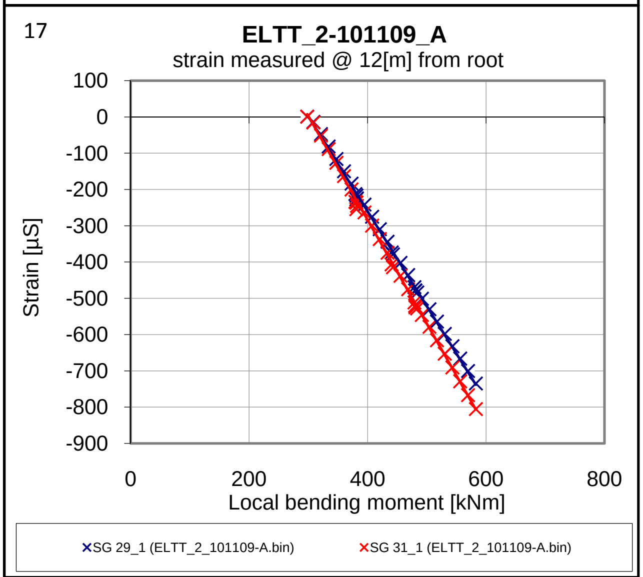
17
ELTT_2-101109_A
strain measured @ 12[m] from root
Strain [µS]
Local bending moment [kNm]
SG 29_1 (ELTT_2_101109-A.bin)
SG 31_1 (ELTT_2_101109-A.bin)

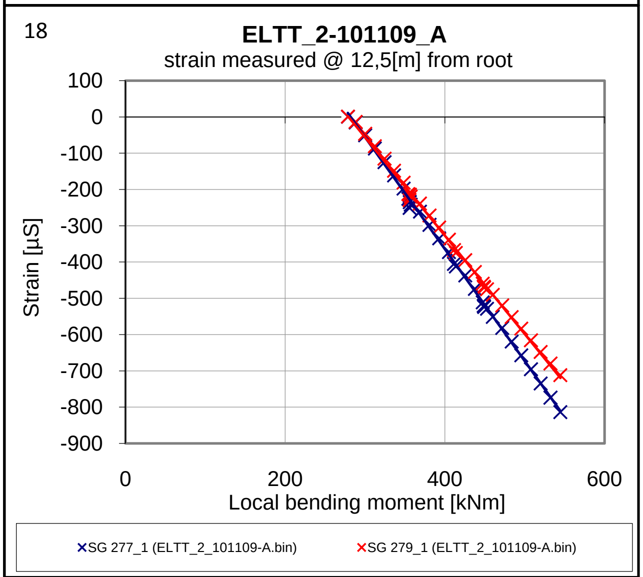
18
ELTT_2-101109_A
strain measured @ 12,5[m] from root
Strain [µS]
Local bending moment [kNm]
SG 277_1 (ELTT_2_101109-A.bin)
SG 279_1 (ELTT_2_101109-A.bin)

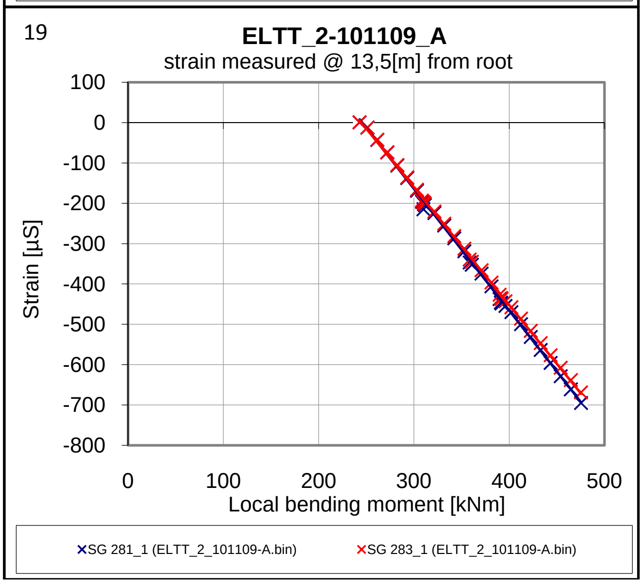
19
ELTT_2-101109_A
strain measured @ 13,5[m] from root
Strain [µS]
Local bending moment [kNm]
SG 281_1 (ELTT_2_101109-A.bin)
SG 283_1 (ELTT_2_101109-A.bin)

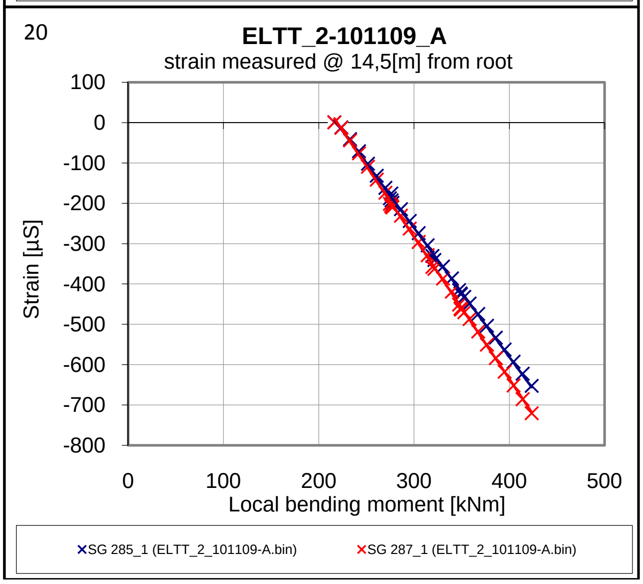
20
ELTT_2-101109_A
strain measured @ 14,5[m] from root
Strain [µS]
Local bending moment [kNm]
SG 285_1 (ELTT_2_101109-A.bin)
SG 287_1 (ELTT_2_101109-A.bin)

B2

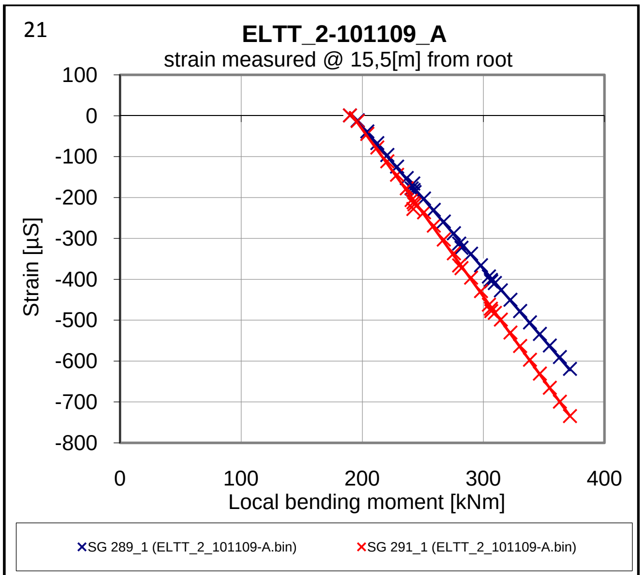
21
ELTT_2-101109_A
strain measured @ 15,5[m] from root
Strain [µS]
100
0
-100
-200
-300
-400
-500
-600
-700
-800
0
100
200
300
400
Local bending moment [kNm]
SG 289_1 (ELTT_2_101109-A.bin)
SG 291_1 (ELTT_2_101109-A.bin)

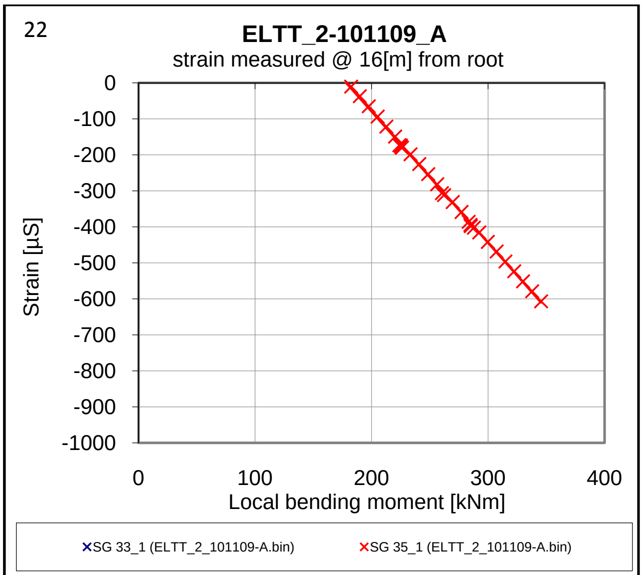
22
ELTT_2-101109_A
strain measured @ 16[m] from root
Strain [µS]
0
-100
-200
-300
-400
-500
-600
-700
-800
-900
-1000
0
100
200
300
400
Local bending moment [kNm]
SG 33_1 (ELTT_2_101109-A.bin)
SG 35_1 (ELTT_2_101109-A.bin)

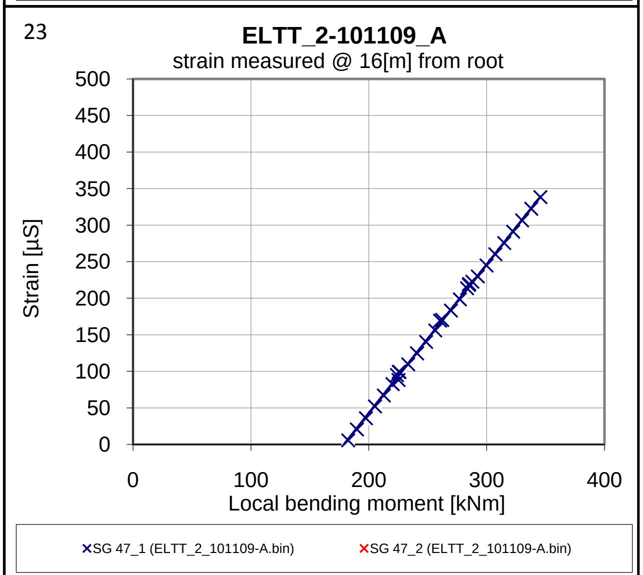
23
ELTT_2-101109_A
strain measured @ 16[m] from root
Strain [µS]
500
450
400
350
300
250
200
150
100
50
0
0
100
200
300
400
Local bending moment [kNm]
SG 47_1 (ELTT_2_101109-A.bin)
SG 47_2 (ELTT_2_101109-A.bin)

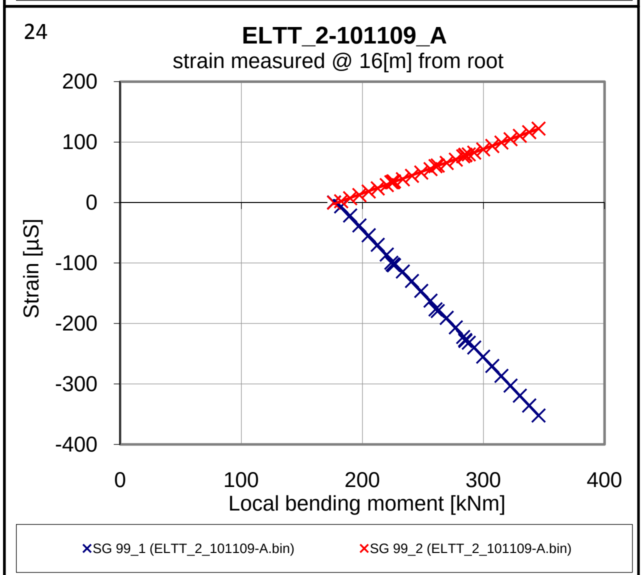
24
ELTT_2-101109_A
strain measured @ 16[m] from root
Strain [µS]
200
100
0
-100
-200
-300
-400
0
100
200
300
400
Local bending moment [kNm]
SG 99_1 (ELTT_2_101109-A.bin)
SG 99_2 (ELTT_2_101109-A.bin)

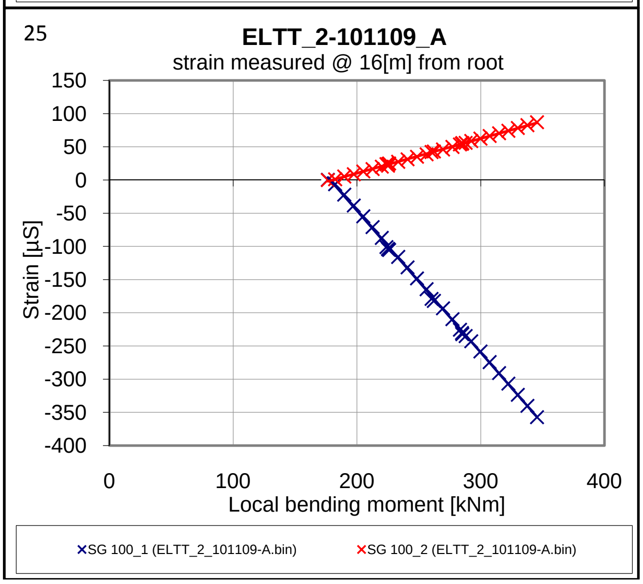
25
ELTT_2-101109_A
strain measured @ 16[m] from root
Strain [µS]
150
100
50
0
-50
-100
-150
-200
-250
-300
-350
-400
0
100
200
300
400
Local bending moment [kNm]
SG 100_1 (ELTT_2_101109-A.bin)
SG 100_2 (ELTT_2_101109-A.bin)

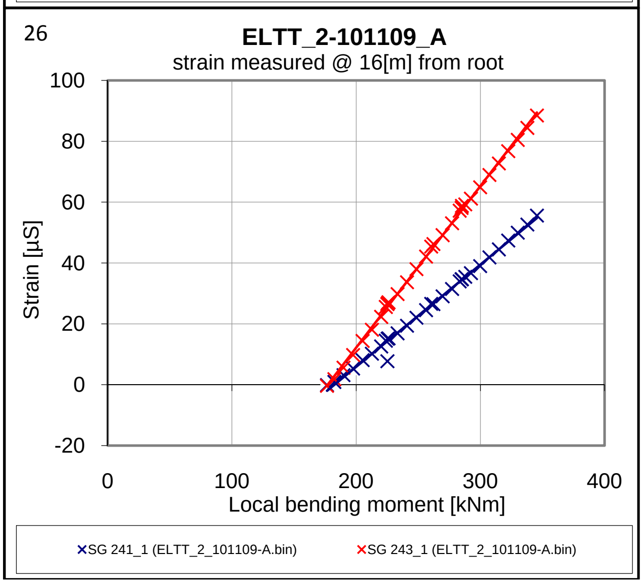
26
ELTT_2-101109_A
strain measured @ 16[m] from root
Strain [µS]
100
80
60
40
20
0
-20
0
100
200
300
400
Local bending moment [kNm]
SG 241_1 (ELTT_2_101109-A.bin)
SG 243_1 (ELTT_2_101109-A.bin)

B2

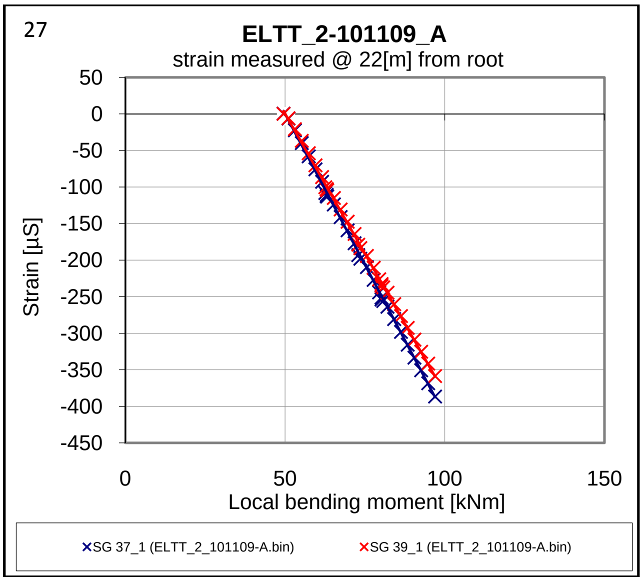
27
ELTT_2-101109_A
strain measured @ 22[m] from root
50
0
-50
-100
-150
-200
-250
-300
-350
-400
-450
Strain [µS]
0
50
100
150
Local bending moment [kNm]
SG 37_1 (ELTT_2_101109-A.bin)
SG 39_1 (ELTT_2_101109-A.bin)

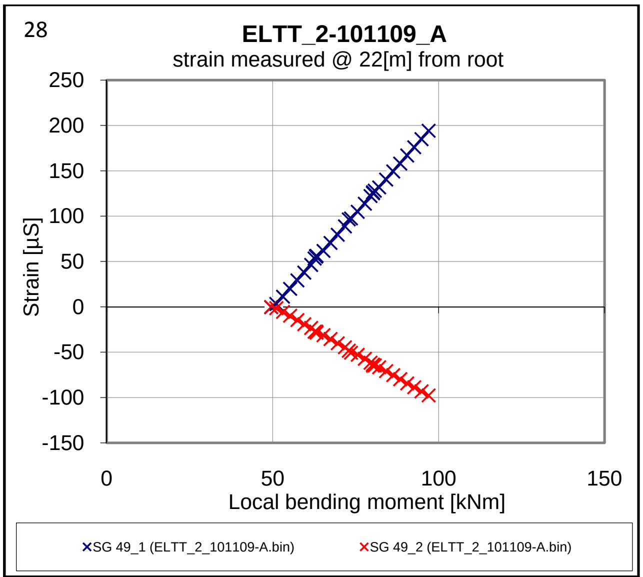
28
ELTT_2-101109_A
strain measured @ 22[m] from root
250
200
150
100
50
0
-50
-100
-150
Strain [µS]
0
50
100
150
Local bending moment [kNm]
SG 49_1 (ELTT_2_101109-A.bin)
SG 49_2 (ELTT_2_101109-A.bin)

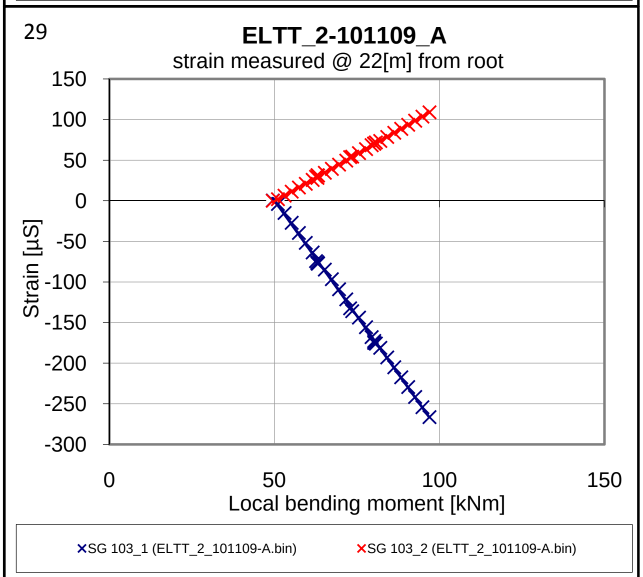
29
ELTT_2-101109_A
strain measured @ 22[m] from root
150
100
50
0
-50
-100
-150
-200
-250
-300
Strain [µS]
0
50
100
150
Local bending moment [kNm]
SG 103_1 (ELTT_2_101109-A.bin)
SG 103_2 (ELTT_2_101109-A.bin)

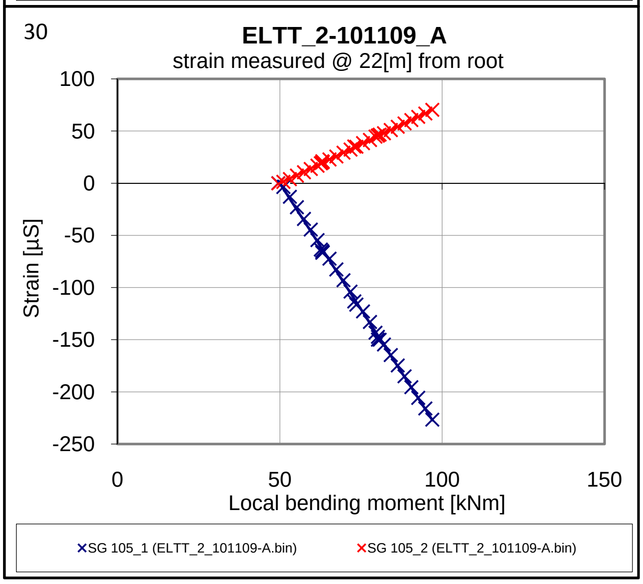
30
ELTT_2-101109_A
strain measured @ 22[m] from root
100
50
0
-50
-100
-150
-200
-250
Strain [µS]
0
50
100
150
Local bending moment [kNm]
SG 105_1 (ELTT_2_101109-A.bin)
SG 105_2 (ELTT_2_101109-A.bin)

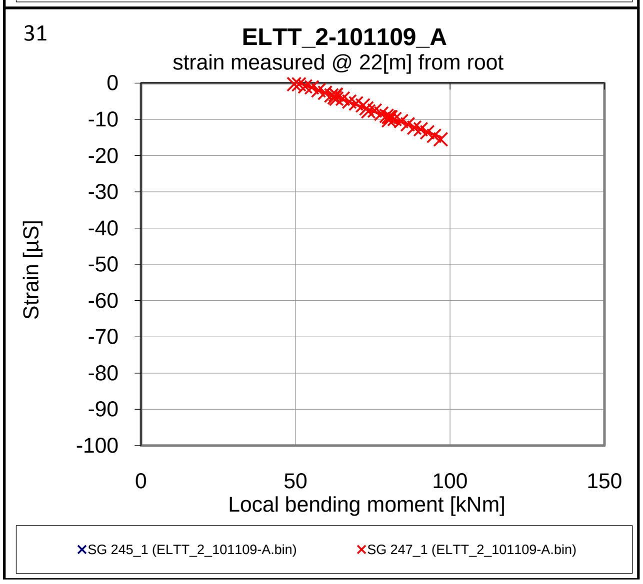
31
ELTT_2-101109_A
strain measured @ 22[m] from root
0
-10
-20
-30
-40
-50
-60
-70
-80
-90
-100
Strain [µS]
0
50
100
150
Local bending moment [kNm]
SG 245_1 (ELTT_2_101109-A.bin)
SG 247_1 (ELTT_2_101109-A.bin)

B3 Measurements obtained from strain gauges in:
Other groups section in test ELTT_3-041109_A

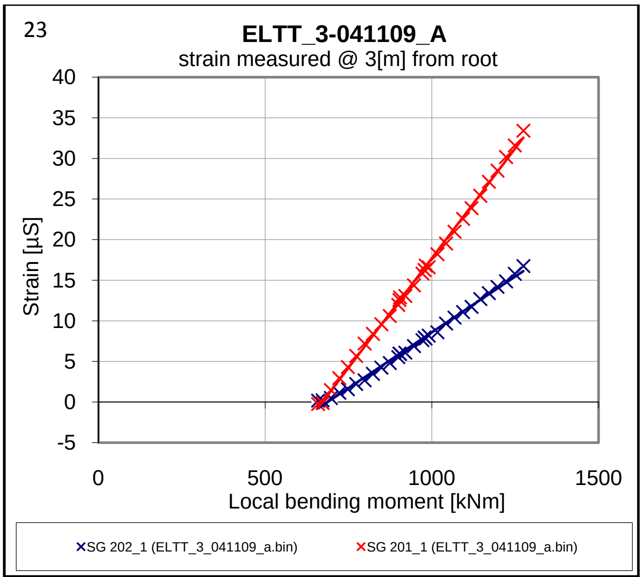

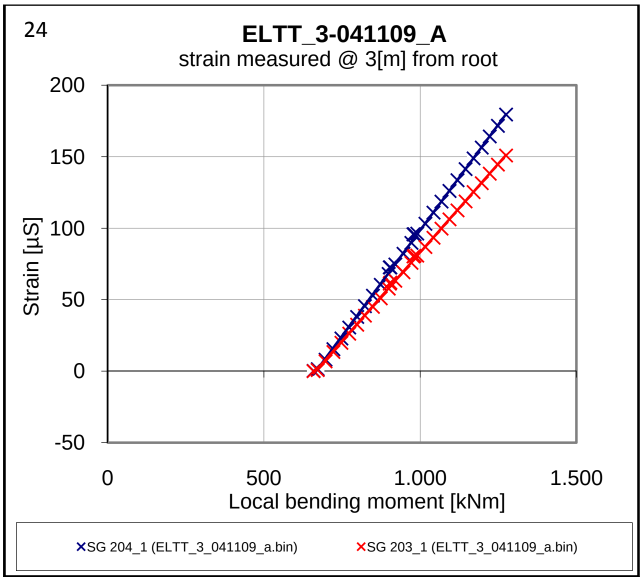

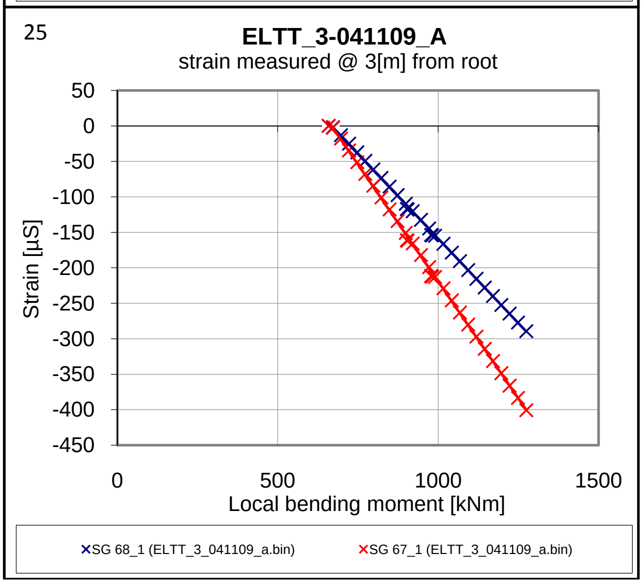

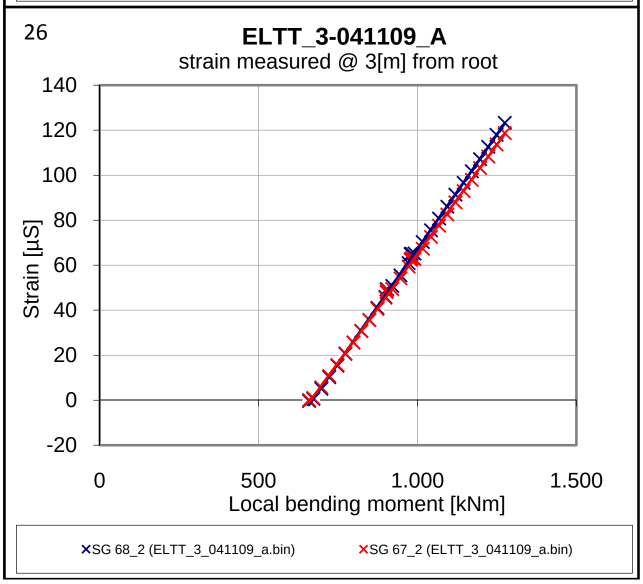

B3

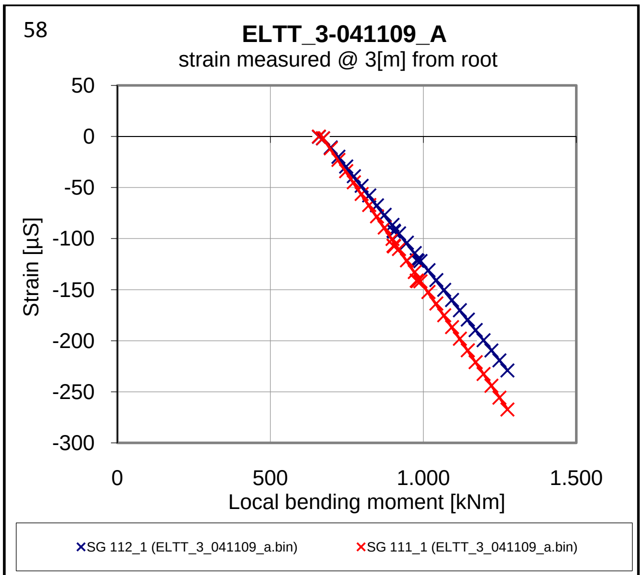
58
ELTT_3-041109_A
strain measured @ 3[m] from root
Strain [µS]
50
0
-50
-100
-150
-200
-250
-300
0
500
1.000
1.500
Local bending moment [kNm]
SG 112_1 (ELTT_3_041109_a.bin)
SG 111_1 (ELTT_3_041109_a.bin)

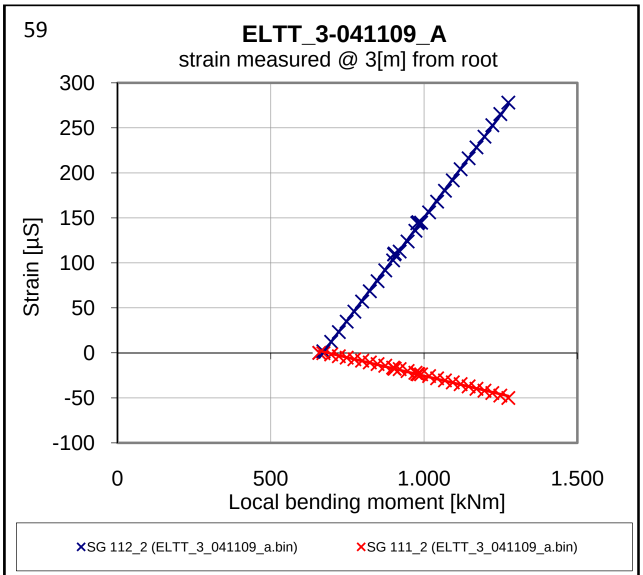
59
ELTT_3-041109_A
strain measured @ 3[m] from root
Strain [µS]
300
250
200
150
100
50
0
-50
-100
0
500
1.000
1.500
Local bending moment [kNm]
SG 112_2 (ELTT_3_041109_a.bin)
SG 111_2 (ELTT_3_041109_a.bin)

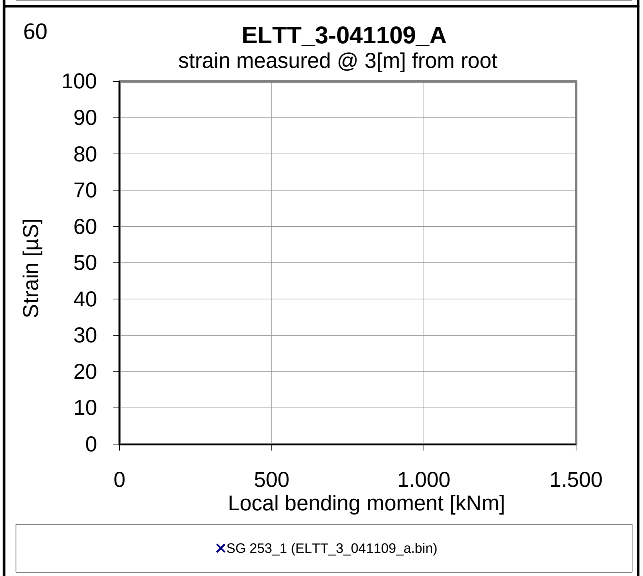
60
ELTT_3-041109_A
strain measured @ 3[m] from root
Strain [µS]
100
90
80
70
60
50
40
30
20
10
0
0
500
1.000
1.500
Local bending moment [kNm]
SG 253_1 (ELTT_3_041109_a.bin)

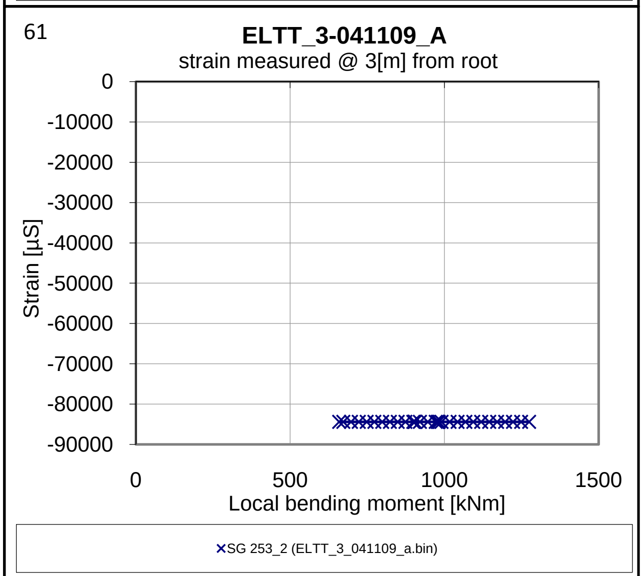
61
ELTT_3-041109_A
strain measured @ 3[m] from root
Strain [µS]
0
-10000
-20000
-30000
-40000
-50000
-60000
-70000
-80000
-90000
0
500
1000
1500
Local bending moment [kNm]
SG 253_2 (ELTT_3_041109_a.bin)

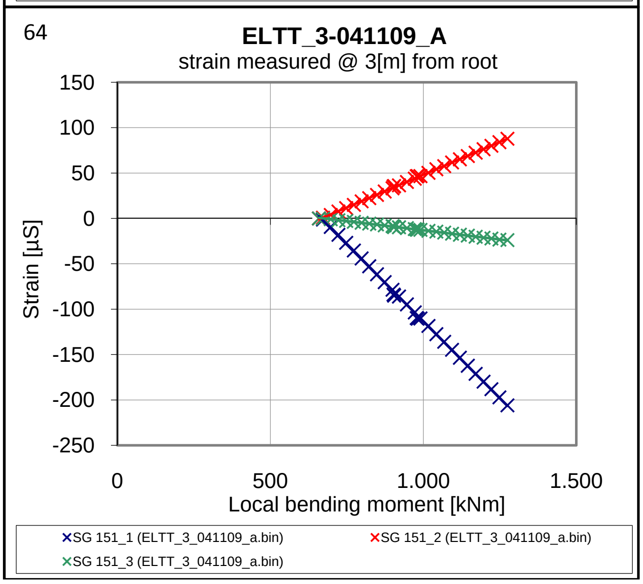
64
ELTT_3-041109_A
strain measured @ 3[m] from root
Strain [µS]
150
100
50
0
-50
-100
-150
-200
-250
0
500
1.000
1.500
Local bending moment [kNm]
SG 151_1 (ELTT_3_041109_a.bin)
SG 151_2 (ELTT_3_041109_a.bin)
SG 151_3 (ELTT_3_041109_a.bin)

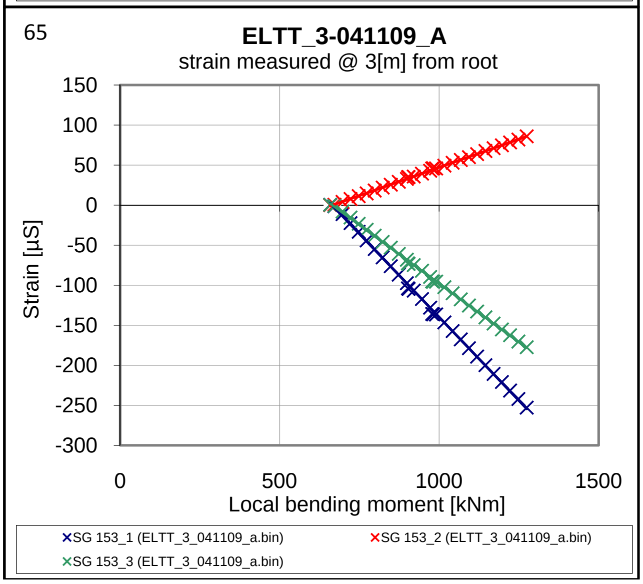
65
ELTT_3-041109_A
strain measured @ 3[m] from root
Strain [µS]
150
100
50
0
-50
-100
-150
-200
-250
-300
0
500
1000
1500
Local bending moment [kNm]
SG 153_1 (ELTT_3_041109_a.bin)
SG 153_2 (ELTT_3_041109_a.bin)
SG 153_3 (ELTT_3_041109_a.bin)

B3

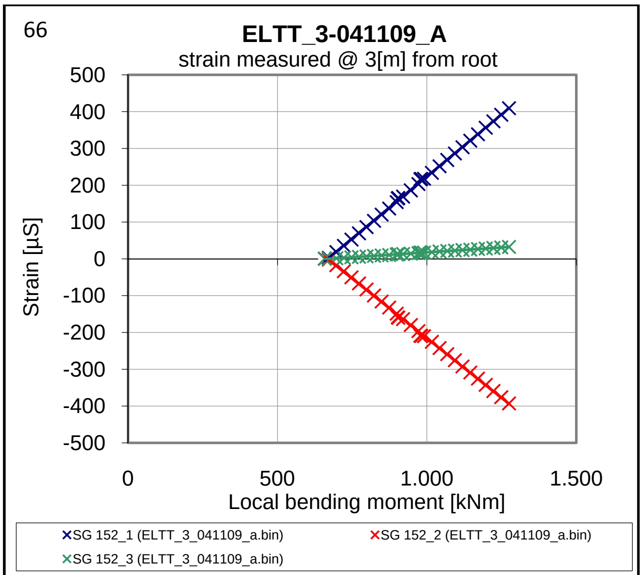
66
ELTT_3-041109_A
strain measured @ 3[m] from root
Strain [µS]
500
400
300
200
100
0
-100
-200
-300
-400
-500
0
500
1.000
1.500
Local bending moment [kNm]
SG 152_1 (ELTT_3_041109_a.bin)
SG 152_2 (ELTT_3_041109_a.bin)
SG 152_3 (ELTT_3_041109_a.bin)

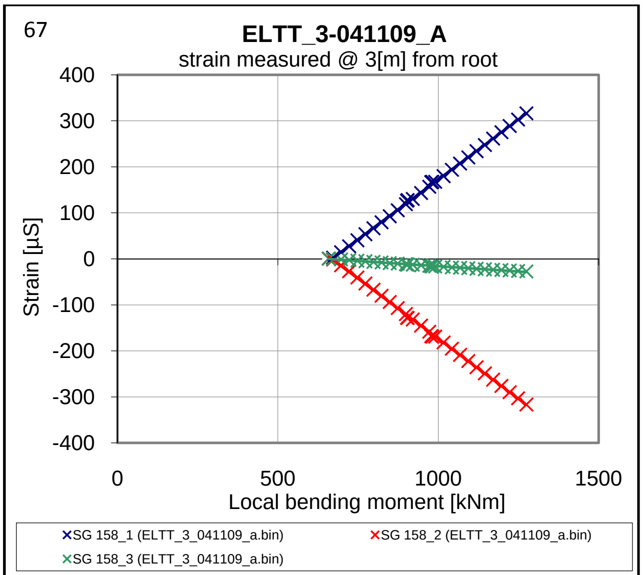
67
ELTT_3-041109_A
strain measured @ 3[m] from root
Strain [µS]
400
300
200
100
0
-100
-200
-300
-400
0
500
1000
1500
Local bending moment [kNm]
SG 158_1 (ELTT_3_041109_a.bin)
SG 158_2 (ELTT_3_041109_a.bin)
SG 158_3 (ELTT_3_041109_a.bin)

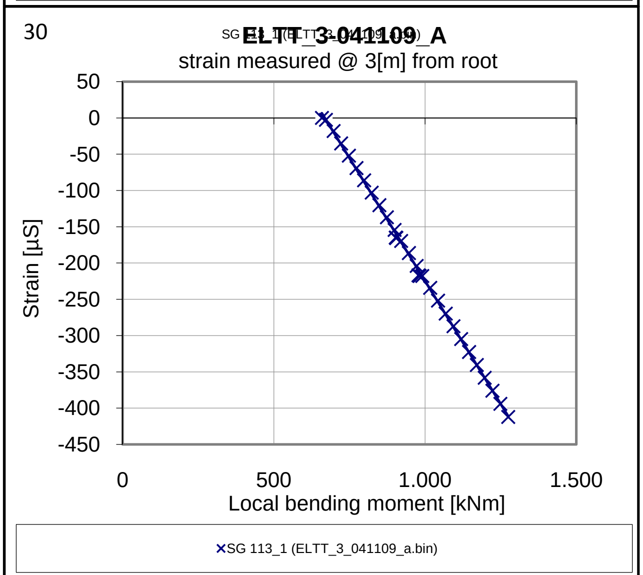
30
ELTT_3-041109_A
strain measured @ 3[m] from root
Strain [µS]
50
0
-50
-100
-150
-200
-250
-300
-350
-400
-450
0
500
1.000
1.500
Local bending moment [kNm]
SG 113_1 (ELTT_3_041109_a.bin)

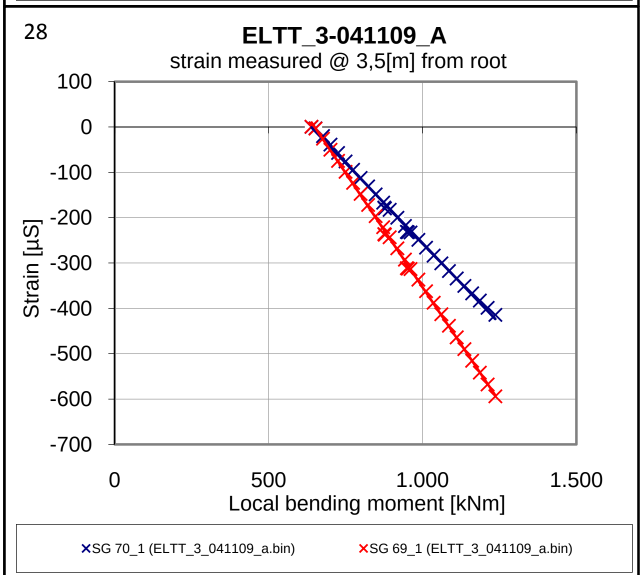
28
ELTT_3-041109_A
strain measured @ 3,5[m] from root
Strain [µS]
100
0
-100
-200
-300
-400
-500
-600
-700
0
500
1.000
1.500
Local bending moment [kNm]
SG 70_1 (ELTT_3_041109_a.bin)
SG 69_1 (ELTT_3_041109_a.bin)

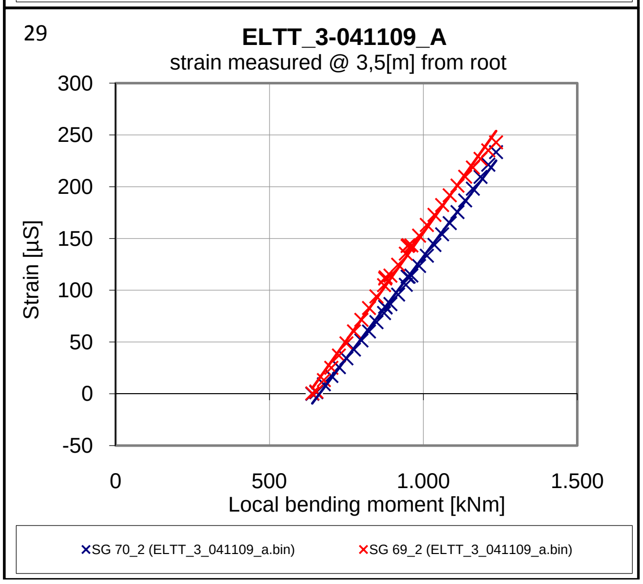
29
ELTT_3-041109_A
strain measured @ 3,5[m] from root
Strain [µS]
300
250
200
150
100
50
0
-50
0
500
1.000
1.500
Local bending moment [kNm]
SG 70_2 (ELTT_3_041109_a.bin)
SG 69_2 (ELTT_3_041109_a.bin)

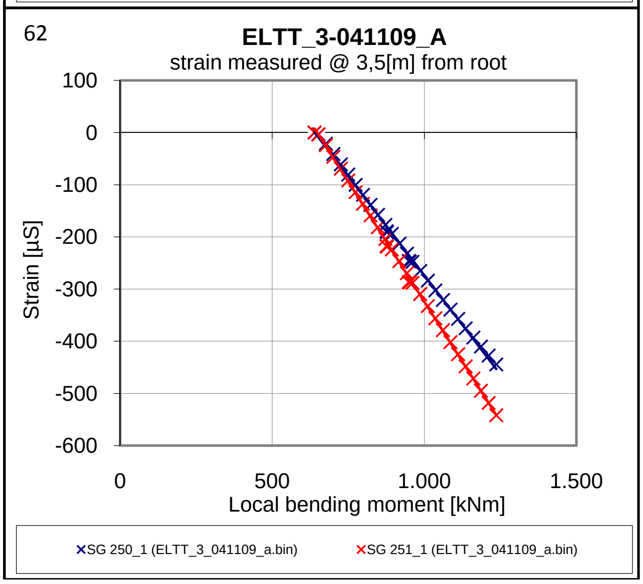
62
ELTT_3-041109_A
strain measured @ 3,5[m] from root
Strain [µS]
100
0
-100
-200
-300
-400
-500
-600
0
500
1.000
1.500
Local bending moment [kNm]
SG 250_1 (ELTT_3_041109_a.bin)
SG 251_1 (ELTT_3_041109_a.bin)

B3

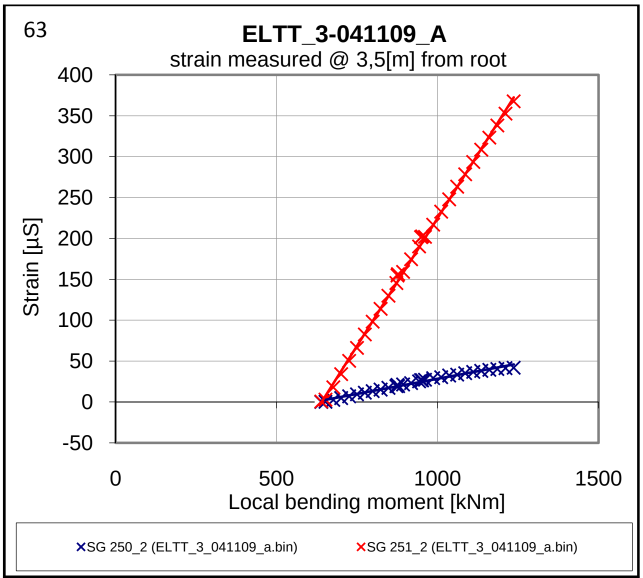
63
ELTT_3-041109_A
strain measured @ 3,5[m] from root
400
350
300
250
200
150
100
50
0
-50
Strain [µS]
0
500
1000
1500
Local bending moment [kNm]
SG 250_2 (ELTT_3_041109_a.bin)
SG 251_2 (ELTT_3_041109_a.bin)

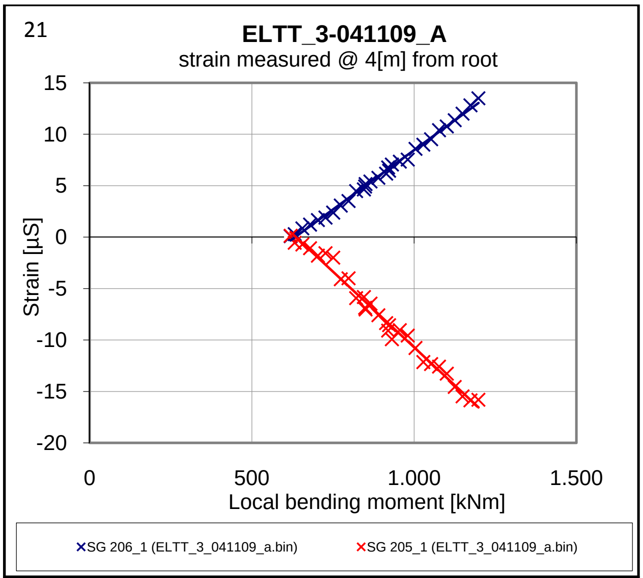
21
ELTT_3-041109_A
strain measured @ 4[m] from root
15
10
5
0
-5
-10
-15
-20
Strain [µS]
0
500
1.000
1.500
Local bending moment [kNm]
SG 206_1 (ELTT_3_041109_a.bin)
SG 205_1 (ELTT_3_041109_a.bin)

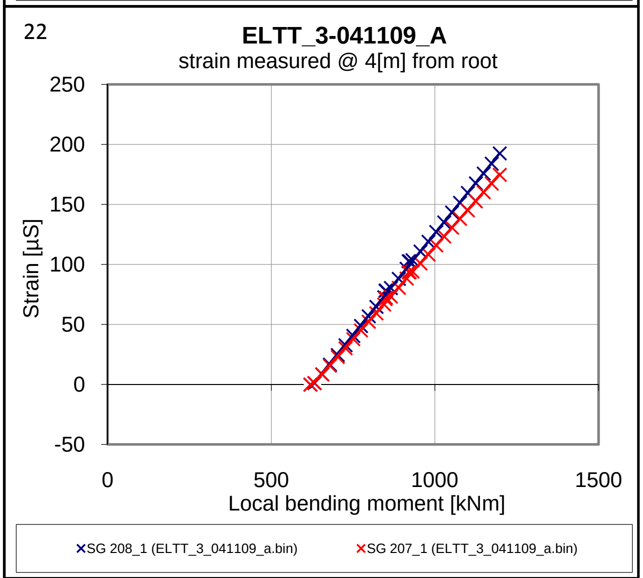
22
ELTT_3-041109_A
strain measured @ 4[m] from root
250
200
150
100
50
0
-50
Strain [µS]
0
500
1000
1500
Local bending moment [kNm]
SG 208_1 (ELTT_3_041109_a.bin)
SG 207_1 (ELTT_3_041109_a.bin)

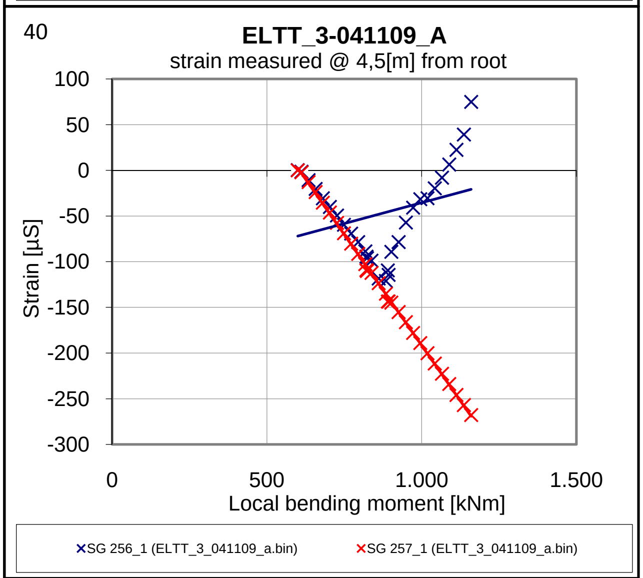
40
ELTT_3-041109_A
strain measured @ 4,5[m] from root
100
50
0
-50
-100
-150
-200
-250
-300
Strain [µS]
0
500
1.000
1.500
Local bending moment [kNm]
SG 256_1 (ELTT_3_041109_a.bin)
SG 257_1 (ELTT_3_041109_a.bin)

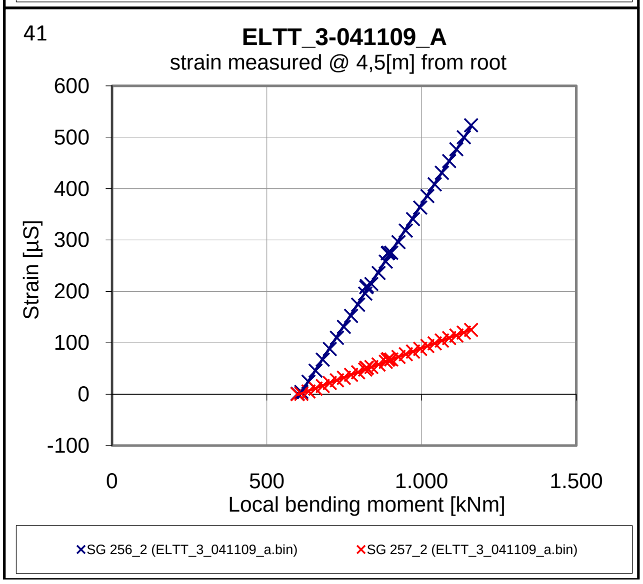
41
ELTT_3-041109_A
strain measured @ 4,5[m] from root
600
500
400
300
200
100
0
-100
Strain [µS]
0
500
1.000
1.500
Local bending moment [kNm]
SG 256_2 (ELTT_3_041109_a.bin)
SG 257_2 (ELTT_3_041109_a.bin)

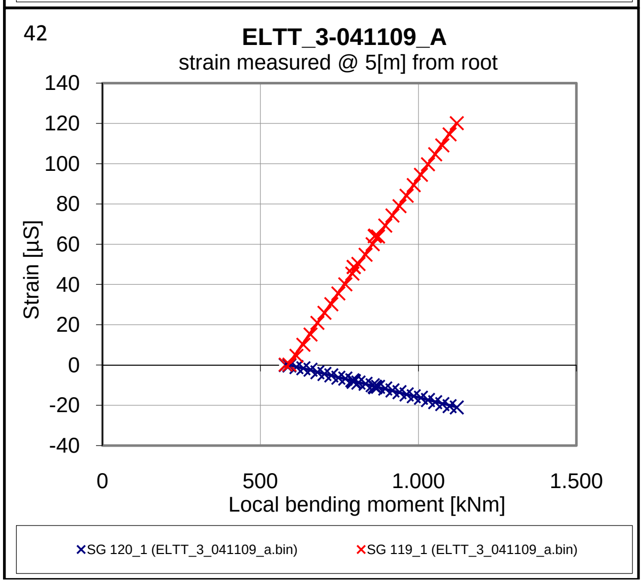
42
ELTT_3-041109_A
strain measured @ 5[m] from root
140
120
100
80
60
40
20
0
-20
-40
Strain [µS]
0
500
1.000
1.500
Local bending moment [kNm]
SG 120_1 (ELTT_3_041109_a.bin)
SG 119_1 (ELTT_3_041109_a.bin)

B3

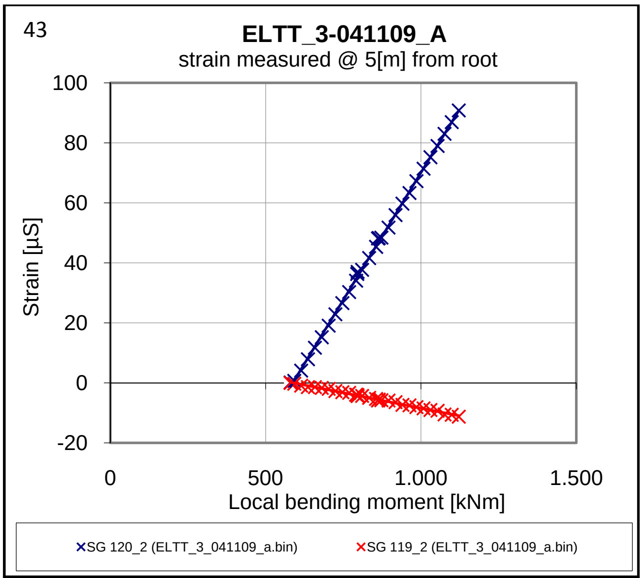
43
ELTT_3-041109_A
strain measured @ 5[m] from root
Strain [µS]
100
80
60
40
20
0
-20
0
500
1.000
1.500
Local bending moment [kNm]
SG 120_2 (ELTT_3_041109_a.bin)
SG 119_2 (ELTT_3_041109_a.bin)

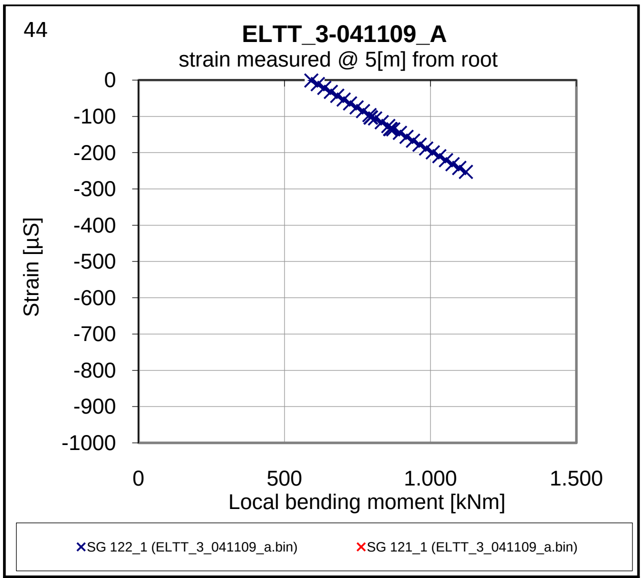
44
ELTT_3-041109_A
strain measured @ 5[m] from root
Strain [µS]
0
-100
-200
-300
-400
-500
-600
-700
-800
-900
-1000
0
500
1.000
1.500
Local bending moment [kNm]
SG 122_1 (ELTT_3_041109_a.bin)
SG 121_1 (ELTT_3_041109_a.bin)

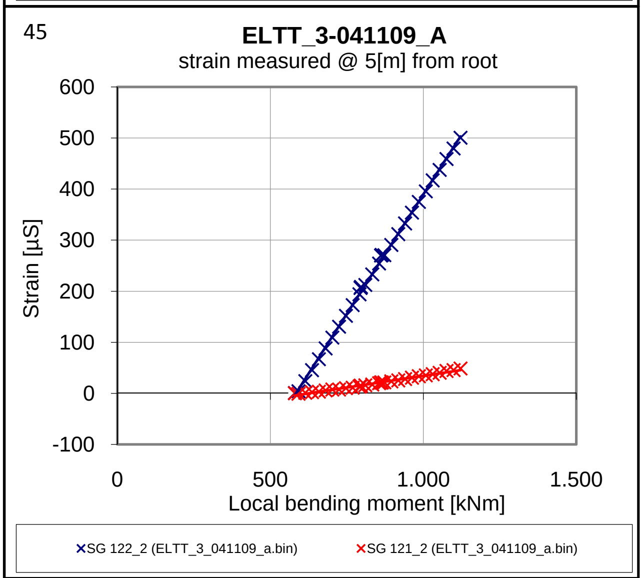
45
ELTT_3-041109_A
strain measured @ 5[m] from root
Strain [µS]
600
500
400
300
200
100
0
-100
0
500
1.000
1.500
Local bending moment [kNm]
SG 122_2 (ELTT_3_041109_a.bin)
SG 121_2 (ELTT_3_041109_a.bin)

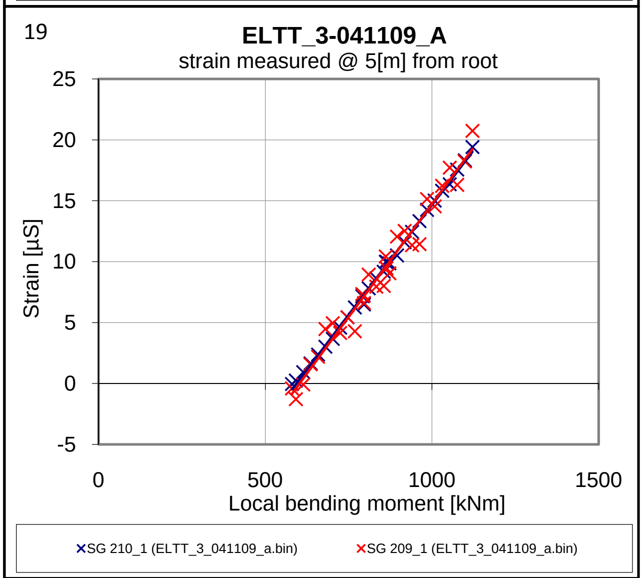
19
ELTT_3-041109_A
strain measured @ 5[m] from root
Strain [µS]
25
20
15
10
5
0
-5
0
500
1000
1500
Local bending moment [kNm]
SG 210_1 (ELTT_3_041109_a.bin)
SG 209_1 (ELTT_3_041109_a.bin)

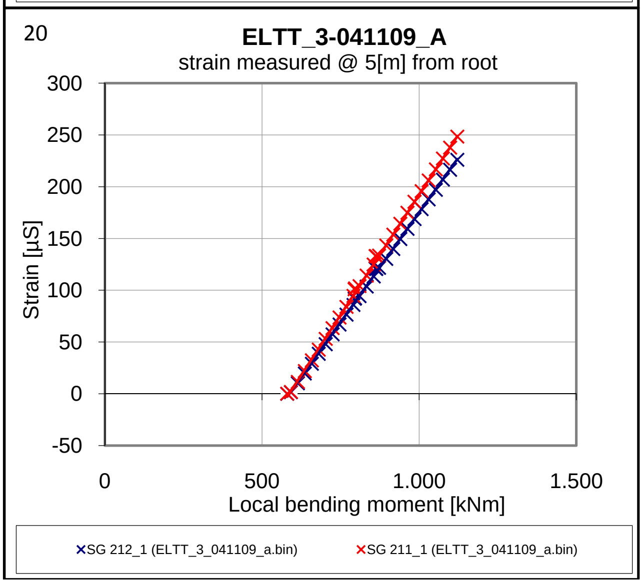
20
ELTT_3-041109_A
strain measured @ 5[m] from root
Strain [µS]
300
250
200
150
100
50
0
-50
0
500
1.000
1.500
Local bending moment [kNm]
SG 212_1 (ELTT_3_041109_a.bin)
SG 211_1 (ELTT_3_041109_a.bin)

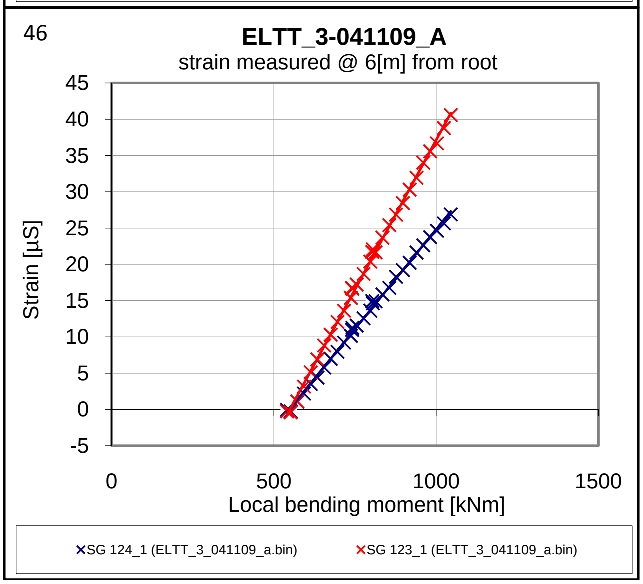
46
ELTT_3-041109_A
strain measured @ 6[m] from root
Strain [µS]
45
40
35
30
25
20
15
10
5
0
-5
0
500
1000
1500
Local bending moment [kNm]
SG 124_1 (ELTT_3_041109_a.bin)
SG 123_1 (ELTT_3_041109_a.bin)

B3

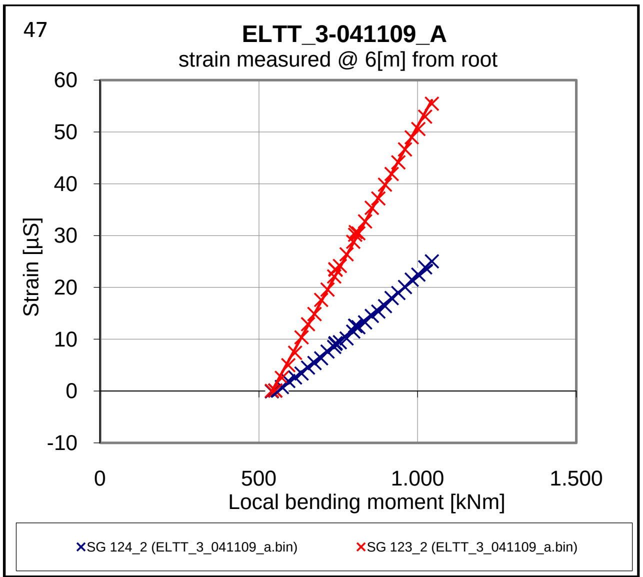
47
ELTT_3-041109_A
strain measured @ 6[m] from root
Strain [µS]
60
50
40
30
20
10
0
-10
0
500
1.000
1.500
Local bending moment [kNm]
SG 124_2 (ELTT_3_041109_a.bin)
SG 123_2 (ELTT_3_041109_a.bin)

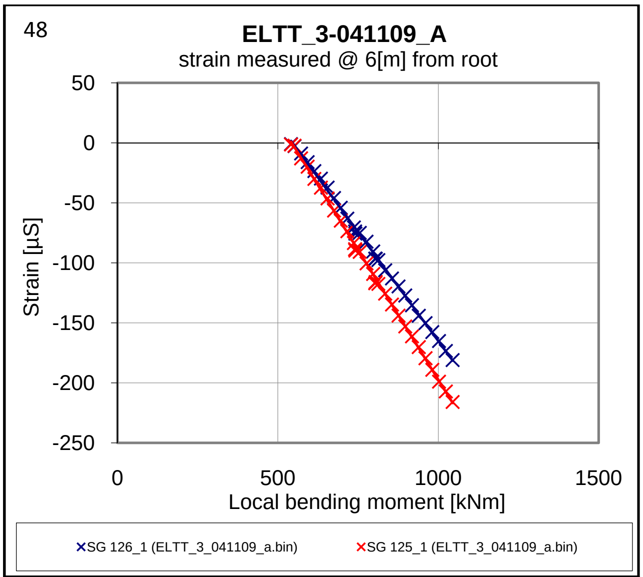
48
ELTT_3-041109_A
strain measured @ 6[m] from root
Strain [µS]
50
0
-50
-100
-150
-200
-250
0
500
1000
1500
Local bending moment [kNm]
SG 126_1 (ELTT_3_041109_a.bin)
SG 125_1 (ELTT_3_041109_a.bin)

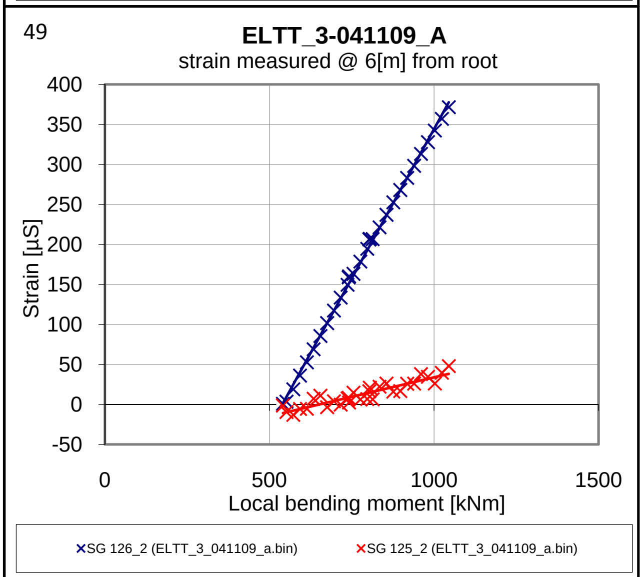
49
ELTT_3-041109_A
strain measured @ 6[m] from root
Strain [µS]
400
350
300
250
200
150
100
50
0
-50
0
500
1000
1500
Local bending moment [kNm]
SG 126_2 (ELTT_3_041109_a.bin)
SG 125_2 (ELTT_3_041109_a.bin)

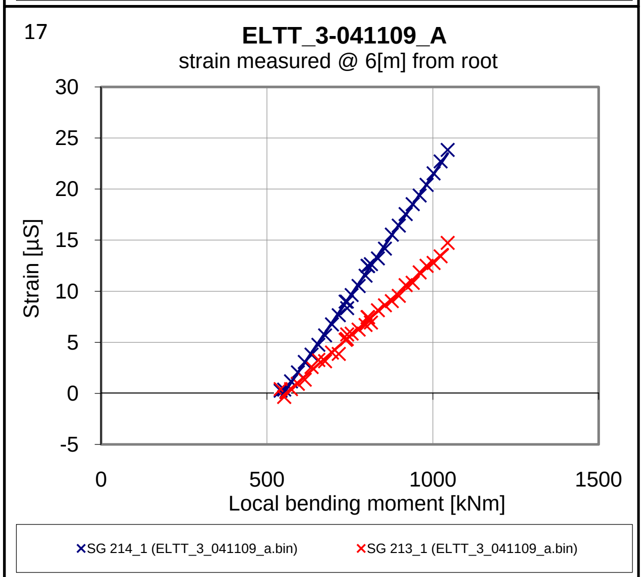
17
ELTT_3-041109_A
strain measured @ 6[m] from root
Strain [µS]
30
25
20
15
10
5
0
-5
0
500
1000
1500
Local bending moment [kNm]
SG 214_1 (ELTT_3_041109_a.bin)
SG 213_1 (ELTT_3_041109_a.bin)

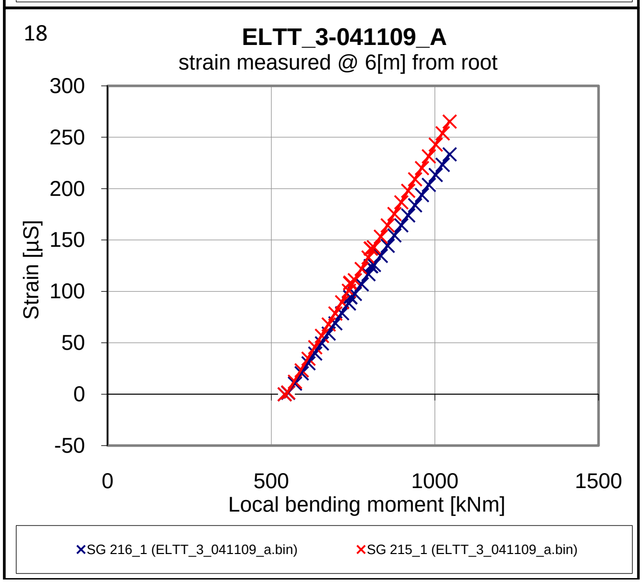
18
ELTT_3-041109_A
strain measured @ 6[m] from root
Strain [µS]
300
250
200
150
100
50
0
-50
0
500
1000
1500
Local bending moment [kNm]
SG 216_1 (ELTT_3_041109_a.bin)
SG 215_1 (ELTT_3_041109_a.bin)

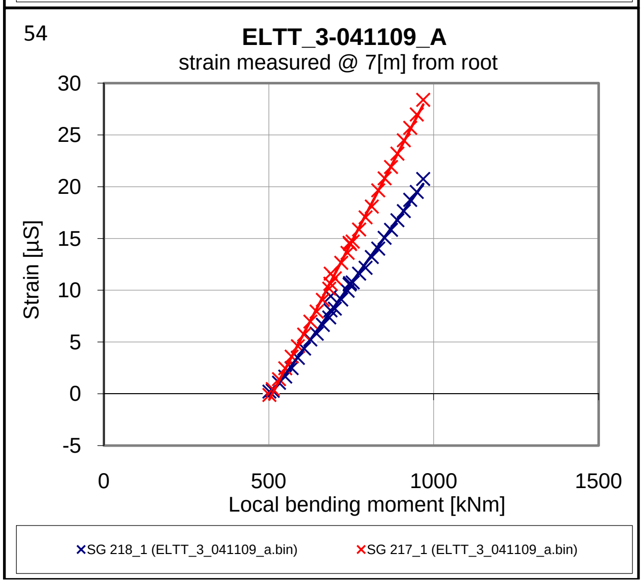
54
ELTT_3-041109_A
strain measured @ 7[m] from root
Strain [µS]
30
25
20
15
10
5
0
-5
0
500
1000
1500
Local bending moment [kNm]
SG 218_1 (ELTT_3_041109_a.bin)
SG 217_1 (ELTT_3_041109_a.bin)

B3

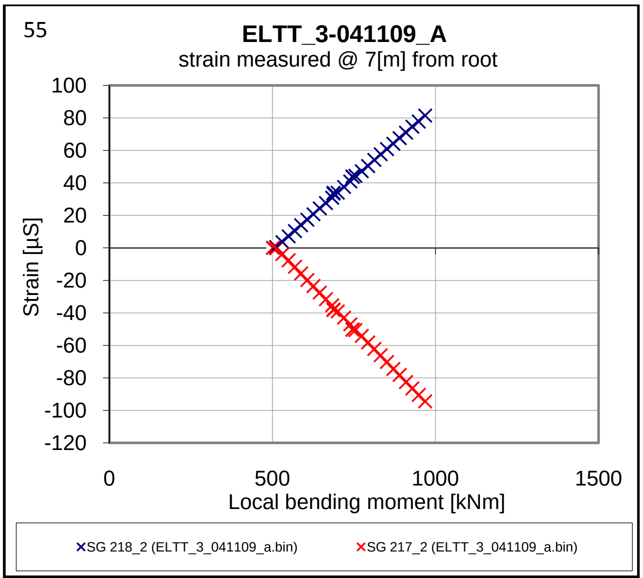
55
ELTT_3-041109_A
strain measured @ 7[m] from root
Strain [µS]
100
80
60
40
20
0
-20
-40
-60
-80
-100
-120
0
500
1000
1500
Local bending moment [kNm]
SG 218_2 (ELTT_3_041109_a.bin)
SG 217_2 (ELTT_3_041109_a.bin)

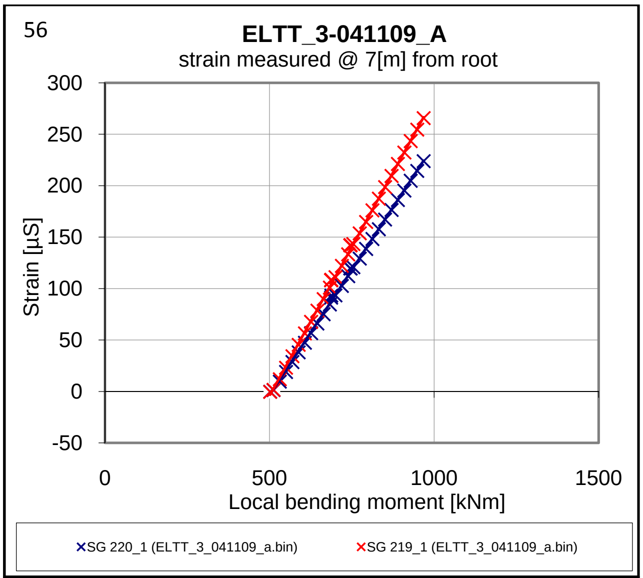
56
ELTT_3-041109_A
strain measured @ 7[m] from root
Strain [µS]
300
250
200
150
100
50
0
-50
0
500
1000
1500
Local bending moment [kNm]
SG 220_1 (ELTT_3_041109_a.bin)
SG 219_1 (ELTT_3_041109_a.bin)

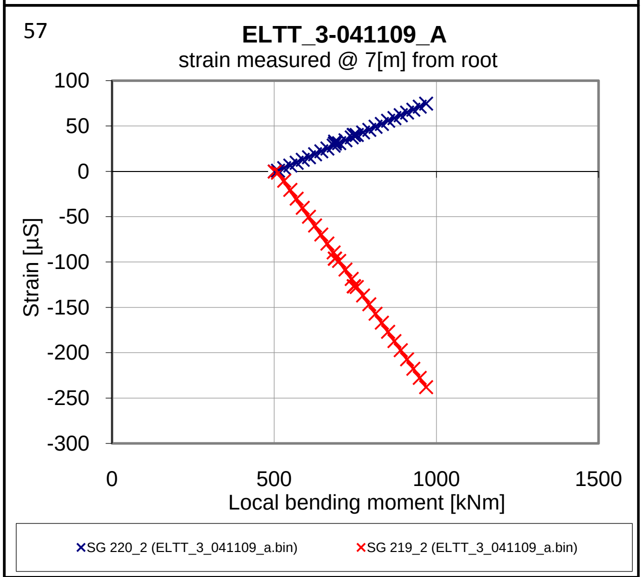
57
ELTT_3-041109_A
strain measured @ 7[m] from root
Strain [µS]
100
50
0
-50
-100
-150
-200
-250
-300
0
500
1000
1500
Local bending moment [kNm]
SG 220_2 (ELTT_3_041109_a.bin)
SG 219_2 (ELTT_3_041109_a.bin)

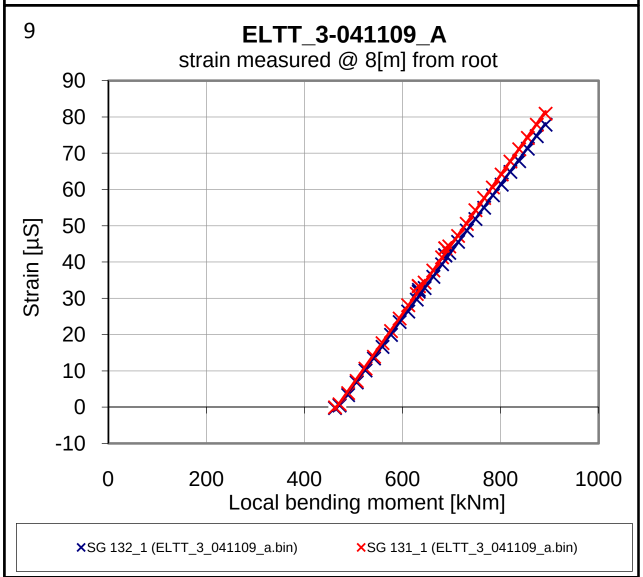
9
ELTT_3-041109_A
strain measured @ 8[m] from root
Strain [µS]
90
80
70
60
50
40
30
20
10
0
-10
0
200
400
600
800
1000
Local bending moment [kNm]
SG 132_1 (ELTT_3_041109_a.bin)
SG 131_1 (ELTT_3_041109_a.bin)

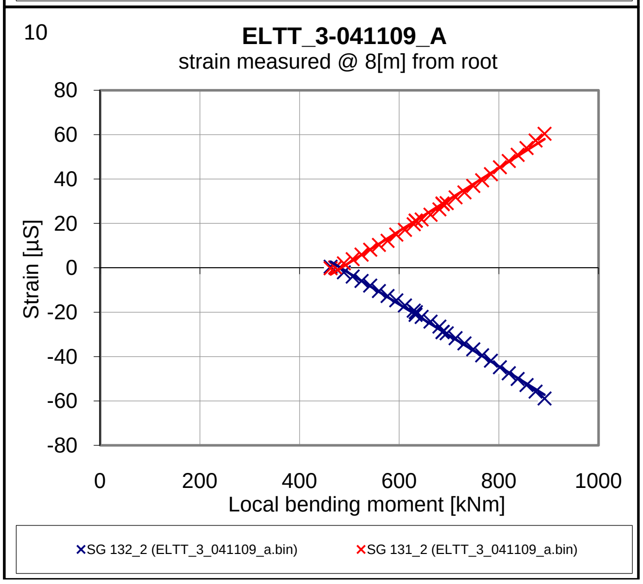
10
ELTT_3-041109_A
strain measured @ 8[m] from root
Strain [µS]
80
60
40
20
0
-20
-40
-60
-80
0
200
400
600
800
1000
Local bending moment [kNm]
SG 132_2 (ELTT_3_041109_a.bin)
SG 131_2 (ELTT_3_041109_a.bin)

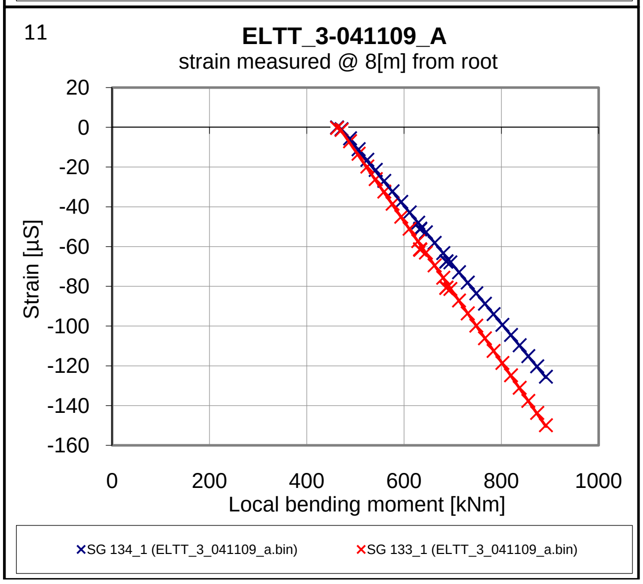
11
ELTT_3-041109_A
strain measured @ 8[m] from root
Strain [µS]
20
0
-20
-40
-60
-80
-100
-120
-140
-160
0
200
400
600
800
1000
Local bending moment [kNm]
SG 134_1 (ELTT_3_041109_a.bin)
SG 133_1 (ELTT_3_041109_a.bin)

B3

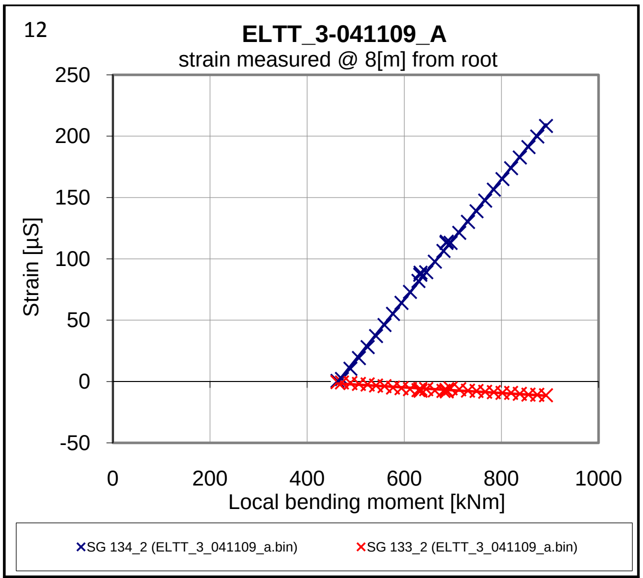
12
ELTT_3-041109_A
strain measured @ 8[m] from root
Strain [µS]
250
200
150
100
50
0
-50
0
200
400
600
800
1000
Local bending moment [kNm]
SG 134_2 (ELTT_3_041109_a.bin)
SG 133_2 (ELTT_3_041109_a.bin)

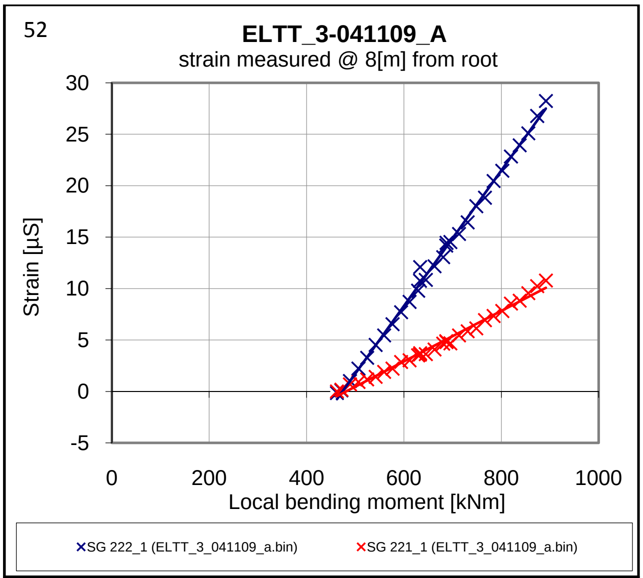
52
ELTT_3-041109_A
strain measured @ 8[m] from root
Strain [µS]
30
25
20
15
10
5
0
-5
0
200
400
600
800
1000
Local bending moment [kNm]
SG 222_1 (ELTT_3_041109_a.bin)
SG 221_1 (ELTT_3_041109_a.bin)

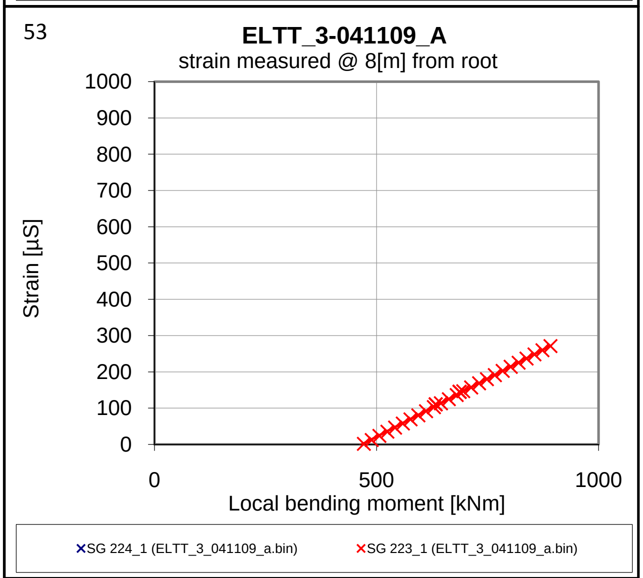
53
ELTT_3-041109_A
strain measured @ 8[m] from root
Strain [µS]
1000
900
800
700
600
500
400
300
200
100
0
0
500
1000
Local bending moment [kNm]
SG 224_1 (ELTT_3_041109_a.bin)
SG 223_1 (ELTT_3_041109_a.bin)

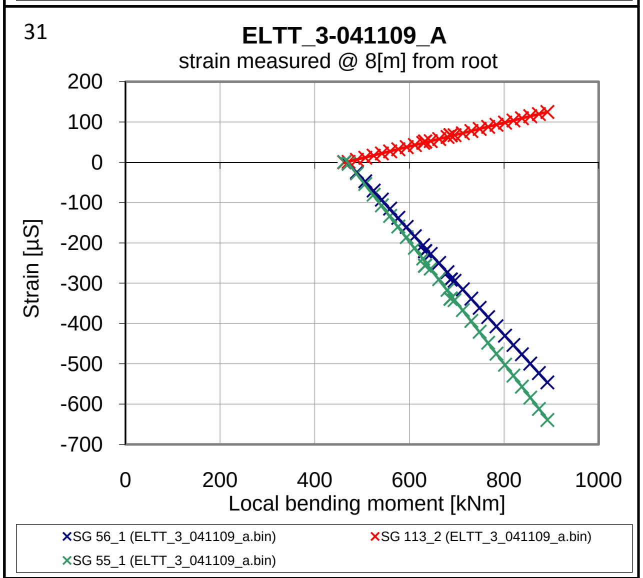
31
ELTT_3-041109_A
strain measured @ 8[m] from root
Strain [µS]
200
100
0
-100
-200
-300
-400
-500
-600
-700
0
200
400
600
800
1000
Local bending moment [kNm]
SG 56_1 (ELTT_3_041109_a.bin)
SG 113_2 (ELTT_3_041109_a.bin)
SG 55_1 (ELTT_3_041109_a.bin)

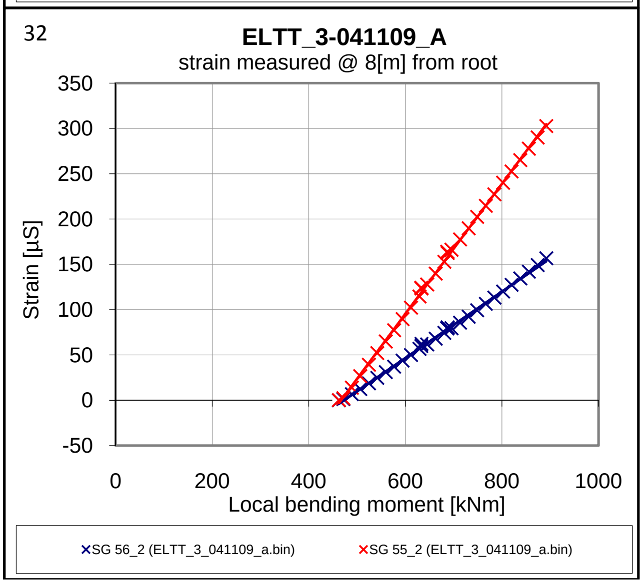
32
ELTT_3-041109_A
strain measured @ 8[m] from root
Strain [µS]
350
300
250
200
150
100
50
0
-50
0
200
400
600
800
1000
Local bending moment [kNm]
SG 56_2 (ELTT_3_041109_a.bin)
SG 55_2 (ELTT_3_041109_a.bin)

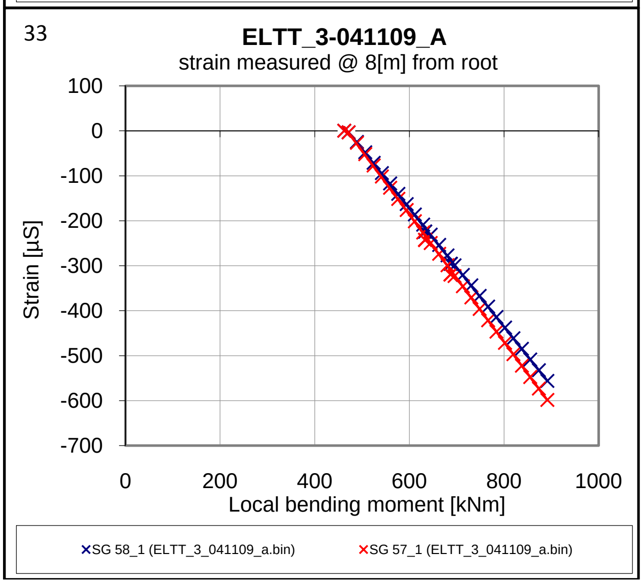
33
ELTT_3-041109_A
strain measured @ 8[m] from root
Strain [µS]
100
0
-100
-200
-300
-400
-500
-600
-700
0
200
400
600
800
1000
Local bending moment [kNm]
SG 58_1 (ELTT_3_041109_a.bin)
SG 57_1 (ELTT_3_041109_a.bin)

B3

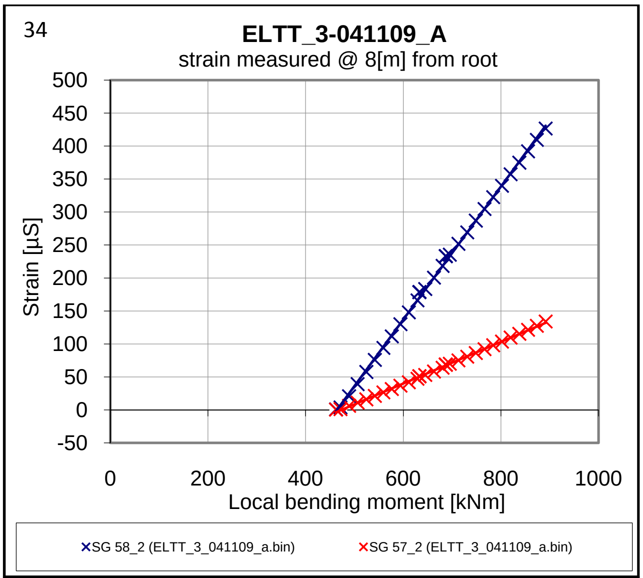
34
ELTT_3-041109_A
strain measured @ 8[m] from root
Strain [µS]
500 450 400 350 300 250 200 150 100 50 0 -50
0 200 400 600 800 1000
Local bending moment [kNm]
SG 58_2 (ELTT_3_041109_a.bin)
SG 57_2 (ELTT_3_041109_a.bin)

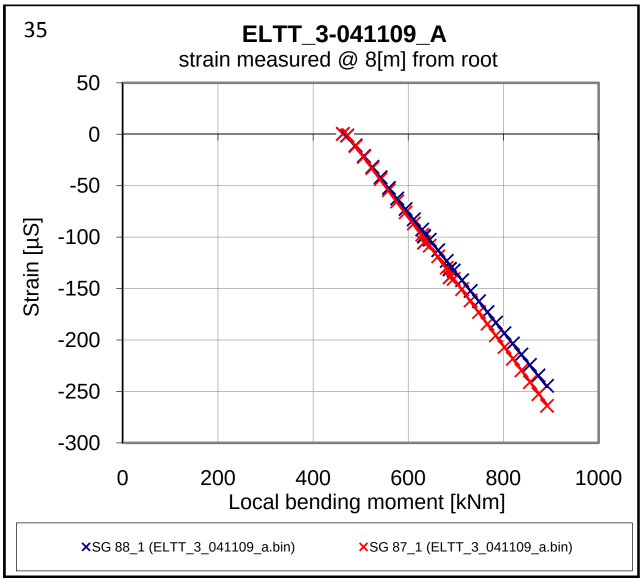
35
ELTT_3-041109_A
strain measured @ 8[m] from root
Strain [µS]
50 0 -50 -100 -150 -200 -250 -300
0 200 400 600 800 1000
Local bending moment [kNm]
SG 88_1 (ELTT_3_041109_a.bin)
SG 87_1 (ELTT_3_041109_a.bin)

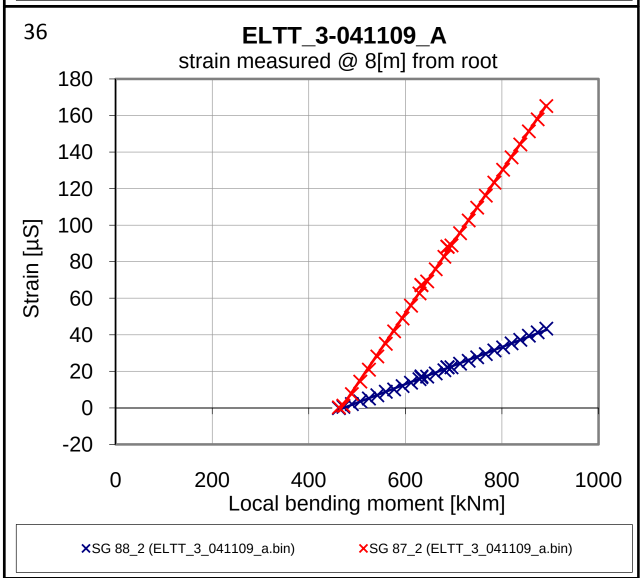
36
ELTT_3-041109_A
strain measured @ 8[m] from root
Strain [µS]
180 160 140 120 100 80 60 40 20 0 -20
0 200 400 600 800 1000
Local bending moment [kNm]
SG 88_2 (ELTT_3_041109_a.bin)
SG 87_2 (ELTT_3_041109_a.bin)

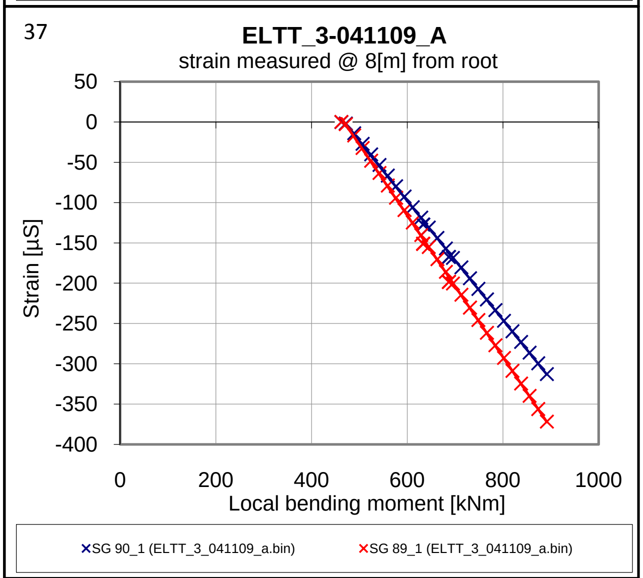
37
ELTT_3-041109_A
strain measured @ 8[m] from root
Strain [µS]
50 0 -50 -100 -150 -200 -250 -300 -350 -400
0 200 400 600 800 1000
Local bending moment [kNm]
SG 90_1 (ELTT_3_041109_a.bin)
SG 89_1 (ELTT_3_041109_a.bin)

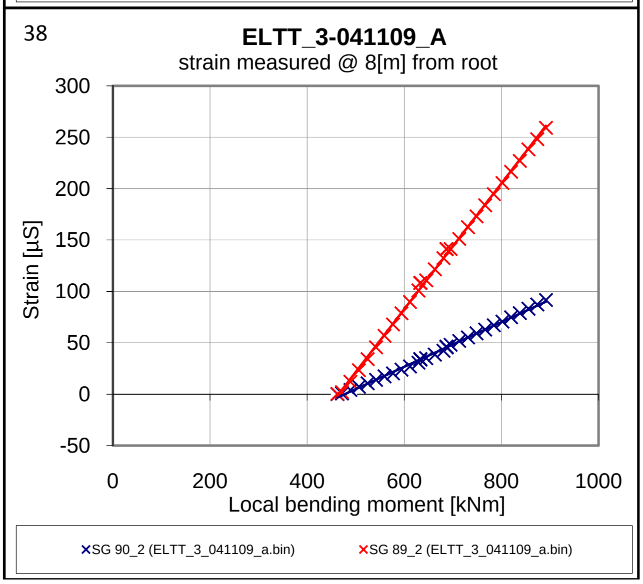
38
ELTT_3-041109_A
strain measured @ 8[m] from root
Strain [µS]
300 250 200 150 100 50 0 -50
0 200 400 600 800 1000
Local bending moment [kNm]
SG 90_2 (ELTT_3_041109_a.bin)
SG 89_2 (ELTT_3_041109_a.bin)

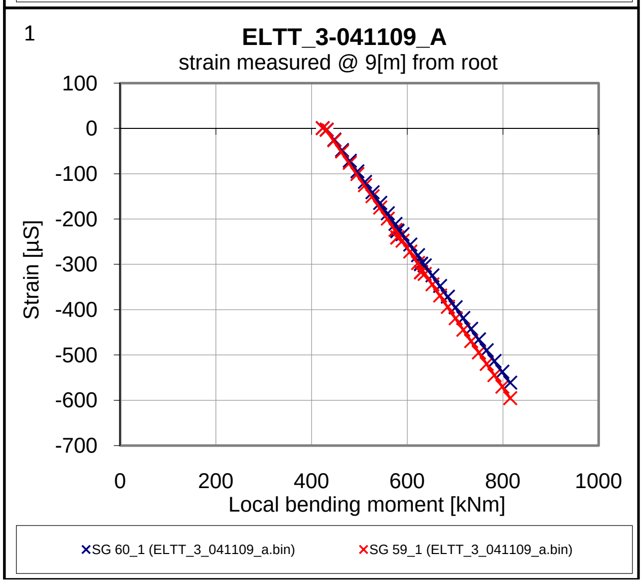
1
ELTT_3-041109_A
strain measured @ 9[m] from root
Strain [µS]
100 0 -100 -200 -300 -400 -500 -600 -700
0 200 400 600 800 1000
Local bending moment [kNm]
SG 60_1 (ELTT_3_041109_a.bin)
SG 59_1 (ELTT_3_041109_a.bin)

B3

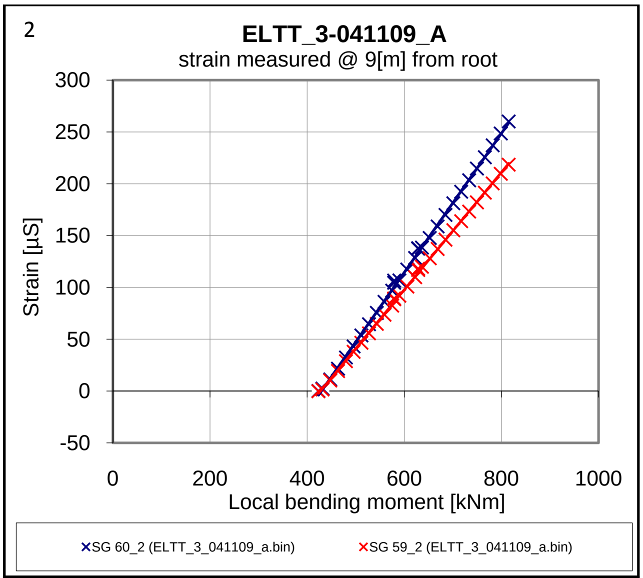
2
ELTT_3-041109_A
strain measured @ 9[m] from root
Strain [µS]
300
250
200
150
100
50
0
-50
0
200
400
600
800
1000
Local bending moment [kNm]
SG 60_2 (ELTT_3_041109_a.bin)
SG 59_2 (ELTT_3_041109_a.bin)

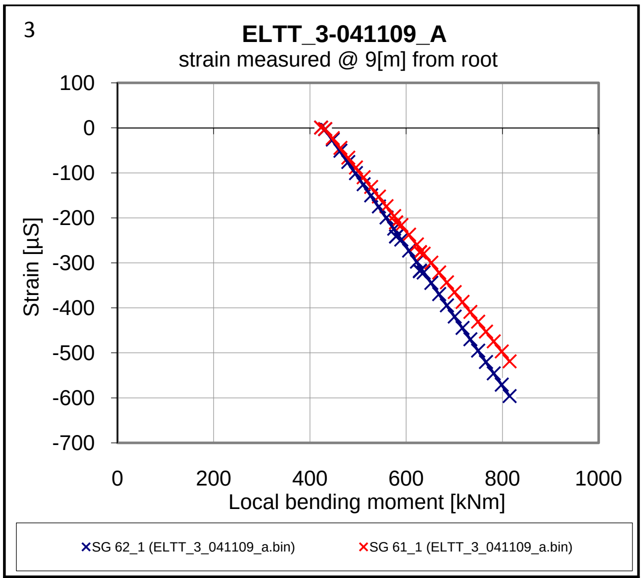
3
ELTT_3-041109_A
strain measured @ 9[m] from root
Strain [µS]
100
0
-100
-200
-300
-400
-500
-600
-700
0
200
400
600
800
1000
Local bending moment [kNm]
SG 62_1 (ELTT_3_041109_a.bin)
SG 61_1 (ELTT_3_041109_a.bin)

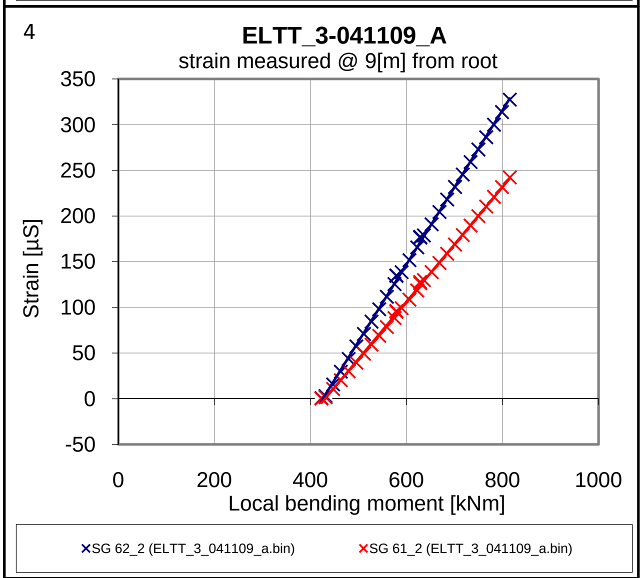
4
ELTT_3-041109_A
strain measured @ 9[m] from root
Strain [µS]
350
300
250
200
150
100
50
0
-50
0
200
400
600
800
1000
Local bending moment [kNm]
SG 62_2 (ELTT_3_041109_a.bin)
SG 61_2 (ELTT_3_041109_a.bin)

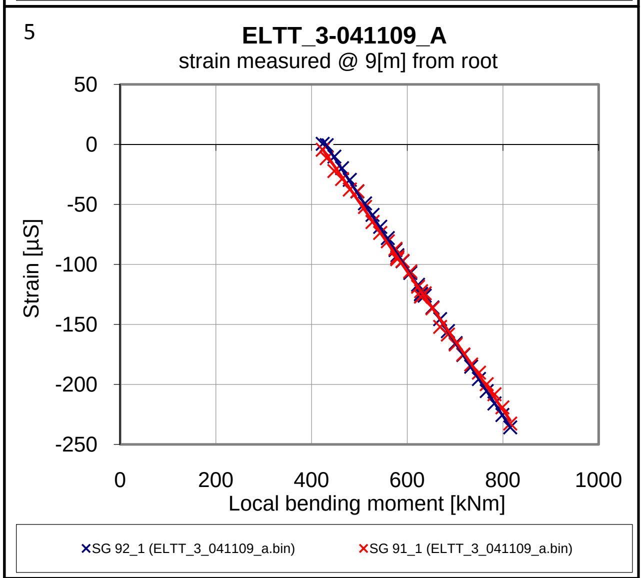
5
ELTT_3-041109_A
strain measured @ 9[m] from root
Strain [µS]
50
0
-50
-100
-150
-200
-250
0
200
400
600
800
1000
Local bending moment [kNm]
SG 92_1 (ELTT_3_041109_a.bin)
SG 91_1 (ELTT_3_041109_a.bin)

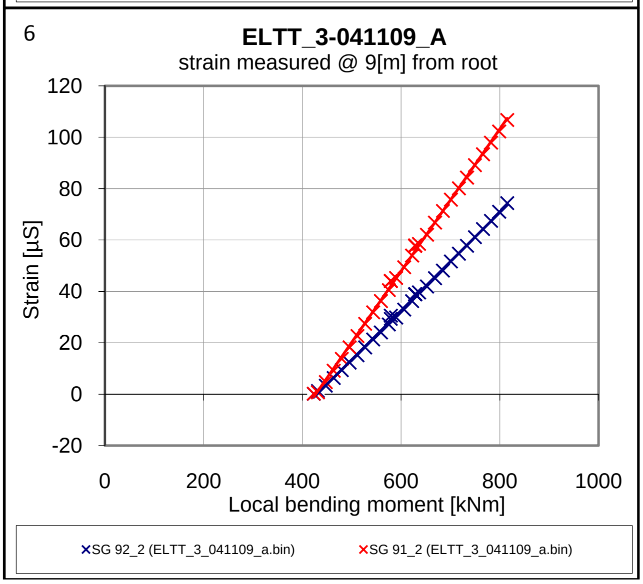
6
ELTT_3-041109_A
strain measured @ 9[m] from root
Strain [µS]
120
100
80
60
40
20
0
-20
0
200
400
600
800
1000
Local bending moment [kNm]
SG 92_2 (ELTT_3_041109_a.bin)
SG 91_2 (ELTT_3_041109_a.bin)

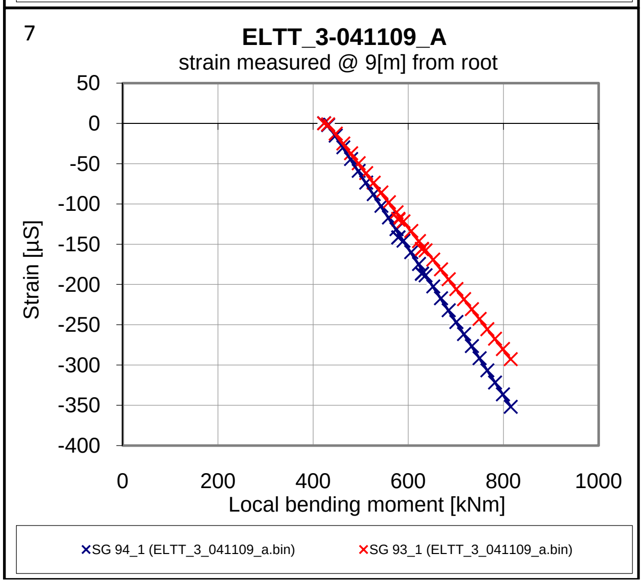
7
ELTT_3-041109_A
strain measured @ 9[m] from root
Strain [µS]
50
0
-50
-100
-150
-200
-250
-300
-350
-400
0
200
400
600
800
1000
Local bending moment [kNm]
SG 94_1 (ELTT_3_041109_a.bin)
SG 93_1 (ELTT_3_041109_a.bin)

B3

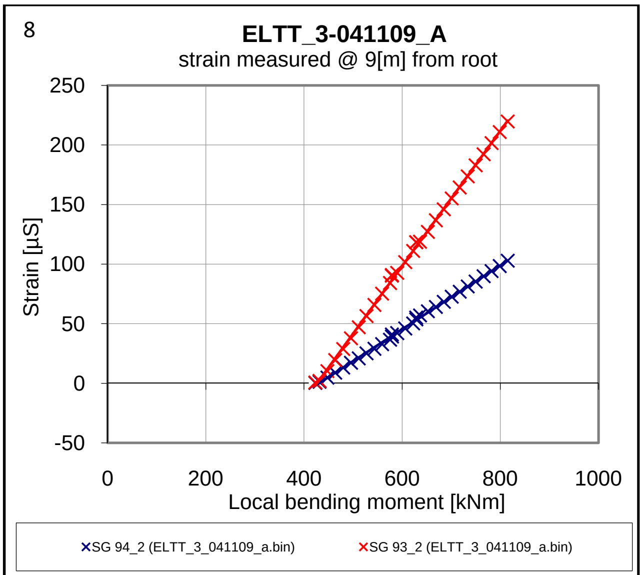
8
ELTT_3-041109_A
strain measured @ 9[m] from root
Strain [µS]
Local bending moment [kNm]
SG 94_2 (ELTT_3_041109_a.bin)
SG 93_2 (ELTT_3_041109_a.bin)

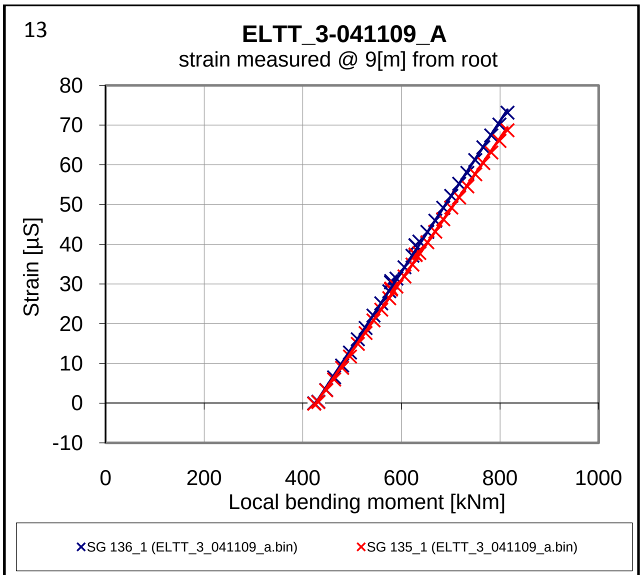
13
ELTT_3-041109_A
strain measured @ 9[m] from root
Strain [µS]
Local bending moment [kNm]
SG 136_1 (ELTT_3_041109_a.bin)
SG 135_1 (ELTT_3_041109_a.bin)

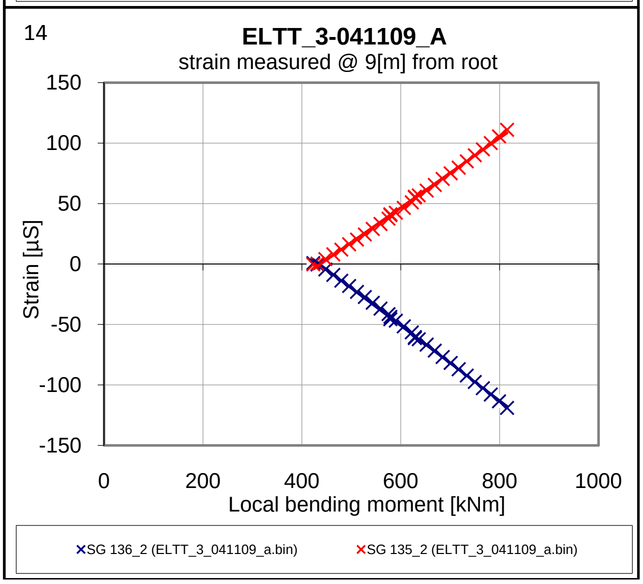
14
ELTT_3-041109_A
strain measured @ 9[m] from root
Strain [µS]
Local bending moment [kNm]
SG 136_2 (ELTT_3_041109_a.bin)
SG 135_2 (ELTT_3_041109_a.bin)

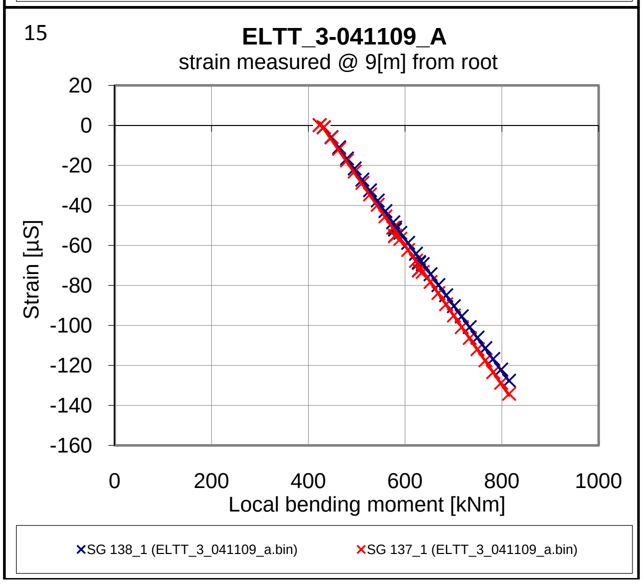
15
ELTT_3-041109_A
strain measured @ 9[m] from root
Strain [µS]
Local bending moment [kNm]
SG 138_1 (ELTT_3_041109_a.bin)
SG 137_1 (ELTT_3_041109_a.bin)

B3

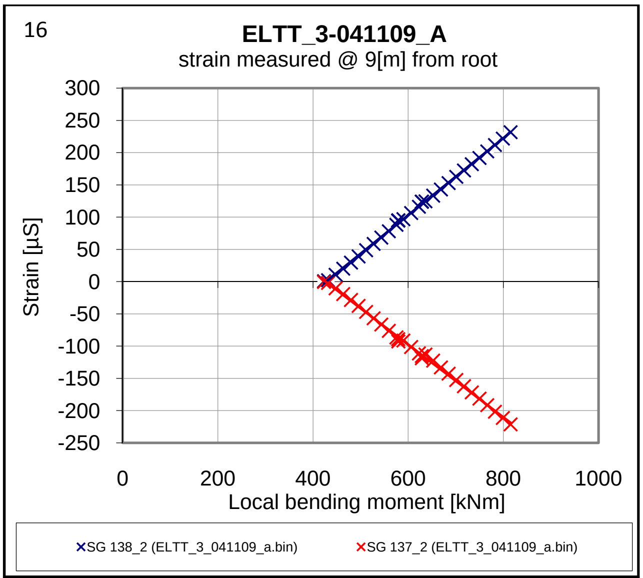
16
ELTT_3-041109_A
strain measured @ 9[m] from root
Strain [µS]
300
250
200
150
100
50
0
-50
-100
-150
-200
-250
0
200
400
600
800
1000
Local bending moment [kNm]
SG 138_2 (ELTT_3_041109_a.bin)
SG 137_2 (ELTT_3_041109_a.bin)

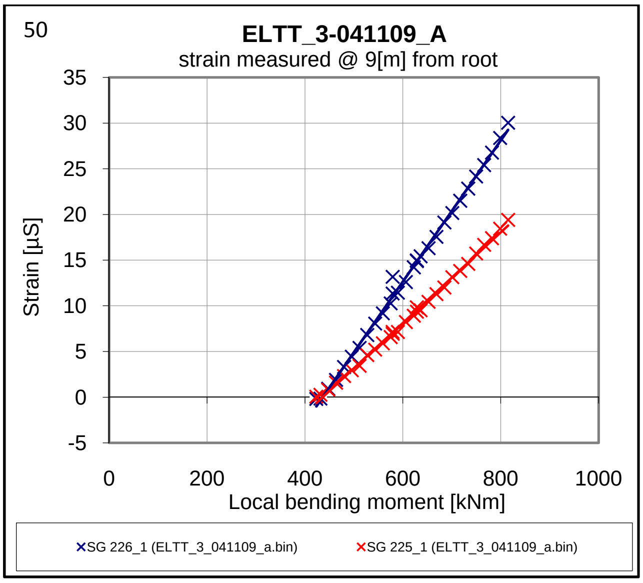
50
ELTT_3-041109_A
strain measured @ 9[m] from root
Strain [µS]
35
30
25
20
15
10
5
0
-5
0
200
400
600
800
1000
Local bending moment [kNm]
SG 226_1 (ELTT_3_041109_a.bin)
SG 225_1 (ELTT_3_041109_a.bin)

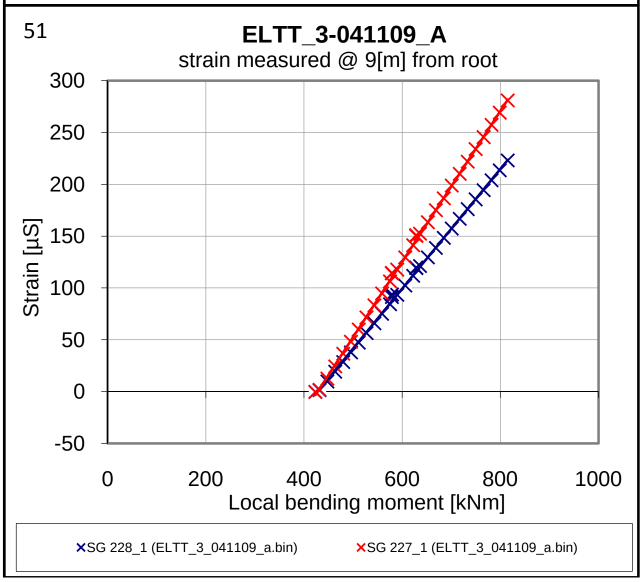
51
ELTT_3-041109_A
strain measured @ 9[m] from root
Strain [µS]
300
250
200
150
100
50
0
-50
0
200
400
600
800
1000
Local bending moment [kNm]
SG 228_1 (ELTT_3_041109_a.bin)
SG 227_1 (ELTT_3_041109_a.bin)

B4 The deflections measurements vs. local bending moment

Deflections measured in test ELTT_1-291009_A

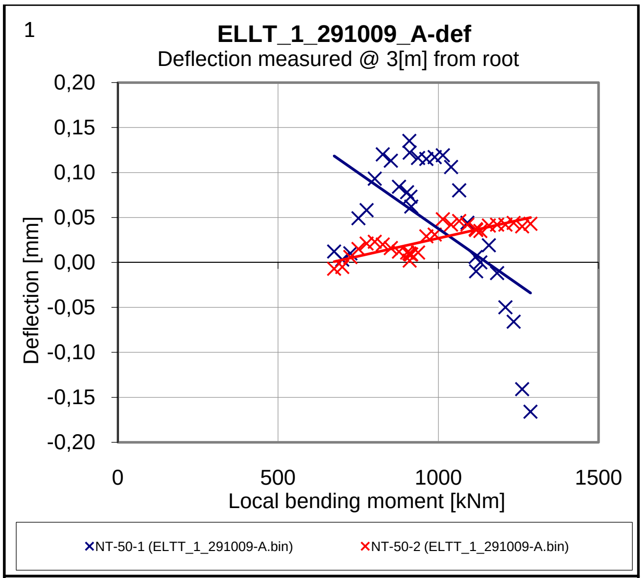

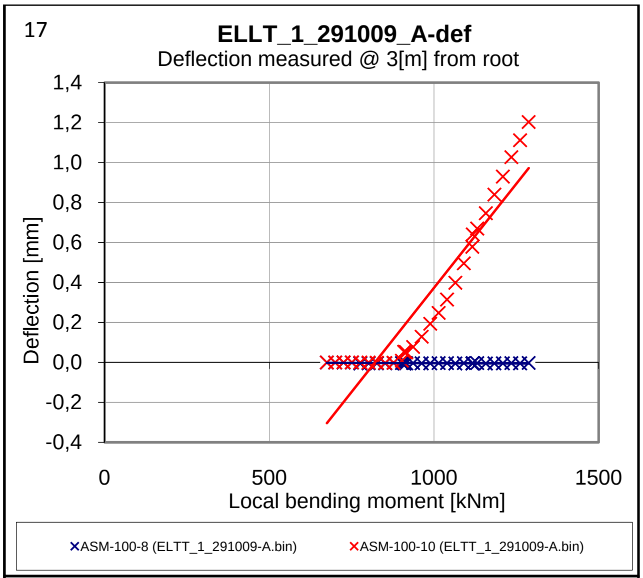

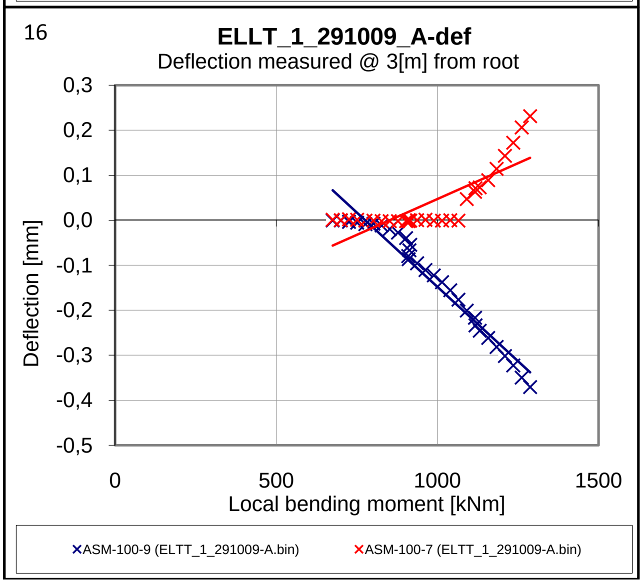

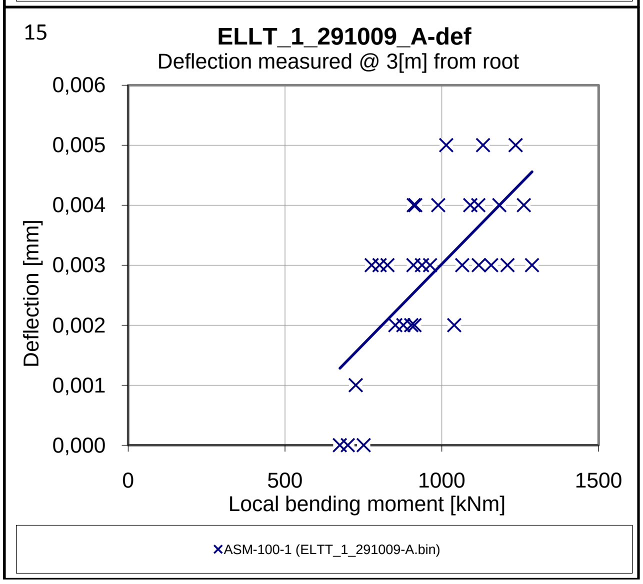

B4

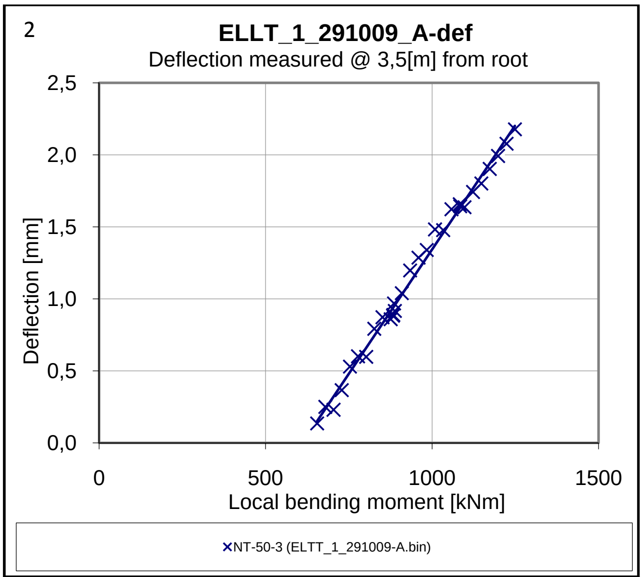
2
ELLT_1_291009_A-def
Deflection measured @ 3,5[m] from root
2,5
2,0
1,5
1,0
0,5
0,0
Deflection [mm]
0
500
1000
1500
Local bending moment [kNm]
NT-50-3 (ELLT_1_291009-A.bin)

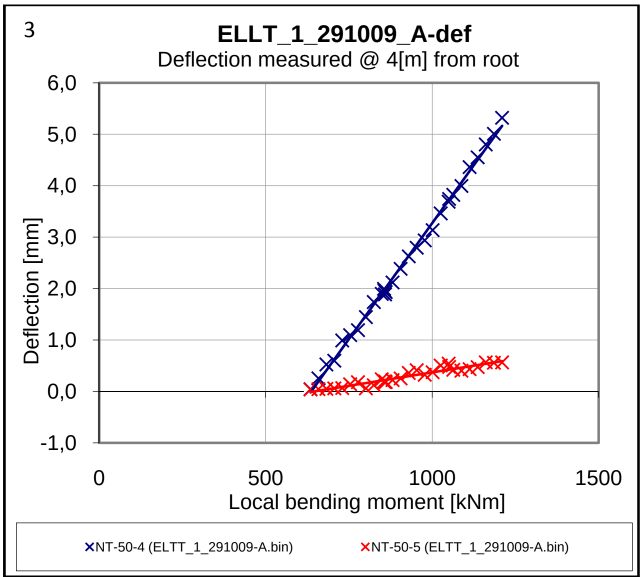
3
ELLT_1_291009_A-def
Deflection measured @ 4[m] from root
6,0
5,0
4,0
3,0
2,0
1,0
0,0
-1,0
Deflection [mm]
0
500
1000
1500
Local bending moment [kNm]
NT-50-4 (ELLT_1_291009-A.bin)
NT-50-5 (ELLT_1_291009-A.bin)

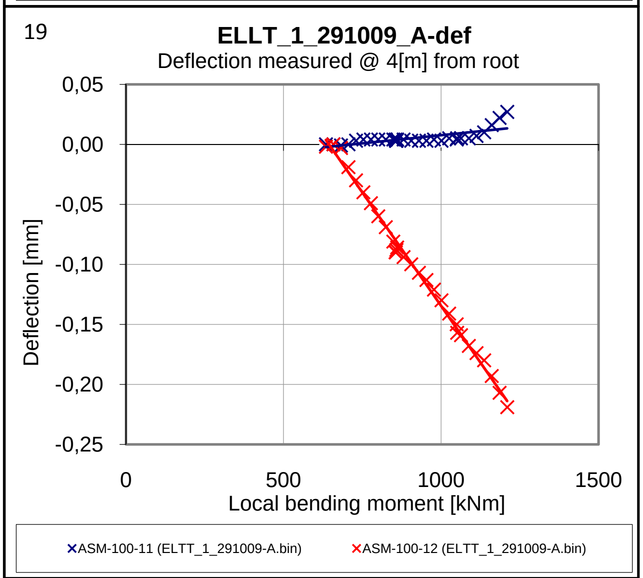
19
ELLT_1_291009_A-def
Deflection measured @ 4[m] from root
0,05
0,00
-0,05
-0,10
-0,15
-0,20
-0,25
Deflection [mm]
0
500
1000
1500
Local bending moment [kNm]
ASM-100-11 (ELLT_1_291009-A.bin)
ASM-100-12 (ELLT_1_291009-A.bin)

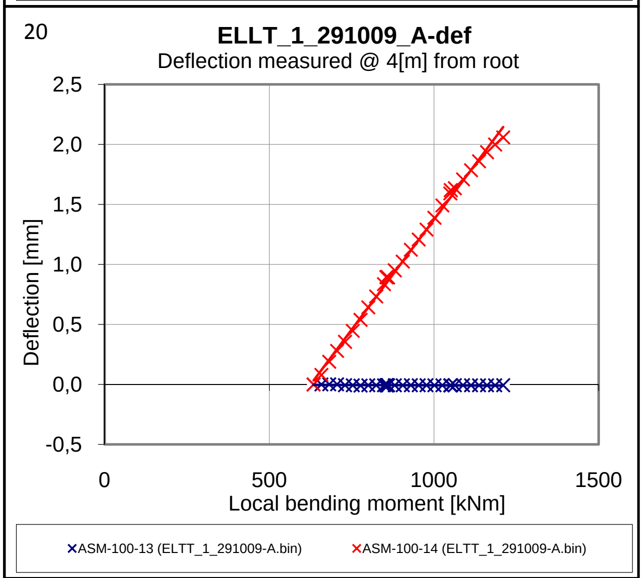
20
ELLT_1_291009_A-def
Deflection measured @ 4[m] from root
2,5
2,0
1,5
1,0
0,5
0,0
-0,5
Deflection [mm]
0
500
1000
1500
Local bending moment [kNm]
ASM-100-13 (ELLT_1_291009-A.bin)
ASM-100-14 (ELLT_1_291009-A.bin)

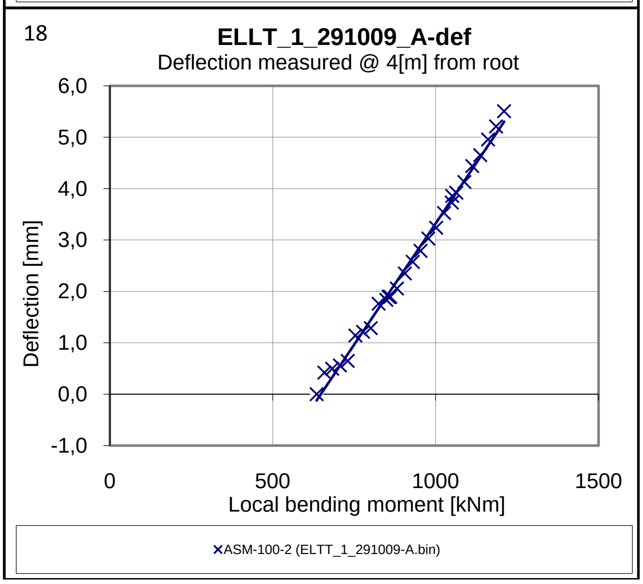
18
ELLT_1_291009_A-def
Deflection measured @ 4[m] from root
6,0
5,0
4,0
3,0
2,0
1,0
0,0
-1,0
Deflection [mm]
0
500
1000
1500
Local bending moment [kNm]
ASM-100-2 (ELLT_1_291009-A.bin)

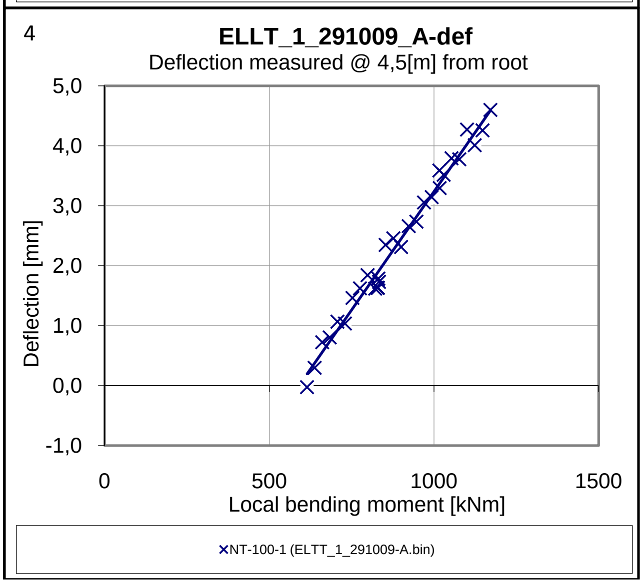
4
ELLT_1_291009_A-def
Deflection measured @ 4,5[m] from root
5,0
4,0
3,0
2,0
1,0
0,0
-1,0
Deflection [mm]
0
500
1000
1500
Local bending moment [kNm]
NT-100-1 (ELLT_1_291009-A.bin)

B4

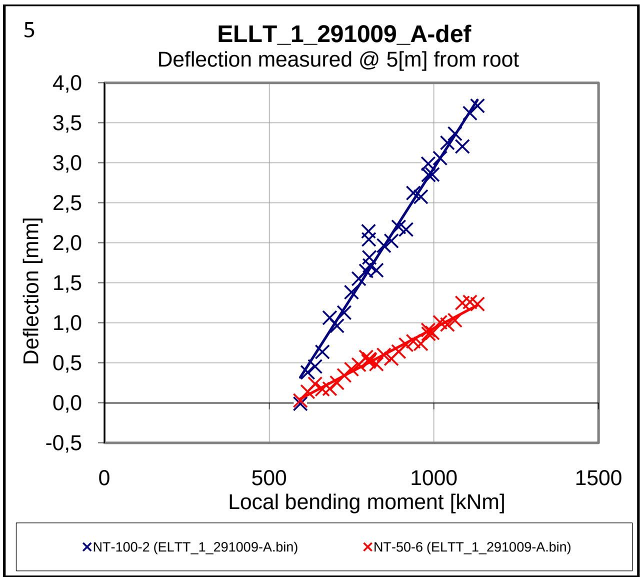
5
ELLT_1_291009_A-def
Deflection measured @ 5[m] from root
Deflection [mm]
Local bending moment [kNm]
4,0
3,5
3,0
2,5
2,0
1,5
1,0
0,5
0,0
-0,5
0
500
1000
1500
NT-100-2 (ELLT_1_291009-A.bin)
NT-50-6 (ELLT_1_291009-A.bin)

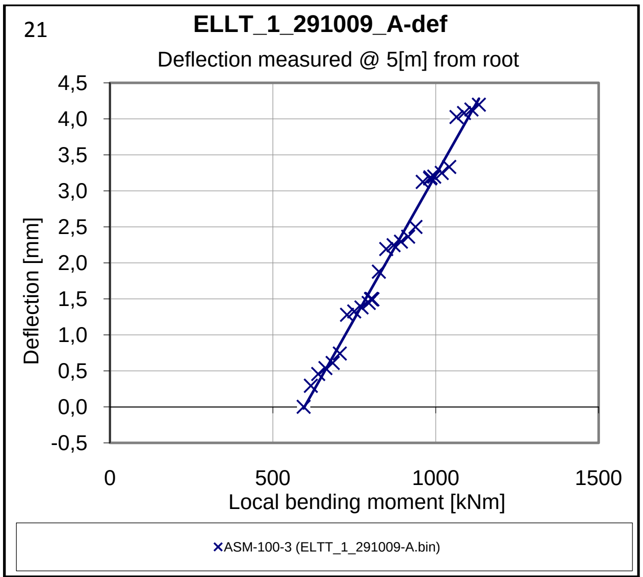
21
ELLT_1_291009_A-def
Deflection measured @ 5[m] from root
Deflection [mm]
Local bending moment [kNm]
4,5
4,0
3,5
3,0
2,5
2,0
1,5
1,0
0,5
0,0
-0,5
0
500
1000
1500
ASM-100-3 (ELLT_1_291009-A.bin)

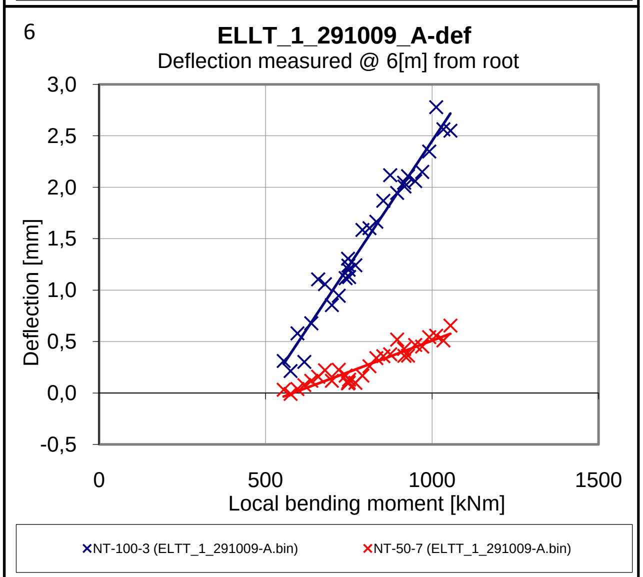
6
ELLT_1_291009_A-def
Deflection measured @ 6[m] from root
Deflection [mm]
Local bending moment [kNm]
3,0
2,5
2,0
1,5
1,0
0,5
0,0
-0,5
0
500
1000
1500
NT-100-3 (ELLT_1_291009-A.bin)
NT-50-7 (ELLT_1_291009-A.bin)

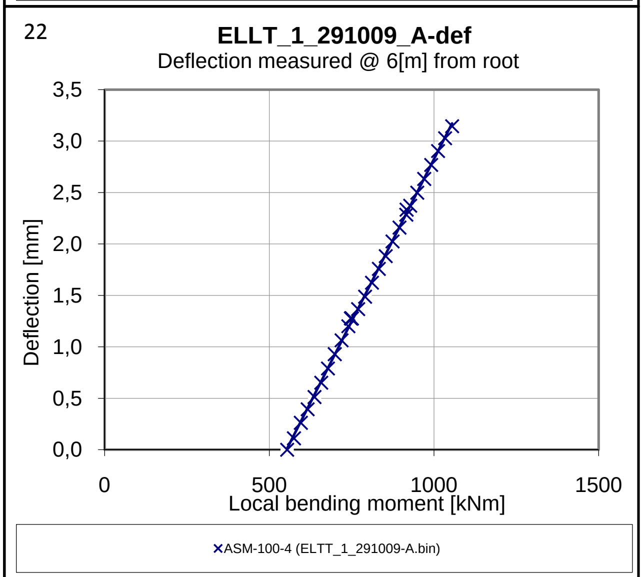
22
ELLT_1_291009_A-def
Deflection measured @ 6[m] from root
Deflection [mm]
Local bending moment [kNm]
3,5
3,0
2,5
2,0
1,5
1,0
0,5
0,0
0
500
1000
1500
ASM-100-4 (ELLT_1_291009-A.bin)

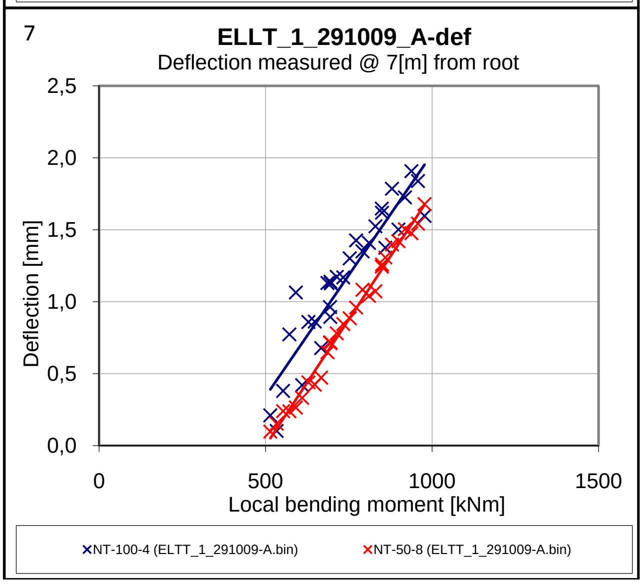
7
ELLT_1_291009_A-def
Deflection measured @ 7[m] from root
Deflection [mm]
Local bending moment [kNm]
2,5
2,0
1,5
1,0
0,5
0,0
0
500
1000
1500
NT-100-4 (ELLT_1_291009-A.bin)
NT-50-8 (ELLT_1_291009-A.bin)

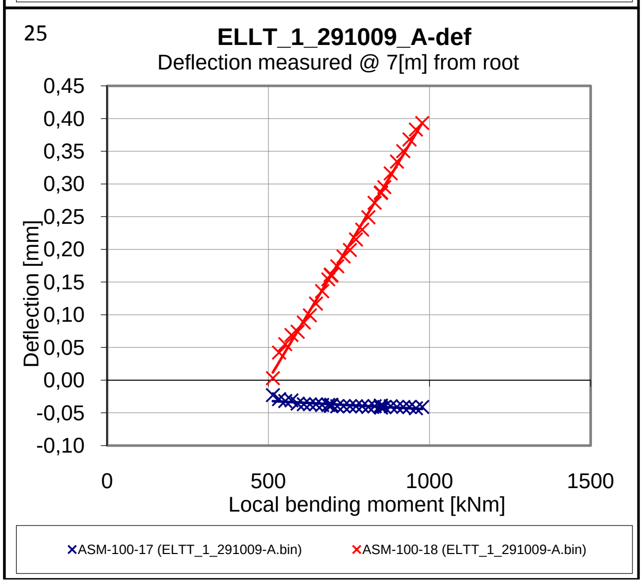
25
ELLT_1_291009_A-def
Deflection measured @ 7[m] from root
Deflection [mm]
Local bending moment [kNm]
0,45
0,40
0,35
0,30
0,25
0,20
0,15
0,10
0,05
0,00
-0,05
-0,10
0
500
1000
1500
ASM-100-17 (ELLT_1_291009-A.bin)
ASM-100-18 (ELLT_1_291009-A.bin)

B4

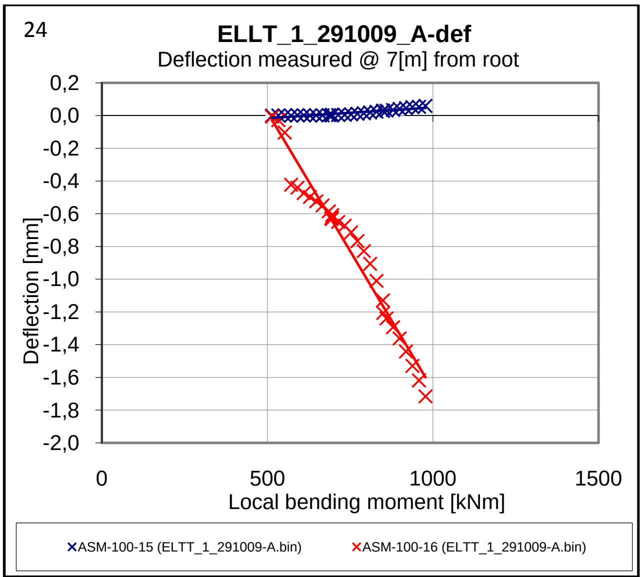
24
ELLT_1_291009_A-def
Deflection measured @ 7[m] from root
Deflection [mm]
Local bending moment [kNm]
ASM-100-15 (ELLT_1_291009-A.bin)
ASM-100-16 (ELLT_1_291009-A.bin)

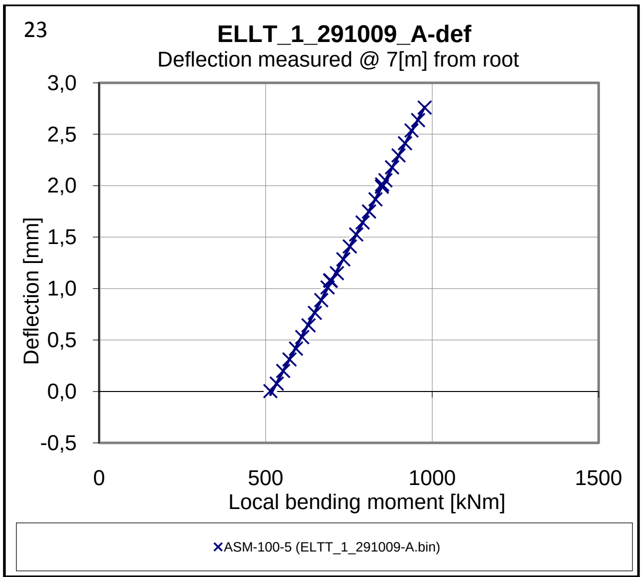
23
ELLT_1_291009_A-def
Deflection measured @ 7[m] from root
Deflection [mm]
Local bending moment [kNm]
ASM-100-5 (ELLT_1_291009-A.bin)

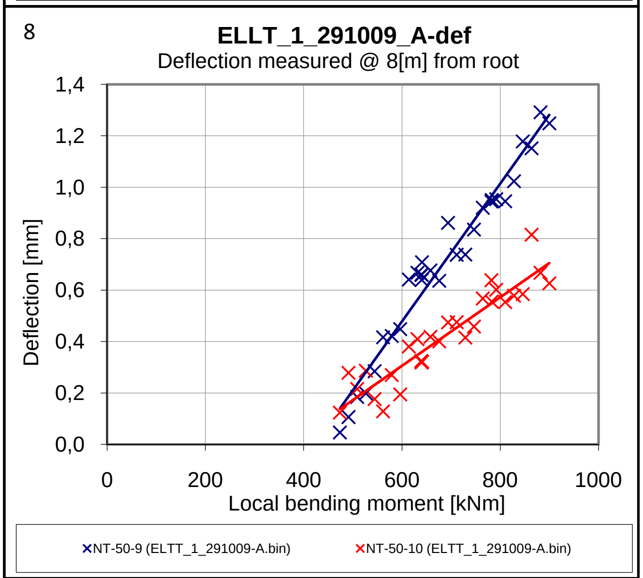
8
ELLT_1_291009_A-def
Deflection measured @ 8[m] from root
Deflection [mm]
Local bending moment [kNm]
NT-50-9 (ELLT_1_291009-A.bin)
NT-50-10 (ELLT_1_291009-A.bin)

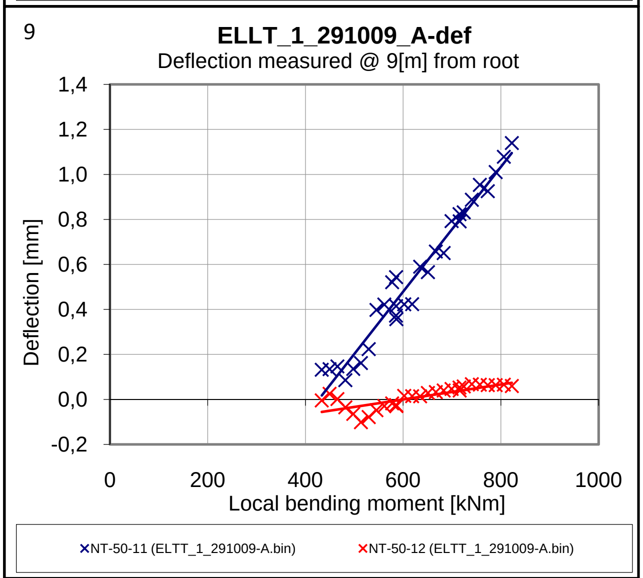
9
ELLT_1_291009_A-def
Deflection measured @ 9[m] from root
Deflection [mm]
Local bending moment [kNm]
NT-50-11 (ELLT_1_291009-A.bin)
NT-50-12 (ELLT_1_291009-A.bin)

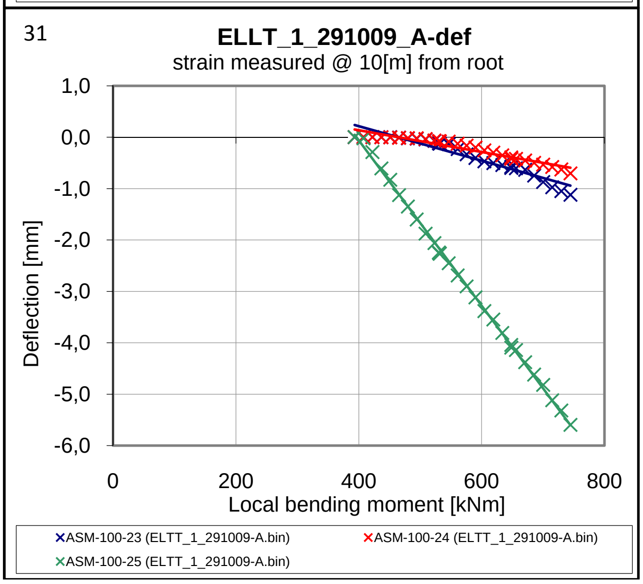
31
ELLT_1_291009_A-def
strain measured @ 10[m] from root
Deflection [mm]
Local bending moment [kNm]
ASM-100-23 (ELLT_1_291009-A.bin)
ASM-100-24 (ELLT_1_291009-A.bin)
ASM-100-25 (ELLT_1_291009-A.bin)

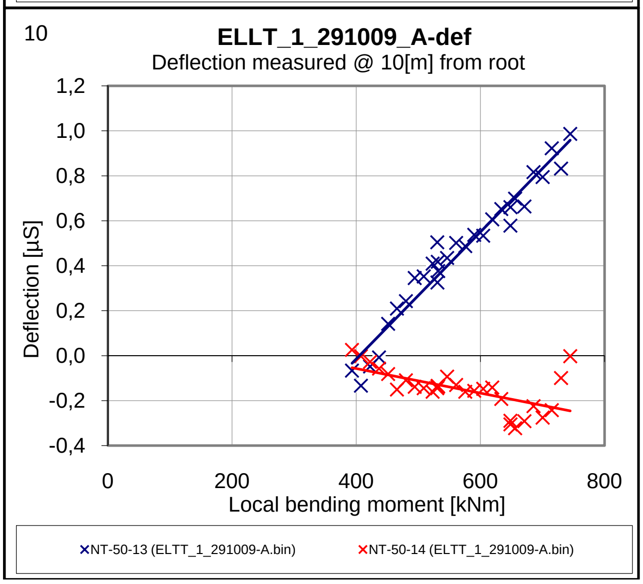
10
ELLT_1_291009_A-def
Deflection measured @ 10[m] from root
Deflection [µS]
Local bending moment [kNm]
NT-50-13 (ELLT_1_291009-A.bin)
NT-50-14 (ELLT_1_291009-A.bin)

B4

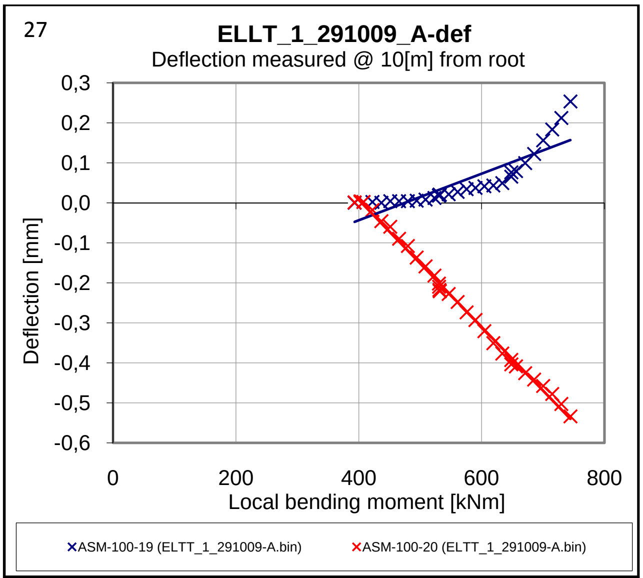
27
ELLT_1_291009_A-def
Deflection measured @ 10[m] from root
0,3
0,2
0,1
0,0
-0,1
-0,2
-0,3
-0,4
-0,5
-0,6
Deflection [mm]
0
200
400
600
800
Local bending moment [kNm]
ASM-100-19 (ELLT_1_291009-A.bin)
ASM-100-20 (ELLT_1_291009-A.bin)

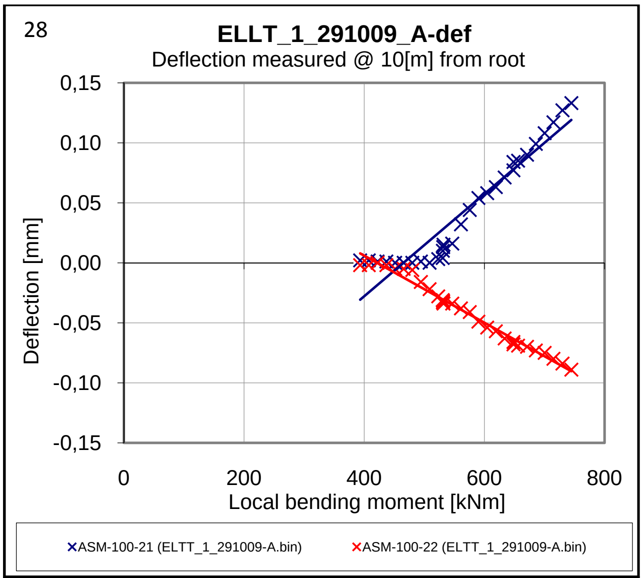
28
ELLT_1_291009_A-def
Deflection measured @ 10[m] from root
0,15
0,10
0,05
0,00
-0,05
-0,10
-0,15
Deflection [mm]
0
200
400
600
800
Local bending moment [kNm]
ASM-100-21 (ELLT_1_291009-A.bin)
ASM-100-22 (ELLT_1_291009-A.bin)

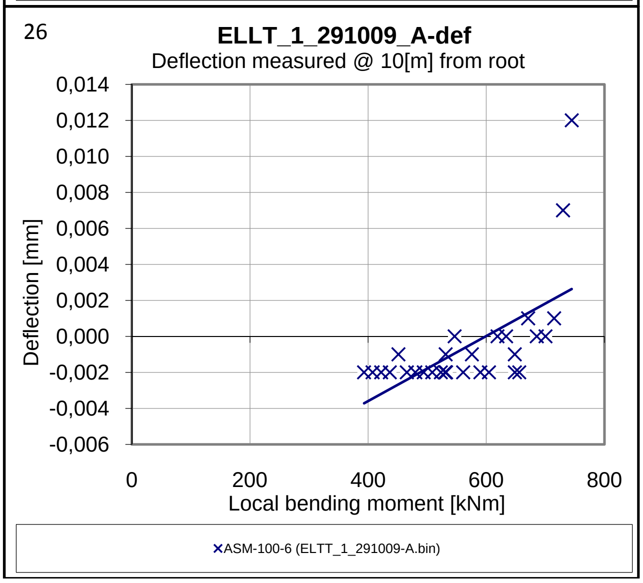
26
ELLT_1_291009_A-def
Deflection measured @ 10[m] from root
0,014
0,012
0,010
0,008
0,006
0,004
0,002
0,000
-0,002
-0,004
-0,006
Deflection [mm]
0
200
400
600
800
Local bending moment [kNm]
ASM-100-6 (ELLT_1_291009-A.bin)

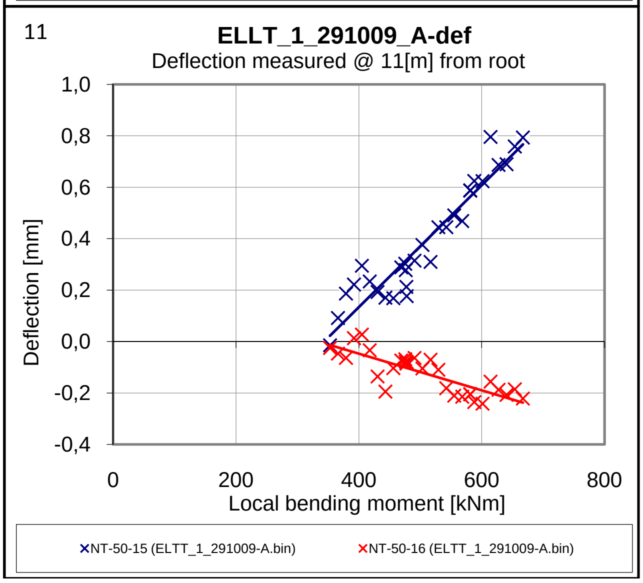
11
ELLT_1_291009_A-def
Deflection measured @ 11[m] from root
1,0
0,8
0,6
0,4
0,2
0,0
-0,2
-0,4
Deflection [mm]
0
200
400
600
800
Local bending moment [kNm]
NT-50-15 (ELLT_1_291009-A.bin)
NT-50-16 (ELLT_1_291009-A.bin)

B4

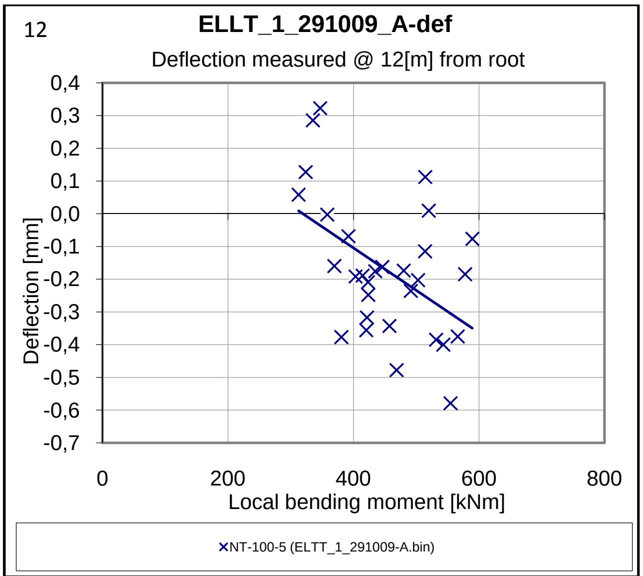
12
ELLT_1_291009_A-def
Deflection measured @ 12[m] from root
Deflection [mm]
0,4
0,3
0,2
0,1
0,0
-0,1
-0,2
-0,3
-0,4
-0,5
-0,6
-0,7
0
200
400
600
800
Local bending moment [kNm]
NT-100-5 (ELLT_1_291009-A.bin)

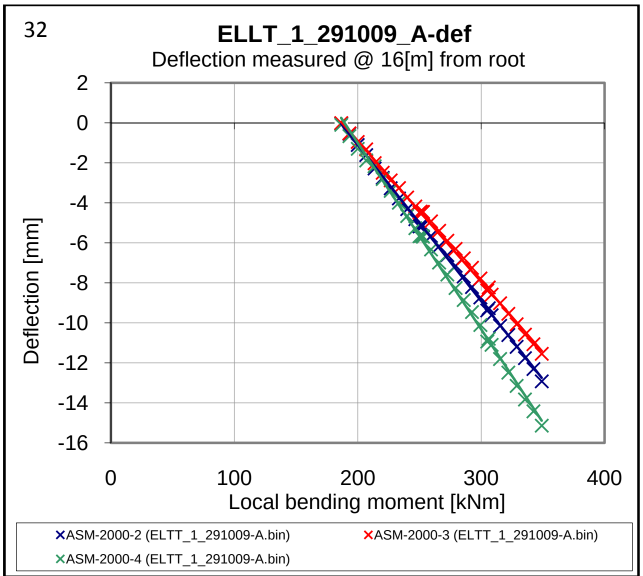
32
ELLT_1_291009_A-def
Deflection measured @ 16[m] from root
Deflection [mm]
2
0
-2
-4
-6
-8
-10
-12
-14
-16
0
100
200
300
400
Local bending moment [kNm]
ASM-2000-2 (ELLT_1_291009-A.bin)
ASM-2000-3 (ELLT_1_291009-A.bin)
ASM-2000-4 (ELLT_1_291009-A.bin)

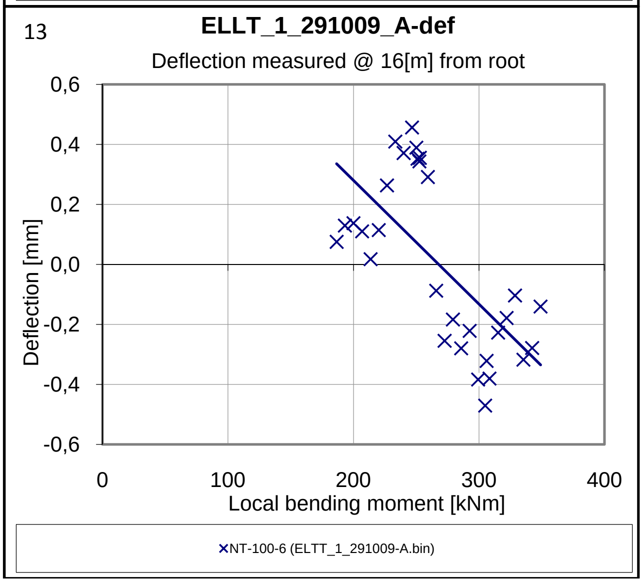
13
ELLT_1_291009_A-def
Deflection measured @ 16[m] from root
Deflection [mm]
0,6
0,4
0,2
0,0
-0,2
-0,4
-0,6
0
100
200
300
400
Local bending moment [kNm]
NT-100-6 (ELLT_1_291009-A.bin)

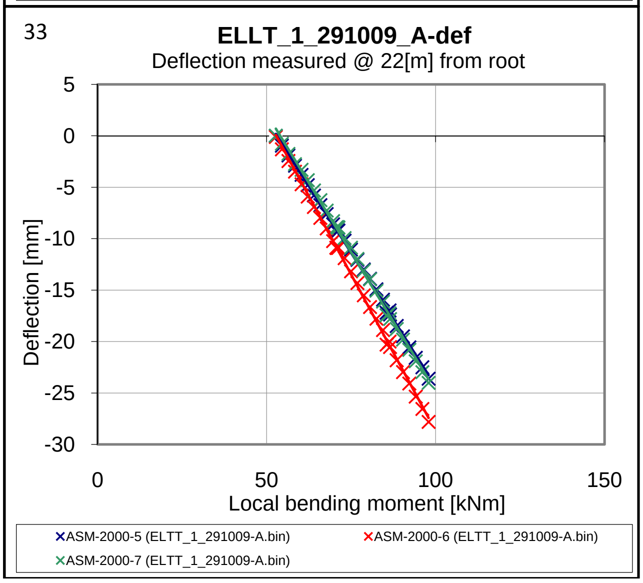
33
ELLT_1_291009_A-def
Deflection measured @ 22[m] from root
Deflection [mm]
5
0
-5
-10
-15
-20
-25
-30
0
50
100
150
Local bending moment [kNm]
ASM-2000-5 (ELLT_1_291009-A.bin)
ASM-2000-6 (ELLT_1_291009-A.bin)
ASM-2000-7 (ELLT_1_291009-A.bin)

B5 Deflections obtained in test ELTT_5-181109_A measured by:
NT-50-17
NT-100-18
NT-50-19
NT-50-20

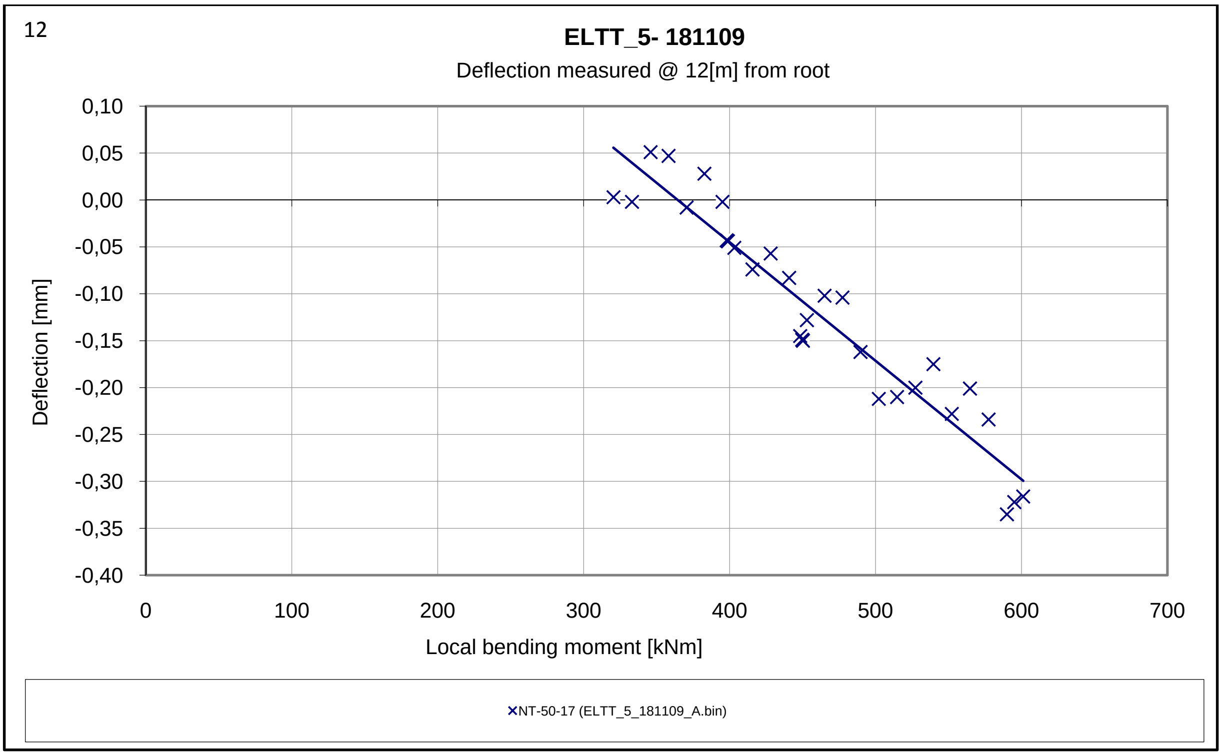

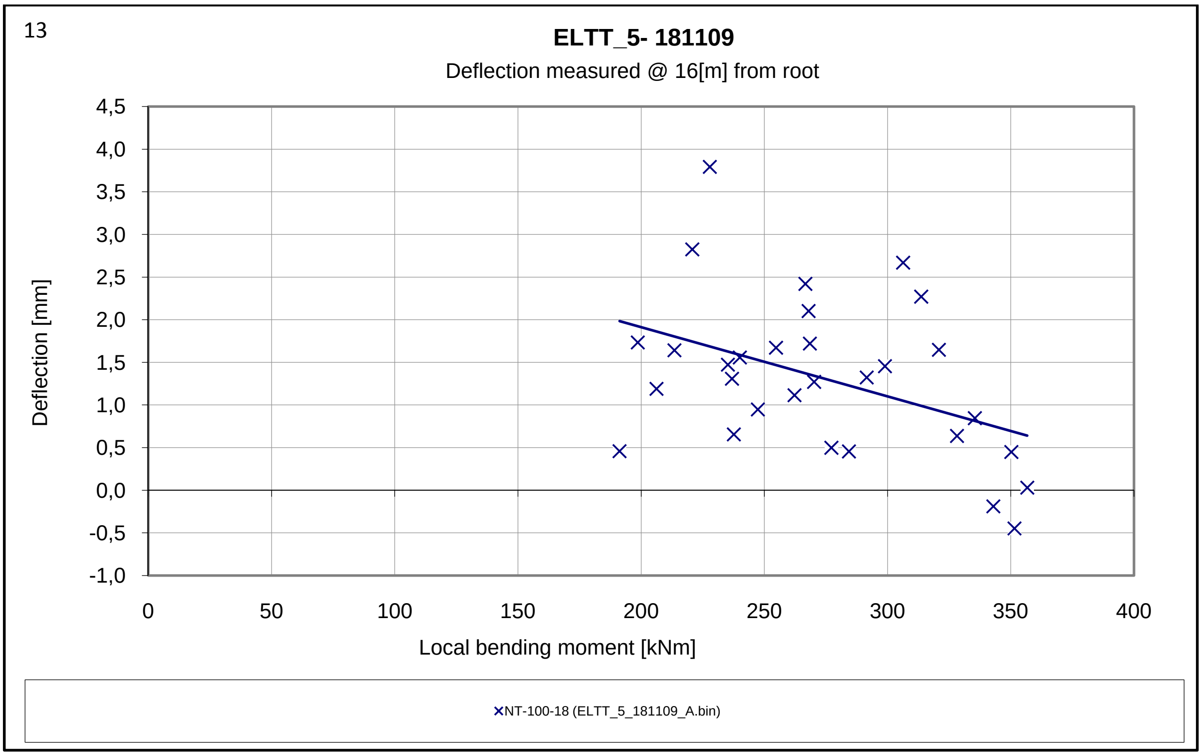

B5

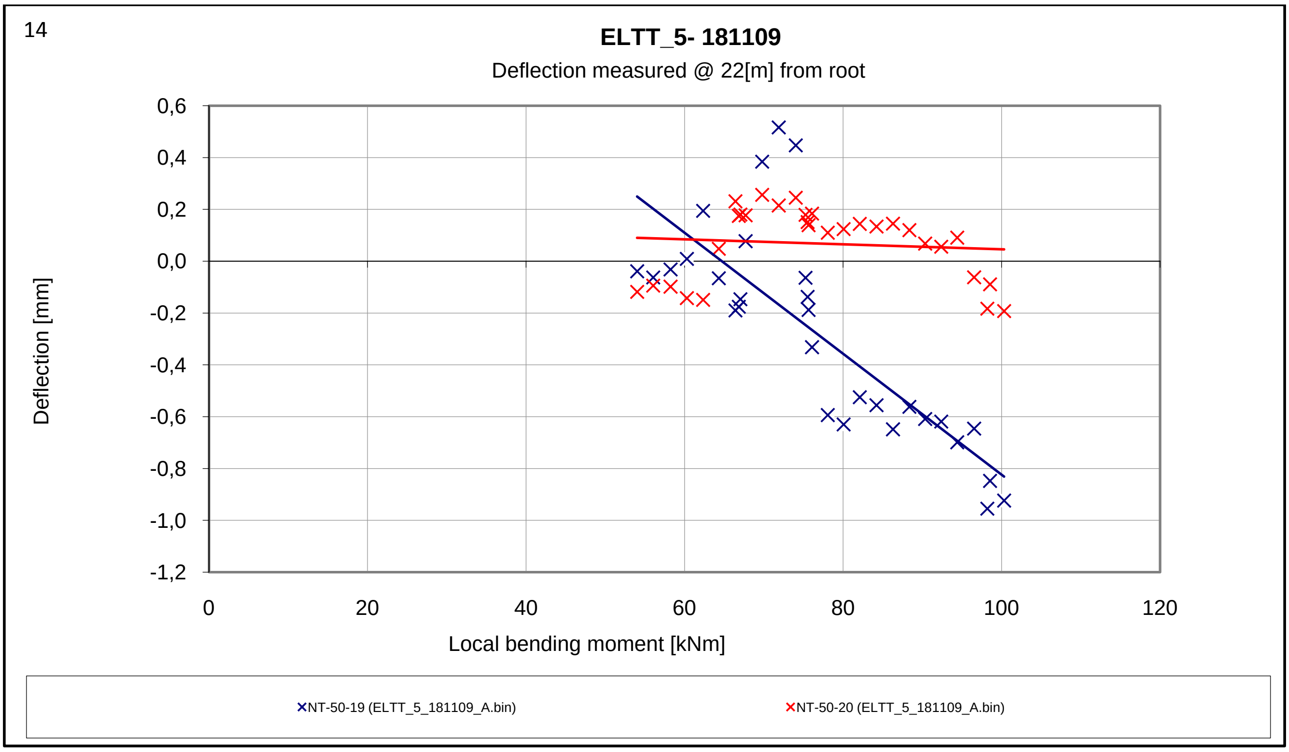
14
ELTT_5- 181109
Deflection measured @ 22[m] from root
Deflection [mm]
0,6
0,4
0,2
0,0
-0,2
-0,4
-0,6
-0,8
-1,0
-1,2
0
20
40
60
80
100
120
Local bending moment [kNm]
NT-50-19 (ELTT_5_181109_A.bin)
NT-50-20 (ELTT_5_181109_A.bin)

B6 The flapwise global deflections measurements vs. root bending moment obtained in test ELTT_1-291009_A

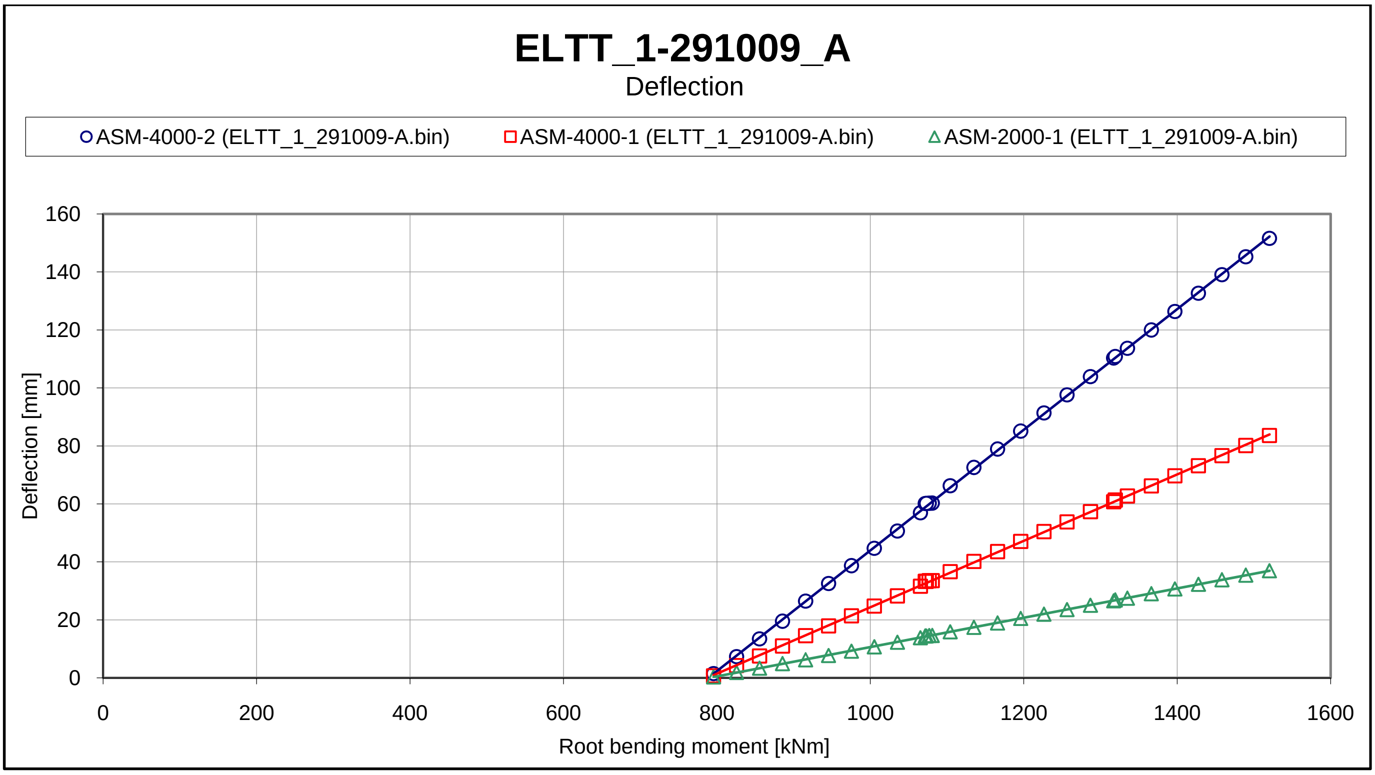

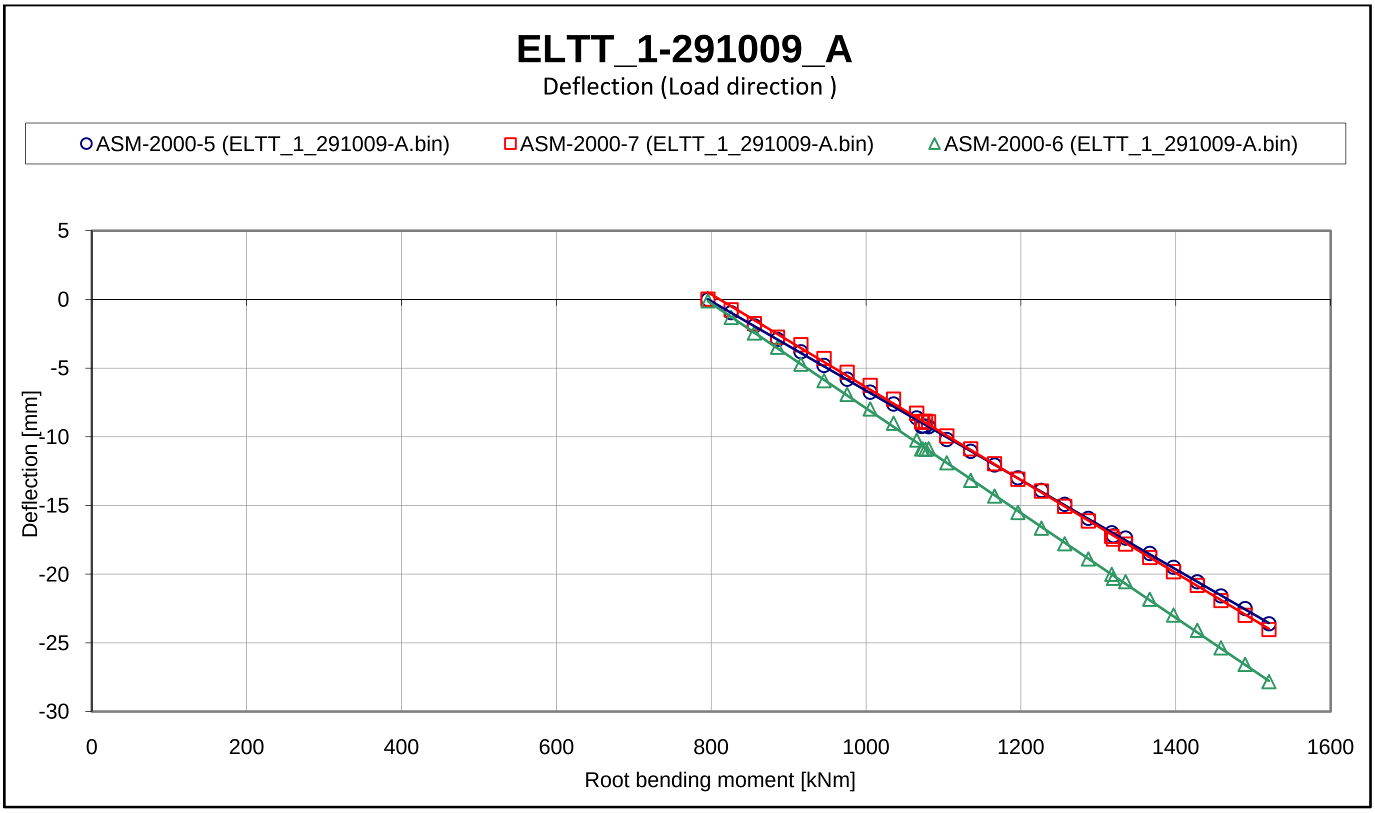

B6

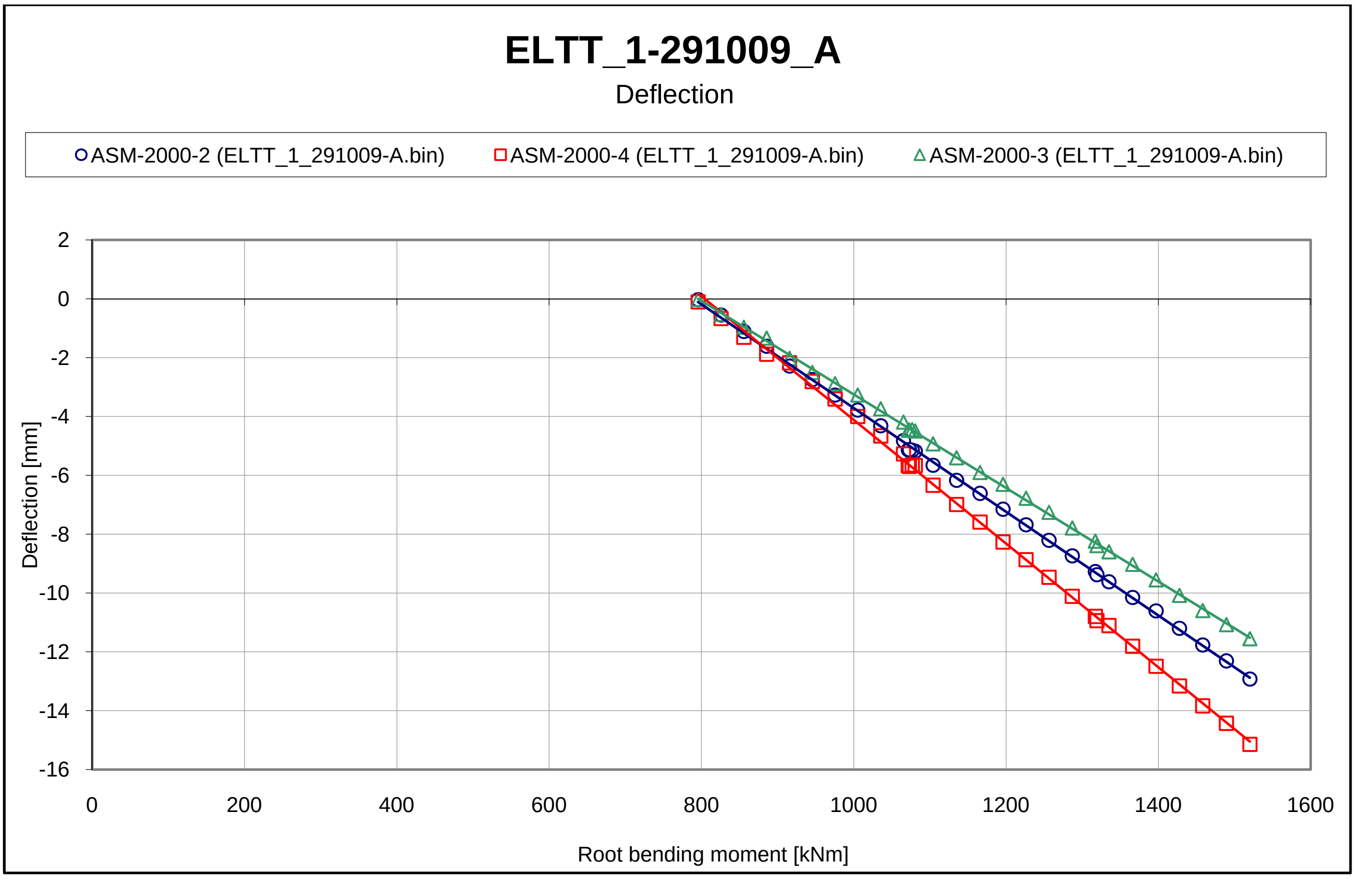

ELTT_1-291009_A
Deflection
ASM-2000-2 (ELTT_1_291009-A.bin)
ASM-2000-4 (ELTT_1_291009-A.bin)
ASM-2000-3 (ELTT_1_291009-A.bin)
Deflection [mm]
2
0
-2
-4
-6
-8
-10
-12
-14
-16
0
200
400
600
800
1000
1200
1400
1600
Root bending moment [kNm]

C Load comparaison

Lastsammenligning.

Da vingens egenvægt belaster vingen ud over den påførte last, er der valgt en løsning hvor egenvægten er repræsenteret ved laster i lastpunkterne.

Den påførte last reduceres derefter med denne værdi.

Beregningerne af lasterne der repræsenterer egenvægten er udført i Mathcad.

Dette er beregnet ud fra oplysninger om vægten af vingen.
Vægten er for 1 m. for hver metersektion af vingen: oplysningerne stammer fra FEM beregninger
A er placeringen af vægten og V er vægten i det respektive område.
Dvs at 1 m vinge mellem 0 og 1 m vejer 290.31 kg.
Ud fra dette har jeg I MathCad beregnet momentfordelingen og den samlede vægt

Jeg har kontrolleret de første bidrag ude fra tippen af momenterne.

$$A := \begin{pmatrix} 0.5 \\ 1.5 \\ 2.5 \\ 3.5 \\ 4.5 \\ 5.5 \\ 6.5 \\ 7.5 \\ 8.5 \\ 9.5 \\ 10.5 \\ 11.5 \\ 12.5 \\ 13.5 \\ 14.5 \\ 15.5 \\ 16.5 \\ 17.5 \\ 18.5 \\ 19.5 \\ 20.5 \\ 21.5 \\ 22.5 \\ 13.5 \\ 24.5 \end{pmatrix} \qquad V := \begin{pmatrix} 290.31 \\ 291.84 \\ 249.6 \\ 234.46 \\ 223.56 \\ 212.88 \\ 199.25 \\ 192.4 \\ 173.24 \\ 156.18 \\ 147.98 \\ 144.52 \\ 152.85 \\ 147.53 \\ 145.66 \\ 145.39 \\ 144.69 \\ 138.11 \\ 137.09 \\ 131.96 \\ 127.49 \\ 110.34 \\ 102.47 \\ 94.86 \\ 83.09 \end{pmatrix}$$

Ma er den samlede masse

$$n := 0..24$$

$$Ma := \sum_{n} V_n$$

$$Ma = 4.178 \times 10^3$$

$$Momentrod := A \cdot V \cdot 10$$

$\text{Momentrod} = 4.19 \times 10^5$

$k := 0..24$

$$Ve(k) := \begin{array}{|l} M \leftarrow -83.09\cdot 5 \\ l \leftarrow 0 \\ Ve \leftarrow 0 \\ \text{while } l \le k \\ \quad \begin{array}{|l} Ve \leftarrow Ve + V_{24-l} \\ l \leftarrow l + 1 \end{array} \\ dM \leftarrow Ve \cdot 10 \\ M \leftarrow M + dM \\ Ve \end{array} \qquad M(k) := \begin{array}{|l} M \leftarrow 0 \\ l \leftarrow 0 \\ \text{while } l \le k - 1 \\ \quad \begin{array}{|l} dM \leftarrow Ve(l)\cdot 10 \\ M \leftarrow M + dM \\ l \leftarrow l + 1 \end{array} \\ M \leftarrow Ve(k)\cdot 5 + M \\ M \end{array}$$

Ve(k) er den summerede vægt fra tippen anvendees kun som krontrol

M(k) er momenten ude fra tippen k = 0 svarer til i 24 m.

k =	M(k) =	Ve(k) =
0	415.45	83.09
1	$1.721\cdot10^3$	177.95
2	$4.013\cdot10^3$	280.42
3	$7.368\cdot10^3$	390.76
4	$1.191\cdot10^4$	518.25
5	$1.776\cdot10^4$	650.21
6	$2.494\cdot10^4$	787.3
7	$3.351\cdot10^4$	925.41
8	$4.348\cdot10^4$	$1.07\cdot10^3$
9	$5.491\cdot10^4$	$1.215\cdot10^3$
10	$6.78\cdot10^4$	$1.361\cdot10^3$
11	$8.214\cdot10^4$	$1.509\cdot10^3$
12	$9.8\cdot10^4$	$1.662\cdot10^3$
13	$1.153\cdot10^5$	$1.806\cdot10^3$
14	$1.341\cdot10^5$	$1.954\cdot10^3$
15	$1.545\cdot10^5$	$2.11\cdot10^3$
16	$1.764\cdot10^5$	$2.283\cdot10^3$
17	$2.002\cdot10^5$	$2.476\cdot10^3$
18	$2.26\cdot10^5$	$2.675\cdot10^3$
19	$2.538\cdot10^5$	$2.888\cdot10^3$
20	$2.838\cdot10^5$	$3.112\cdot10^3$
21	$3.161\cdot10^5$	$3.346\cdot10^3$
22	$3.508\cdot10^5$	$3.596\cdot10^3$
23	$3.882\cdot10^5$	$3.887\cdot10^3$
24	$4.285\cdot10^5$	$4.178\cdot10^3$

Kontrol af momentberegningerne

k =1

$83.09\cdot 5 + (83.09)\cdot 10 + 94.86\cdot 5 = 1.721 \times 10^3$

k =2

$1721 + 177.95\cdot 10 + 102.47\cdot 5 = 4.013 \times 10^3$

Med værdierne herfra ønsker jeg at få momentkurven til at passe i 25, 18.61,13.21 og 4 m.
Se nedstående kurve. Det giver en rodmoment på 371400 der skal korreigeres for med lasterne.

$$K := \begin{pmatrix} 0 \\ 21350 \\ 82140 \\ 283800 \\ 371400 \end{pmatrix} \qquad y := \begin{pmatrix} 25 \\ 18.61 \\ 13.21 \\ 4 \\ 0 \end{pmatrix}$$

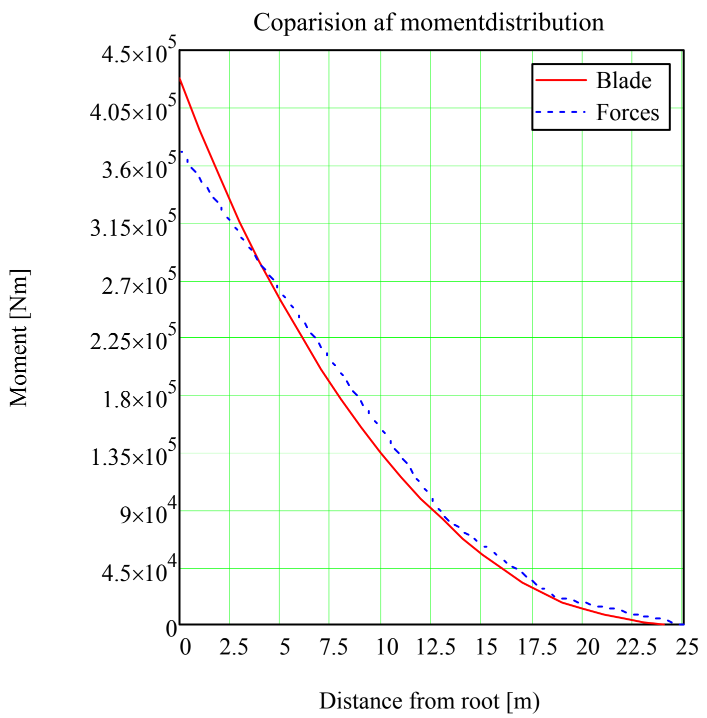

For at få samme Moment i 18.61 13.21 og 4 m. beregnes værdien hvormed kræfterne i i trækpunkterne skal reduceres.

For at få samme moment i 18.61 m. skal kraften i 25 m reduceres med. Enheden er N.

$$\frac{21350}{24.91 - 18.61} = 3.389 \times 10^{3}$$

I 18.61 m skal kraften reduceres med

$$\frac{82140 - 3389 \cdot (24.91 - 13.21)}{18.61 - 13.21} = 7.868 \times 10^{3}$$

I 13.21 m skal kraften reduceres med

$$\frac{371400 - 3389 \cdot 24.91 - 7868 \cdot 18.61}{13.21} = 1.064 \times 10^{4}$$

Ud fra ovenstående at repræsentere egenvægten ved

$$F_{egen} := \begin{pmatrix} 3500 \\ 8000 \\ 10000 \end{pmatrix}$$

$$F_{max} := \begin{pmatrix} 58099 \\ 31675 \\ 40013 \end{pmatrix}$$

Dette er ELLT 100% last.

Da egenvægten er påført fra start vil lasten have en angivet størrelse når testen startes.
Da lasten ønsket påført ens i alle lastpunkter (Samme prosentvise værdi af Extreme load) skal værdien for hvilken procentvise last der startes med ved hver ny test bestemmes.

$$F_{begyndelseslast} := \frac{F_{max}}{4} - F_{egen}$$

$$F_{begyndelseslast} = \begin{pmatrix} 1.102 \times 10^{4} \\ -81.25 \\ 3.25 \end{pmatrix}$$

Dette resultat giver at den mindste last der kan påføres så alle 3 lastpunkter belastes ens er er over 25% belastning.

Da trækket udføres med spil er det væsentlig for at wiren ikke ruller sig op at det er forbelastet.

valget er derfor faldet på at trækkene starter ved en belastning på 30%.

D Testplan

Test plan

Test Name: ELTT_1-030909_A	
Date and Time: 21.08.09	
Responsible for the test including understanding the purpose of the test: fimj	
Load applied before [x] New load area [ ]	
Responsible for applying load: magd	
Responsible for safety during the test: magd	
Responsible for Data acquisition: vatr	
Responsible for Aramis: pber	
Responsible for Acoustic emission: mamc	
Responsible for operation of camera: vatr	

Purpose of the test:

1) Use Aramis measurements to see if it is possible to localise where the waves of the trailing edge panels are located. Based on these measurements the NT's and ASM's(inside)-might be moved.
2) Due to not having taking the gravity into account in the previous test and load calculations, the forces and the distribution have changed. Furthermore the way to plot the forces in the graphs have been reconsidered.
3) Get experiences with the acoustic emission equipment for the particularly blade and load case. The load range has been reached before so not much noise is expected.
4) To observe the global deformation of the blade in section 4m and 7m, using additional installed ASMs: ASM-100-29, ASM-100-30, ASM-100-31, ASM-100-32, ASM-100-33, ASM-100-34
Test the sewing of the blade from 3 to 4.5 m.

Planned load range:

1) Around 60% of (These percentages includes the weight from the blade) extreme loads. This load has been reached several times before in test series 1 and trial tests, so no problems are expected. Load intervals can be done in big steps and since we expect to repeat the test later on we do not need to adjust the load accurately at each load level. It has therefore been decided that the measurements won't exceed Moment distribution made in previous test. The test expects to be repeated several times since Aramis equipment will be moved around in different length positions and on both suction and pressure side,. The most important place to carry out Aramis measurements are at 4 m. pressure side.

2) The procedure under test will be. The blade will be loaded until 25% of extreme loads. (Here the loads includes the contributions from the load from the weight of the blade). At 25% extreme load all the measure equipment except the Force transducers will be reset to zero point. The measurements from Aramis and the Acoustic emission will be started at this point as well.

For this test the forces applied on the blade, 25% of Extreme forces will be F1(tip)=11000 N F2(18.61)= 0N and F3(13.21)= 0 N. At 60% loads the Applied loads will be be F1(tip)=31000 N F2(18.61)= 11000N F3(13.21)= 14000 N.

3) Large load steps without to many breaks will be executed since most of the consideration are made on beforehand (in previous tests) and the new test equipment and load range do not require to many load stops.
4) Since no plans are to continuing loading after 60% have been reached, the unloading will make take place right after the 60% load has been reached.
5) Wire holes etc. should be ready as soon as possible so test can be performed with wires between the trailing edge panels. The wave location has to be known before optimal position can be placed. Tension metres could be considered to measure the force in the wire: Action Magda

Potential failure mechanism which has to be followed during the test:
1- Global buckling of the trailing edge: At the Sparkær test in 2003 the trailing edge showed stable buckling in the range 60-80% load. The global buckling was observed in 15m region by studying the longitudinal SG on the trailing edge. In the test with the new SSP-blade tested without a wooden clamp the buckling load can be reduced. On the other hand the new SSP-blade has been reinforced by extra UD-laminate in the trailing edge.

2- Local buckling of the trailing edge panels: FE-studies show large panel deformations in the region 3-4m. The suction side panesl have shown the larges deformations (9mm in 4m) but pressure side could also to be considered if it is not to time consuming to measure + post process etc.

Measurement equipment:
Position for SG-group has been changed to Main section(group 1) since SG's measurement in 4m is important. Regarding global buckling of the trailing edge the SG in position B can be used.

2- Local buckling of the trailing edge panels: FE-studies show large panel deformations in the region 3-4m. This have been confirmed by the first test and especially 4m suction side panel show large deformation (9mm)

Others:
Since no critical failures are expected real time graphs are not necessary.

Comments for future test:
-Extra (and faster) laptop including wireless internet connection are needed to get both real time and camera to work at the same task. Action: vatr
-Microphone(s) in the test facility is needed. Action:vatr
-Cables for canhead has been ordered so global ASM-deformations can be measured in 4m and 7m. Action/responsible: karm
-Wire holes etc. should be ready as soon as possible so test can be performed with wires between the trailing edge panels.

1. Real Time graphs	
1- Global buckling of the trailing edge	XXX
2- Local buckling of the trailing edge panels:	XX
Others	
Comments/Observations	

Comments/Observations during and after test	
Comments/Observations	

2 . Test informations

Strain gauge group: **1: Main** ☐ **2: AED + Global** ☐ **3: Other groups** ☐	**Excluding sensors** **Including sensors**
NT list:	**Including sensors** **Excluding sensors**
ASM list:	**Including sensors** **Excluding sensors**
Name of report/results	**Data** **Aramis** **Acoustic emission**
Comments/Observations	

E Measurement equipment

Strain gauge

Strain gauges principle

Strain gauge is a device that measures elongation by means of the electrical resistance. A coil of certain resistance is attached to the examined part. When a strain occurs, the length of the coil changes and so does resistivity. Simple, unidirectional strain gauges (UD) measure the relative strain only in one direction. In case one needs to measure both directions (0 and 90 degrees), so called Biax (Bx), the system of two perpendicular gauges, is applied. In order to measure the elongation in 3 directions: 0, 45 and 90 degree, the triax-rosettes (Tx) were used.

Figure . The directions of the strain measurements.

E LT-NT

The sensors are attached to the metal frame, which is fastened to the blade with a stripe. The force in stripes cannot be too high in order to prevent the deformation of the blade. The deflection is measured by means of the electrical resistance. The sensors were calibrated and the measurements have plus values when the measuring part goes out.

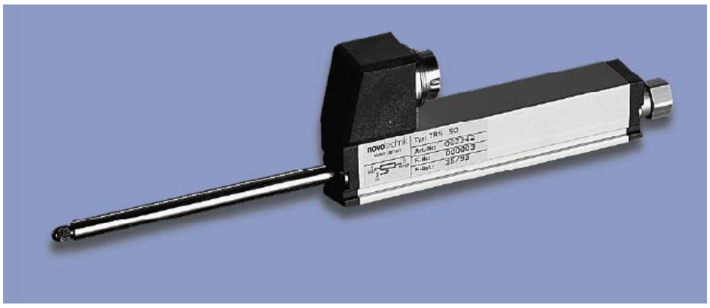

Figure 3. LT-NT- Length Transducer from NovoTechnik

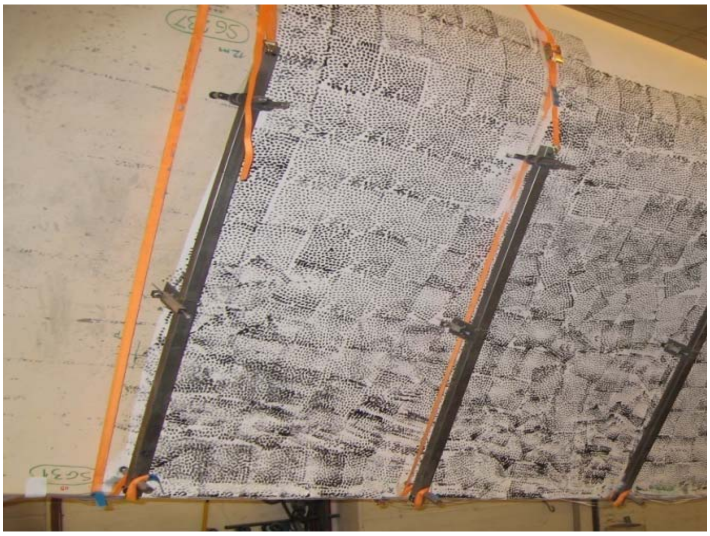

Figure 4. LT-NTs' frames mounted to the blade.

E LT-ASM

Position sensors LT-ASM transform position of a linear guided movement into an electrical signal. Linear motion of the measuring cable is converted into rotation by means of precision cable drum. A spring motor provides torque for the cable retraction. Special design assures precise and reproducible winding of the measuring cable. Cable extraction or retraction is transformed into an electrical signal.

Figure 2. Length Transducer from ASM.

Cable extraction or retraction is seen by the system as measurement with + or -. This is depending on the sensor.

E Force transducer

The force transducer is a commonly used instrument all over the industry, to measure force in tensile or compressive. The type that is used in this experiment measure the force which is applied by the winches to blade. The device is mounted in the link between the winch and the blade so all the force is transferred through the force transducer. The force transducer consists of block of metal that is able to carry the load, but is also able to deflect. This deflection is measured by a strain gauge mounted the block of metal, the result of the strain gauge can the tell load on the force transducer.

DIC (Aramis)

In principle the ARAMIS system works by analysis of the acquired images. Undeformed stage is used as a reference and multiple deformed stages are recorded during a test.
Multiple subsets of image pixels are analyzed by a grey-value correlation technique in the undeformed and the deformed state.

Figure 1. *ARAMIS equipment (facing towards the tip).*

Aramis is an optical measurement system which can measure deflection in three directions at the same time. The system uses two cameras detecting the difference in measured pattern. This technique can measure the deflection in an area of 2.5m by 2.5m for a four Mega pixel system. The ARAMIS equipment is produced by GOM and the measurements were performed by GOM / Zebicon.

Acoustic emission

When certain dynamic processes occur in the material, some of the released energy generates elastic stress waves, we might say vibrations. These stress waves are propagated from the source and can be detected by sensitive transducers. Once amplified, the signal from these transducers is available for further analysis. Information about the location, severity and nature of the event causing the stress wave emission can be deduced from the received signals.
When loaded, a structural polymer composite material emits a huge number of these transient stress waves as a result of non-reversible (plastic) micro-damage events such as matrix cracking, tribology at delaminations,

fiber fracture, etc. This multitude of small-scale events is detectable long before a reduction in structure stiffness and/or the appearance of visible (macro-scale) crack.

Figure 2. Acoustic emission sensors used Holroyd instrument AE- SS1

When a composite structure is loaded up to critical levels, a significant increase in general stress wave activity can be expected. In the case of a structure loaded within working limits, any area which has already sustained local damage (as the result of for instance an impact, static overload, or severe fatigue) will also return an increase in local stress wave emission activity relative to the structurally unchanged ambient material.

Therefore it is possible to locate defects and damaged areas in composite structures, by monitoring the transient stress waves, before they become threatening to the structure integrity. In this manner we may also chart the progress of structural response to loading towards ultimate failure.

As the signal frequency generally does not fall in the human audible range, the term acoustic emission (AE) is a misnomer and the alternative term stress wave emission (SWE) would be a more accurate description of the phenomenon. Both of them are valid but acoustic emission is the expression in more widespread use.

Data acquisition system

MGCPlus

MGCPlus is a multichannel computer-controllable signal conditioning and Data Acquisition (DAQ) system developed by HBM. The MGCPlus acquires data from a variety of sensors placed on the wing, including strain gages, force transducers and LVTDs, and presents it to engineers in native or engineering units.

Our MGCPlus system can be connected with up to 24 CANHEAD's with 10 channels per CANHEAD, which gives us up to 240 physical channels.

CANHEADS

The CANHEAD amplifier module is the heart of the system. This standard amplifier module can be used for all measured quantities and circuit variants, and is suited for use with all base module types. The amplifier module can be removed and re-inserted in a matter of seconds. This allows the amplifier module to be quickly and flexibly interchanged between the different measurement configurations. Important feature is, that it does not matter in which order we connect our CANHEAD's because they will be recognised automatically in our system.

CANHEAD base modules are, in principle, intelligent junction boxes. They permit sensors to be directly connected in close proximity to the measuring point and to stay integrated in the cabling. Information specific to each measuring point is permanently stored in the base module. The CANHEAD base modules are available in three variants for feeding and connecting different strain gage circuits and transducers.

Key Features:

- 10-channel amplifier modules for installation close to measuring points.
- Measured data transmission to communication master via field bus.
- Base modules for individual strain gages, strain gage full and half bridges, DC voltage sources.
- Connection of amplifier module/base module by simply plugging in.
- Automatic recognition in our system, so we don't have to connect them in any specific order.

Data acquisition system

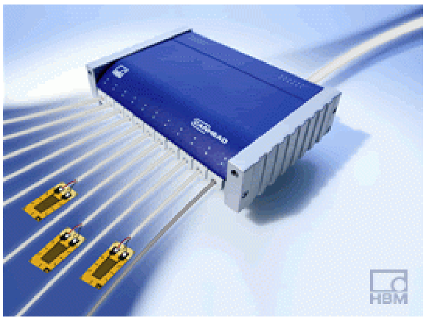

Catman Professional

Catman Professional is software which enables us to easily configure connected amplifiers and intuitively define, run and automate our measurement sequences without any programming knowledge. Measured values can be visualized in real time or after measurement has been concluded for reporting purposes. Recurring measurement tasks are greatly simplified as Catman can be used to automate each sequence.

Key Features:

- The software package for configuration, measurement, visualization, analysis and documentation.
- Free definition of individual interfaces for graphical visualization.
- Over 400 post-process analysis functions (statistics, signal analysis etc.)
- Creation of measurement reports complete with traceability data.
- Automation of individual measurement sequences.

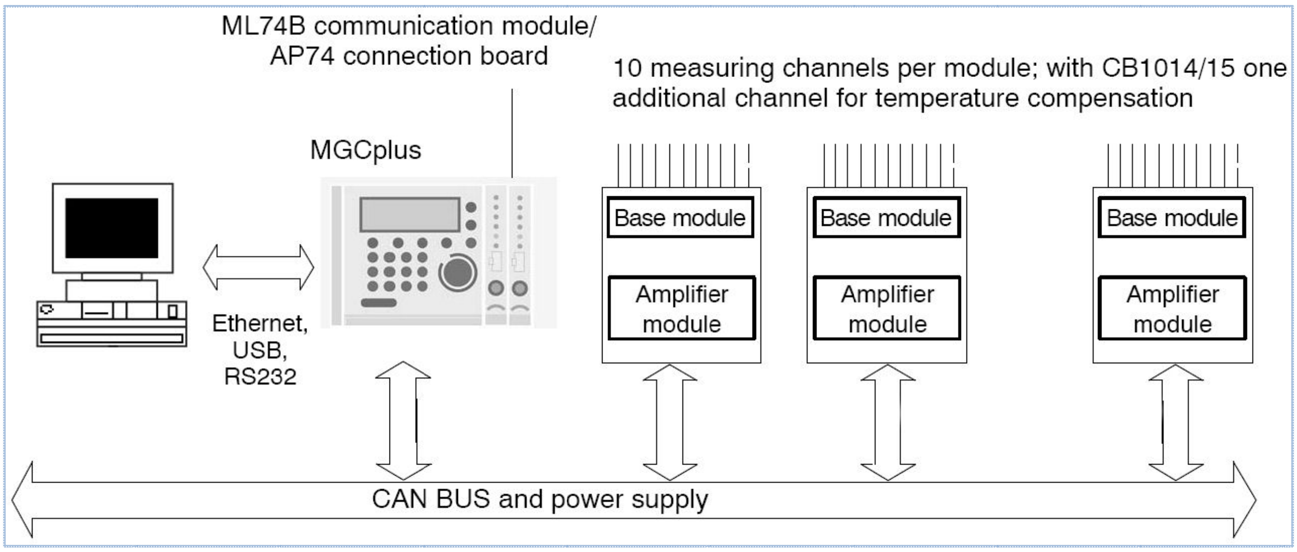

F Calibration

LT-NTs calibration

LT-NT – Length transducer from NovoTechnik (see figure 1) - are another type of measure equipment used in the experimental tests. The range of such a transducer is 100mm. It is used for measurements of the local blade deflection while buckling. It is attached to the metal frame, which is fastened to the blade with a stripe. The force in stripes cannot be too high in order to avoid blade deformation (see figure 2).

Figure1. LT- NT

Figure 2. LT-NTs mounted on the blade

LT-NTs have the same numbers what fallow them cables. Therefore the calibration must be conduct while they are assembled and mounted on the blade. After the all equipment is mounted on the blade one can perform adjustment and necessary calibration. First thing to remember is to adjust LT-NT in the way so the “zero position” enables movement of the measuring rod in both directions. To the calibration process one should use the calibration block with known thickness (during our calibrations block with thickness of 10,0mm was used). While calibrating LT-NTs first zero position must be determined. It is done while one calibration block is placed between blade and tip of the LT-NT rod. Implementation of the block between blade and rod while determining “zero position” is necessary because blade surface is not even. Calibration block provides efficient surface quality and prevents from incorrect calibration (see figure 3). After “zero position” establishment, second block with known thickness is placed between blade and LT-NT rod. In the CATMAN system, obtained measure is set as precise thickens of the calibration block (in our calibration as 10,0mm). This step provides final calibration of the measure equipment (see figure 4).

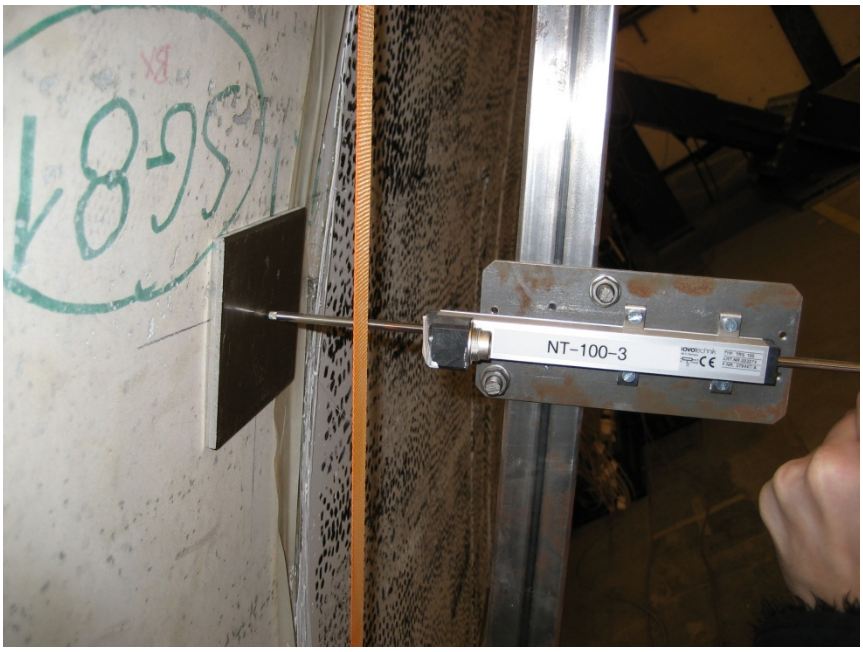

Figure2. One element between blade and LT-NT rod

Figure3. Two elements between blade and LT-NT rod

Kalibrering af krafttransducere.

Kalibreringen blev fortaget ved at sammenligne en måling udført med en kalibreret krafttransducer med værdierne der blev vist på de øvrige krafttransducere.

Kalibreret føler PFV 7	412/1947	viste	8,309 kN
Krafttransducer 1	5962291 A		8,285 kN
Krafttransducer 2	2 576255 A		8,293 kN
Krafttransducer 3	596283 A		8,28 kN

Strain gauge calibration

Dehnungsmeßstreifen
Strain Gauges
Jauges d'extensométrie

Bestellnummer Order No. No. de référence			K-LY41-10/350-4-10M
Typ Type Type			10/350LY41-4-10M
Widerstand Resistance Résistance	350 Ω ± 0.35 %	Stückzahl Contents Quantité	10
k-Faktor Gauge factor Facteur k	2.09 ± 1 %	Temperaturkoeffizient des k-Faktors Temperature coefficient of gauge factor Coefficient de température du facteur k	104 ±10 [10^{-6} / °C] (-10...+45°C)
Querempfindlichkeit Transverse Sensitivity Sensibilité transverse	-0.3 %	Folienlos Lot Lot de la feuille	A398/21
		Herstellungslos Batch Lot de fabrication	812035234

Temperaturkompensation: Angepaßt für Ferritischen Stahl mit
Temperature Compensation: Compensated for Steel with
Compensation de température: Compensation pour Acier avec

α = 10.8 [10^{-6} / °C]

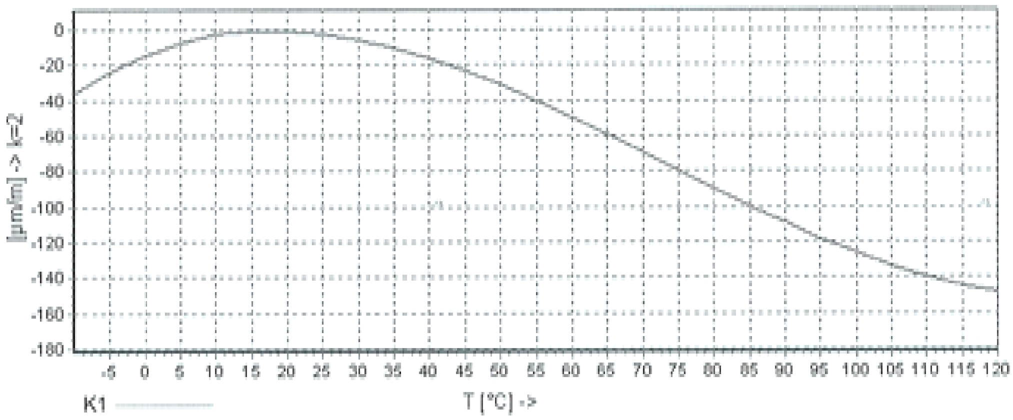

ε_S (T) = -11.1 +1.41 * T -4.97 * 10^{-2} * T^2 +2.27 * 10^{-4} * T^3 + 0.172 * (T-20) µm/m ± 0.3 (µm/m) $°C^{-1}$

Alle technischen Daten nach OIML IR 62, bei Beachtung der abweichenden Toleranzangaben auch nach VDI/VDE 2635. Geben Sie bei Rückfragen bitte DMS-Typ und Herstellungs-Los an.

All technical data in accordance with OIML IR 62, also compliant with C VDI/VDE 2635 if deviating tolerances are observed. In case of further inquiries please indicate gauge type and batch number.

Toutes caractéristiques techniques selon OIML IR 62 et VDI/VDE 2635 pour les indications différentes de tolérance. Pour toutes questions, indiquer le type de la jauge ainsi que le lot de fabrication.

Temperaturgang der Dehnungsmeßstreifen bei Applikationen mit umseitig angegebenen Wärmeausdehnungskoeffizienten α. Gemessen bei kontinuierlicher Temperaturänderung.

Kennlinie 1: DMS mit nicht kürzbaren Teflonanschlußbändchen.
T = Temperatur in °C

Comportement en température des jauges d'extensométrie appliquées sur des matériaux dont les coefficients de dilatation termique α sont indiqués au verso. Mesuré au d'une variation continue de la température.

Courbe 1: Jauges avec fils de sortie de Teflon.
T = température en °C

The **Thermal output** refers to strain gauges when bonded to materials with coefficient of thermal expansion α given overleaf. Values are measured at a continous temperature progression.

Curve 1: Gauges with Teflon connecting leads.
T = temperature in °C

HBM

Dehnungsmeßstreifen
Strain Gauges
Jauges d'extensométrie

Widerstand Resistance Résistance	350 Ω ± 0.35 %	Bestellnummer Order No. No. de référence	**K-XY31-6/350-4-10M**
		Typ Type Type	6/350XY31-4-10M
		Stückzahl Contents Quantité	5
k-Faktor Gauge factor Facteur k	Gitter A: 2.07 ± 1 % Gitter B: 2.06 ± 1 % Gitter C: 2.07 ± 1 %	Temperaturkoeffizient des k-Faktors Temperature coefficient of gauge factor Coefficient de température du facteur k	104 ±10 $[10^{-6} / °C]$ (-10...+45°C)
Querempfindlichkeit Transverse Sensitivity Sensibilité transverse	Gitter A: 0.1 % Gitter B: 0.9 % Gitter C: 0.1 %	Folienlos Lot Lot de la feuille	A398/21
		Herstellungslos Batch Lot de fabrication	812035235

Temperaturkompensation: Angepaßt für Ferritischen Stahl mit
Temperature Compensation: Compensated for Steel with
Compensation de température: Compensation pour Acier avec

α = 10.8 $[10^{-6} / °C]$

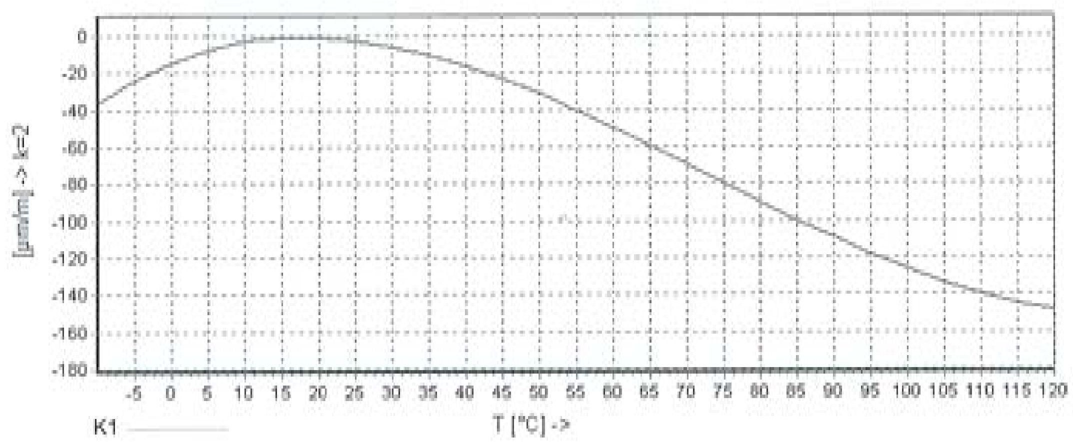

$$\varepsilon_S(T) = -11{,}1 + 1{,}41 \cdot T - 4{,}97 \cdot 10^{-2} \cdot T^2 + 2{,}27 \cdot 10^{-4} \cdot T^3 + 0{,}172 \cdot (T-20)\ \mu m/m \pm 0{,}3\ (\mu m/m)\ °C^{-1}$$

Alle technischen Daten nach OIML IR 62, bei Beachtung der abweichenden Toleranzangaben auch nach VDI/VDE 2635. Geben Sie bei Rückfragen bitte DMS-Typ und Herstellungs-Los an.

All technical data in accordance with OIML IR 62, also compliant with C'VDI/VDE 2635 if deviating tolerances are observed. In case of further inquiries please indicate gauge type and batch number.

Toutes caractéristiques techniques selon OIML IR 62 et VDI/VDE 2635 pour les indications différentes de tolérance. Pour toutes questions, indiquer le type de la jauge ainsi que le lot de fabrication.

Temperaturgang der Dehnungsmeßstreifen bei Applikationen mit umseitig angegebenen Wärmeausdehnungskoeffizienten α. Gemessen bei kontinuierlicher Temperaturänderung.

Kennlinie 1: DMS mit nicht kürzbaren Teflonanschlußbändchen.
T = Temperatur in °C

Comportement en température des jauges d'extensométrie appliquées sur des matériaux dont les coefficients de dilatation termique α sont indiqués au verso. Mesuré au d'une variation continue de la température.

Courbe 1: Jauges avec fils de sortie de Teflon.
T = température en °C

The **Thermal output** refers to strain gauges when bonded to materials with coefficient of thermal expansion α given overleaf. Values are measured at a continuous temperature progression.

Curve 1: Gauges with Teflon connecting leads.
T = temperature in °C

The information's given above are incorrect. It was given update form HBM Company :

Gaue factor:	Sensitivity:
Gitter A: 2.07	Gitter A: 0.1%
Gitter B: 2.07	Gitter B: 0.9%

	Dehnungsmeßstreifen **Strain Gauges** **Jauges d'extensométrie**	Bestellnummer Order No. No. de référence	**K-RY81-6/350-4-10M**
		Typ Type Type	6/350RY81-4-10M
Widerstand Resistance Résistance	350 Ω ± 0.35 %	Stückzahl Contents Quantité	5
k-Faktor Gauge factor Facteur k	Gitter A: 2.07 ± 1 % Gitter B: 2.07 ± 1 % Gitter C: 2.07 ± 1 %	Temperaturkoeffizient des k-Faktors Temperature coefficient of gauge factor Coefficient de température du facteur k	104 ±10 [10^{-6} / °C] (-10...+45°C)
Querempfindlichkeit Transverse Sensitivity Sensibilité transverse	Gitter A: 0 % Gitter B: -0.2 % Gitter C: 0 %	Folienlos Lot Lot de la feuille	A396/04
		Herstellungslos Batch Lot de fabrication	812035933

Temperaturkompensation: Angepaßt für Temperature Compensation: Compensated for Compensation de température: Compensation pour	Ferritischen Stahl mit Steel with Acier avec	α =	10.8 [10^{-6} / °C]

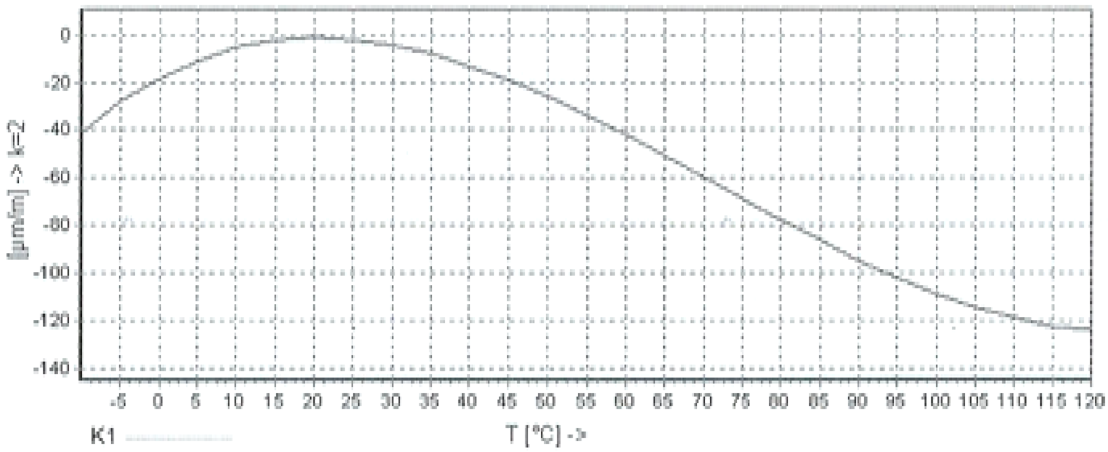

$$\varepsilon_S(T) = -16.7 + 1.69 \cdot T - 4.99 \cdot 10^{-2} \cdot T^2 + 2.32 \cdot 10^{-4} \cdot T^3 + 0.071 \cdot (T-20)\ \mu m/m \pm 0.3\ (\mu m/m)\ °C^{-1}$$

Alle technischen Daten nach OIML IR 62, bei Beachtung der abweichenden Toleranzangaben auch nach VDI/VDE 2635. Geben Sie bei Rückfragen bitte DMS-Typ und Herstellungs-Los an.

All technical data in accordance with OIML IR 62, also compliant with C VDI/VDE 2635 if deviating tolerances are observed. In case of further inquiries please indicate gauge type and batch number.

Toutes caractéristiques techniques selon OIML IR 62 et VDI/VDE 2635 pour les indications différentes de tolérance. Pour toutes questions, indiquer le type de la jauge ainsi que le lot de fabrication.

Temperaturgang der Dehnungsmeßstreifen bei Applikationen mit umseitig angegebenen Wärmeausdehnungskoeffizienten α. Gemessen bei kontinuierlicher Temperaturänderung.

Kennlinie 1: DMS mit nicht kürzbaren Teflonanschlußbändchen.
T = Temperatur in °C

Comportement en température des jauges d'extensométrie appliquées sur des matériaux dont les coefficients de dilatation termique α sont indiqués au verso. Mesuré au d'une variation continue de la température.

Courbe 1: Jauges avec fils de sortie de Teflon.
T = température en °C

The Thermal output refers to strain gauges when bonded to materials with coefficient of thermal expansion α given overleaf. Values are measured at a continous temperature progression.

Curve 1: Gauges with Teflon connecting leads.
T = temperature in °C

G DIC Results

Test: ELTT_1_191009_A

The measurement was started at 30% load.

The maximum load during this test was 60%.

The DIC - measurement was conducted in the 16 meter region on the suction side of the blade, see snapshot below.

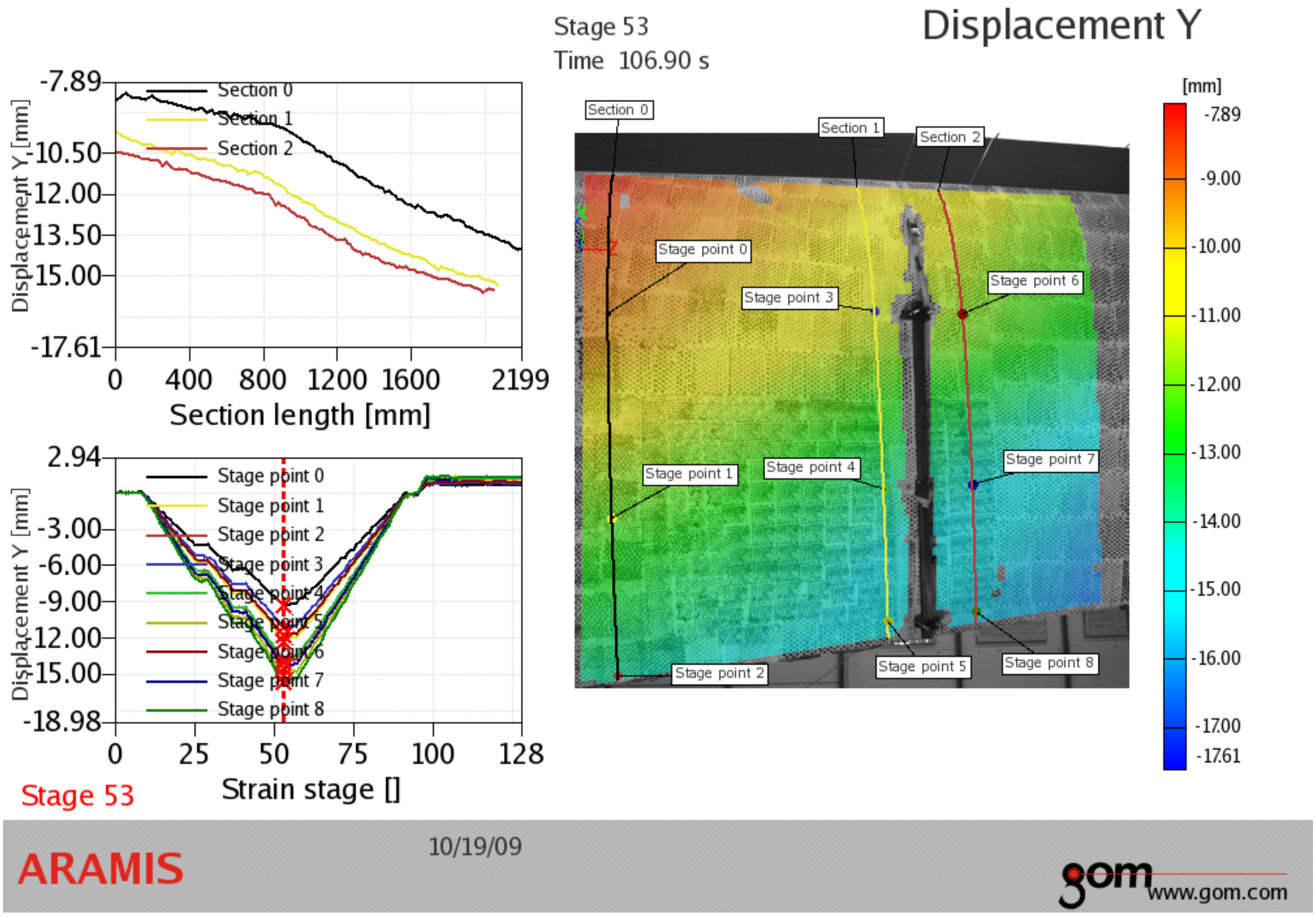

Input of data from DIC - measurement (area is collapsed)

The “local deformation” of the sandwich panels are determined applying the method described in the main report, see capture 5. These determined deformations are comparable with the NT- measurements.

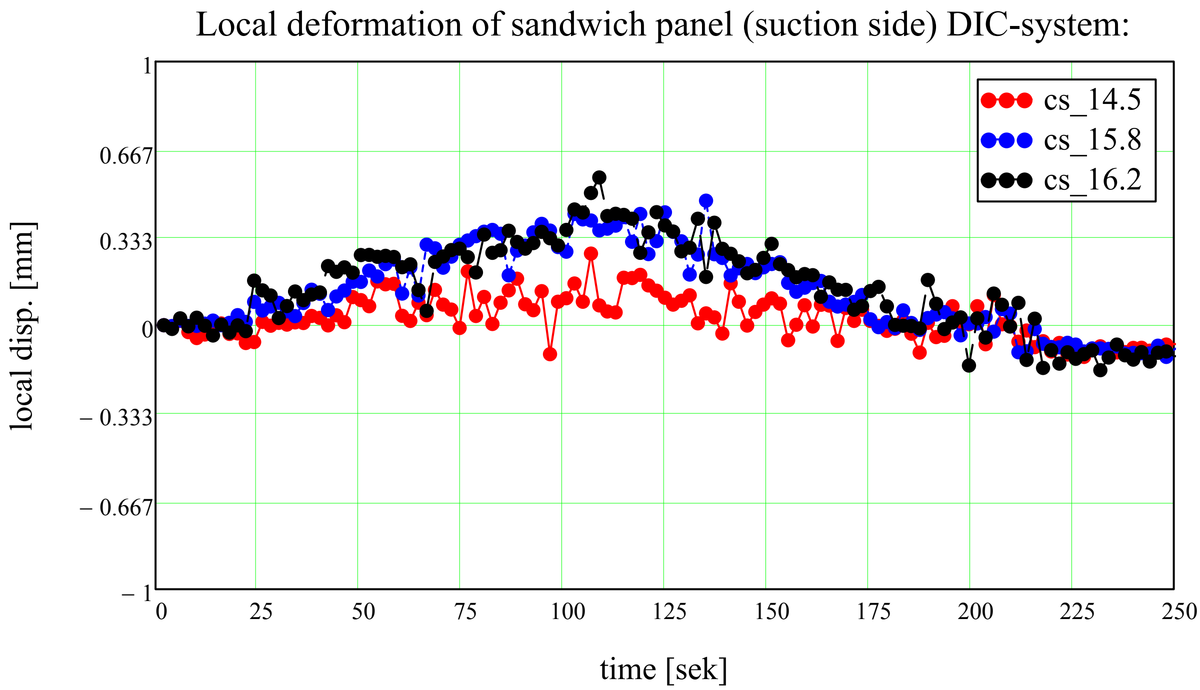

Rigid body movement transformation

The “rigid body movement” transformation is performed by determining the rotations and displacements of the “stiff” cap and then subtracting this movement from the deformed cross section. This gives a fairly god estimate of the local cross sectional displacements. The rotations and displacement are determined by applying the least squares algorithmdescribed in the main report, see chapter 5.

measuring points on the cap: $n_1 := 5$ $n_2 := 30$ $n_{a1} := n_1$ $n_{a2} := n_2$ $sf := 10$

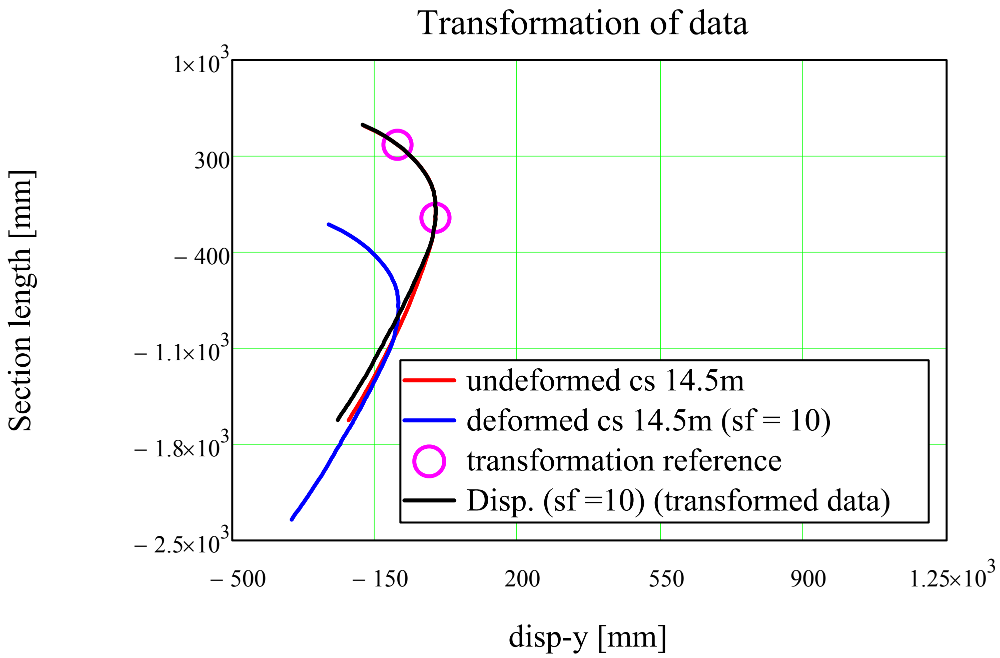

Rigid body movement transformation

measuring points on the cap: $n_1 := 5$ $n_2 := 30$ $n_{b1} := n_1$ $n_{b2} := n_2$ $sf := 10$

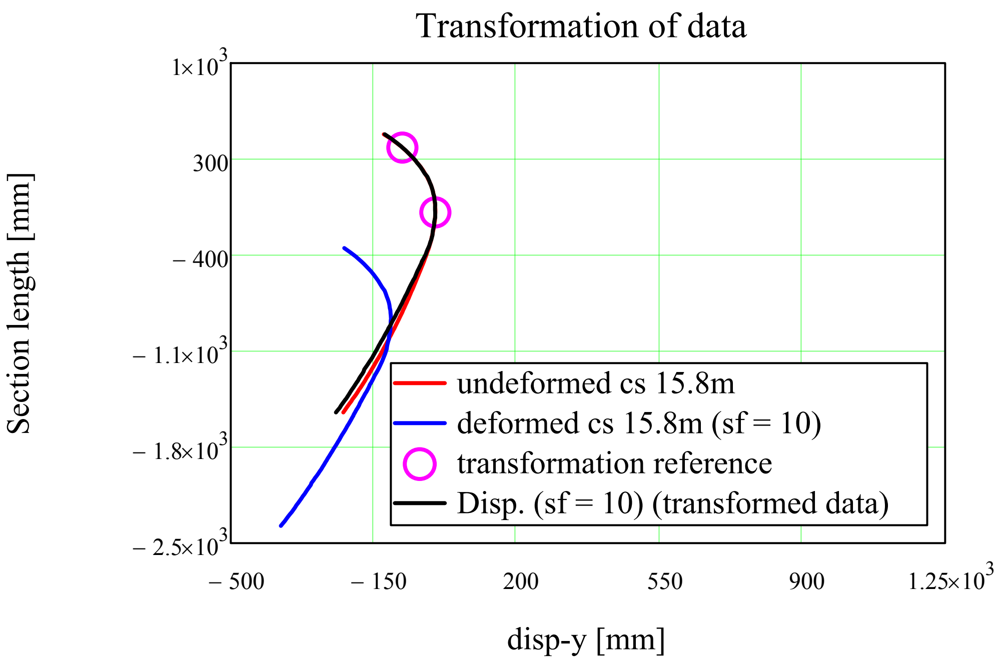

Rigid body movement transformation

measuring points on the cap: $n_1 := 5$ $n_2 := 30$ $n_{c1} := n_1$ $n_{c2} := n_2$ $sf := 10$

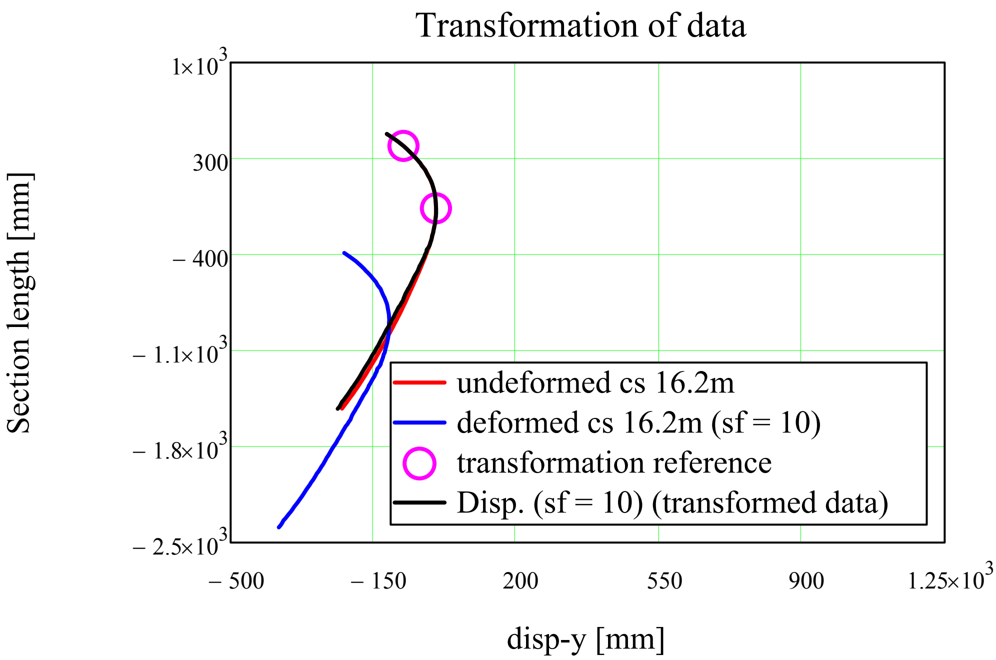

Presented below are the transformed (rigid body movement are subtracted) relative y - displacements:

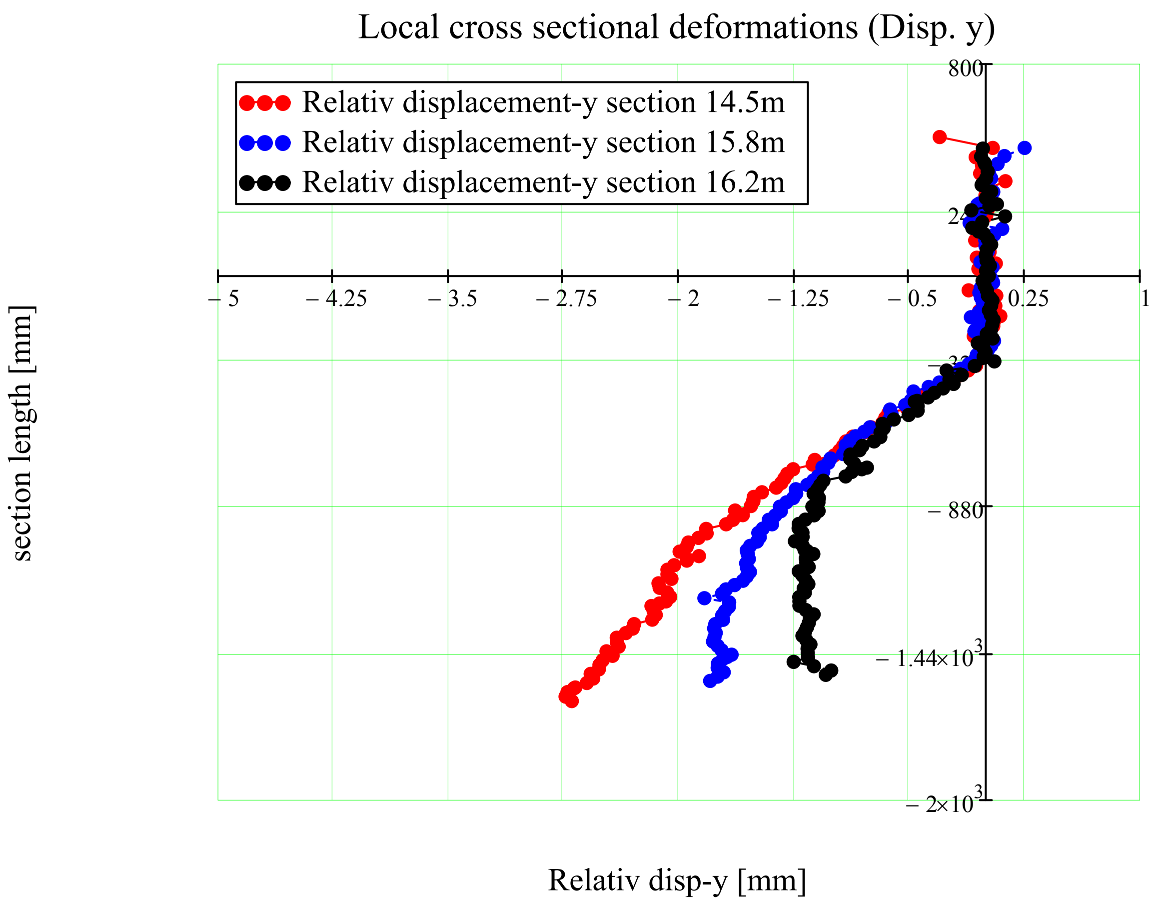

Presented below are the relative y - displacements with out the transformation:

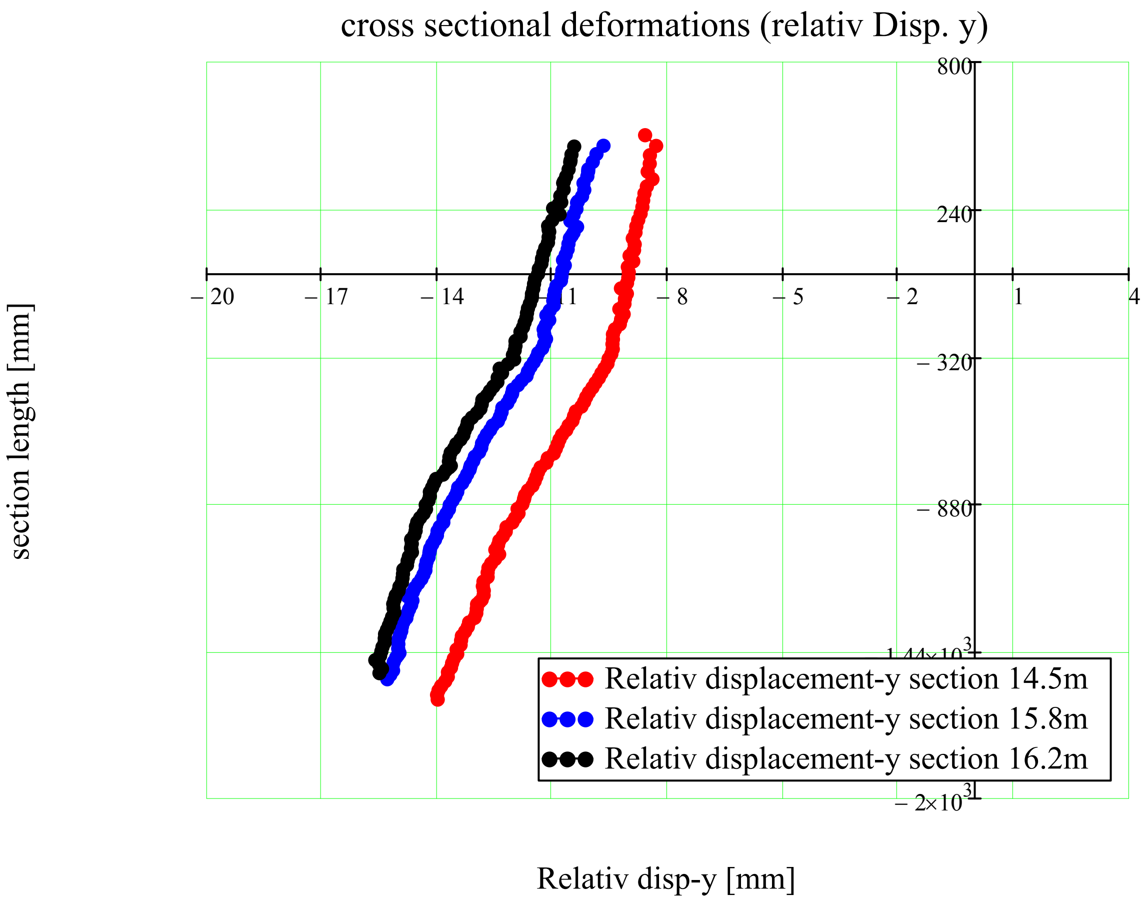

Global deformation determined based on the DIC - measurement

The global deformation is determined by applying the least squares algorithm described in the main report, see chapter 5.

Cross section [m]	Disp. Ux [mm]	Disp. Uy [mm]	Disp. Uz [mm]	Rot. Rx [deg]	Rot. Ry [deg]	Rot. Rz [deg]
14.50	-72.8487	-8.8865	4.6258	####	0.5025	0.0801
15.80	-83.0705	-10.5289	5.2029	####	0.5374	0.1012
16.20	-86.9461	-11.0572	5.4707	####	0.5473	0.1158

Test: ELTT_1_201009_A

The measurement was started at 30% load.

The maximum load during this test was 60%.

The DIC - measurement was conducted in the 16 meter region on the suction side of the blade, see snapshot below.

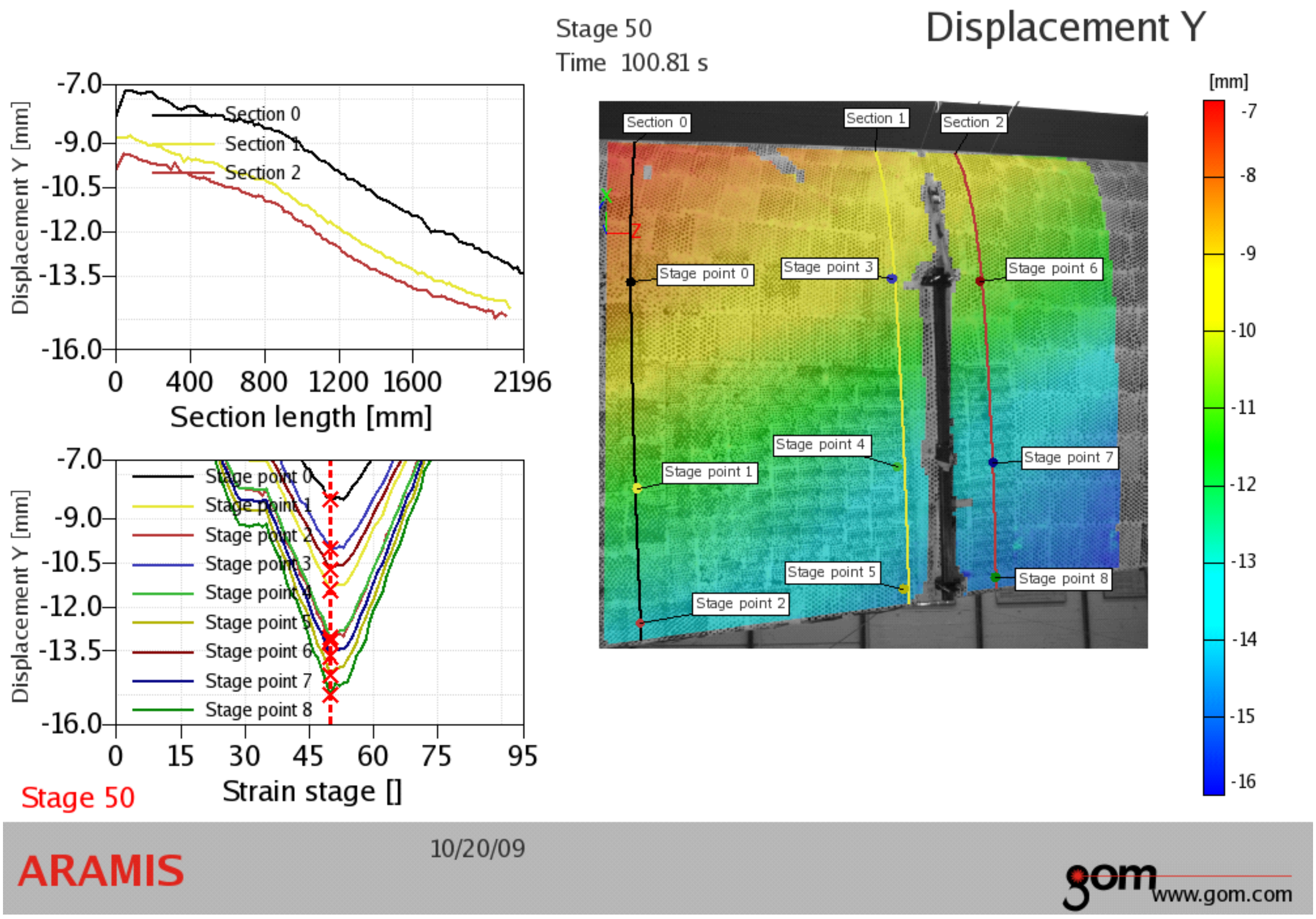

Input of data from DIC - measurement (area is collapsed)

The “local deformation” of the sandwich panels are determined applying the method described in the main report, see capture 5. These determined deformations are comparable with the NT- measurements.

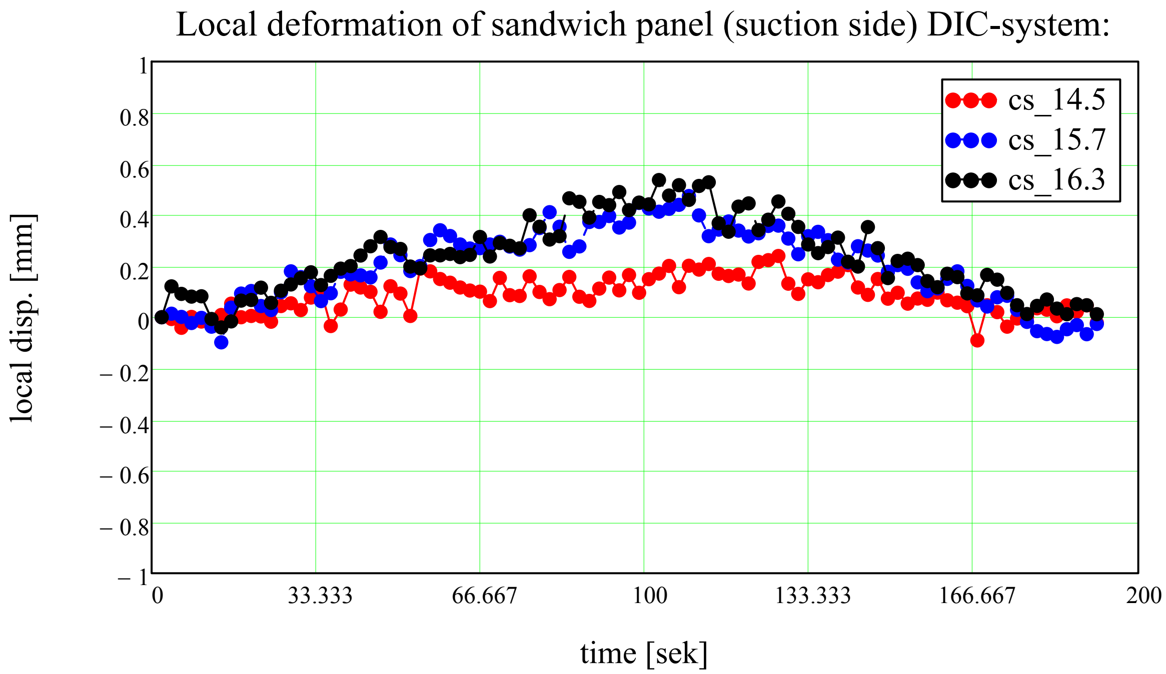

Rigid body movement transformation

The “rigid body movement” transformation is performed by determining the rotations and displacements of the “stiff” cap and then subtracting this movement from the deformed cross section. This gives a fairly god estimate of the local cross sectional displacements. The rotations and displacement are determined by applying the least squares algorithmdescribed in the main report, see chapter 5.

measuring points on the cap: $n_1 := 7$ $n_2 := 32$ $n_{a1} := n_1$ $n_{a2} := n_2$ $sf := 10$

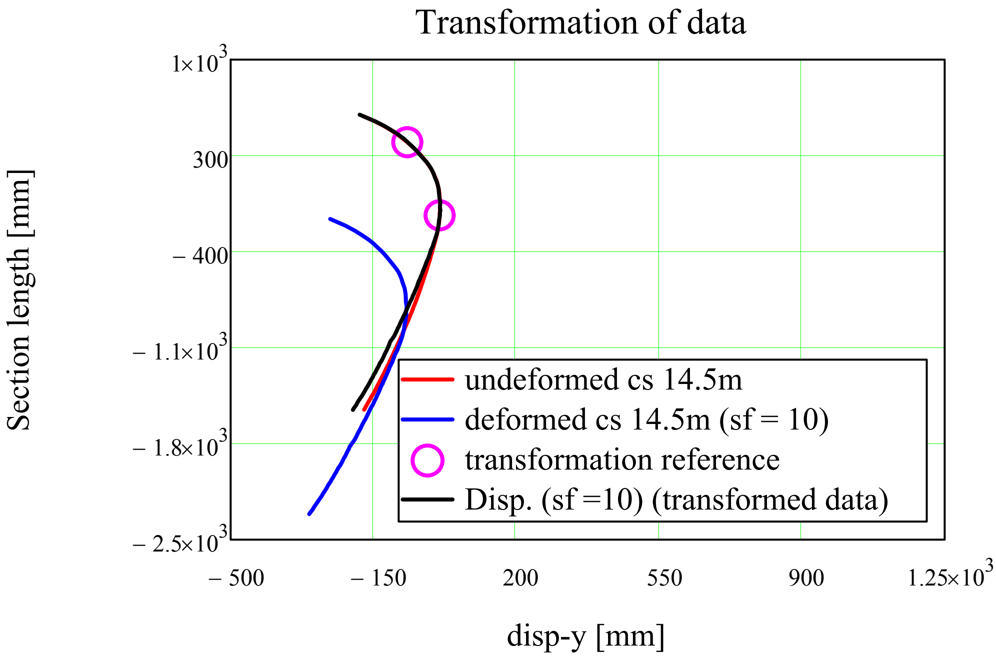

Rigid body movement transformation

measuring points on the cap: $n_1 := 7$ $n_2 := 32$ $n_{b1} := n_1$ $n_{b2} := n_2$ $sf := 10$

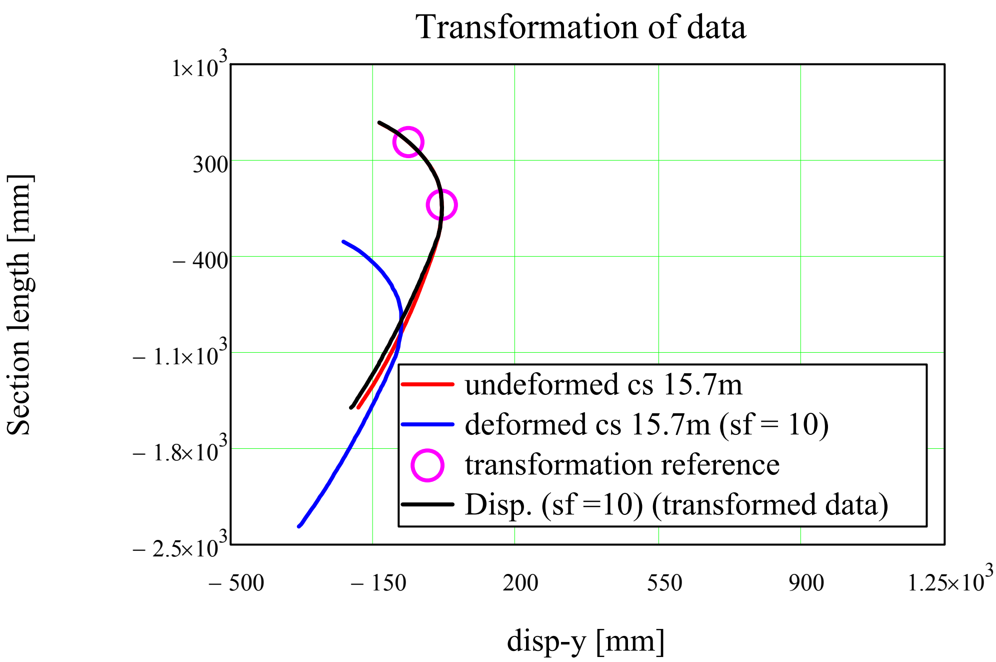

Rigid body movement transformation

measuring points on the cap: $n_1 := 7$ $n_2 := 32$ $n_{c1} := n_1$ $n_{c2} := n_2$ $sf := 10$

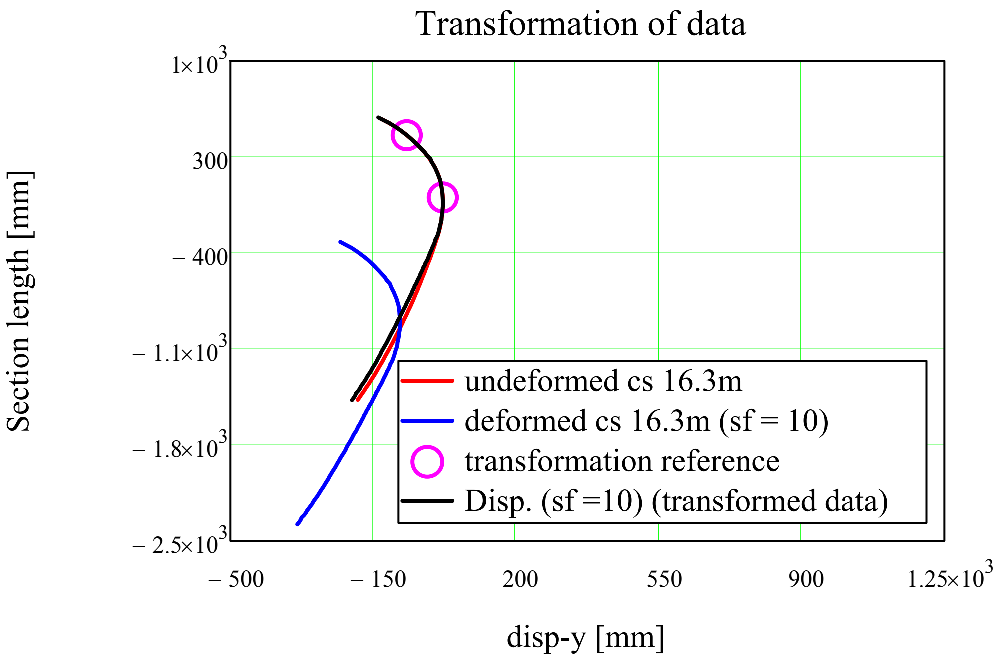

Presented below are the transformed (rigid body movement are subtracted) relative y - displacements:

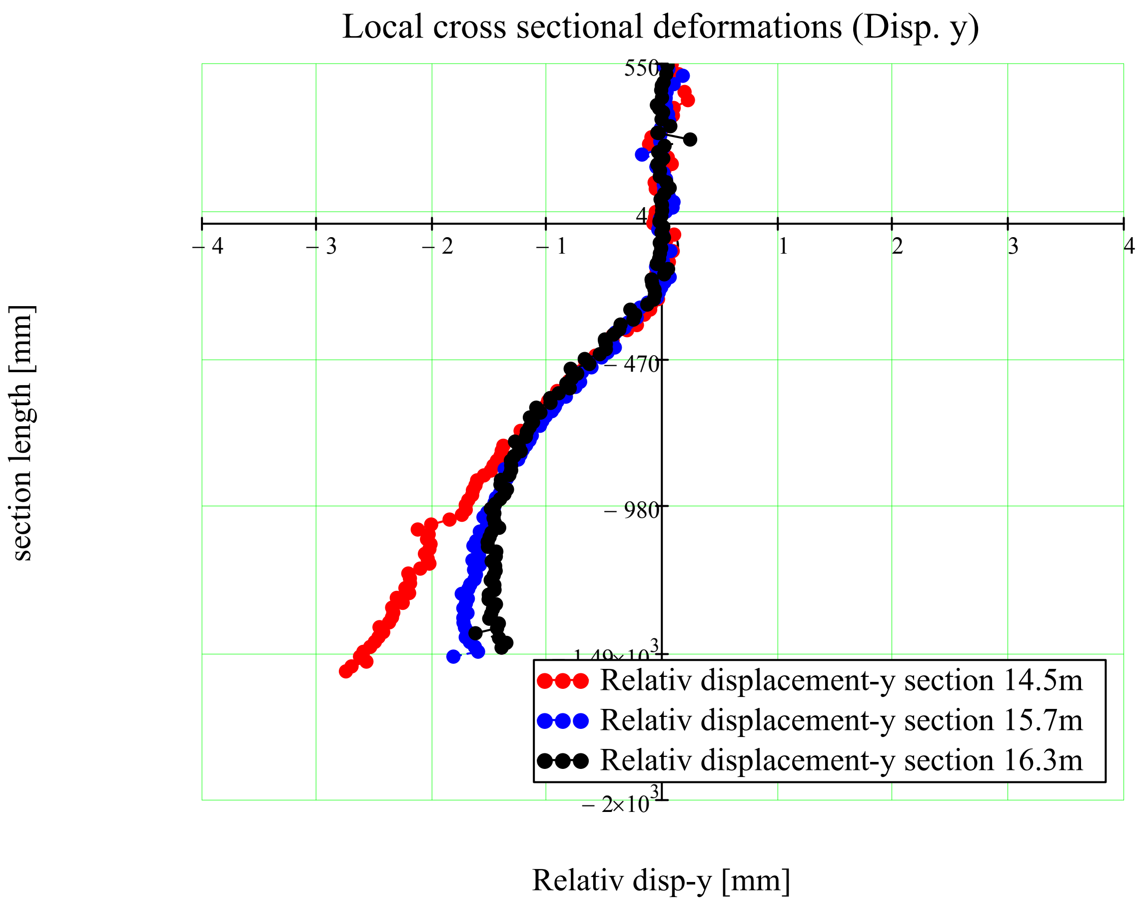

Presented below are the relative y - displacements with out the transformation:

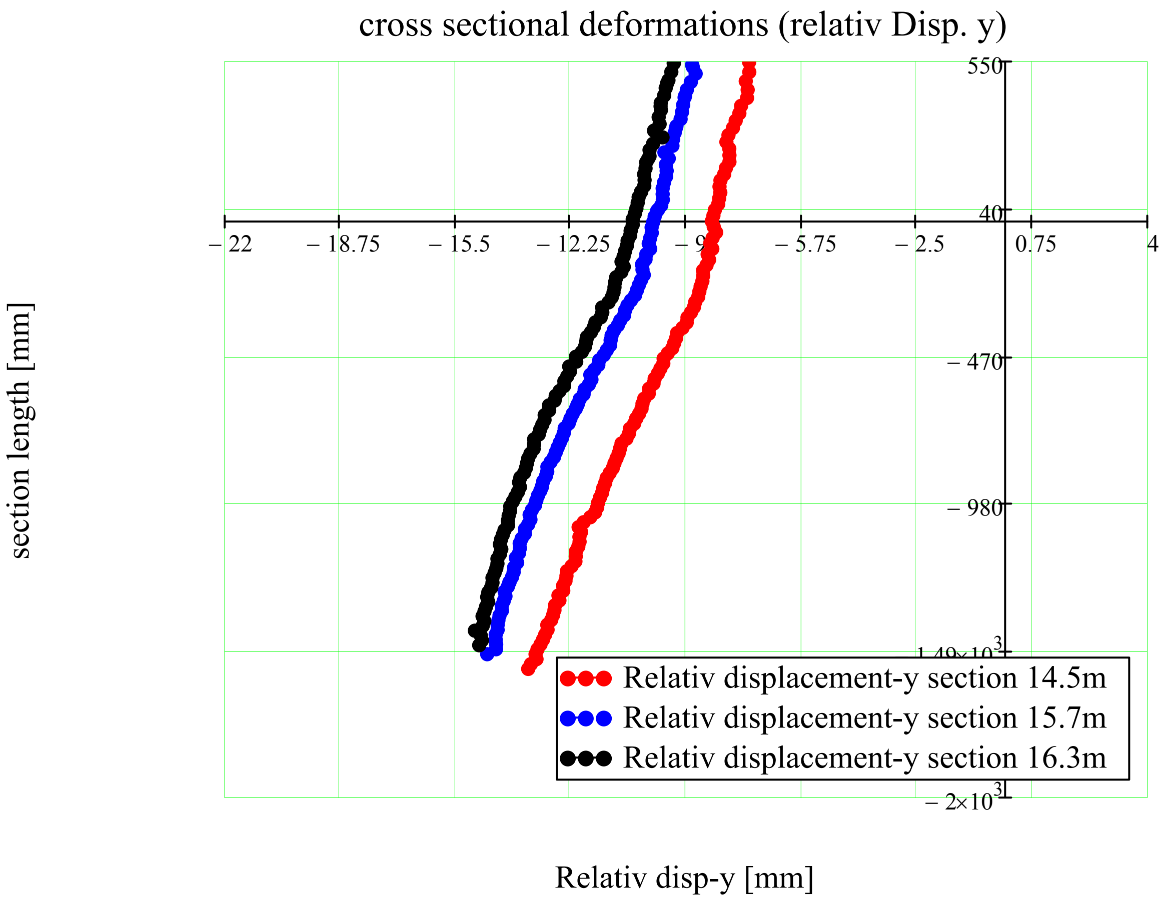

Global deformation determined based on the DIC - measurement

The global deformation is determined by applying the least squares algorithm described in the main report, see chapter 5.

Cross section [m]	Disp. Ux [mm]	Disp. Uy [mm]	Disp. Uz [mm]	Rot. Rx [deg]	Rot. Ry [deg]	Rot. Rz [deg]
14.50	-76.3345	-7.9961	4.4774	####	0.5291	0.0926
15.70	-86.9887	-9.5002	5.4366	####	0.5639	0.1106
16.30	-91.0254	-10.0259	5.7233	####	0.5750	0.1148

Test: ELTT_1_291009_A

The measurement was started at 30% load.

The maximum load during this test was 60%.

The DIC - measurement was conducted in the 20 meter region on the suction side of the blade, see snapshot below.

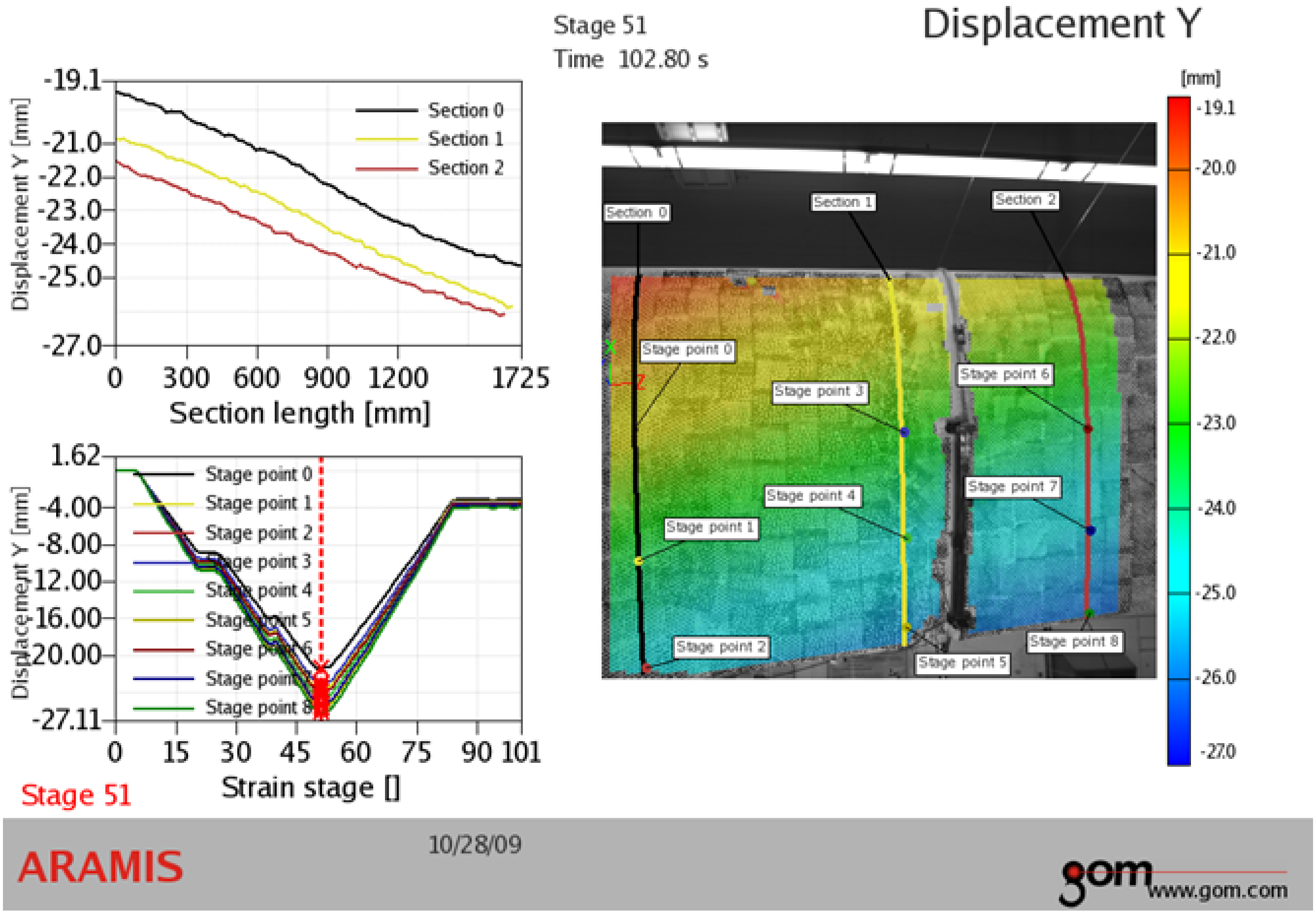

Input of data from DIC - measurement (area is collapsed)

The “local deformation” of the sandwich panels are determined applying the method described in the main report, see capture 5. These determined deformations are comparable with the NT- measurements.

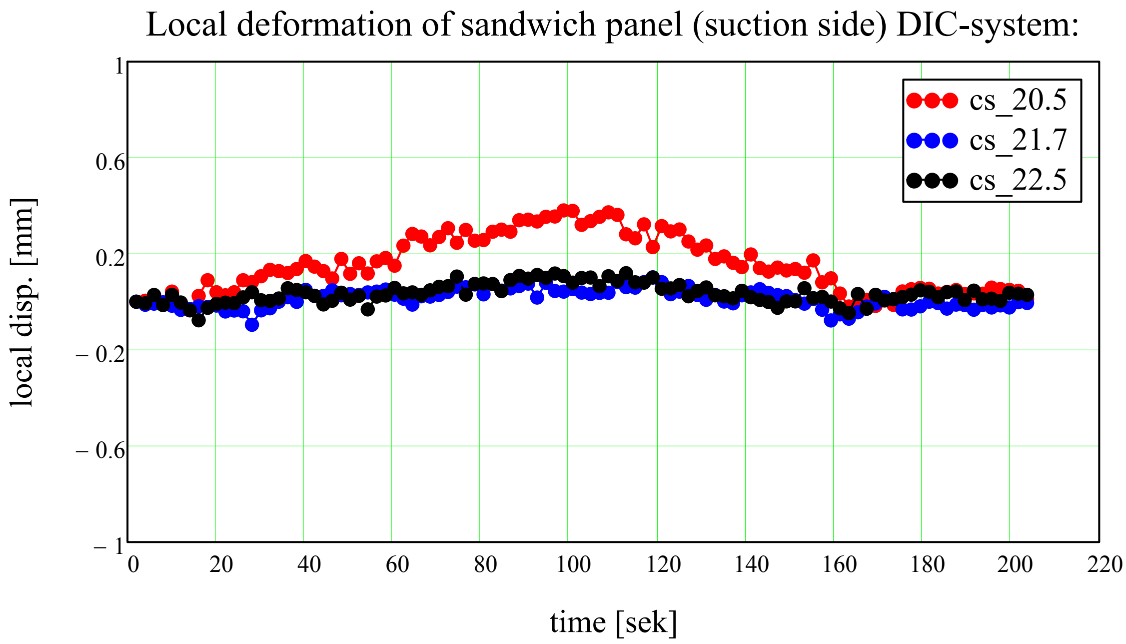

Verification of the DIC-measurement (Comparison between the NT- and DIC- measurement)

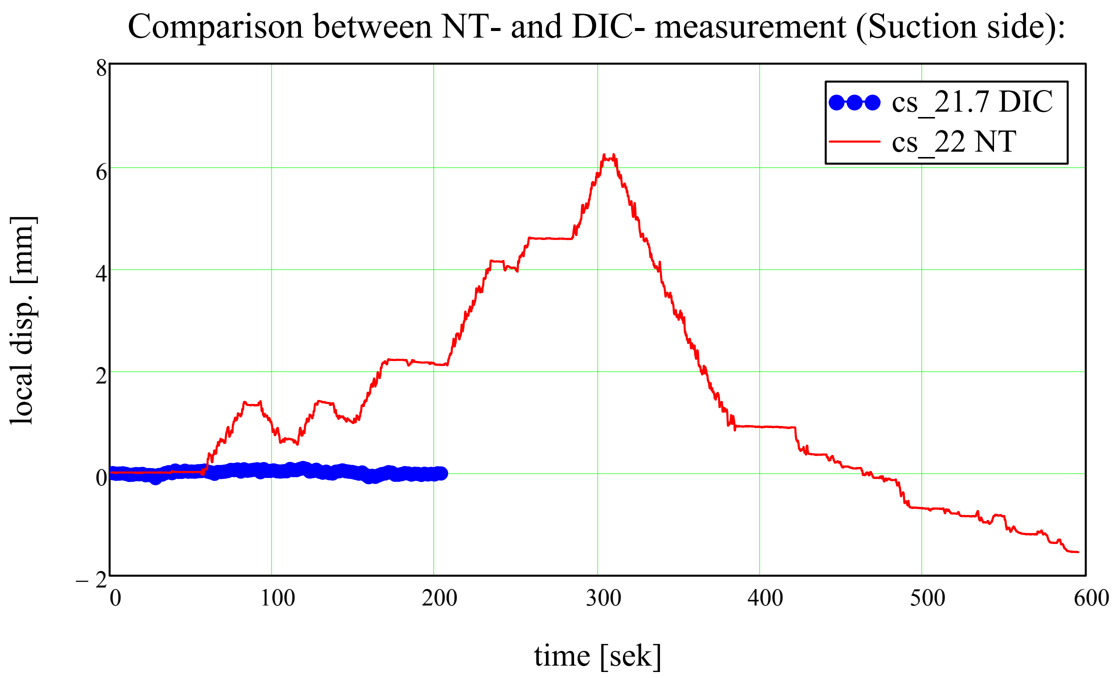

Rigid body movement transformation

The “rigid body movement” transformation is performed by determining the rotations and displacements of the “stiff” cap and then subtracting this movement from the deformed cross section. This gives a fairly god estimate of the local cross sectional displacements. The rotations and displacement are determined by applying the least squares algorithmdescribed in the main report, see chapter 5.

measuring points on the cap: $n_1 := 5$ $n_2 := 30$ $n_{a1} := n_1$ $n_{a2} := n_2$ $sf := 10$

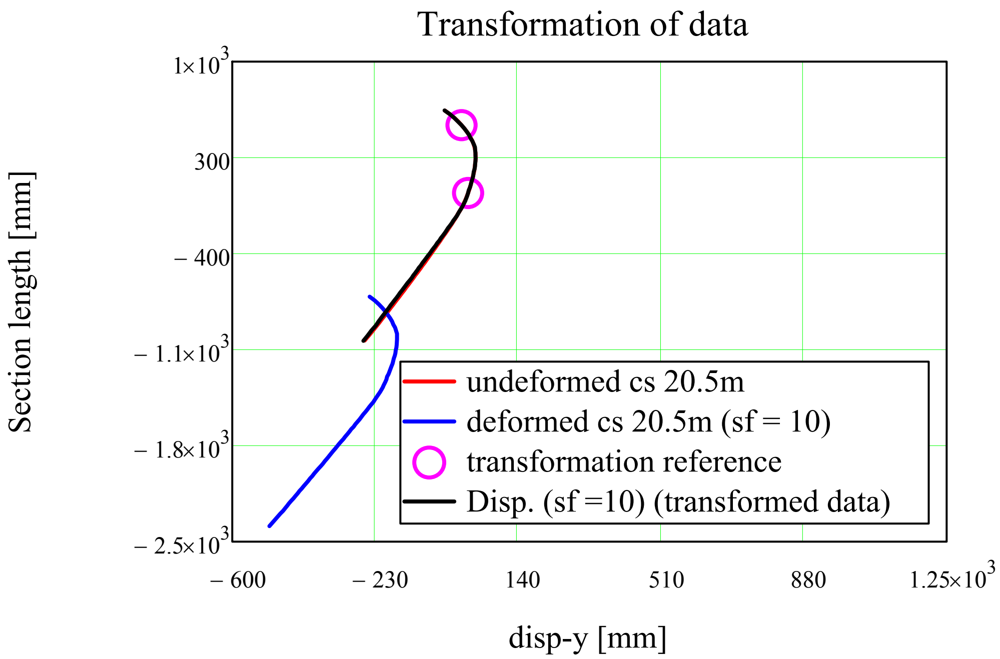

Rigid body movement transformation

measuring points on the cap: $n_1 := 5$ $n_2 := 30$ $n_{b1} := n_1$ $n_{b2} := n_2$ $sf := 10$

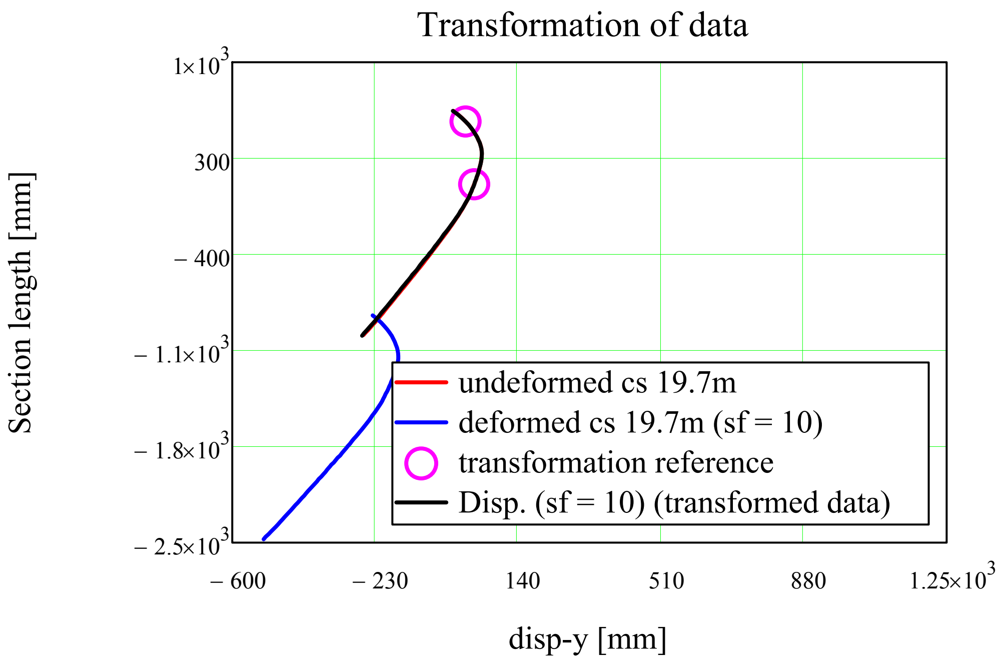

Rigid body movement transformation

measuring points on the cap: $n_1 := 5$ $n_2 := 30$ $n_{c1} := n_1$ $n_{c2} := n_2$ $sf := 10$

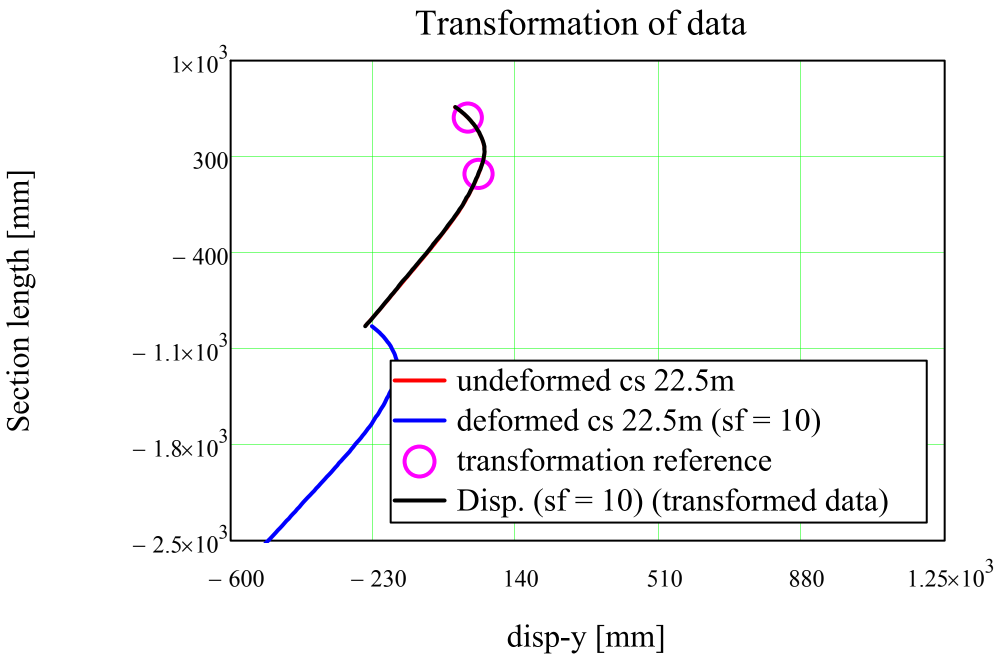

Presented below are the transformed (rigid body movement are subtracted) relative y - displacements:

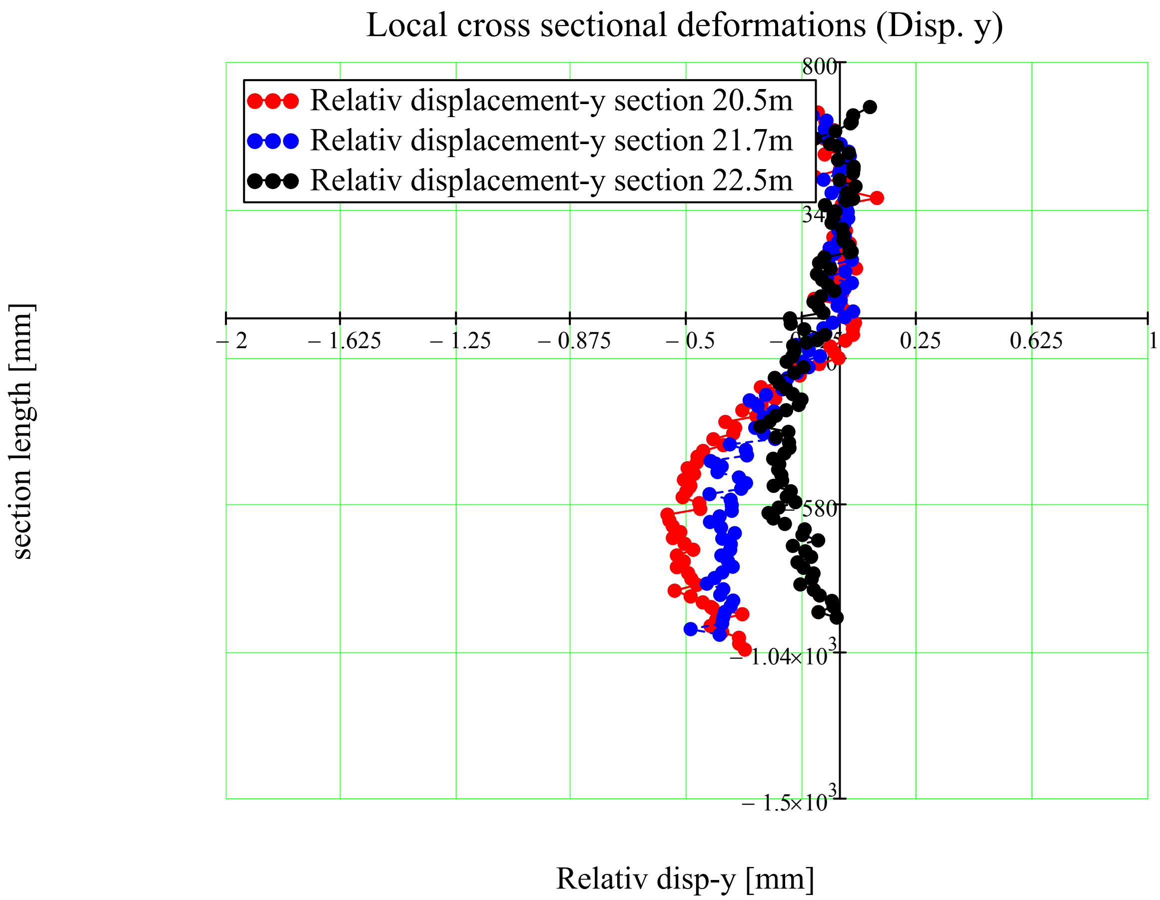

Presented below are the relative y - displacements with out the transformation:

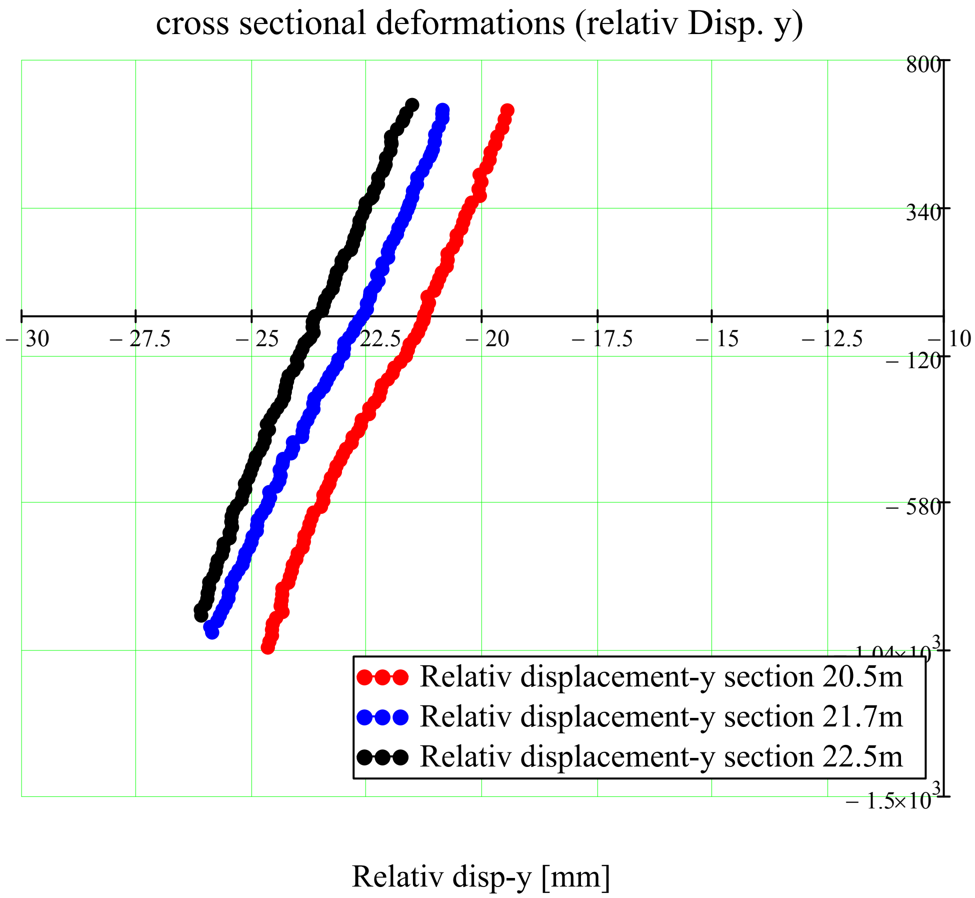

Global deformation determined based on the DIC - measurement

The global deformation is determined by applying the least squares algorithm described in the main report, see chapter 5.

Cross section [m]	Disp. Ux [mm]	Disp. Uy [mm]	Disp. Uz [mm]	Rot. Rx [deg]	Rot. Ry [deg]	Rot. Rz [deg]
20.50	-135.9536	-20.4531	7.0808	0.0418	0.6619	0.1693
21.70	-149.2300	-21.6431	7.7095	0.0413	0.6866	0.1658
22.50	-159.9864	-22.4290	8.2046	0.0298	0.7075	0.1604

Test: ELTT_2_101109_A

The measurement was started at 30% load.

The maximum load during this test was 60%.

The DIC - measurement was conducted in the 4 meter region on the pressure side of the blade, see snapshot below.

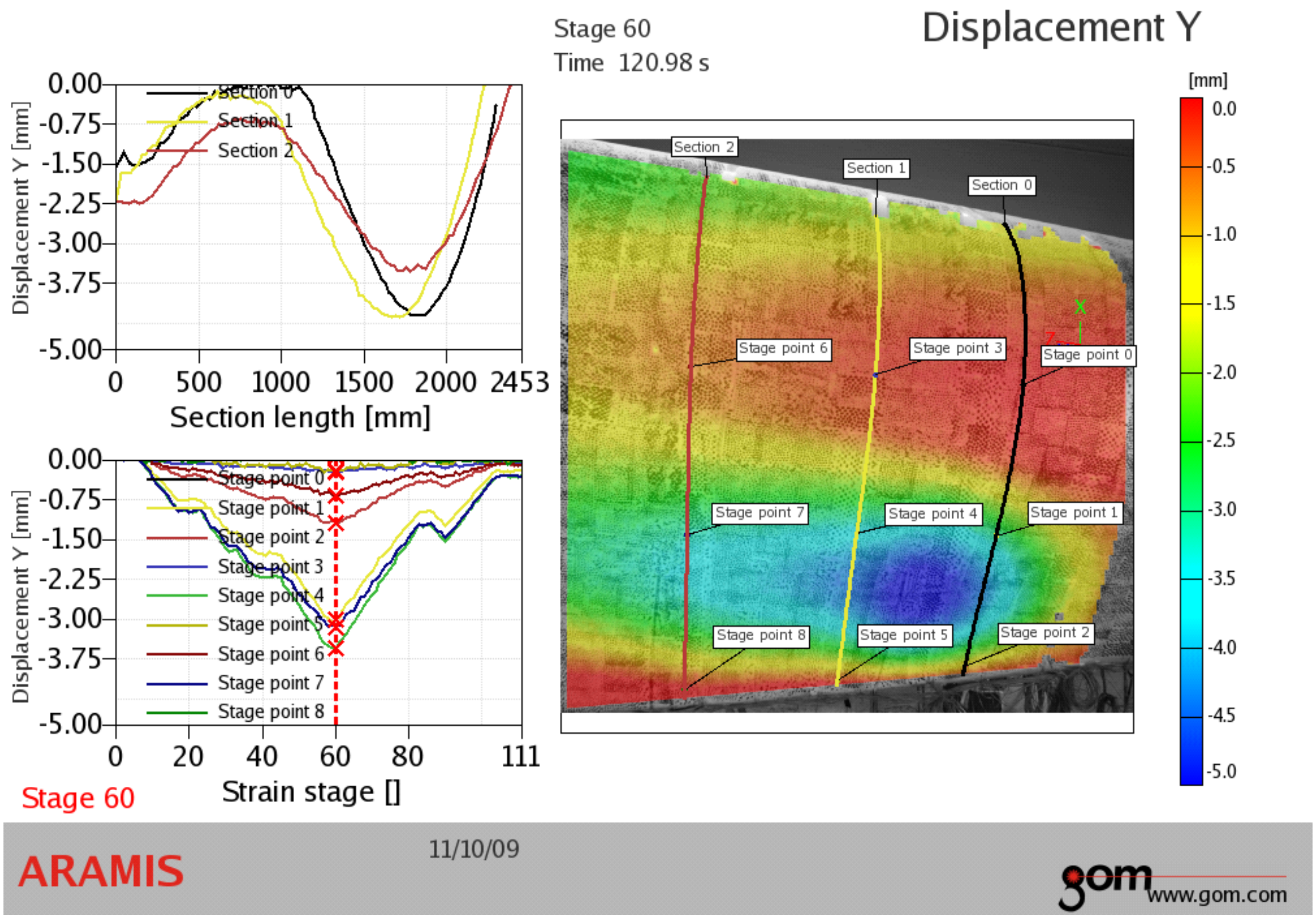

Input of data from DIC - measurement (area is collapsed)

The “local deformation” of the sandwich panels are determined applying the method described in the main report, see capture 5. These determined deformations are comparable with the NT- measurements.

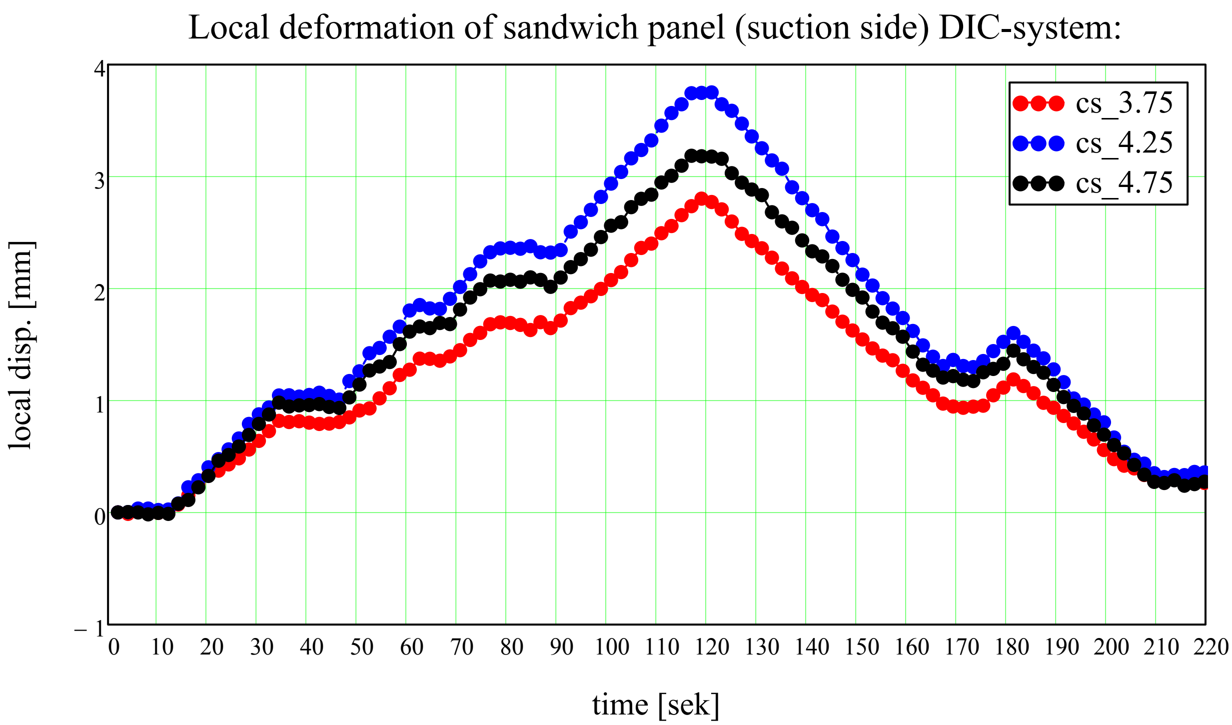

Rigid body movement transformation

The “rigid body movement” transformation is performed by determining the rotations and displacements of the “stiff” cap and then subtracting this movement from the deformed cross section. This gives a fairly god estimate of the local cross sectional displacements. The rotations and displacement are determined by applying the least squares algorithmdescribed in the main report, see chapter 5.

measuring points on the cap: $n_1 := 20$ $n_2 := 45$ $n_{a1} := n_1$ $n_{a2} := n_2$ $sf := 10$

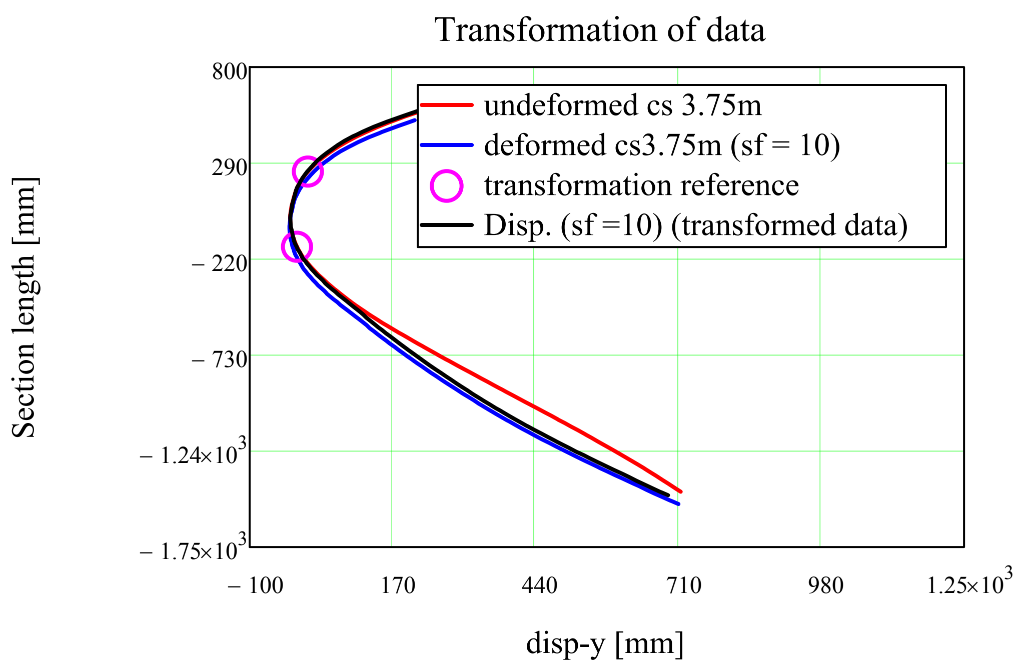

Rigid body movement transformation

measuring points on the cap: $n_1 := 20$ $n_2 := 45$ $n_{b1} := n_1$ $n_{b2} := n_2$ $sf := 10$

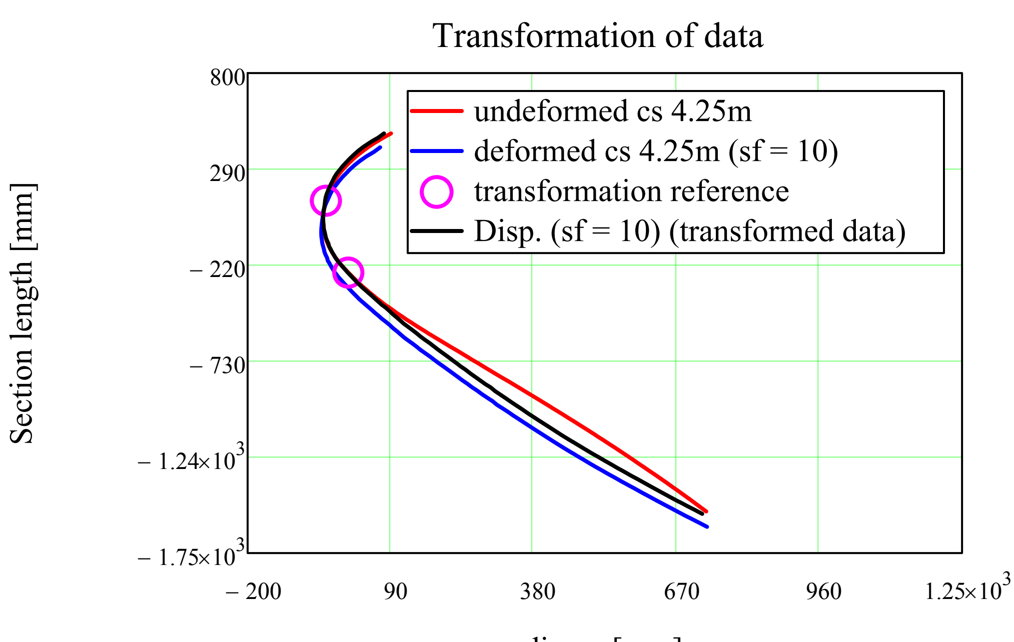

Rigid body movement transformation

measuring points on the cap: $n_1 := 20$ $n_2 := 45$ $n_{c1} := n_1$ $n_{c2} := n_2$ $sf := 10$

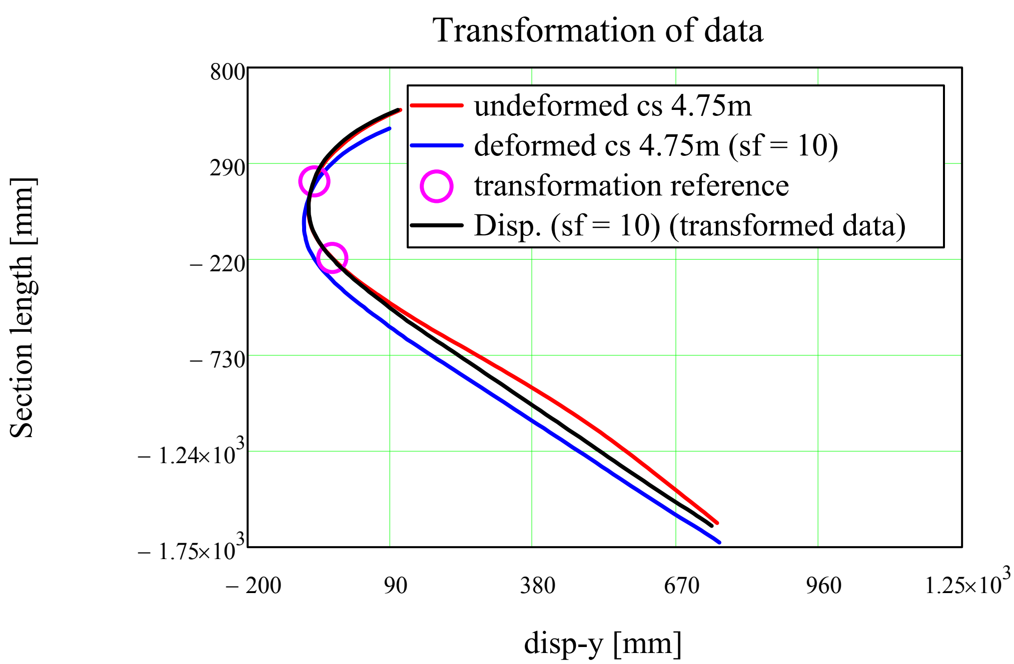

Presented below are the transformed (rigid body movement are subtracted) relative y - displacements:

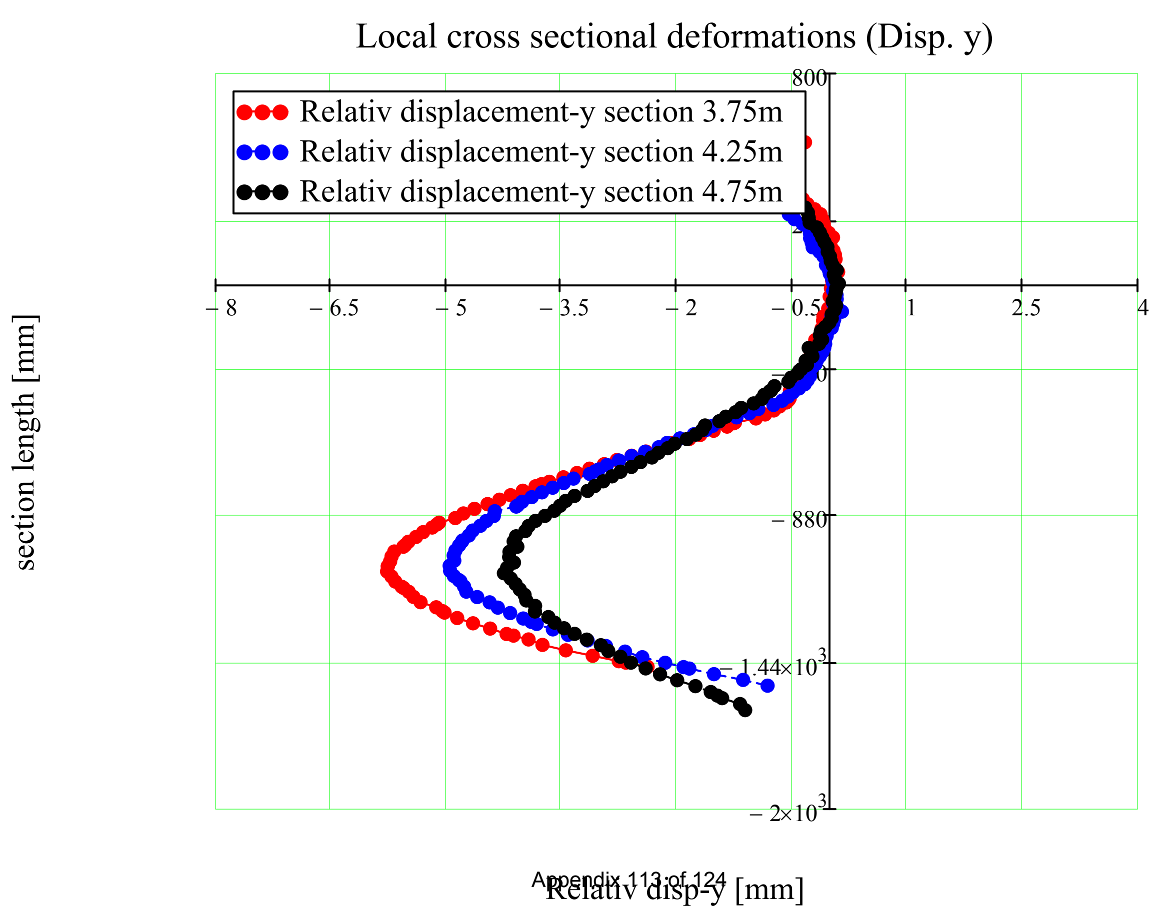

Presented below are the relative y - displacements with out the transformation:

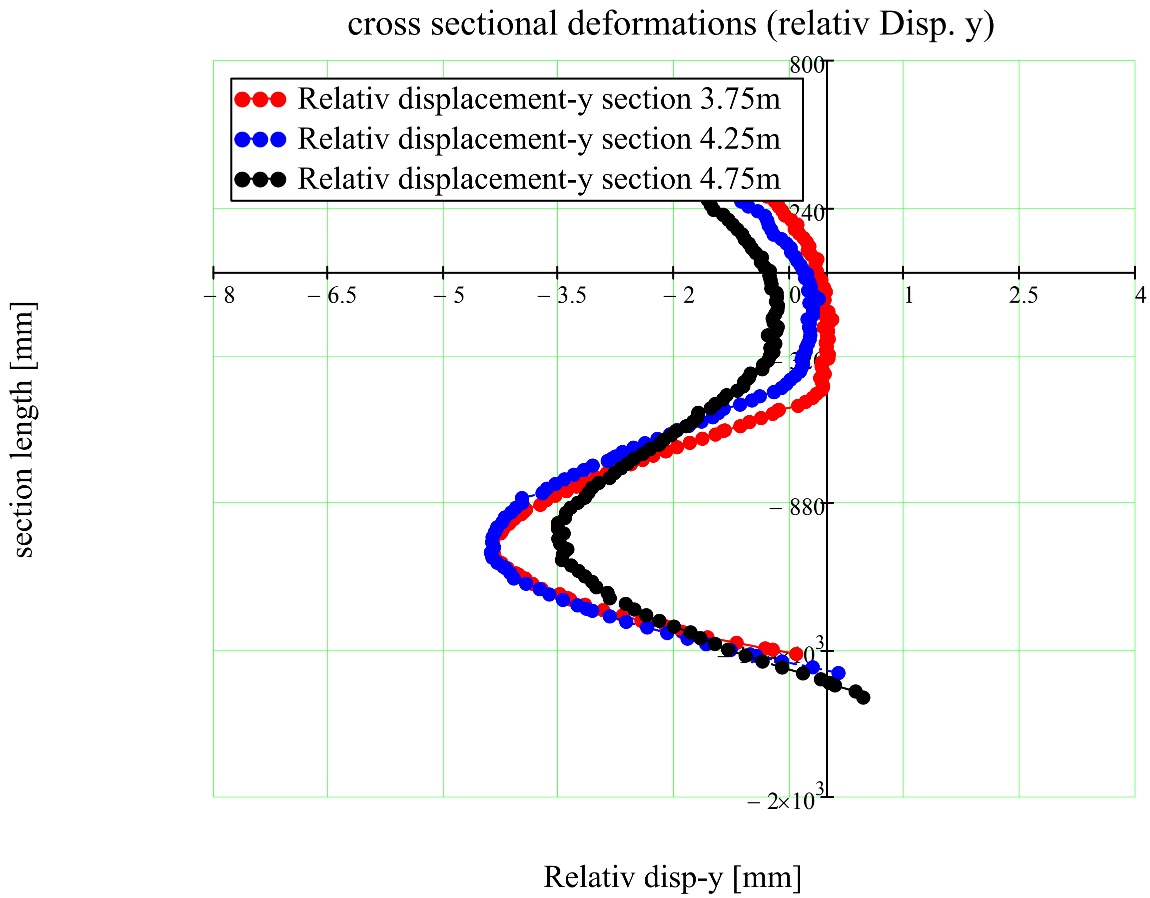

Global deformation determined based on the DIC - measurement

The global deformation is determined by applying the least squares algorithm described in the main report, see chapter 5.

Cross section [m]	Disp. Ux [mm]	Disp. Uy [mm]	Disp. Uz [mm]	Rot. Rx [deg]	Rot. Ry [deg]	Rot. Rz [deg]
3.75	-5.7070	-0.2334	0.9974	####	0.1441	-0.0842
4.25	-7.5344	-0.2955	0.6790	####	0.1723	-0.0493
4.75	-10.0761	-0.8469	0.8198	####	0.2024	-0.0860

Test: ELTT_2_171109_A

The measurement was started at 30% load.

The maximum load during this test was 60%.

The DIC - measurement was conducted in the 4 meter region on the suction side of the blade, see snapshot below.

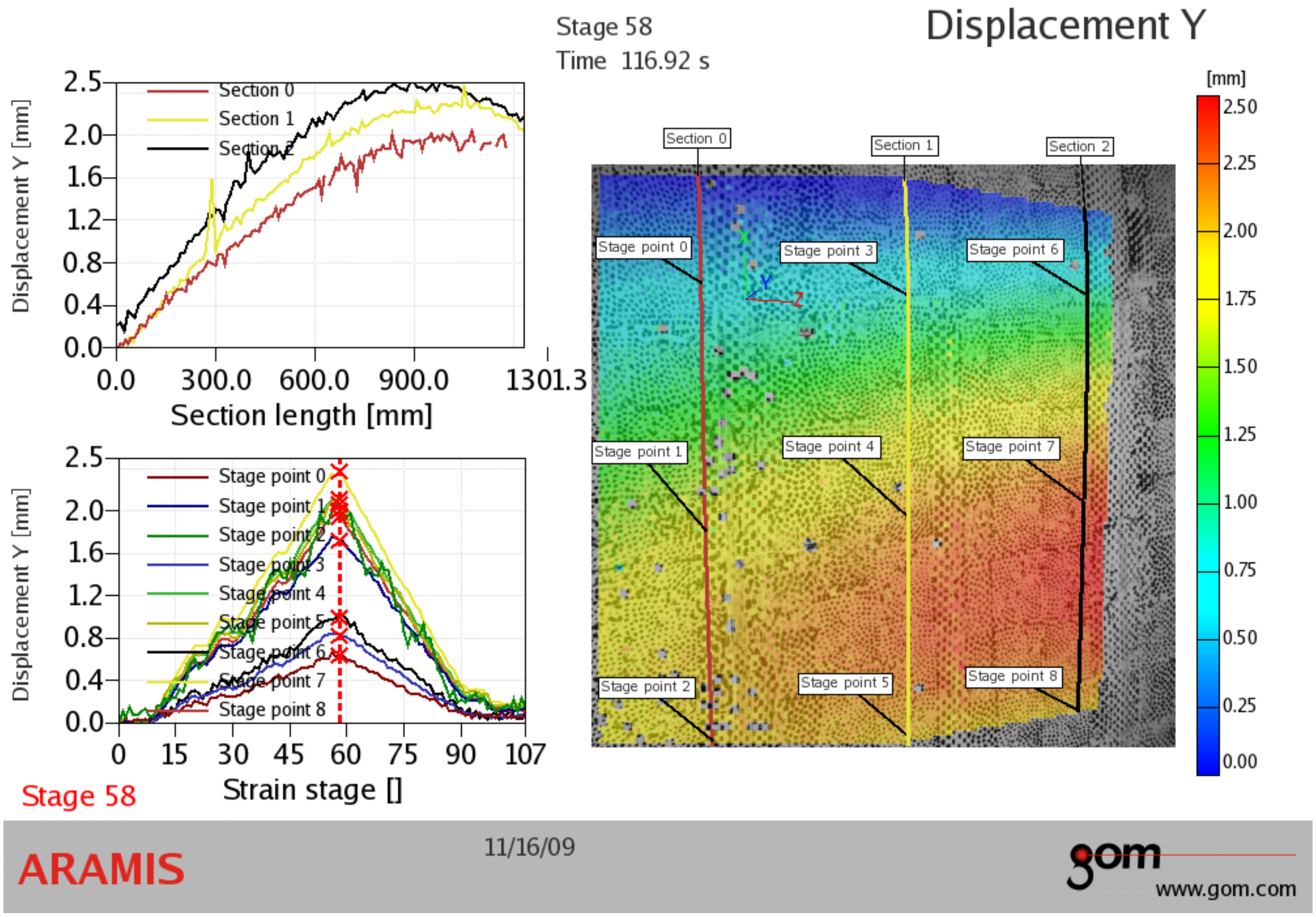

Input of data from DIC - measurement (area is collapsed)

The “local deformation” of the sandwich panels are determined applying the method described in the main report, see capture 5. These determined deformations are comparable with the NT- measurements.

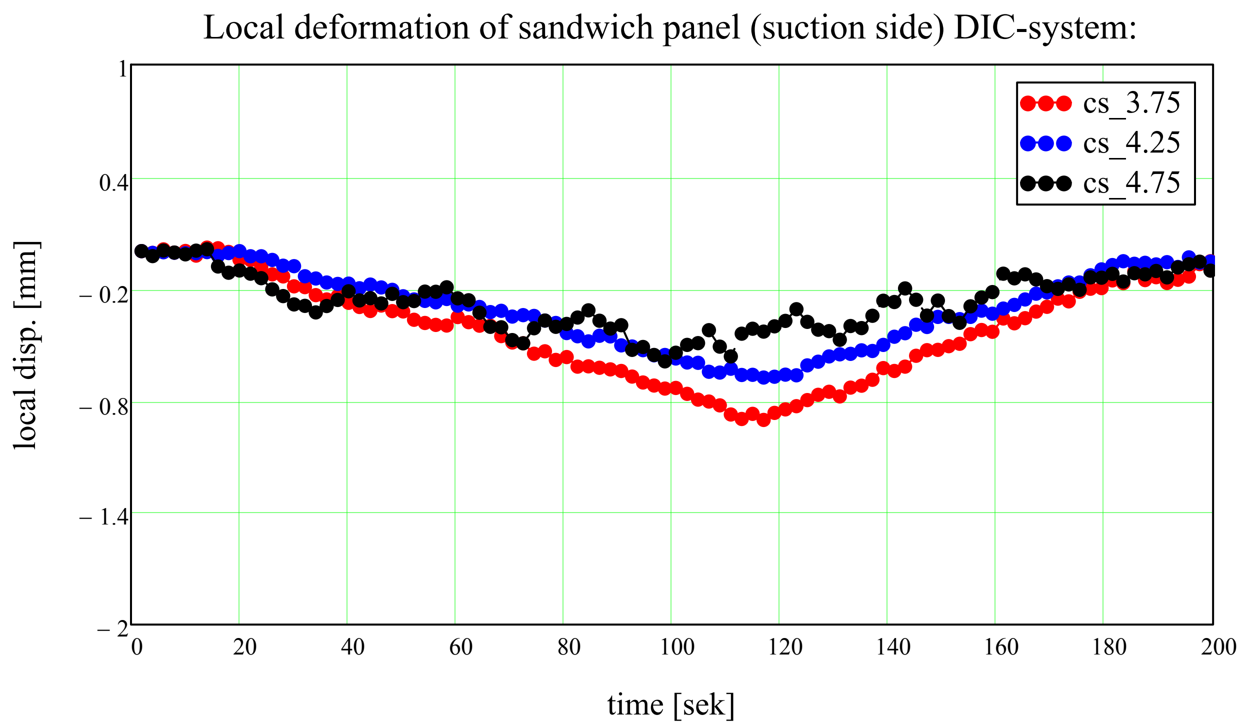

Rigid body movement transformation

The “rigid body movement” transformation is performed by determining the rotations and displacements of the “stiff” cap and then subtracting this movement from the deformed cross section. This gives a fairly god estimate of the local cross sectional displacements. The rotations and displacement are determined by applying the least squares algorithmdescribed in the main report, see chapter 5.

measuring points on the cap: $n_1 := 1$ $n_2 := 25$ $n_{a1} := n_1$ $n_{a2} := n_2$ $sf := 10$

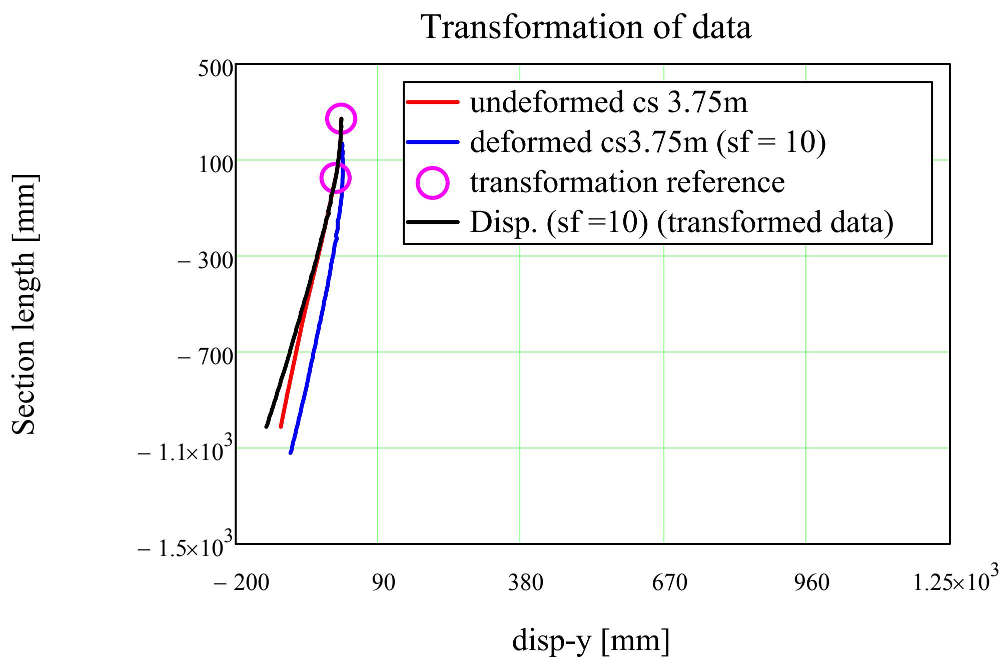

Rigid body movement transformation

measuring points on the cap: $n_1 := 1$ $n_2 := 25$ $n_{b1} := n_1$ $n_{b2} := n_2$ $sf := 10$

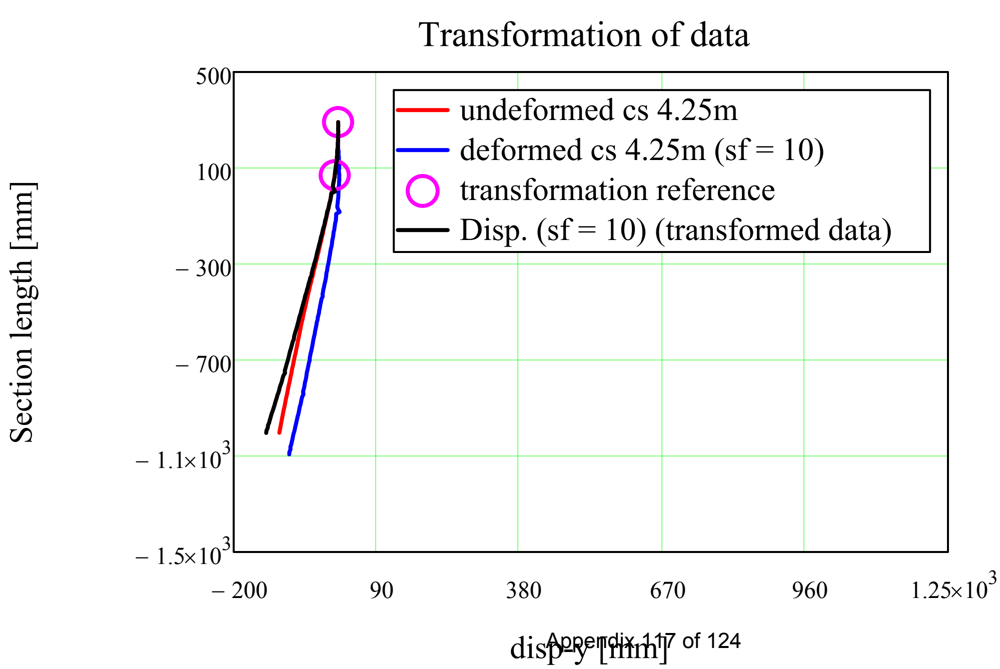

Rigid body movement transformation

measuring points on the cap: $n_1 := 1$ $n_2 := 25$ $n_{c1} := n_1$ $n_{c2} := n_2$ $sf := 10$

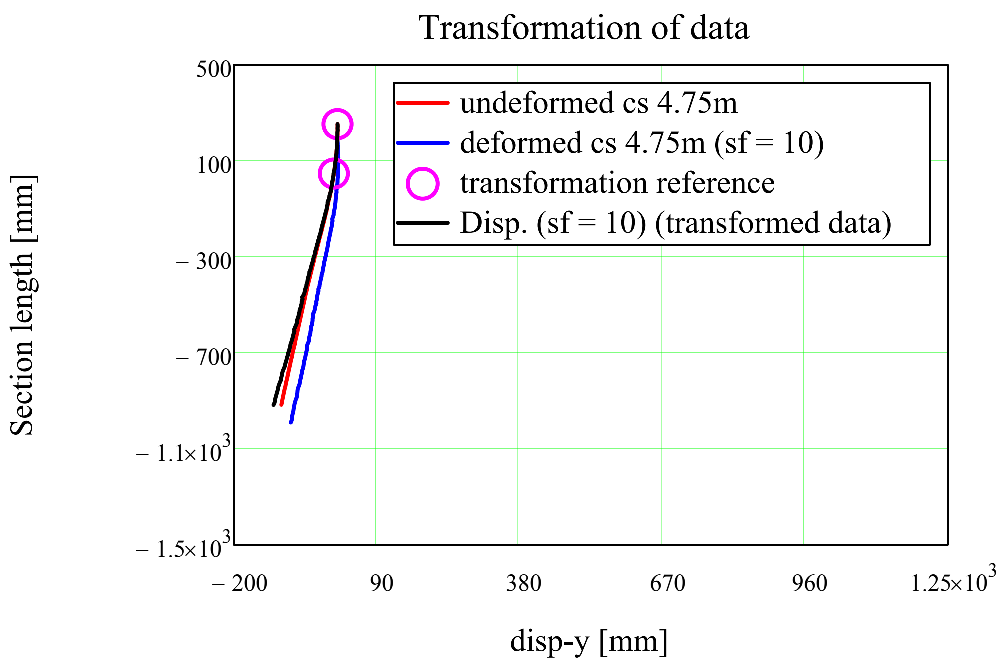

Presented below are the transformed (rigid body movement are subtracted) relative y - displacements:

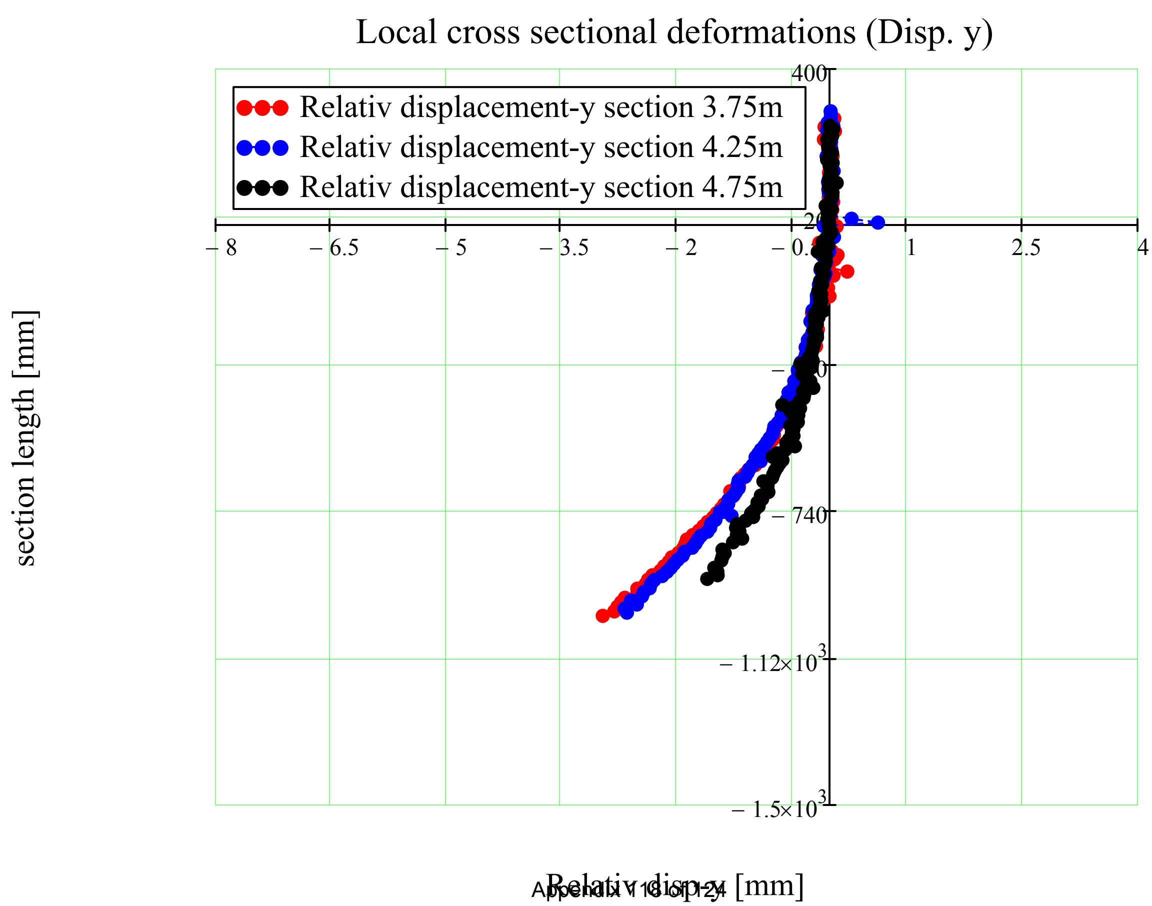

Presented below are the relative y - displacements with out the transformation:

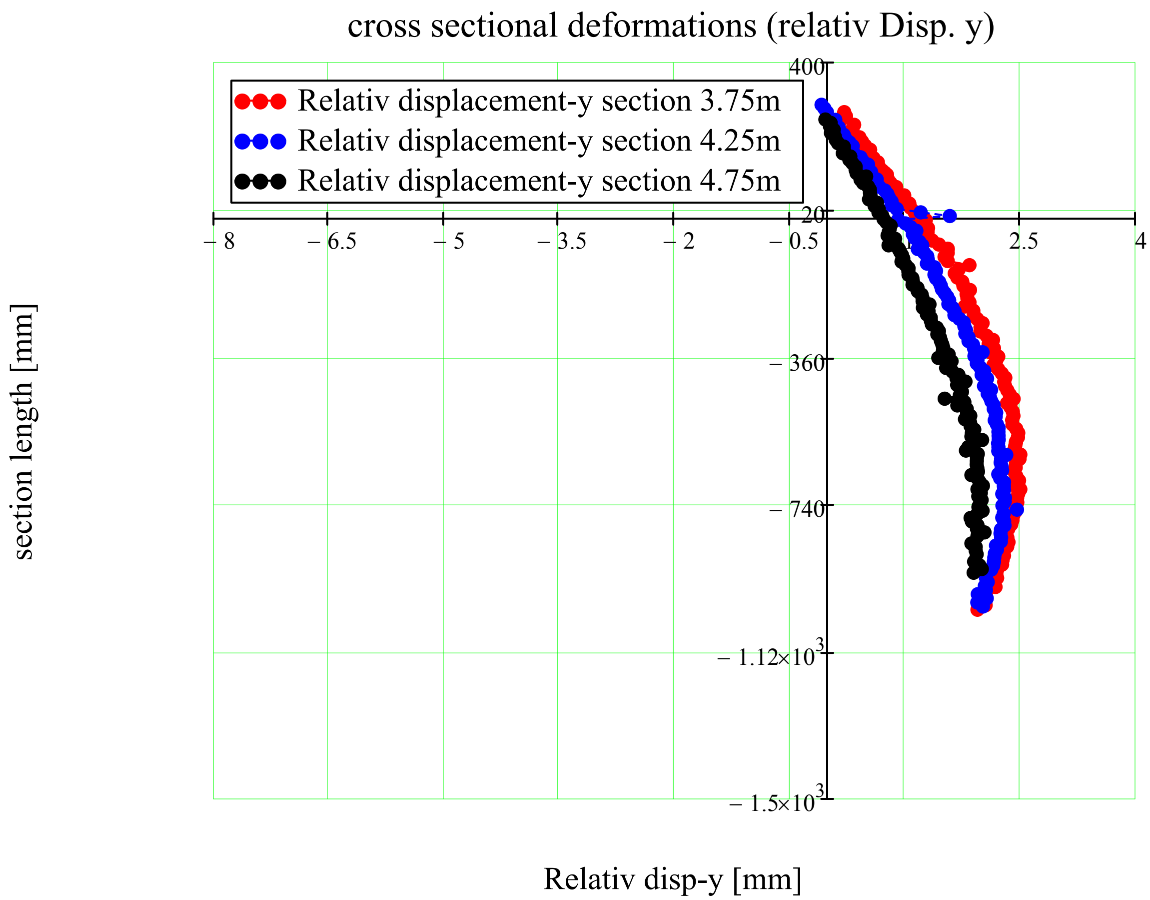

Global deformation determined based on the DIC - measurement

The global deformation is determined by applying the least squares algorithm described in the main report, see chapter 5.

Cross section [m]	Disp. Ux [mm]	Disp. Uy [mm]	Disp. Uz [mm]	Rot. Rx [deg]	Rot. Ry [deg]	Rot. Rz [deg]
3.75	-10.3892	0.6242	0.7271	####	0.2177	-0.2118
4.25	-8.5248	0.3275	0.7994	####	0.1885	-0.2102
4.75	-6.9651	0.2859	0.6931	####	0.1605	-0.1727

Test: ELTT_4_131009_A

The measurement was started at 30% load.

The maximum load during this test was 60%.

The DIC - measurement was conducted in the 10 meter region on the pressure side of the blade, see snapshot below.

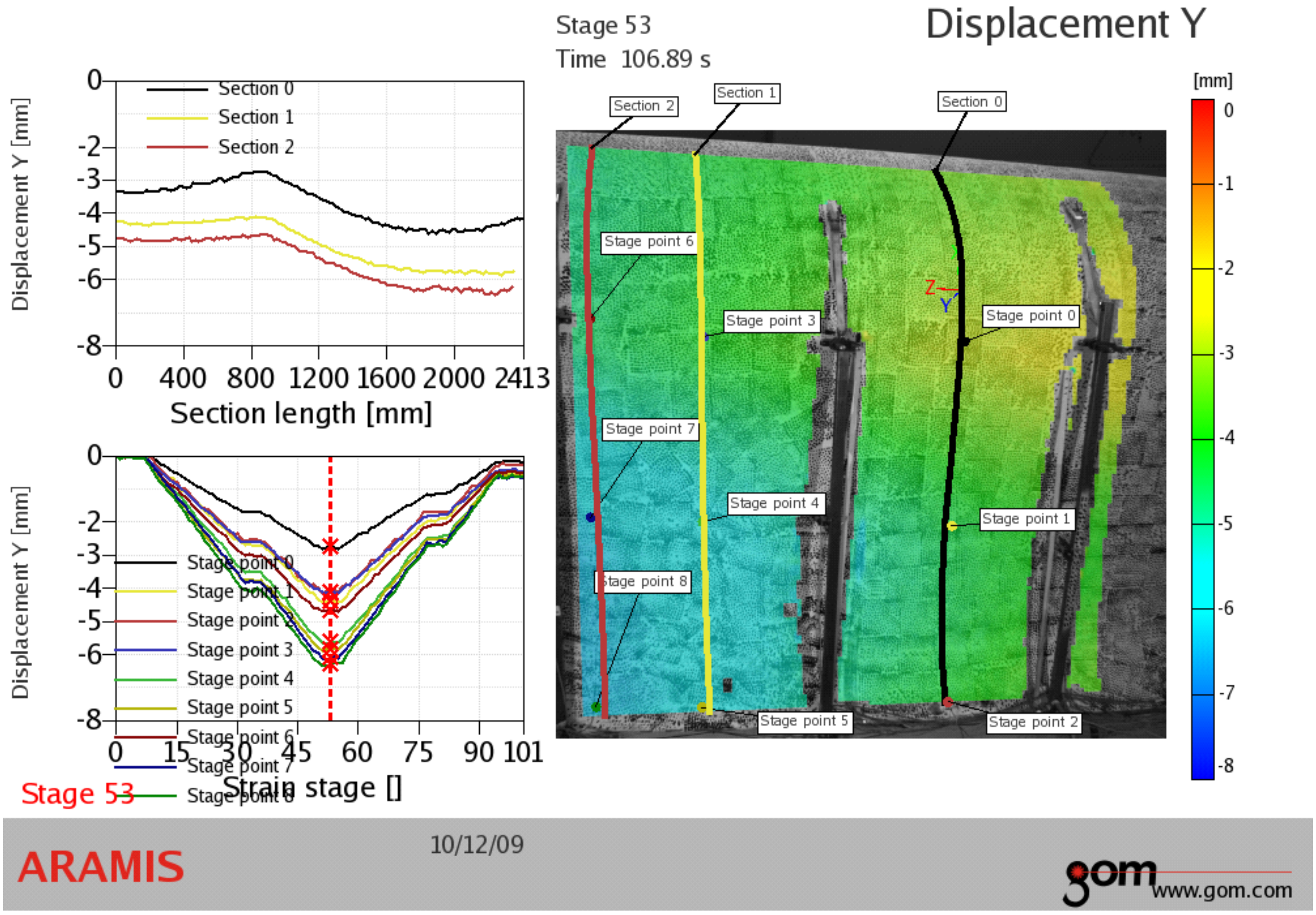

Input of data from DIC - measurement (area is collapsed)

The "local deformation" of the sandwich panels are determined applying the method described in the main report, see capture 5. These determined deformations are comparable with the NT- measurements.

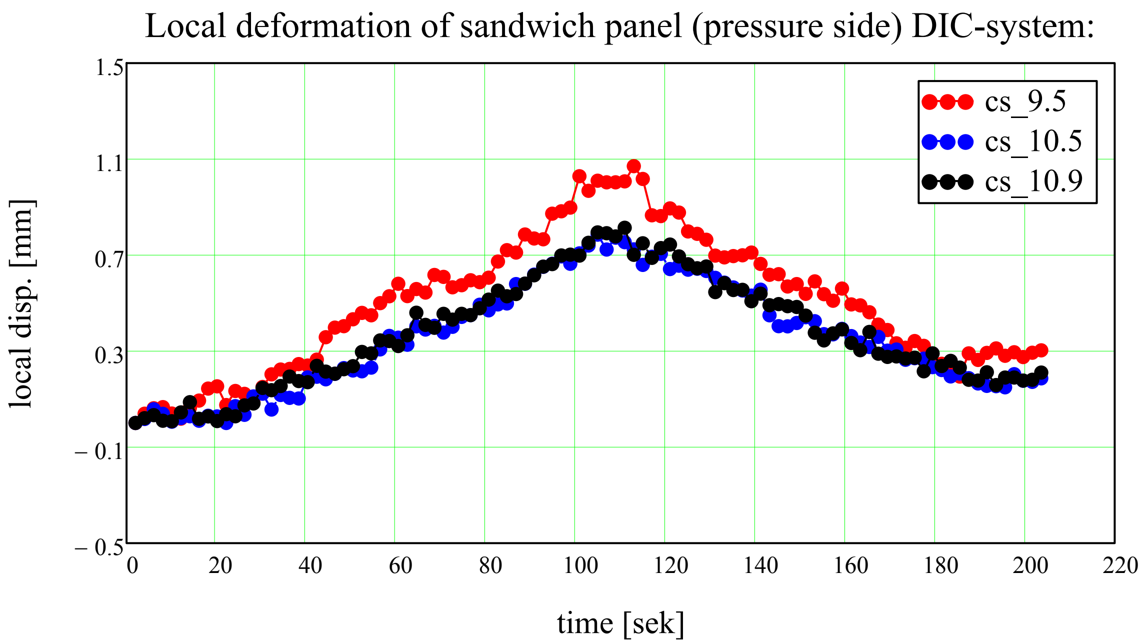

Verification of the DIC-measurement (Comparison between the NT- and DIC- measurement)

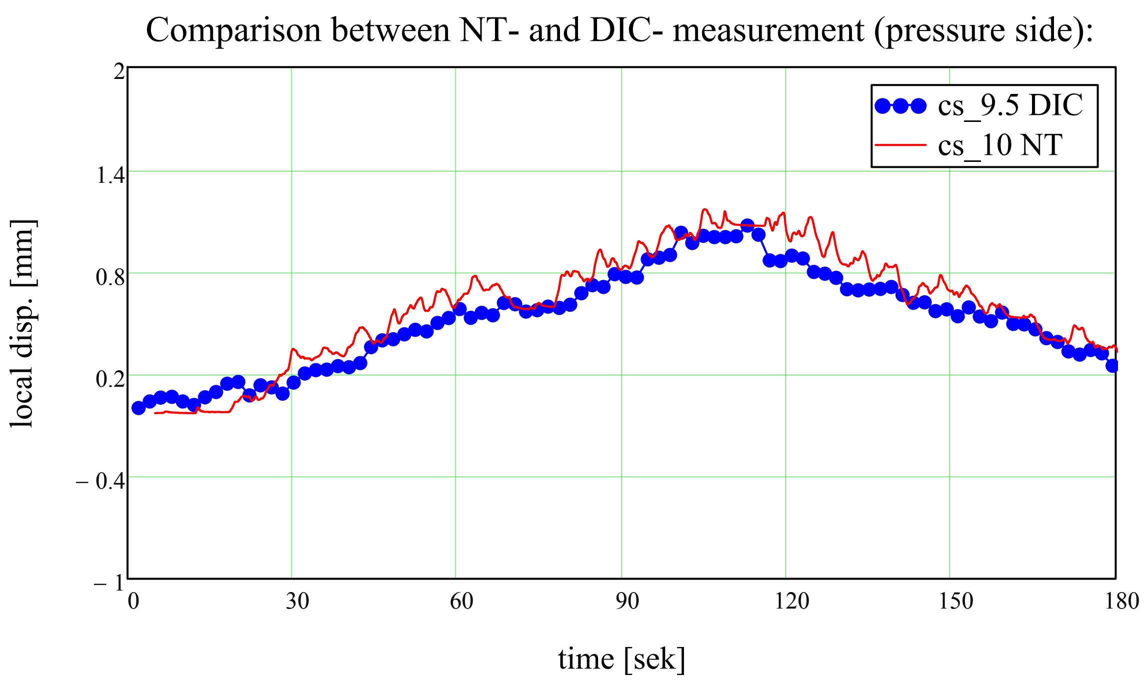

Rigid body movement transformation

The “rigid body movement” transformation is performed by determining the rotations and displacements of the “stiff” cap and then subtracting this movement from the deformed cross section. This gives a fairly god estimate of the local cross sectional displacements. The rotations and displacement are determined by applying the least squares algorithmdescribed in the main report, see chapter 5.

measuring points on the cap: $n_1 := 7$ $n_2 := 32$ $n_{a1} := n_1$ $n_{a2} := n_2$ $sf := 10$

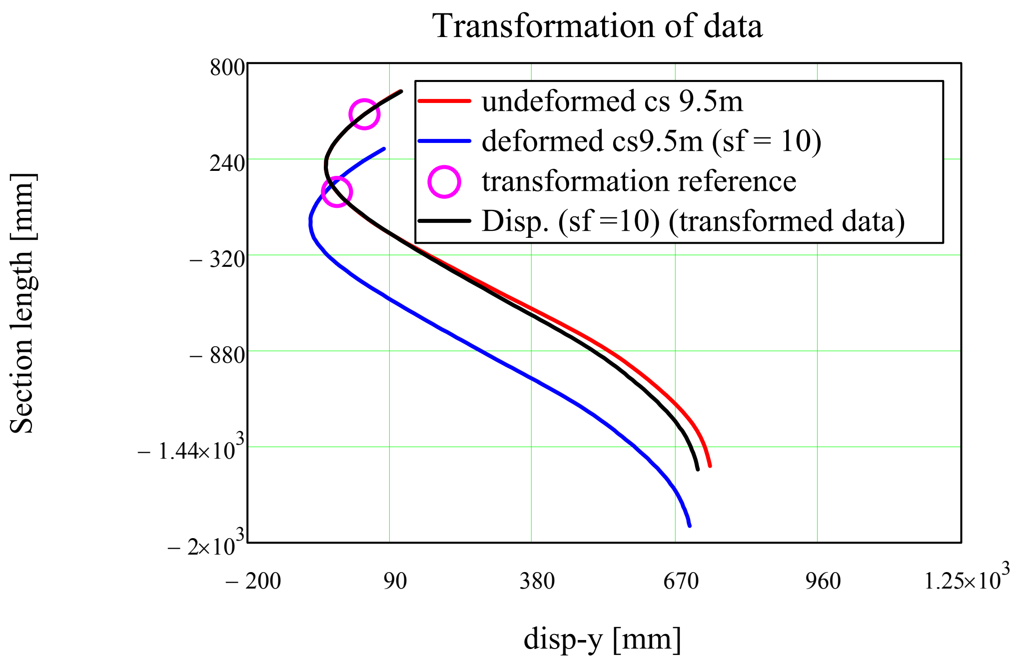

Rigid body movement transformation

measuring points on the cap: $n_1 := 7$ $n_2 := 32$ $n_{b1} := n_1$ $n_{b2} := n_2$ $sf := 10$

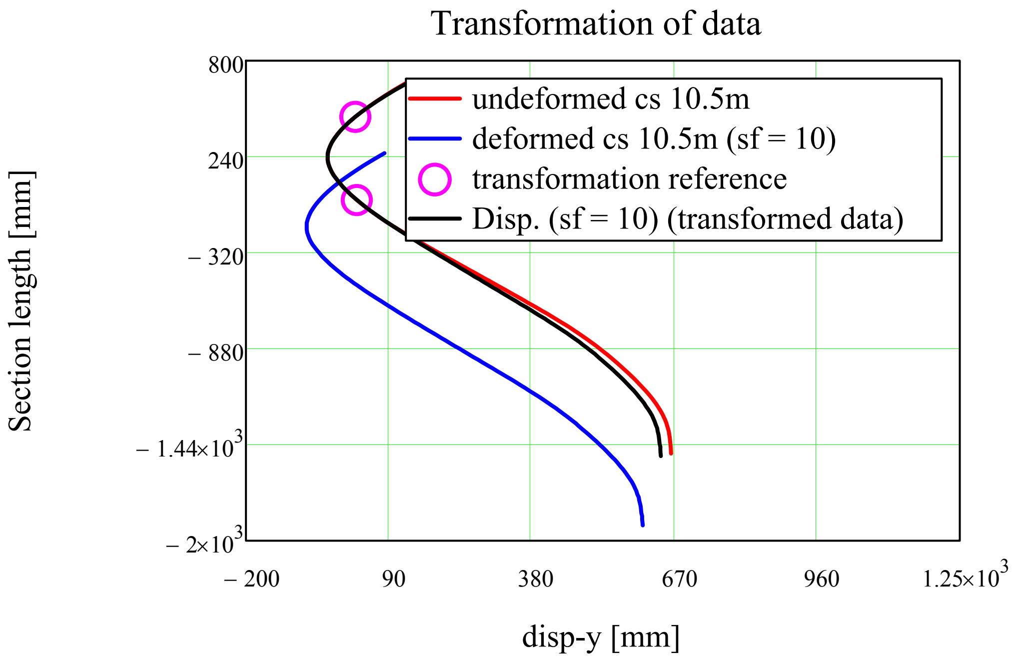

Rigid body movement transformation

measuring points on the cap: $n_1 := 7$ $n_2 := 32$ $n_{c1} := n_1$ $n_{c2} := n_2$ $sf := 10$

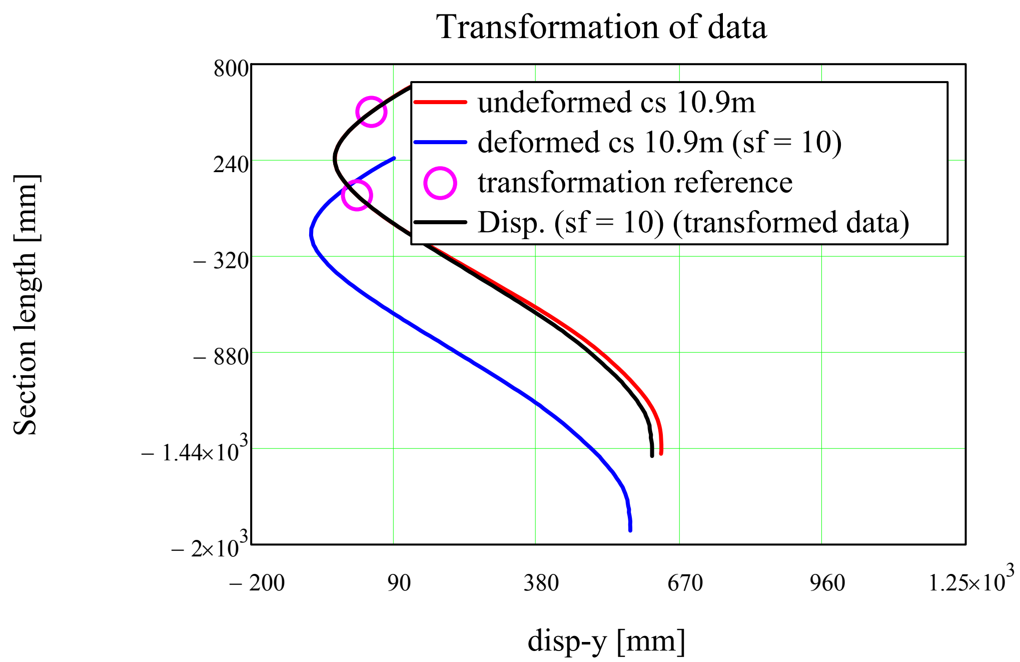

Presented below are the transformed (rigid body movement are subtracted) relative y - displacements:

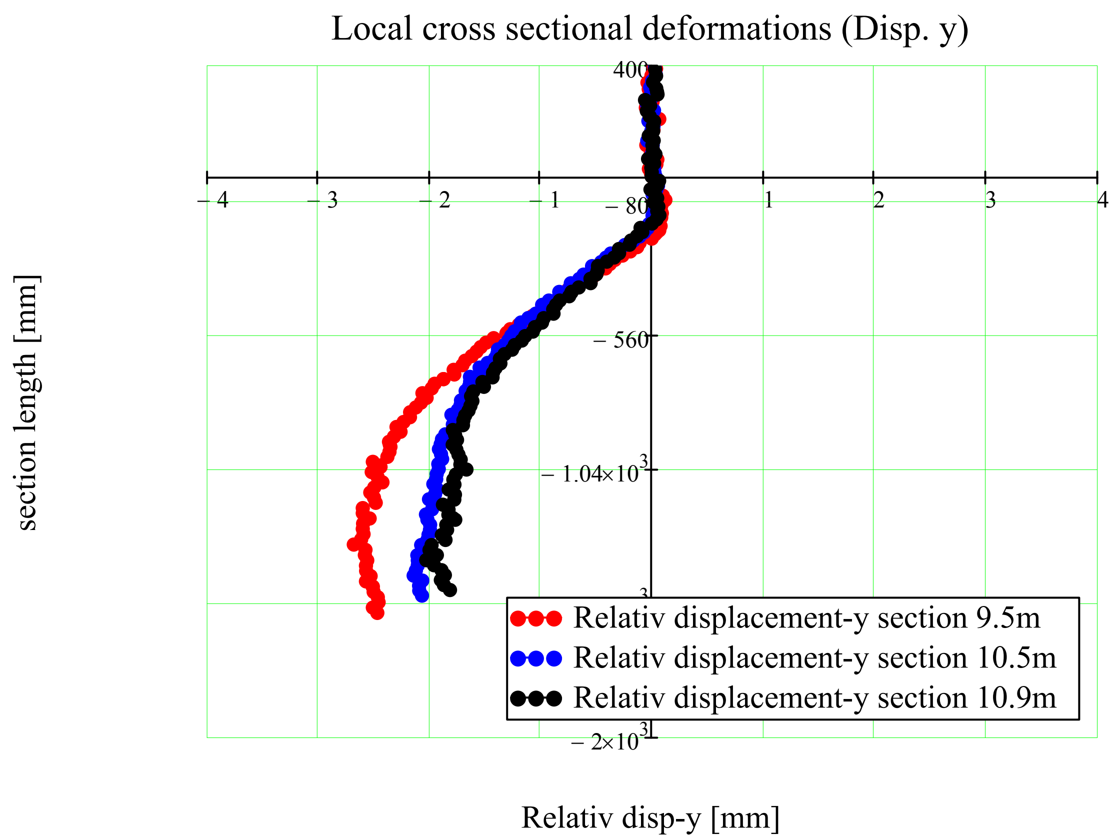

Presented below are the relative y - displacements with out the transformation:

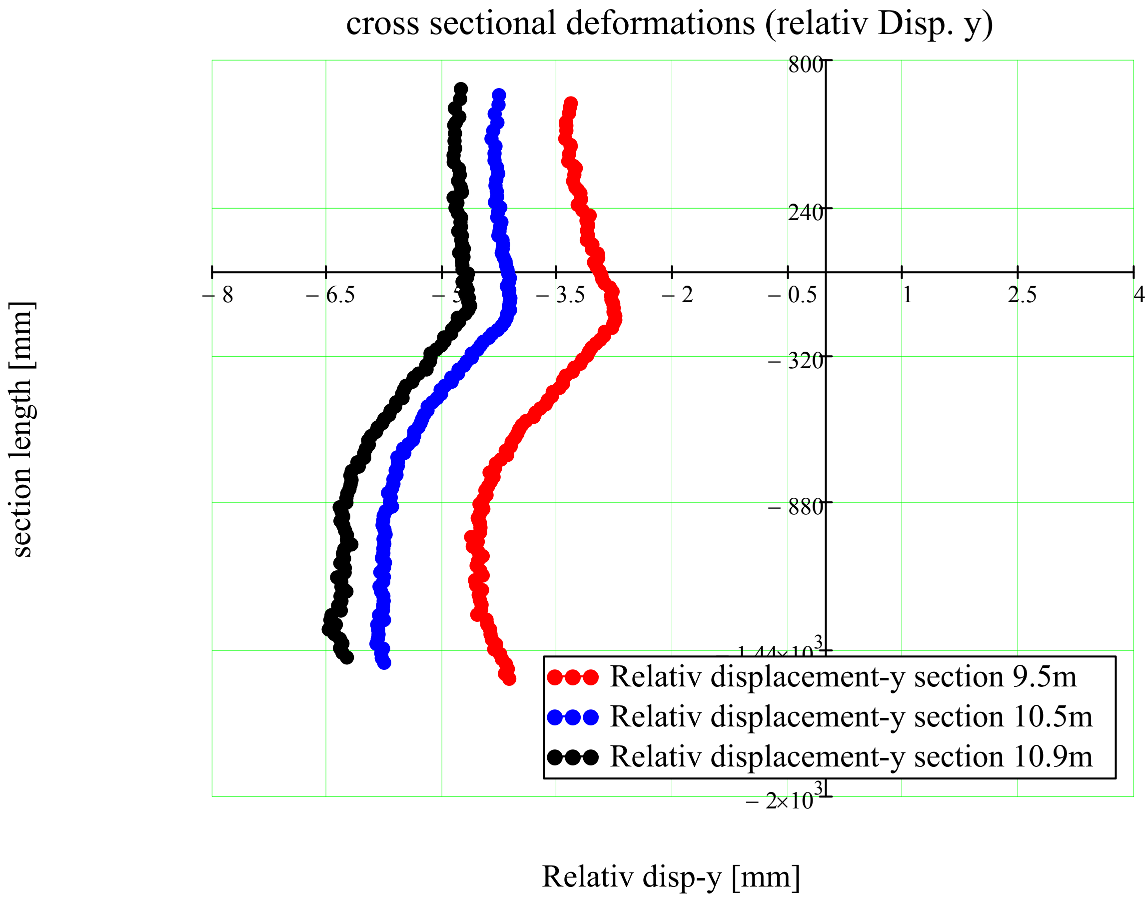

Global deformation determined based on the DIC - measurement

The global deformation is determined by applying the least squares algorithm described in the main report, see chapter 5.

Cross section [m]	Disp. Ux [mm]	Disp. Uy [mm]	Disp. Uz [mm]	Rot. Rx [deg]	Rot. Ry [deg]	Rot. Rz [deg]
9.50	-33.5984	-3.1956	2.7304	#####	0.3770	-0.1189
10.50	-40.6052	-4.2533	2.4165	#####	0.4168	-0.0190
10.90	-43.5984	-4.7866	2.7923	#####	0.4262	-0.0119